YGS OPEN FILE 2010-19

Report on a Quantec Titan-24 geophysical survey over the Minto Mine, central Yukon

A. Verweerd and K. Killin (Quantec Geoscience Ltd.)
Preface by M. Colpron (Yukon Geological Survey) and B. Mercer (Capstone Mining Corp.)

YUKON GEOLOGICAL SURVEY
Capstone Mining Corp.
Quantec Geoscience
Yukon Energy, Mines and Resources

Published under the authority of the Minister of Energy, Mines and Resources, Government of Yukon, http://www.emr.gov.yk.ca

Published in Whitehorse, Yukon, 2010

Publié avec l'autorisation du ministre de l'Énergie, des Mines et des Ressources du gouvernement du Yukon, http://www.emr.gov.yk.ca

Publié à Whitehorse (Yukon) en 2010

This, and other Yukon Geological Survey publications, may be obtained from:
Geoscience Information and Sales
Yukon Geological Survey
102-300 Main Street
Box 2703 (K-102)
Whitehorse, Yukon, Canada Y1A 2C6

phone (867) 667-3201, fax (867) 667-3198, e-mail geosales@gov.yk.ca

Visit the Yukon Geological Survey website at www.geology.gov.yk.ca

In referring to this publication, please use the following citation:
Verweerd, A. and Killin, K., 2010. Report on a Quantec Titan-24 geophysical survey over the Minto Mine, central Yukon. Yukon Geological Survey Open File 2010-19.

Front cover photograph:
Minto Mine, central Yukon.

Report on a Quantec Titan-24 geophysical survey over the Minto Mine, central Yukon

PREFACE

Capstone Mining Corp.'s Minto Mine comprises a cluster of 4 deposits which together define a mineral resource of ~30 million tons with an average grade of 1.22% Cu, 0.45 g/t Au and 4.48 g/t Ag (Capstone Mining Corp., December 2009). Additional mineralization has also been intersected in a number of significant prospects, which together with the known deposits define a NNW-trending exploration corridor on the Minto property. At the time of publication of this report, the Minto Mine is the only producing mine in Yukon.

Copper-gold mineralization at Minto occurs in a series of stacked, shallowly northward-dipping foliated zones located within more massive rocks of the Minto pluton (part of the Granite Mountain batholith), composed predominantly of granodiorite of Early Jurassic age. The Minto pluton is part of a regional suite of Late Triassic to Early Jurassic plutons that occur in two parallel belts associated with the arc terranes of Quesnellia and Stikinia. These terranes extend the length of the Canadian Cordillera, from southern British Columbia to west-central Yukon (Fig. 1). In British Columbia, these plutons are host to a number of world-class Cu-Au(Mo) porphyry deposits. In Yukon, the Minto and Carmacks Copper deposits define the Carmacks Copper belt. Minto is located near the northern apex of this plutonic suite, where Quesnellia and Stikinia merge together. The Minto pluton intrudes along the contact between the Yukon-Tanana terrane (mid- to late Paleozoic metamorphosed continental margin and arc terrane) and Stikinia (mainly Late Triassic arc rocks of the Lewes River Group).

The origin of the Minto deposits is enigmatic. A number of deposit types have been suggested since the initial discovery of the Main Minto deposit in 1973, with Porphyry Copper and Iron Oxide Copper Gold (IOCG) types being the most recently proposed models. In order to better characterize the style of mineralization found at Minto, the Yukon Geological Survey is collaborating with Minto Explorations Limited (a subsidiary of Capstone Mining Corp.) on a number of initiatives, including an ongoing structural and paragenetic study (conducted by the Mineral Deposit Research Unit of the University of British Columbia) and a geochemical and isotopic study (in collaboration with the Geological Survey of Canada).

The following report by Quantec Geosciences Ltd. presents the results of a Titan-24 geophysical survey that was co-funded by Capstone Mining Corp. and the Yukon Geological Survey. Titan-24 is a geophysical exploration method combining DC resistivity/IP chargeability and magnetotellurics; a pole-dipole geometry with 100 m station spacing was used in this survey. This survey was designed to image the known mineralization along the Minto exploration corridor in order to better understand the geometry of the deposits. The Titan-24 survey successfully imaged very well all of the known deposits and confirmed the overall shallow northerly dip of the stacked mineralized system. These results also suggest that the favourable horizons extend to the north of the survey area. This survey has also identified a number of additional exploration targets, at least one of which led to the discovery of a new deposit in 2009, known as Minto East. After this successful "proof of concept" survey in 2009, Minto Explorations Limited is now planning an expanded Titan-24 survey for 2010 that will image more than 80% of the Minto property.

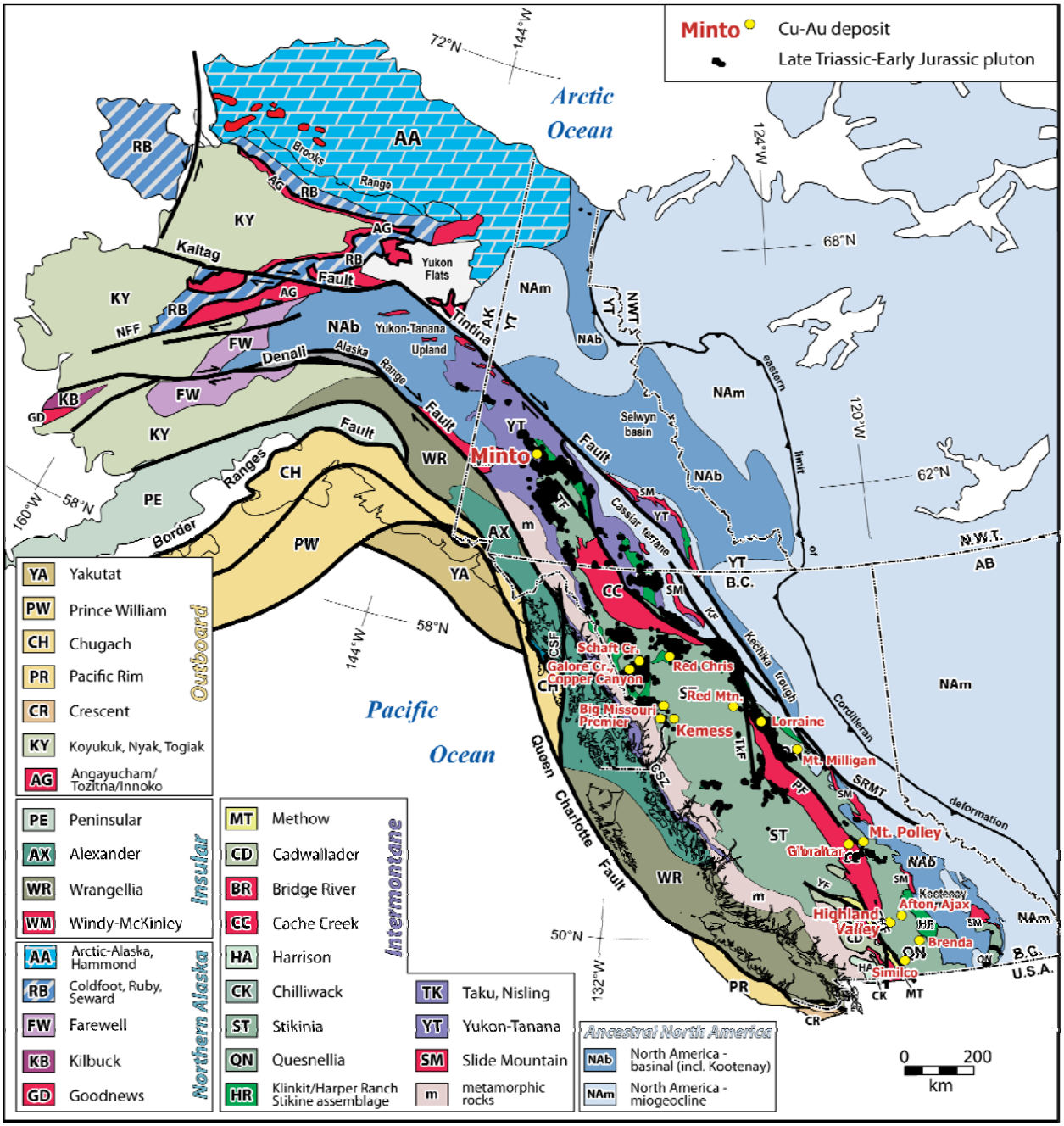

Figure 1. Terrane map of the northern Cordillera showing the distribution of Late Triassic-Early Jurassic plutons and their associated Cu-Au deposits.

It is hoped that the results from this 2009 proof of concept geophysical survey will assist in the design of exploration strategies within the Carmacks Copper belt.

Maurice Colpron
Yukon Geological Survey

Brad Mercer
Capstone Mining Corp.

Quantec Geoscience Ltd.
116 Spadina Ave., Suite 400
Toronto, ON, M5V 2K6
Phone (416) 306 1941
Fax (416) 306 1949

Geophysical Survey Interpretation Report

Quantec Titan-24 Distributed Acquisition System DC RESISTIVITY, INDUCED POLARIZATION AND MT RESISTIVITY Survey over the Minto Mine near Pelly Crossing, Yukon on behalf of Capstone Mining Corporation, Vancouver, B.C. Canada

A. Verweerd
K. Killin

CA00656T
September, 2009

EXECUTIVE SUMMARY

Introduction

A Titan-24 survey was carried out over the Minto mine area, near the town Pelly Crossing, Yukon, Canada between July 29th and August 8th, 2009. The survey included three (3) double spread DC/IP and MT lines totalling 14.7 line- km (21 including current extensions). Each line was surveyed with a pole-dipole geometry with a dipole spacing of 100m. The data were inverted using 2D inversion algorithms to produce maps of DC and MT resistivity and chargeability of the subsurface.

Survey Objectives

The primary objective of the project is to locate potential copper-gold mineralization targets to a depth of 750 m and also large scale structures over the Minto Mine area. The maps of resistivity and chargeability are used to identify and characterize the anomalous targets for focus drilling and further exploration.

Results

The Titan-24 survey over the Minto mine was able to map the resistivity and chargeability response of the major units very well. Correlation between known geology and geophysics is very good,

- Data quality was very good, especially for an active mine site, Typical measurement errors for DC were well below 0.5% and around 5% for the IP data (at the larger N-spacing). MT data had good quality in the range of 10 kHz to 0.01 Hz for most of the sites.
- The existing deposits identified as (Ridge Top) Area 2 and Area 118 correlate very well with chargeability and relatively resistive anomalies.
- The Minto North deposits appear as near surface conductive and chargeable features in the models
- Several deep conductive and chargeable anomalies are observed towards the north and south of the Minto mine pit
- Steeply dipping fault-like structures with an estimated 70 degree dip are observed throughout the sections

Recommendations

Several targets were picked for follow-up with a diamond drilling campaign, (see Table 1). It is also a recommendation to follow-up the current Titan-24 survey with a second survey, with lines parallel to the existing lines. Also a borehole EM and/or DC/IP survey should be considered to validate data and potential off hole anomalies.

In addition to the new measurements, a modelling study has been started at the time of writing of this report, which includes referenced 2D inversions and 3D inversions of the DC and IP data utilising both the inline and the crossline dipoles.

Line ID	Anomaly ID	DDH Location	DDH orientation	Est. Depth of intercept	End of Hole	DC signature	IP signature	MT signature	Priority	DDH ID
L1E	A	250N	-80S	410 m	550 m	moderate	moderate	moderate	3	DDH-01
L1E	E	1610N	-70S	100 m	330 m	Moderate-high	high	Moderate-high	1	DDH-02
L1E	K & I	2940N	-70S	130 m & 580 m	700 m	Moderate & moderate	High & high	Moderate-high & Moderate-high	1	DDH-03
L1E	M	3500N	-70S	250	450 m	moderate	Moderate	Moderate-high	2	DDH-04
L2E	A	100N	-70S	375	650 m	Moderate-high	High	Moderate-High	1	DDH-05
L2E	B	870N	-90	50 m	420 m	Moderate-high	high	Moderate-high	1	DDH-06
L2E	H	2140N	-70S	90 m	350 m	Moderate-low	high	Moderate-low	1	DDH-07
L2E	I	2650N	-80S	420 m	700 m	moderate	high	Moderate-low	1	DDH-08
L2E	M	3180N	-70S	280 m	430 m	moderate	Moderate-low	moderate	3	DDH-09
L2E	N	3540N	-70S	270 m	450 m	moderate	moderate	Moderate-low	2	DDH-10
L3E	A	110N	-80 S	200 m	550 m	Moderate-low	high	Moderate-low	1	DDH-11
L3E	C	1050N	-80S	80 m	280 m	moderate	hugh	low	1	DDH-12
L3E	E	1490N	-80S	160 m	360 m	moderate	high	moderate	1	DDH-13
L3E	F	1840N	-80S	120 m	340 m	low	high	moderate	1	DDH-14

Line ID	Anomaly ID	DDH Location	DDH orientation	Est. Depth of intercept	End of Hole	DC signature	IP signature	MT signature	Priority	DDH ID
L3E	I	2250N	90S	230 m	520 m	Moderate-high	high	Moderate-high	1	DDH-15
L3E	K & J	2840N	90S	60 m & 460 m	630	Moderate-low & moderate	High & high	Moderate-low & moderate-high	1	DDH-16
L3E	L	3180	-70S	90 m	240 m	low	high	low	1	DDH-17
L3E	N	3440N	90S	290 m	510 m	Moderate-low	high	moderate	2	DDH-18
L3E	O	4180N	90S	260 m	530 m	moderate	high	-	3	DDH-19

Table 1: Geophysical targets for the Minto Mine Project

TABLE OF CONTENTS

LIST OF FIGURES

LIST OF TABLES

LIST OF APPENDICES:

1. INTRODUCTION

A Titan-24 DC/IP survey was carried out on behalf of Capstone Mining Corporation, Vancouver BC., Canada, between July 29 and August 8th 2009, over the Minto Mine. The Minto Mine is located 30 minutes off the Klondike Highway between the hamlets of Carmacks and Pelly Crossing in Yukon, Canada (Figure 1). The Minto mine is a copper/gold and silver producer, in operation since 2006.

This survey includes three (3) Titan-24 DC/IP and MT lines with a total length of 21 line km (including current extensions) crossing the Minto Main pit with an azimuth of 341 Degrees (True North).

Each Titan-24 line was surveyed using a pole-dipole geometry with dipole spacing of 100m. The array length was 2.4 km and two arrays were used with 400-500 m overlap to measure the 4 km long line (7.4-7.5 km with current extensions)

The objective of the Titan 24 DC/IP survey is to map potential mineralization targets to a depth of 750 m within the survey area, and identification of the geophysical signature of known deposits for further exploration around the Minto mine.

Figure 1, Minto Project general location map[1]

[1] *Map after* "Technical Report Minto Mine, Yukon" by SRK Consulting, Vancouver

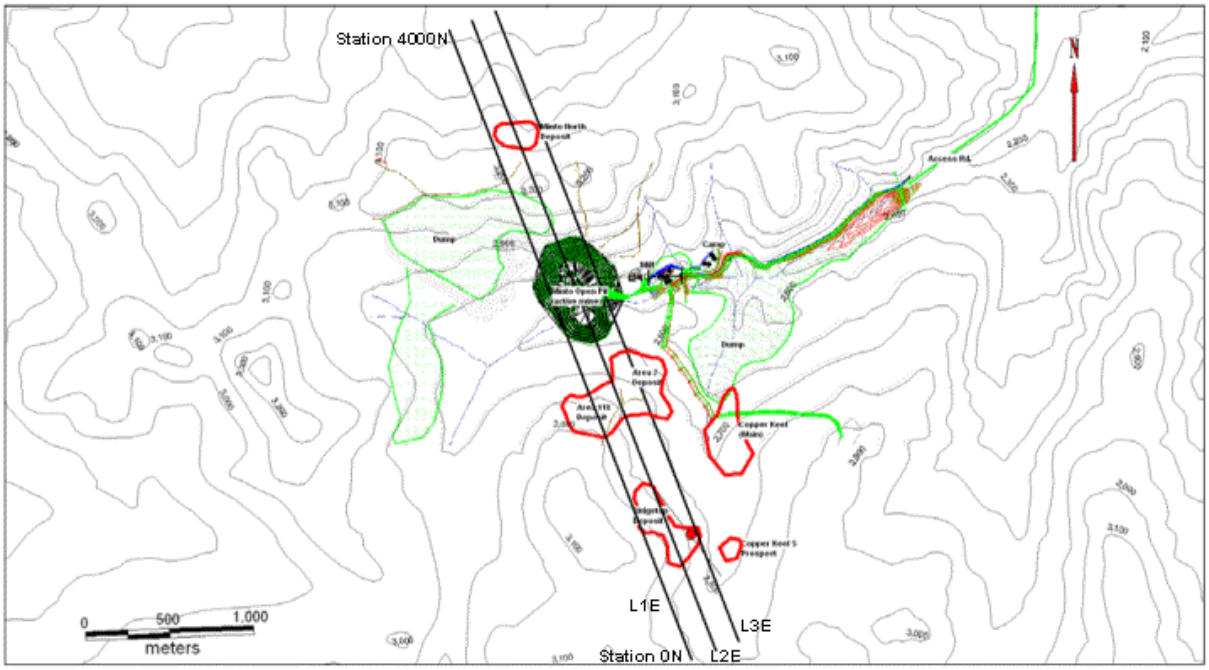

Figure 2: Titan-24 grid and lines location map (ideal lines).

1.1 PROJECT GEOLOGY AND PREVIOUS EXPLORATION[2]

The Minto claims were staked in 1971 after a stream sediment geochemical survey. During the following years a series of geophysical surveys, soil sampling and mapping was completed as was a diamond drilling program, which lead to the discovery of the Minto Main body in 1973

The Minto Property and surrounding area are underlain by plutonic rocks of the Granite Mountain Batholith. They vary in composition from quartz diorite and granodiorite to quartz monzonite. The batholith is unconformably overlain by clastic sedimentary rocks of the Tantalus Formation and andesitic to basaltic volcanic rocks of the Carmacks Group, both are assigned a Late Cretaceous age. Immediately flanking the Granite Mountain Batholith, to the east, is a package of undated mafic volcanic rocks, outcropping on the shores of the Yukon River.

[2] Personal communication with Mr. B.Mercer and "Technical Report Minto Mine, Yukon" by SRK Consulting, Vancouver

The area is divided into several E-W trending zones, divided by two main faults: The Minto Creek fault and the DEF fault, both are dipping steeply north-northeast (approx. 70 degrees)

Mineralization in the Minto deposits are primarily sulphide minerals, occurring as disseminations and stringers along foliation plains in the deformed granodiorite. This deformed granodiorite occurs in sub-horizontal horizons and are often stacked in parallel or sub-parallel sequences.

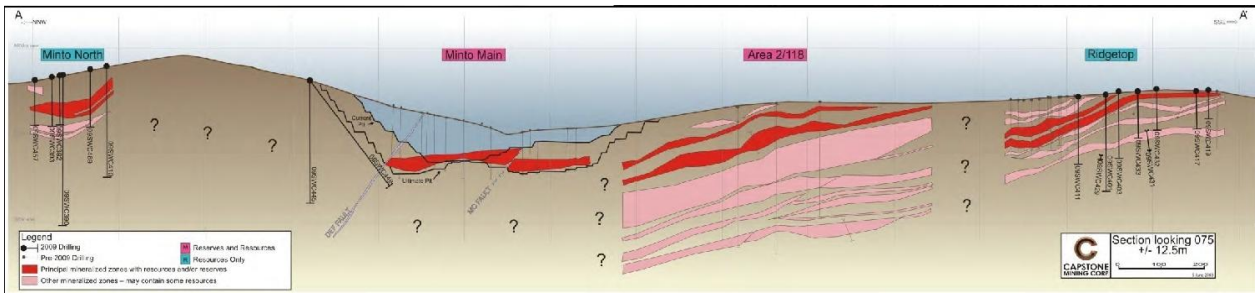

Figure 3: Geology of the Minto Mine[3]

[3] Image obtained from a PowerPoint presentation by Capstone Mining Corp. “Profitable Growth Producing Copper”, June 2009

2. SURVEY DESCRIPTION

2.1.1 DC/IP Surveys

- **Survey Array:** Dipole-Pole-Dipole Array (combined PDR & PDL, see ***Figure 4***)
- **Receiver Configuration**: 24-25 Ex = Continuous In-line voltages (see Figure 5)
  13 Ey = Alternating (2-station) cross-line voltages[4]
- **Array Length:** 2400-2500 meters
- **Number of Arrays/line:** 2
- **Dipole spacing:** 100 meters
- **Sampling Interval:** Ex = 100 meters
  Ey = 200 meters
- **Rx-Tx Separation:** N-spacing (Pn-Cn min) = 0.5 to 39.5 (with current extensions)
  Current electrodes at midpoints between potential electrodes (see Figure 5).
- **Infinite Pole Location:** UTM: 392344E, 6948844N (NAD83, Z08V);
  Grid Coords.: 8837E, 2992N
- **Spectral Domain:** Tx = Frequency-domain square-wave current
  Rx = Full waveform time-series acquisition
  Data processing/output in frequency-domain

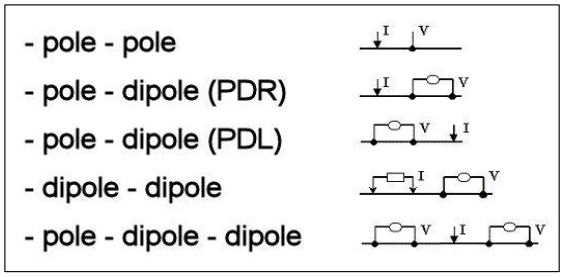

Figure 4: Common DC/IP Survey Layouts

[4] *Note: Cross-Line Ey voltages obtained for future reference purposes – not presented in cross-sectional plots or taken into account in the 2D inversion of the DC and IP data.*

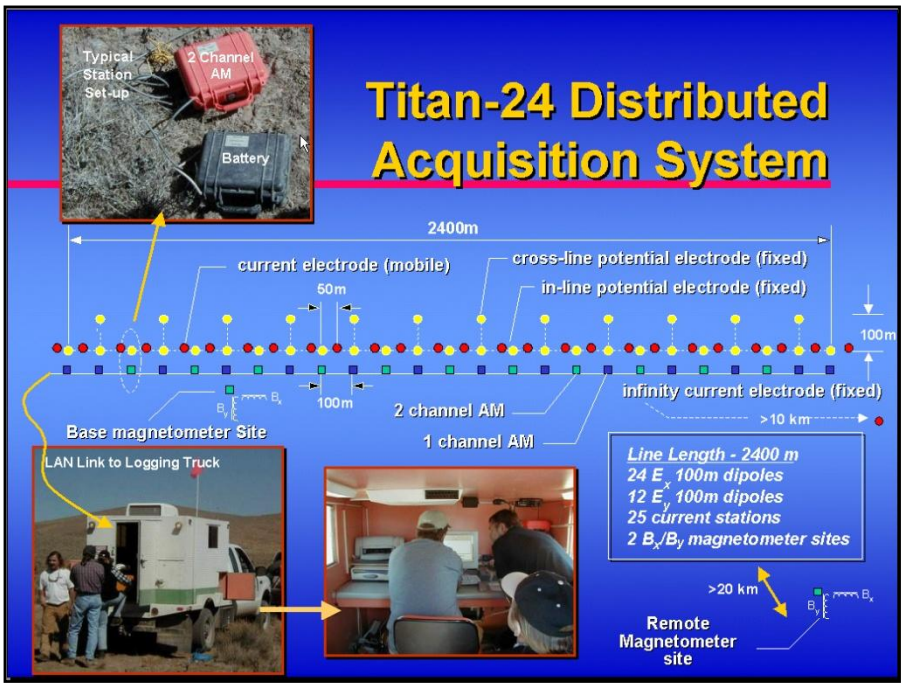

Figure 5: Titan Tensor MT and DC/IP Schematic Survey Layout.

2.1.2 MT Surveys

- **Technique:** Tensor soundings, remote-referenced
- **Base Configuration:** 24-25 Ex = Continuous In-line E-fields
  13 Ey = Alternating (2-stations) cross-line E-fields
  1 pair LF coils
  1 pair HF coils
- **Remote Configuration** 1 Ex = in line E-fields
  1 Ey = cross-line E fields
  1 pair LF coils
  1 pair HF coils
- **Array Length:** 2400-2500 meters
- **Number of Arrays/line:** 2
- **Dipole Spacing:** 100 meters
- **Sampling Interval:** Ex = 100 meters
  Ey = 200 meters
- **Ex/Ey Sampling Ratio:** 2:1
- **E/H Sampling Ratio:** Ex = 24:1 and 25:1
  Ey = 13:1
- **Remote-reference Measurements:** 1 Hx/Hy set (1 Ey/Ex set for verification/monitoring)
- **Remote Reference Position:** 424855E; 7001518N (NAD 83, Zone 08V)
- **Frequency bandwidth:** 0.01 to 10000 Hz

- **Data Acquisition:** Full-waveform time-series acquisition
  Data processing/output in frequency-domain.

2.2 SURVEY COVERAGE

2.2.1 DC/IP Survey

LINE	SETUP	Min P1	Max P2	Min Tx	Max Tx	Coverage (km) without Rx overlap	Coverage (km) with Rx overlap	Coverage (km) with Tx extension
L1E	1	0N	2500N	-50	3150	2.5	2.5	3.2
L1E	2	1600N	4000N	1150	4250	1.5	2.4	3.1
L2E	1	0N	2500N	-650	3250	2.5	2.5	3.9
L2E	2	1600N	4000N	1150	4650	1.5	2.4	3.5
L3E	1	0N	2500N	-650	3150	2.5	2.5	3.8
L3E	2	1600N	4000N	1150	4650	1.5	2.4	3.5
Total						**12**	**14.7**	**21**

Table 2: Minto Mine Grid - Max and Min Pole-Dipole Electrode Position

2.2.2 MT Survey

LINE	SETUP	Min EXTENT (m)	Max EXTENT (m)	Coverage (km)	Coverage (km) with Rx overlap
L1E	1	0N	2500N	2.5	2.5
L1E	2	1600N	4000N	1.5	2.4
L2E	1	0N	2500N	2.5	2.5
L2E	2	1600N	4000N	1.5	2.4
L3E	1	0N	2500N	2.5	2.5
L3E	2	1600N	4000N	1.5	2.4
Total				**12**	**14.7**

Table 3: Minto Mine Grid - MT Survey Coverage (Electrode to Electrode)

3. INVERSIONS AND THE RESULTS

In this section, results of the 2D inversion of the Titan-24 data are presented as cross-sections along each survey line. The observed anomalies are described and discussed as potential drilling targets.

The Titan-24 system acquired three types of geophysical data; direct current (DC) resistivity, MT resistivity, and induced polarization (IP). The DC resistivity method is used to resolve resistivity distribution of the subsurface by measuring the electric potential due to a very low frequency current injection. The MT resistivity is acquired by measuring the variation of natural source electric and magnetic fields to determine the apparent resistivity distribution at depth.

In the induced polarization method, electrical capacitance or chargeability of the subsurface is measured. Chargeability data can be used to locate zones of massive or disseminated mineralization in the subsurface. Sulphides and graphitic minerals are considered as materials with strong chargeability response, therefore the IP method is effectively used in base-metal explorations.

Detailed description of the DC, IP and MT methods used in this survey can be found in Appendices E and F. The preliminary results inversion results, including observed data, error distribution and forward calculated response presented as pseudo sections are presented in Appendix G.

3.1 OVERVIEW OF INVERSION AND INTERPRETATION PROCEDURE

3.1.1 Inversion of Direct Current (DC) and Induced Polarization (IP) data

The Titan-24 DC and IP data were inverted to produce cross-sections of the resistivity and chargeability distribution below the survey lines. The UBC DCIP2D inversion code was used for the 2D inversion of the DC and IP data. Three 2D inversions were carried out along each line. Electrical potential difference (voltage) and phase values were used as input data in the DC and IP inversions, respectively. The DC data was inverted using an unconstrained 2D inversion with a homogenous half-space of average raw data resistivity as starting model. The IP data was inverted using two different reference models. The first IP inversion utilized a reference resistivity model result from the inversion of the DC data (Smooth). In the second IP inversion, a homogenous half-space model of constant resistivity (Null) was used as the reference model. This model is included to test the validity of chargeability anomalies, and to limit the possibility of inversion artefacts in the IP model due to the use of the DC model as a reference.

The parameters of the inversion procedure and model were selected based on the DC/IP survey parameters. The survey was carried out with dipole spacing of 100 m. Therefore, for horizontal grid size in the inversion model, three cells were used between each dipole location. For vertical mesh, a fine mesh of 20 m was used from the surface to a depth of approximately 500 m. below this depth the cell size increases exponentially. For each inversion, a few trials were carried out using different data error conditioning to find the optimum error value that allows the inversion process to converge while preserving the subtle features of the dataset. The error conditioning is dataset dependent and must be evaluated for each individual dataset.

3.1.2 Magnetotellurics (MT)

The MT method is a natural source method that measures the variation of both the electric (E) and magnetic (H) field on the surface of the earth to determine the distribution at depth of the resistivity of rocks. Natural time variations in the Earth's magnetic field, due to oscillations of the ionosphere and lightning, induce electric currents in the ground. The depth of investigation is determined primarily by the frequency of the measurement, and it can be large. Depth estimates from any individual sounding may

easily exceed 20 km. A complete review of the method may be found in Vozoff (1972)[5] or in Orange (1989)[6]. Several of the main points are commented on below.

The measured MT impedance Z, defined by the ratio between the E and H fields, is a tensor of complex numbers. This tensor is represented by its two off-diagonal elements, the TE (Transverse Electric; E parallel to the strike) and the TM (Transverse Magnetic; E perpendicular to the strike) modes. In a 1D earth model, i.e. the resistivity varies only with depth, there is no strike direction and the TE and TM impedances are equal. In the 2D case, i.e. when the resistivity varies with depth and perpendicularly to the strike, TE and TM mode measurements are not equal but reflect the variation of the resistivity along two directions, one parallel and the other perpendicular to the strike.

Both TE and TM impedances are represented by an apparent resistivity (a parameter proportional to the modulus of Z) and a phase (argument of Z). The variation of those parameters with frequency relates the variations of the resistivity with depth, the high frequencies sampling the sub-surface and the low frequencies the deeper part of the earth. However the apparent resistivity and the phase have an opposite behaviour. An increase of the phase indicates a more conductive zone than the host rocks, and is associated with a decrease of the apparent resistivity. The objective of the inversion of MT data is to compute a distribution of the resistivity of the surface that explains the variations of the MT parameters, i.e. the response of the model that fits the observed data. The solution however is not unique and different inversions must be performed (different programs, different conditions) in order to test and compare solutions for artefacts versus a target anomaly.

A brief introduction to the Titan-24 approach to MT can be found in Appendix E. The depth of investigation is determined primarily by the frequency content of the measurement and can be to great depth. Depth estimates from any individual sounding may easily exceed 20 km. However, the data can only be confidently interpreted when the aperture of the array is comparable to the depth of investigation. In the instance of Titan 24 surveys, inversion depth is generally limited to about half the length of the survey line or profile.

The primary tool for evaluating the Titan MT data is 2D inversion. A discussion of inversion, focusing on the Titan-24 approach, is presented in Appendix E The inversion model is dependent on the data, but also on the associated data errors, and the model norm. The inversion models are not unique, may contain artefacts of the inversion process, and may not therefore accurately reflect all of the information apparent in the actual data. Inversions are a tool, but not a “solution”. Inversion models need to be reviewed in context of the observed data, model fit, an understanding of the model norm used and if the model is geologically plausible.

3.2 2D INVERSION RESULTS (SECTION MAPS)

The MT, DC and IP 2D inversions were completed along the three (3) lines over the Minto project. Topography data along the survey lines were incorporated in the inversion process. The survey lines are oriented with a 341 degrees azimuth but vary in proximity of the minto mine pit due to acquisition logistics around existing and temporary obstacles and mine workings

In the following sections, results of the 2D inversion of the MT, DC and IP with smooth resistivity reference model for each line are illustrated and the observed anomalous features are described. A logarithmic scale of 10 Ohm-m to 100.000 Ohm-m for the resistivity and a linear colour scale of 0 milliradians (mrad) to 25 mrad for the chargeability cross-sections are used consistently for all images. As an indication of the validity of the provided smooth resistivity IP model and it the interpretation based on that model, the Null conductivity IP model is also presented and briefly discussed for each line.

[7] *K., Vozoff, K., (1972). “The Magnetotelluric method in the Exploration of Sedimentary basins”. Geophysics, 37, 98-141.*
[8] *A.S., Orange, (1989). “Magnetotelluric exploration for hydrocarbons” Proceedings of the IEEE, 77, 287–317.*

3.2.1 Line 1

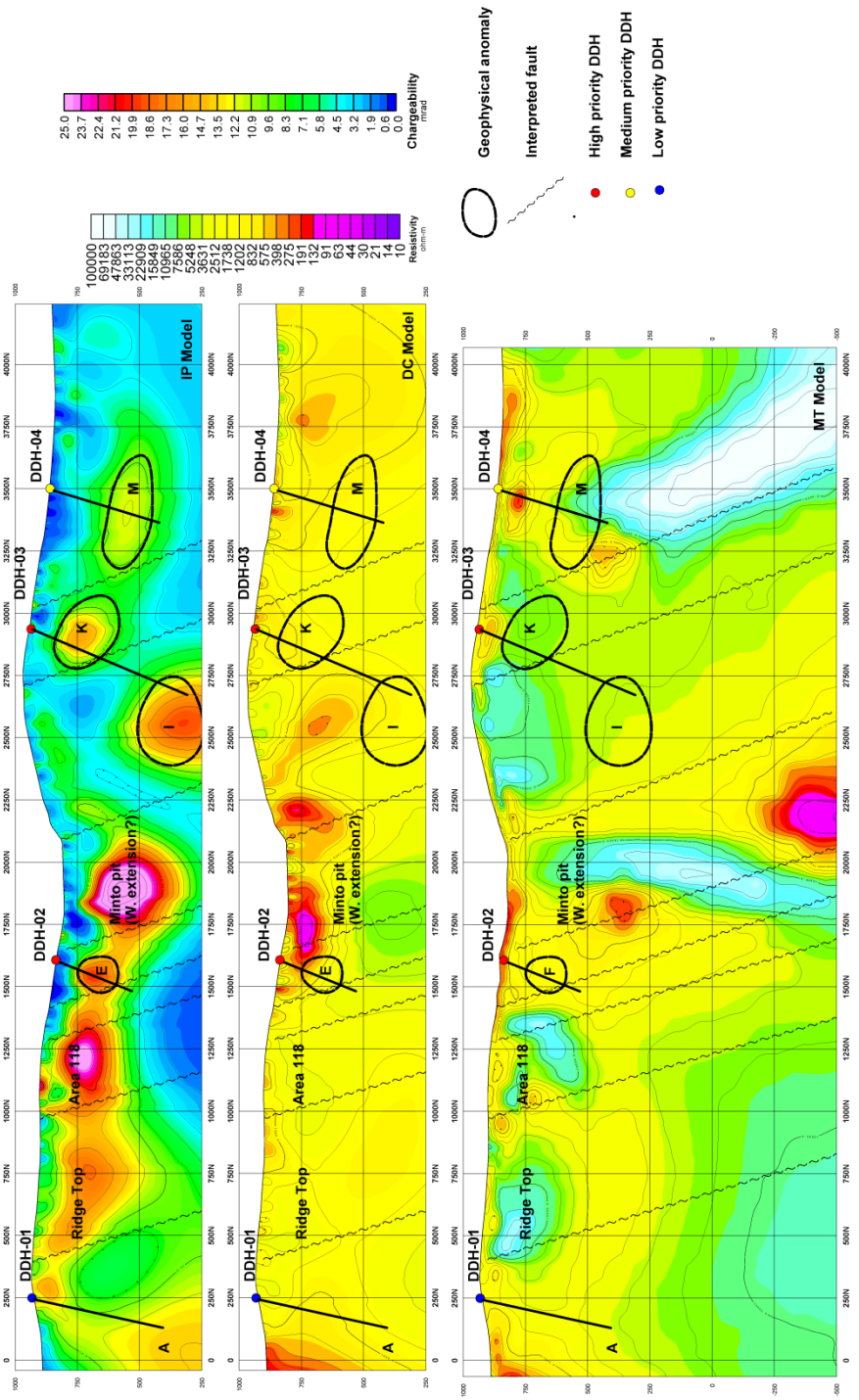

Figure 6: 2D inversion results Line 1

Line 1 is the western most line of the MInto grid, and shows most of the known features of the Minto project. On the southern half of the line the Ridge Top and Area 118 are observed as high chargeability and slightly resistive features (in both DC and MT models). Both zones are located at a similar depth, located between 100 m and 350 m below the surface. Deeper, and located at the far southern side another chargeable zones is observed and identified as anomaly A. Typically this anomaly would not be identified as a target due to the limited depth of penetration caused by the survey geometry at this location, but Anomaly A can also be identified in the two other lines, and therefore classifies as a low priority target (DDH-01).

Following the Ridge Top and Area 118 north Anomaly E is encountered, and appears to part of the same larger scale feature as Ridge Top and Area 118, although it doesn't seem to be associated with a slightly resistive zone. Anomaly E could be targeted with DDH-02 (a high priority borehole).

Near surface around the Minto main open pit is characterized by a very conductive 100-150 m thick zone, without a chargeability signature. Below the conductive zone (again associated with a slightly resistive anomaly) a large chargeable feature is observed up to a depth of 400 m below the surface.

Further north a second deep chargeable zone is observed (Anomaly I), with a very similar signature as Anomaly A. Both chargeable zones are located below a conductive zone, but have background resistivity values themselves and are located at similar depths (600 m below the surface). Anomaly I can be targeted in combination with Anomaly K by high priority borehole DDH-03. Anomaly K fits the same description as Ridge Top and Area 118, a chargeable feature, approximately 200 m below the surface within a slightly resistive environment. Anomaly K could be related to the Minto North zone intersected by line 2.

The final anomaly identified on Line 1 is anomaly M, located around 320 m below the surface, and also associated with a more resistive zone. The depth of anomaly M makes it a medium priority target (DDH-04), to be tested after DDH-02 and DDH-03.

The MT model section shows several steeply north dipping features at depth, which can be used in the chargeability model to separate the chargeability anomalies. The DEF fault is located just north of the Minto Pit, and has a 70 degree northern dip, correlating very well with the interpreted faults. The different depths and broken up nature of the IP anomalies could be explained by a series of north dipping fault-blocks.

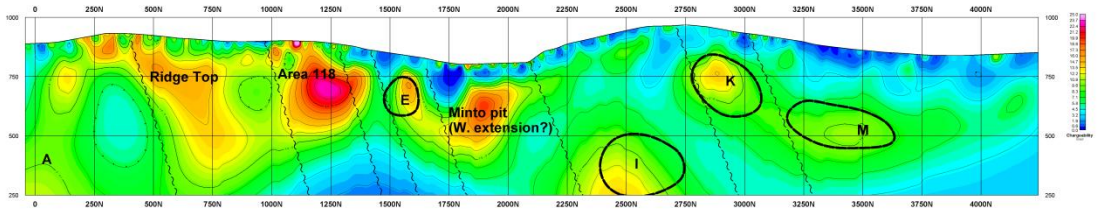

Figure 7: Null conductivity IP Model Line 1

The null conductivity IP model confirms the location of the anomalies picked in the DC referenced IP model. Also the fault-like features at 70 degree dip angles and broken up nature of the IP anomalies is well represented in the Null conductivity IP model.

3.2.2 *Line 2*

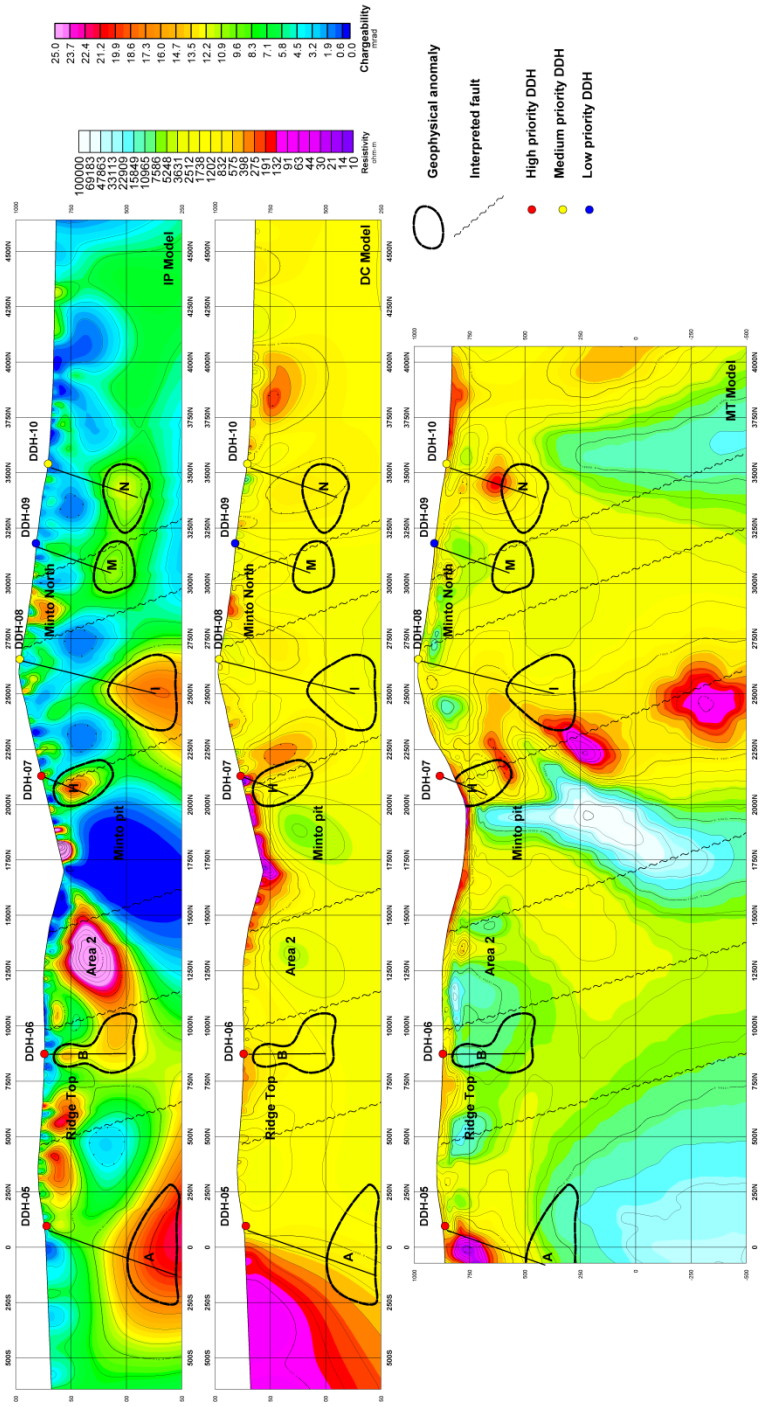

Figure 8: 2D inversion results Line 2

Line 2 is the centre line of the survey and intersect most known zones of mineralization.Line 2 was measured with the use of current extensions, which is the reason why the DC and IP sections are longer than the MT section. The southern part of the line has a similar deep chargeable feature (Anomaly A) as was observed on line 1.Both shape of the anomaly and its occurrence below a conductive zone in DC and MT models are very similar to Anomaly A observed on line 1. A suitable position for drilltesting of this anomaly would be DDH-05.

North of the deep chargeable feautre, located below the overburden within a slightly resistive zone the ridge top anoamlies can be observed again, also a small feature, possibly a remainder of Area 118 is observed, and identified as Anomaly B (to be tested by high priotity DDH-06). At depth this chagreable feature could be connected to the largest chargeabilty anomaly on this line: Area 2, also a known mineralized feature.

Apart from some small chargeability anoamlies below the surface (correlating with a very conductive zone in both DC and MT models), no further features below the Minto Main pit are observed. Both DC and MT show another resistive zone below the pit, potentially with a deep root, as is suggested by the MT model. To the north of the Minto pit a sucession of conductive zones is observed in the MT model, the centres of these anomalies match the 70 degree northern dip of the DEF fault very well. Below the most shallow conductor chargeability anomaly H is observed, with very similar characteristics as previously described zones. This makes Anomaly H a high priority target, abmn DDH-07 is proposed as a suitbale place to test this anomaly.

On the northern side of the fault-like feautre another deep charegeable zone is observed (Anomaly I), which also is present on line 1, again with a very similar signature. North of the top of the hill the Minto North deposit is located, identified as a chargeability and conductivity anomaly at the surface.

Finally two anomalies identified on line 2 are Anomalies M and N, both moderate-low chargeabile zones, similar to the ones observed on line 1.The depth and amplitude of these zones makes the low and medium priority targets (DDH-08 and DDH-09).

Again the IP model can be divided by sharply northward dipping fault like feaures over the whole section, potentially related to the Minto creek and DEF faults

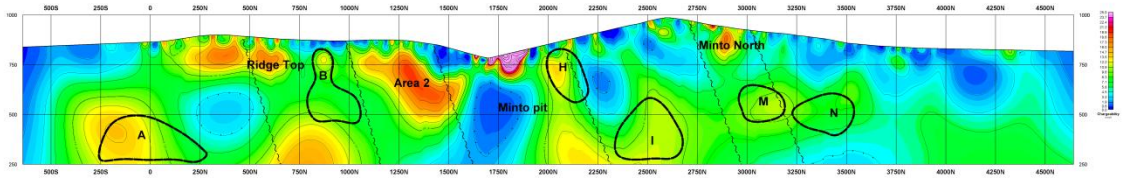

Figure 9: Null conductivity IP model line 2

As was the case in line 1, the IP model calculated without a reference from the DC model, shows most of the features in the same location. The main difference can be found in anomalies A and B, where the null conductivity model shows the center of anomaly further south and the deeper extension of anomaly B as a separate feature in the bottom part of the model. This identifies both anomalies as lesser priority targets than the other anomalies identified on line 2.

3.2.3 Line 3

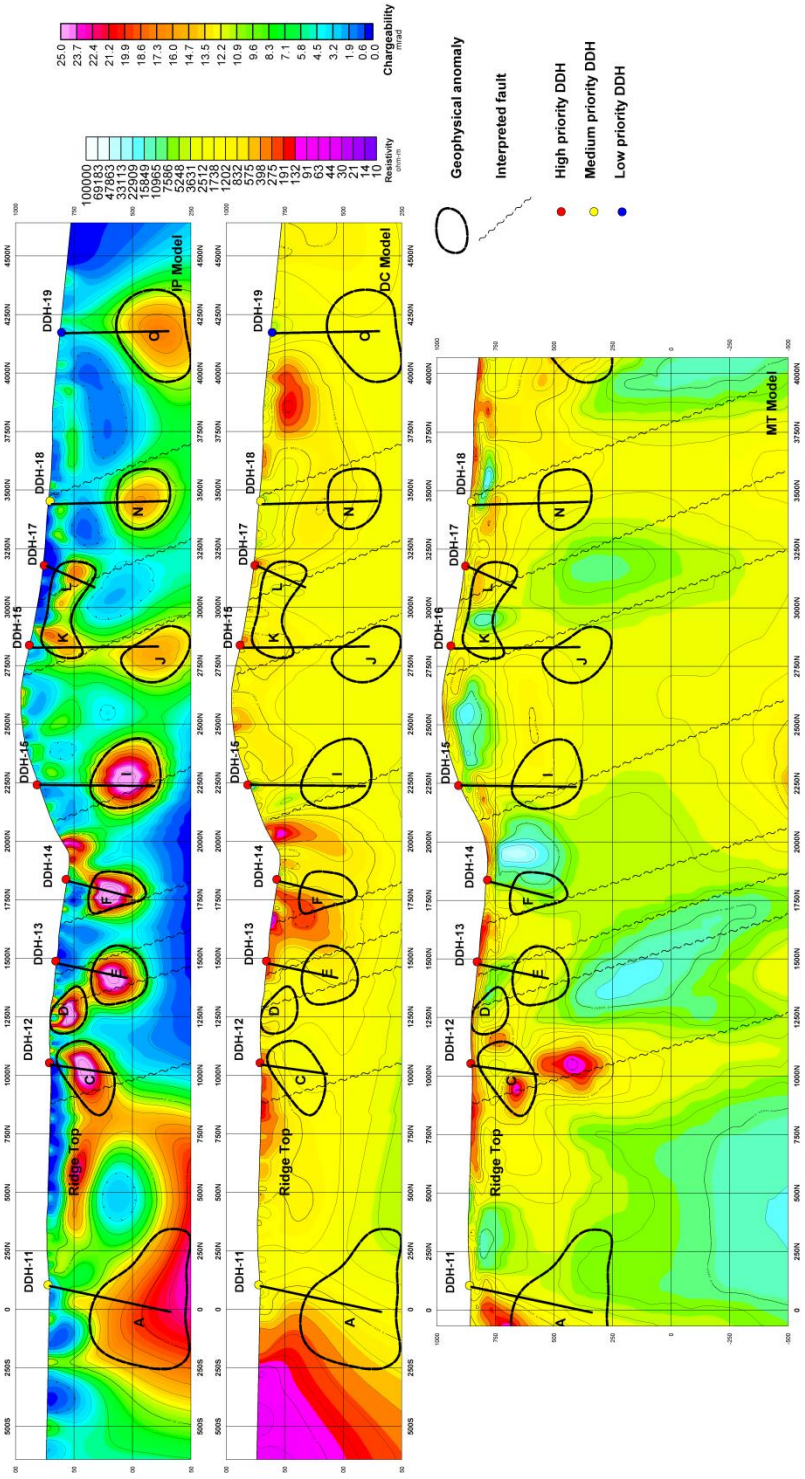

Figure 10: 2D inversion results Line 3

Line 3 is the eastern most line, and also had 6 current injection extensions to the north and south of the line, to facilitate better depth of investigaton at the edge of the lines. The IP model shows the southern anomaly (Anomaly A) again, potentially coming closer to the surface. As was observed in the previous lines, this anomaly is located below a conductive zone in both the DC and MT models. Borehole DDH-10 is proposed to test this moderate priority target.

The Ridge Top anomaly is also represented very well on line 3, as a sub horizontal chargeable feature, approximately 100 m thick and located 100 m below the surface. The northern end of the flat Ridge Top anomaly can be interpreted as a separate feature: Anomaly C. A similar, though smaller, feature was also observed on line 2, and similarly to the Ridge Top, Area 118 and Zone 2 anomalies, this feature is located in a slightly resistive zone. Anomaly C therefore is another high priority target and could be tested by DDH-11. Two similar chargeable features are located slightly to the north of Anomaly C. Both Anomaly D and Anomaly E also are high chargeability targets with a similar resistive signature as observed in previous cases. The location and shape of both anomalies fit very well with a 70 degree dipping fault, as indicated on the section. Anomaly D could potentially be tested by trenching due to its location close to the surface, anomaly E could be tested by DDH-12, the second high priority target on line 3.

The next chargeability anomaly (anomaly I) is located approximately below the minto pit, and also fits the 70 degree dipping nature of the faulting in the area closely, as was the case with anomaly A; this feature also is located below a conductive feature, in a more resistive zone. DDH-13 is proposed to test this anomaly. Anomaly I is the last very high chargeable feature on line 3, also orientated along a 70 degree dip (as is the corresponding narrow resistor in the DC model).

The anomalies in the northern half of the section can be divided into two groups, anomalies J,N and O are large, smooth features located at depth, and anomalies K and L are small scale near surface chargeability highs, potentially related to Minto North. Boreholes DDH-15 and DDH-16 are proposed to test these near surface (approximately 100 m below the surface) targets. DDH-15 can be extended to also test anomaly J at depth. The other two deep anomalies (Anomaly N and O) are lower priority targets due to their depth and in the case of anomaly location, at the edge of the line, DDH-17 and DDH-18 are proposed to test these zones.

The deeper part of the MT model shows a very good correlation with the faults identified in the IP model, where many interpreted faults match contacts between conductive and resistive zones. Also the DC and MT model, confirm most of the resistivity features in the upper 500 m, even though the contrast between resistors and conductors less pronounced in the DC model.

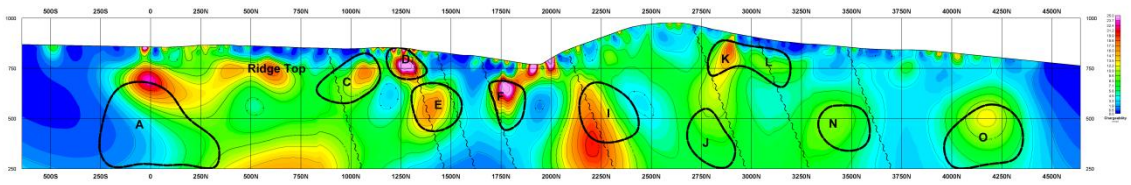

Figure 11: Null conductivity IP model Line L3

The anomalies on the northern half of Line 3 are well represented in the null conductivity model, but the deeper extension of anomaly A seem to be absent. The top of Anomaly A can be identified again, validating that part of Anomaly A as a target, the deeper extend however, could be partially due to inversion artefacts. The very deep chargeable feature just to the north of anomaly A (below Ridge top), however is represented in both models, and could be the feature responsible for the pull up below the top of Anomaly A (the inversion correctly identifies a deep chargeability feature, but by implementing the DC model, it exaggerates the anomaly and misplaces it by joining the deep feature with anomaly A).

3.3 2D INVERSION RESULTS (PLAN MAPS)

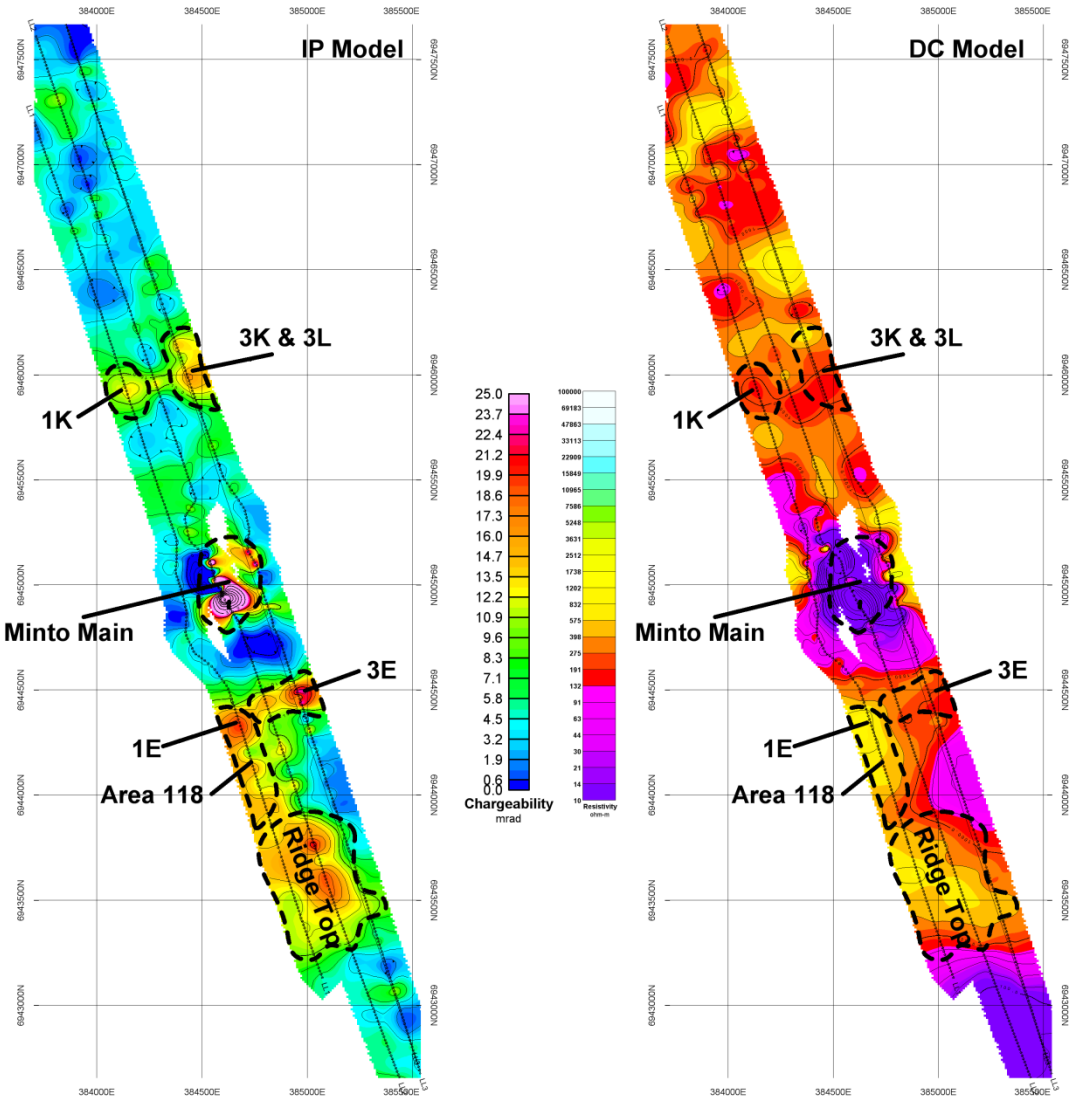

Figure 12: DC and IP model extracted plan maps (elevation level 800 m)

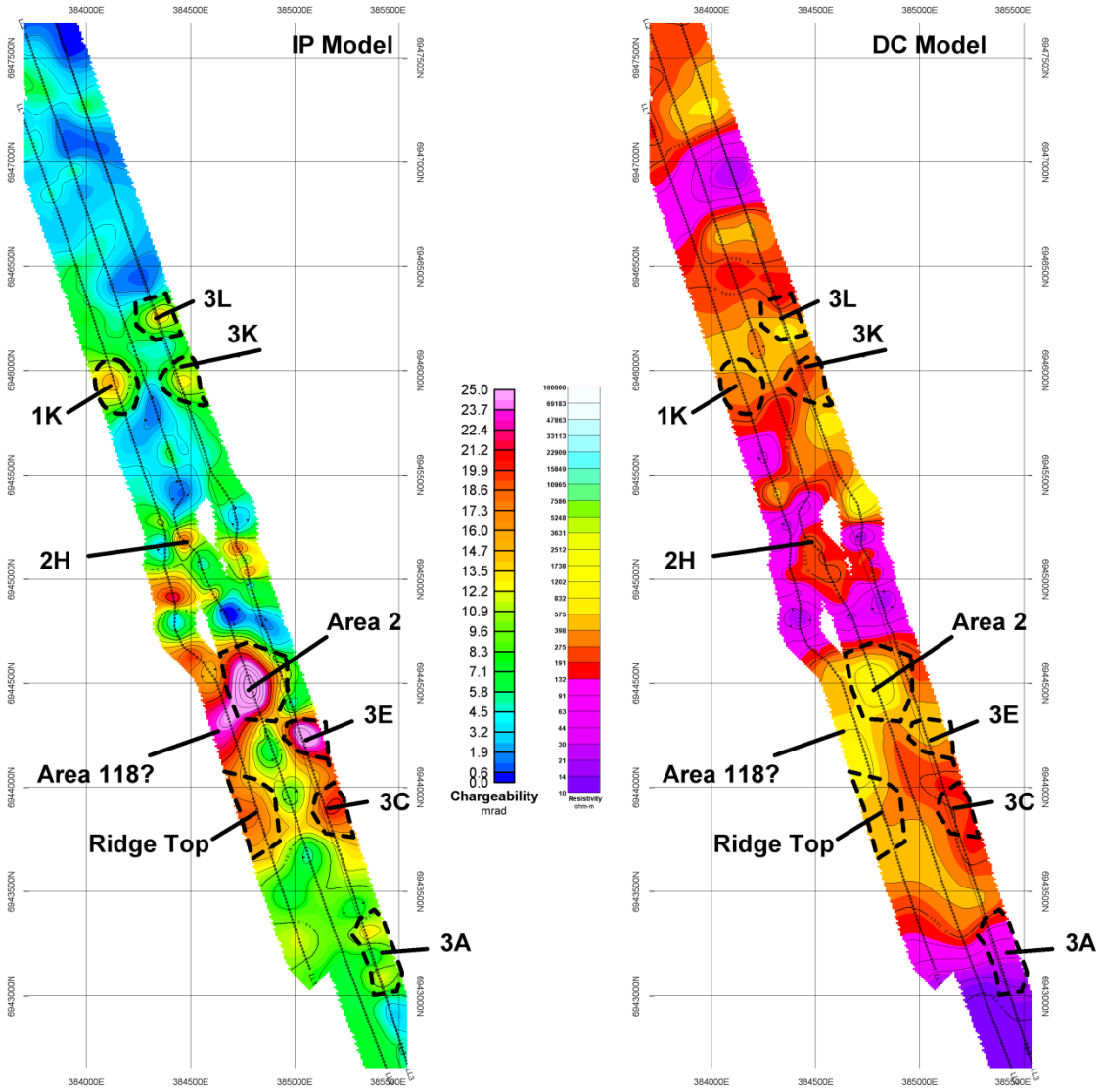

Figure 13: DC and IP model extracted plan maps (elevation level 700 m)

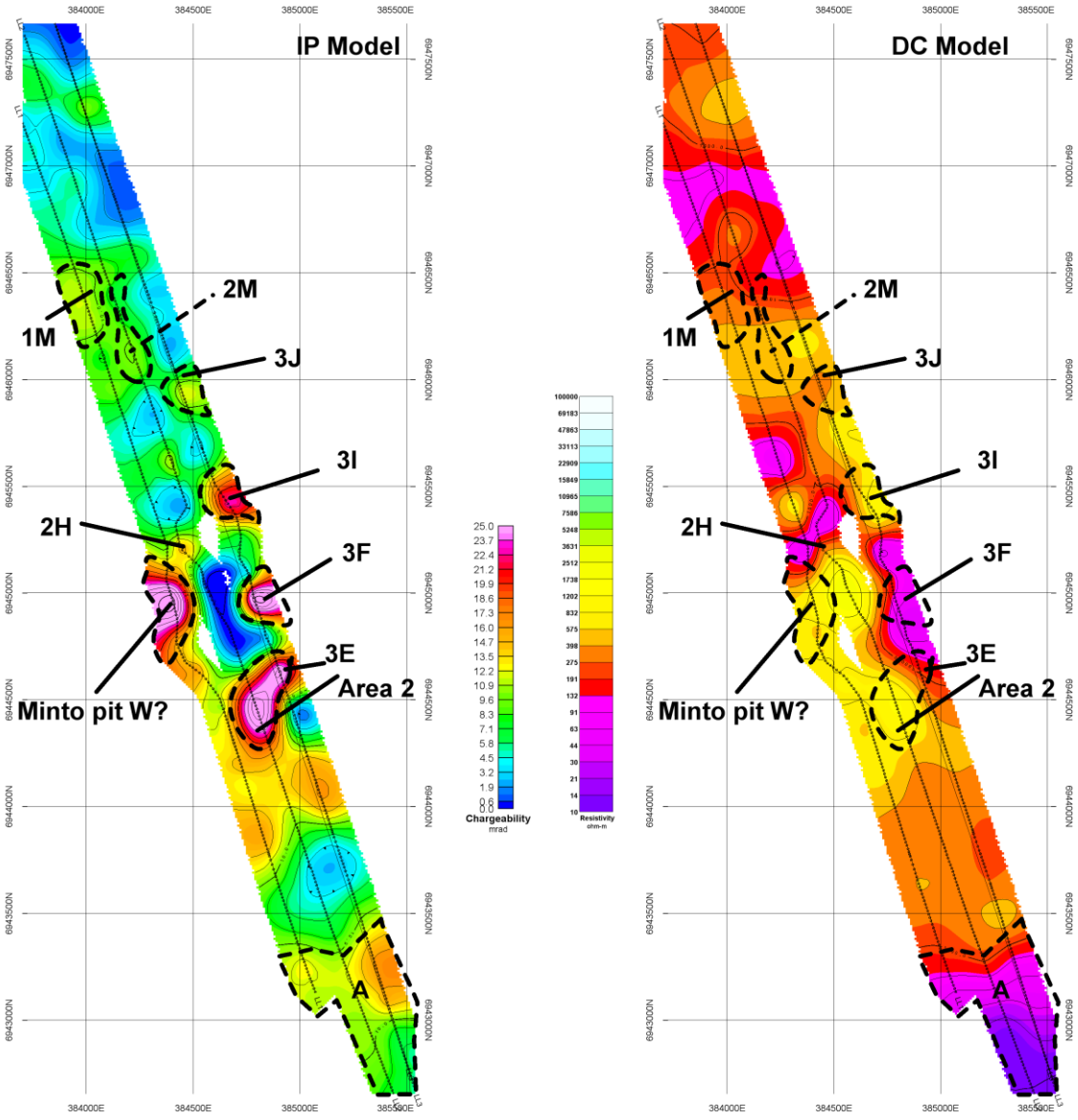

Figure 14: DC and IP models, extracted as plan maps (600 m elevation)

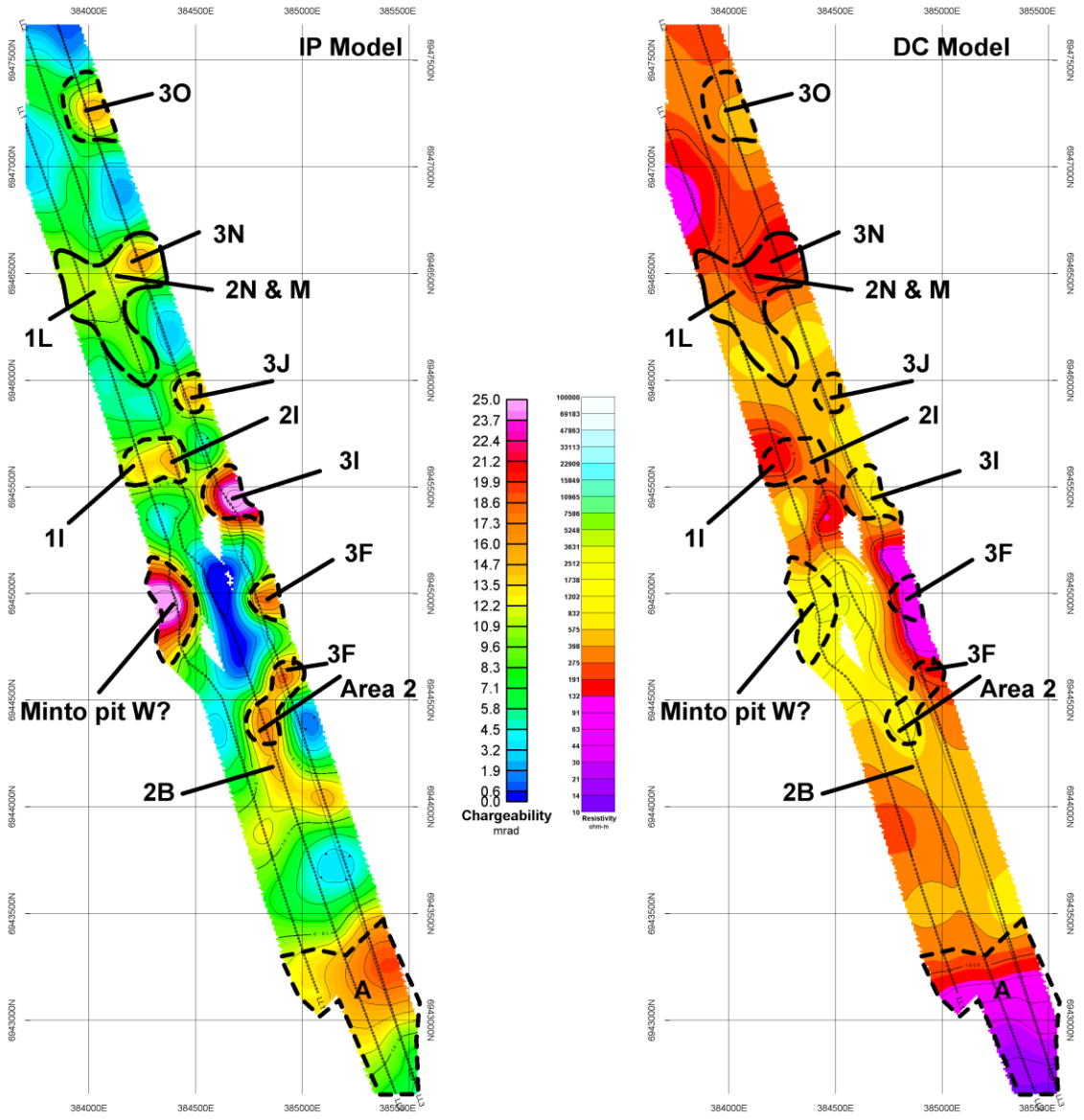

Figure 15: DC and IP models extracted as plan maps (500 m elevation))

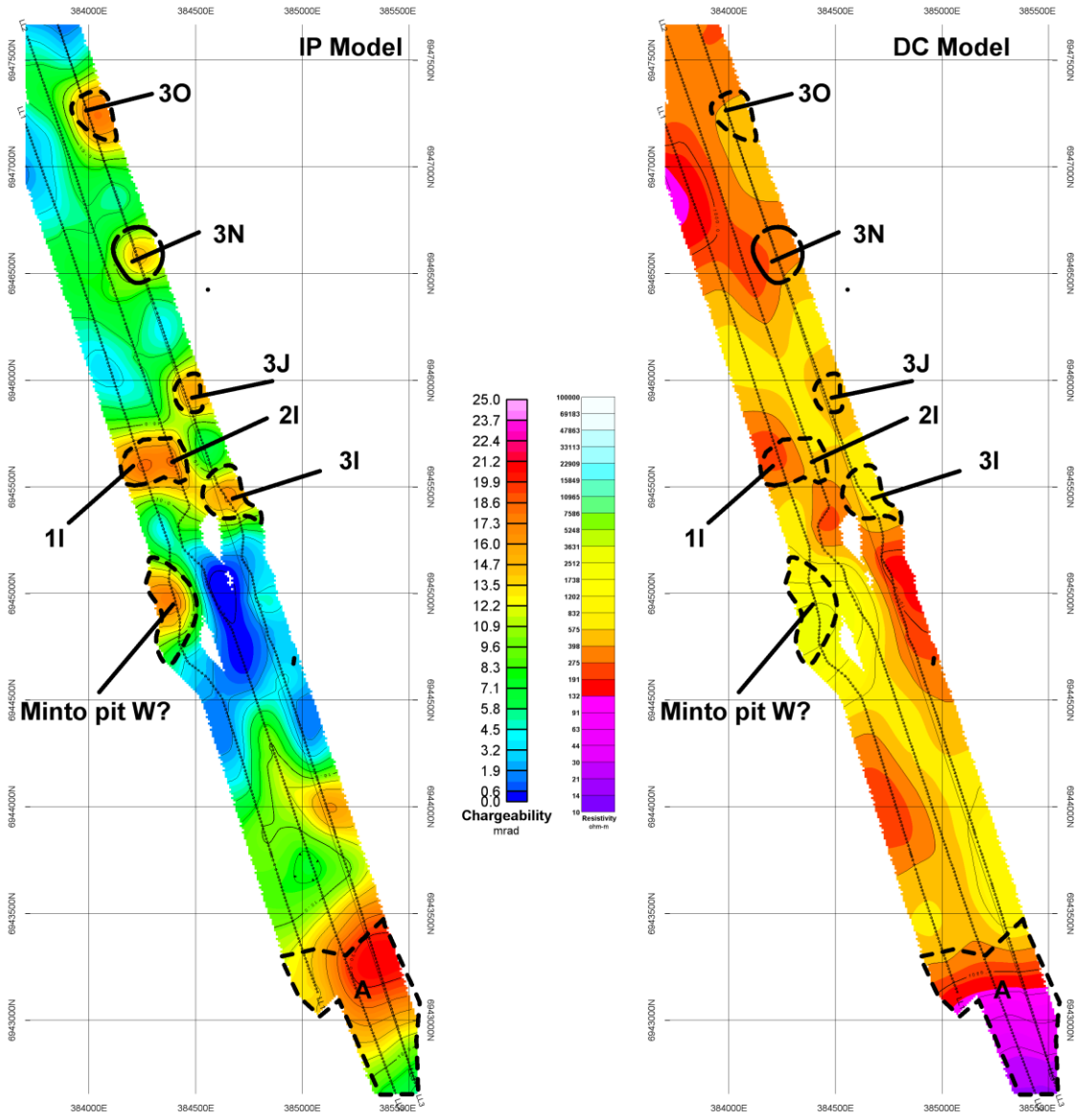

Figure 16: DC and IP model extracted plan maps (400 m elevation)

The different DC and IP plan maps presented in this section (figures 12-16) allow correlation of several anomalies form line to line. Four levels have been plotted at 100 m intervals, starting from 800 m elevation to the 400 m elevation level (approximately 400 m below the minto pit and 600 m below the highest point on the line).

The southern portion of the project area has a very conductive nature, related to an abrupt change in geology, at the edge of the conductor chargeability anomaly A provides a good target, potentially plunging towards the west and extending further east (although its depth extension could be limited).

Near to the surface known deposits of Ridge top, Area 118 and Area 2 are clearly identified. The Ridge Top anomaly is more pronounced on the western side of the project, and Area 2 is a large scale feature, extending to depth, potentially moving towards the east (where it meets up with anomaly 3E).

Below the Minto main deposit only a small near surface chargeability feature is observed, but towards the east and west high chargeability anomalies are observed. Similar features are observed in the DC model where at shallow depth the whole Minto Main is characterized as conductive, and at depth only the edges.

To the north, anomalies 1D, 3H and 3I form a continuous band of chargeability highs at shallow depth (Figure 13). Followed by a more NW-SE striking band on anomalies at greater depth, connecting anomalies M and N and 3G to a single linear feature (Figure 14. A similar striking band of chargeability anomalies can be observed at greater depth (see Figure 15) with anomalies I

The MT model plan maps are plotted at 200 m intervals from 800 m to the -200 m elevation level. For the first two levels (Figure 17) the correlation between the DC and MT maps is very good, the Minto main deposit has a similar signature; a shallow conductive zone, changing into a donut shaped conductor at depth. The conductor located at the north of the main deposit can be followed for a considerable depth, and could be related to the DEF fault bounding the minto main deposit.

The resistive signatures of the Ridge Top, Area 118 and Area 2 anomalies are well represented in the shallow MT plans, and the conductive southern edge of the survey area. At greater depth below the southern conductor a more resistive zone is observed, which makes up one of the three deep resistive zones at depth. The other two resistive zones are located below the Minto main deposit and at the northern edge of the project area. Apart from the conductors correlating with the DEF fault, no other distinct conductors are observed.

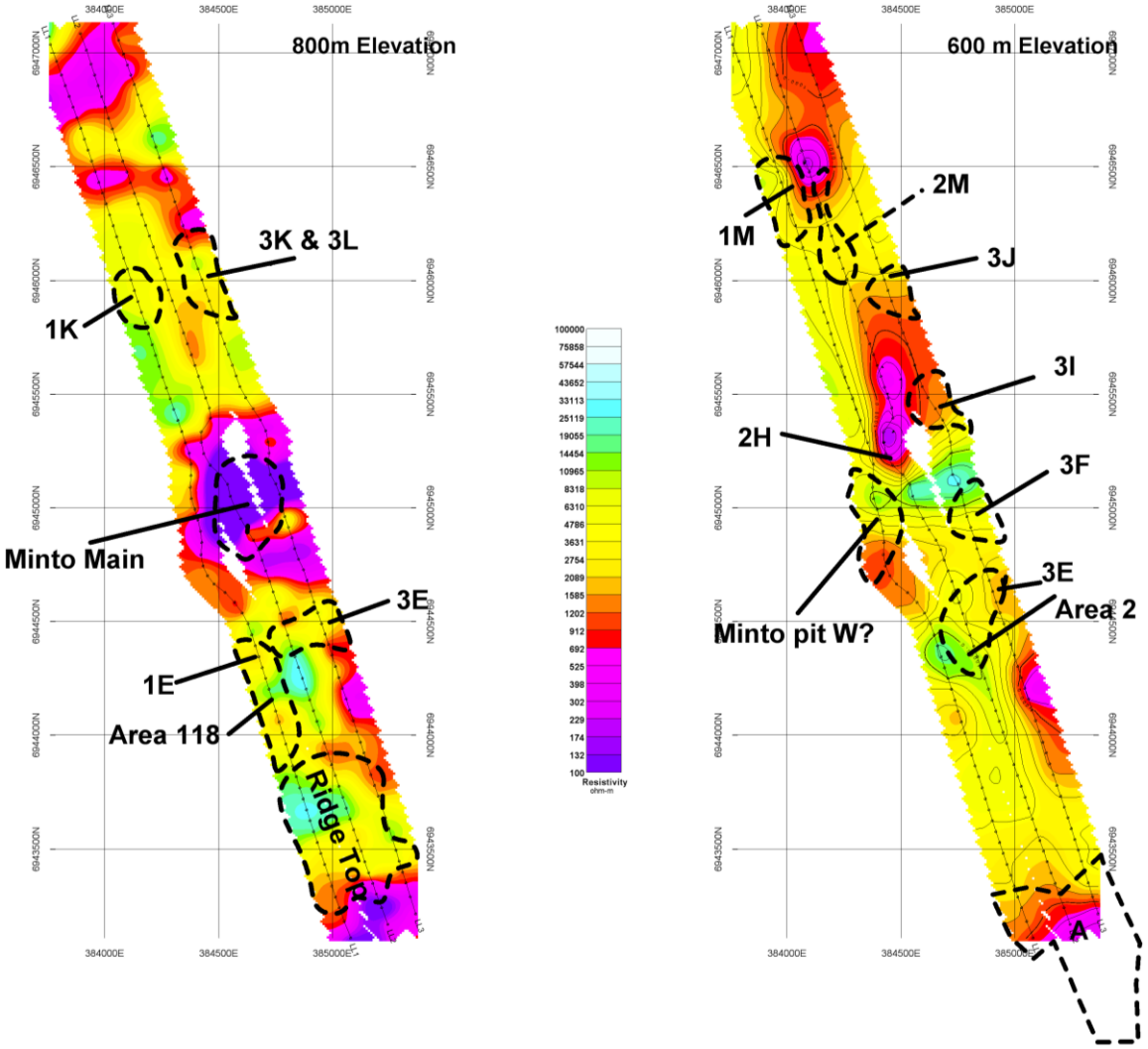

Figure 17: MT model plan maps, 800 m and 600 m elevation

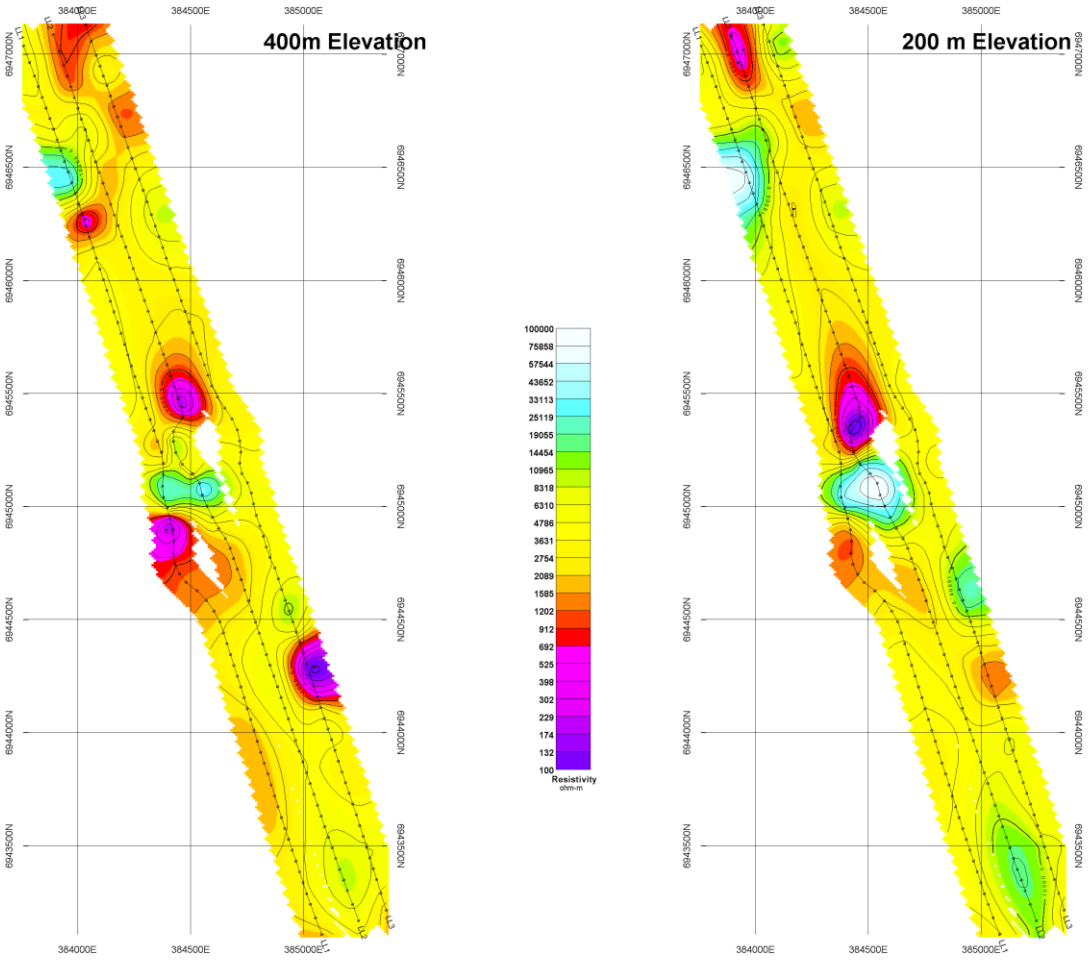

Figure 18: MT model plan maps: 400 m and 200 m elevation

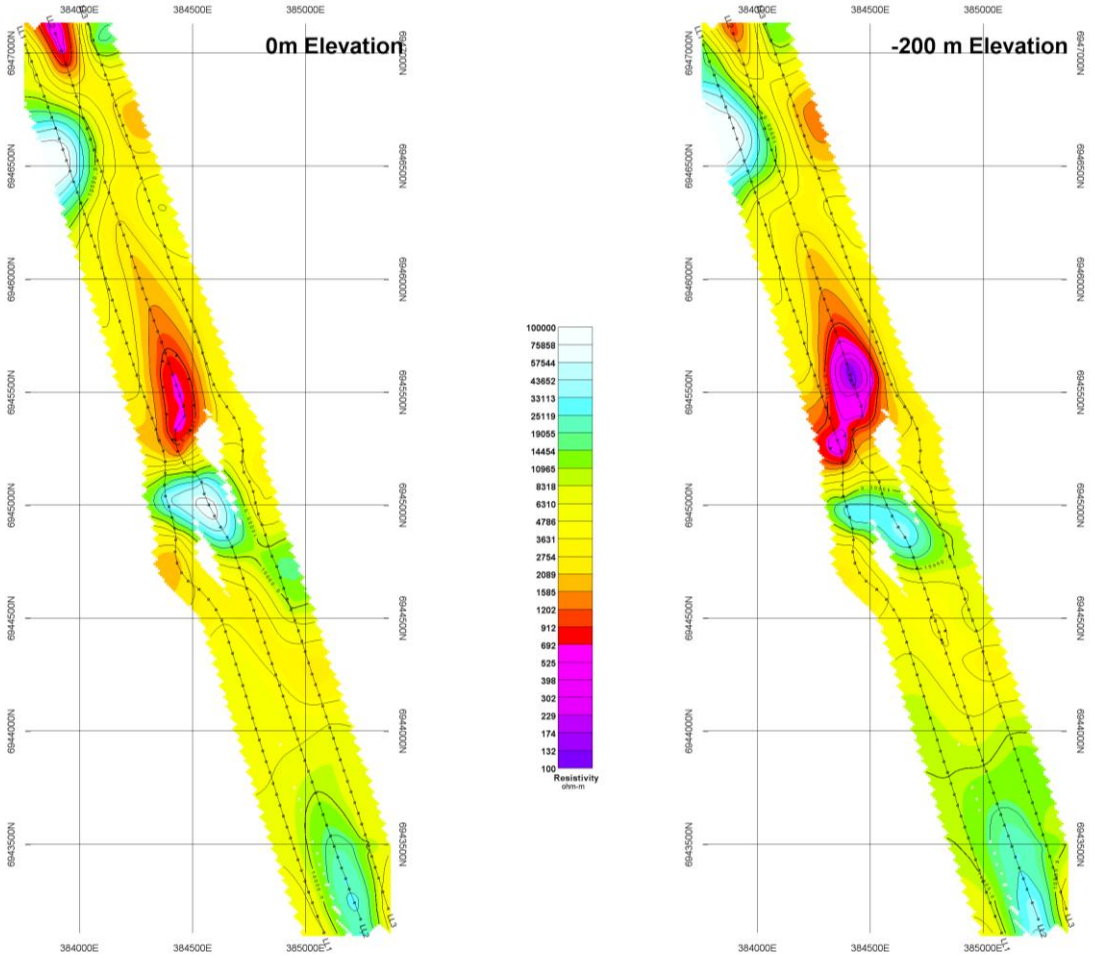

Figure 19: MT model plan maps 0 m and -200 m elevation

3.4 DEPTH OF INVESTIGATION STUDY

A measure of the depth of investigation of any inversion result can be obtained by comparison of two inversions of the same data set, each one calculated with a different reference model[7]. This technique images the difference between the two models, thus indicating zones in the model which are more influenced by the reference model than by the data misfit criteria of the inversion algorithm. By introducing a typical cut-off value, as a measure of how close the comparison between both models is.

For this project Line 2 was chosen as a representative line for the survey and a default DC reference model (average half space resistivity) was compared to a 10 kOhm-m halfspace reference. For the IP models the smooth DC and Null conductivity IP models were used.

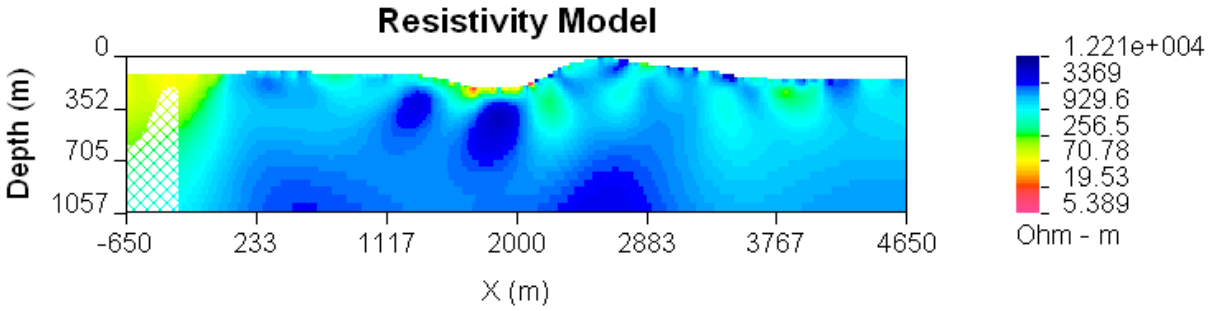

Figure 20: Depth of investigation for DC model Line L2

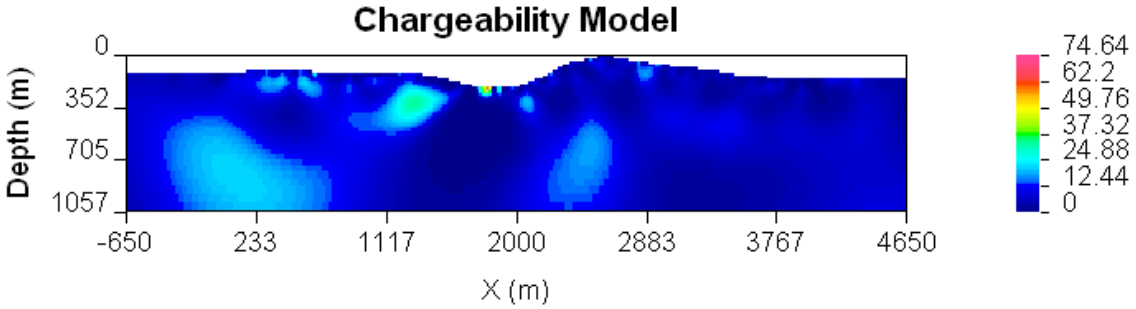

Figure 21: Depth of investigation for DC model line L2E

Both resistivity and chargeability models show a very similar image, the results of the inversion modelling doesn't impose any additional zones of uncertainty (i.e. where the model results are not stable) expect for a zones at the southern edge of the line. The actual depth of penetration still is controlled by the geometry of the survey and will be largest at the centre of the line, where a depth around 750 m below the surface can be assumed

[7] See Oldenburg & Li, "Estimating depth of investigation in DC resistivity and IP surveys" GEOPHYSICS, VOL. 64, NO. 2 (MARCH-APRIL 1999); P. 403–416

4. CONCLUSIONS AND RECOMMENDATIONS

A Titan-24 DC/IP and MT survey was carried out over the Minto Mine property. The survey grid includes three (3) lines consisting of 2 spreads along 4 line-km (two lines had 600 m current extension). Each line was surveyed with a pole-dipole geometry with a dipole spacing of 100 m and 400-500 m receiver overlap.

The data were inverted using the 2D inversion algorithms to produce section maps of resistivity and chargeability distributions of the subsurface. These maps are used to locate potential copper/gold mineralization targets to a depth of 750 m within the survey area. The MT data was inverted separately and provided an image of the resistivity distribution up to 1500 m below the surface.

4.1 CONCLUSIONS

Correlation with the known geology was made available by Capstone Mining Corporation, which supplied georeferenced solids of known reserves of the Ridge Top, Area 118, Area 2, Minto deposit and Minto North. The following conclusions can be drawn from the results of this survey:

- The existing deposits identified as the ridge top, area 118 and Area 2 deposits correlate very well with chargeability and relatively resistive anomalies
- The Minto north deposits appears as a conductive and chargeable feature in the models
- Several deep conductive and chargeable anomalies are observed towards the north and south of the Minto mine pit
- Steeply dipping fault-like structures with an estimated 70 degree dip are observed throughout the sections

4.2 RECOMMENDATIONS

At the time of the writing of this report an additional modelling study is already underway which will include referenced 2D inversions, in an attempt to better place the chargeability anomalies. Also a 3D DC and IP inversion is being calculated including the Ey (cross line) data, collected during the survey, but not included in typical inversion and modelling.

In the interpretation, based on the 2D inversion results, several anomalies have been identified as candidates to be followed up by a drilling campaign. Criteria for the priority of targeting were mainly based on the size and magnitude of the chargeability anomaly, but also the resistivity regime (moderate-high to high, corresponding to the signature of Ridge Top, Area 118 and Area 2) and depth below the surface were taken into account. The boreholes proposed for testing the most prominent anomalies are listed in Table 4, with priorities ranging from: 1 (high) to 3 (low).

Line ID	Anomaly ID	DDH Location	DDH orientation	Est. Depth of intercept	End of Hole	DC signature	IP signature	MT signature	Priority	DDH ID
L1E	A	250N	-80S	410 m	550 m	moderate	moderate	moderate	3	DDH-01
L1E	E	1610N	-70S	100 m	330 m	Moderate-high	high	Moderate-high	1	DDH-02
L1E	K & I	2940N	-70S	130 m & 580 m	700 m	Moderate & moderate	High & high	Moderate-high & Moderate-high	1	DDH-03
L1E	M	3500N	-70S	250	450 m	moderate	Moderate	Moderate-high	2	DDH-04
L2E	A	100N	-70S	375	650 m	Moderate-high	High	Moderate-High	1	DDH-05
L2E	B	870N	-90	50 m	420 m	Moderate-high	high	Moderate-high	1	DDH-06
L2E	H	2140N	-70S	90 m	350 m	Moderate-low	high	Moderate-low	1	DDH-07
L2E	I	2650N	-80S	420 m	700 m	moderate	high	Moderate-low	1	DDH-08
L2E	M	3180N	-70S	280 m	430 m	moderate	Moderate-low	moderate	3	DDH-09
L2E	N	3540N	-70S	270 m	450 m	moderate	moderate	Moderate-low	2	DDH-10

Line ID	Anomaly ID	DDH Location	DDH orientation	Est. Depth of intercept	End of Hole	DC signature	IP signature	MT signature	Priority	DDH ID
L3E	A	110N	-80 S	200 m	550 m	Moderate-low	high	Moderate-low	1	DDH-11
L3E	C	1050N	-80S	80 m	280 m	moderate	hugh	low	1	DDH-12
L3E	E	1490N	-80S	160 m	360 m	moderate	high	moderate	1	DDH-13
L3E	F	1840N	-80S	120 m	340 m	low	high	moderate	1	DDH-14
L3E	I	2250N	90S	230 m	520 m	Moderate-high	high	Moderate-high	1	DDH-15
L3E	K & J	2840N	90S	60 m & 460 m	630	Moderate-low & moderate	High & high	Moderate-low & moderate-high	1	DDH-16
L3E	L	3180	-70S	90 m	240 m	low	high	low	1	DDH-17
L3E	N	3440N	90S	290 m	510 m	Moderate-low	high	moderate	2	DDH-18
L3E	O	4180N	90S	260 m	530 m	moderate	high	-	3	DDH-19

Table 4: Geophysical target Minto Mine project

It is highly recommended to expand the existing dataset with additional lines to the east and west of the current group of three (3) lines. Orientation of these lines and line spacing should be kept equal to the current data set. Also the line length of 4 km, with 100 m station spacing and 4 to 5 receiver station overlap should be used for the follow-up survey.

As part of the follow-up survey, if existing drill holes remain open, a borehole EM survey would provide valuable insight on potential off-hole anomalies. Also a combination of a borehole and surface DC/IP survey could bring additional information, similar to a mise-a-la-masse type survey where current is injected down hole directly into the mineralized zones and receivers are positioned on the surface.

Combined inversion of borehole and surface DC/IP data and incorporation of other geophysical methods would be a second step in further understanding and validation of the models.

Respectfully Submitted

QUANTEC GEOSCIENCE LTD.

Arre Verweerd, Dr. Rer. Nat

Titan-24 Interpretation

.

Kevin Killin

Senior Manager, Titan Interpretation Group

APPENDIX A: STATEMENT OF QUALIFICATIONS

I, Arre Verweerd, declare that

- I am a consultant with residence in Toronto, Ontario and am presently employed in this capacity with Quantec Geoscience Ltd., Toronto, Ontario;
- I obtained a Doctorandus Degree (MSc. equivalent) in Geophysics, from the Universiteit Utrecht, Utrecht, the Netherlands in 2001. I also obtained a Doctorate Degree in the Natural Sciences (Dr. Rer. Nat.), subject Applied Geophysics from the Rheinische-Friedrich-Wilhelms-Universität-zu-Bonn, Bonn, Germany in 2007;
- I have practiced my profession continuously since January 2002, in Europe, North and South America and Africa.
- I am a member of the European Association of Geoscientists and Engineers (EAGE), the European Geosciences Union (EGU), the Environmental and Engineering Geophysical Society (EEGS), the society of Exploration Geophysicists (SEG) and the Canadian Exploration Geophyical Society (KEGS).
- I have no interest, nor do I expect to receive any interest in the properties or securities of Capstone Mining Corporation, its subsidiaries or its joint-venture partners.
- I am the project supervisor, in charge of data acquisition quality control for this project. I have written the interpretation report and survey results and calculated all geophysical model results described in it. I can attest that these accurately and faithfully reflect the data acquired on site. The statements made in this report represent my professional opinion based on my consideration of the information available to me at the time of writing this report.

Toronto, Ontario

September, 2009

Arre Job Verweerd, Dr. Rer. Nat.

Titan-24 Interpretation Group

Quantec Geoscience Ltd.

I, Kevin J. Killin, declare that:

- I am a consultant with residence in Whitby, Ontario and am presently employed in this capacity with Quantec Geoscience Ltd., Toronto, Ontario.
- I obtained an Honours Bachelor of Science Degree (HBSc), in Geological Geophysics from the University of Western Ontario in London Ontario, in 1986, including a Geology degree and Geophysics degree.
- I have worked continuously since December, 1986, in North-America, Europe, South-America, The Middle East and Asia in the exploration industry.
- I am a member of the Prospectors and Developers Association of Canada (PDAC), and the Canadian Exploration Geophysics Society (KEGS).
- I have no interest, nor do I expect to receive any interest in the properties or securities of Capstone Mining Corporation, its subsidiaries or its joint-venture partners.
- I have reviewed the survey results, oversaw the preparation and reviewed this interpretation report. I can attest that these accurately and faithfully reflect the data acquired on site.
- The statements made in this report represent my opinion in consideration of the information available to me at the time of writing this report.

Toronto, Ontario
September, 2009

Kevin Killin, HBSc
Senior Manager Titan-24 Interpretation Group
Quantec Geoscience Ltd.

DATE	FIELD ACTIVITIES AND OBSERVATIONS	PROCESSOR COMMENTS AND OBSERVATIONS	LINE	SPREAD	IP OVERLAP (km)	MT OVERLAP (km)	LINE START	LINE END	TX START	TX END	READ (km)		
											MT	IP	IP CURRENT EXTENSIONS
CA00656T- MINTO MINE PROJECT APPENDIX B-PRODUCTION SUMMARY Capstone Mining Corporation													
29-Jul-09	Mob to Minto Mine from Casion Camp, Orientation	Mob from Casino Camp to Minto Mine & do mine orientation											
30-Jul-09	Set Up 1.5km on the first line, and Put out infinite. Could not access pit area until all mine supervisor's are informed. PST, start looking for remote site	Remote search, layout infinite and setup line	**L1E**	**S1**									
31-Jul-09	Had a meeting with the mine supervisors and went through what we will be doing and where in the open pit we will be. Set up the rest of the line for MT, located remote site in the morning in time for MT in the evening	PST, finish line setup & Survey MT	**L1E**	**S1**			**0N**	**2500N**			**2.5**		
1-Aug-09	results to change lines. Had to drive to Pelly Crossing in the afternoon to pick up remote data, could not upload onto FTP site for	Survey IP (difficulty getting remote data, so MT processing finsihed late to move the line)	**L1E**	**S1**			**0N**	**2500N**	**50S**	**3150N**	**0**	**2.5**	**0.7**
2-Aug-09	Change lines in the morniing and read IP, Read MT in the evening	Survey IP Survey MT	**L1E**	**S2**	**0.9**	**0.9**	**1600N**	**4000N**	**1150N**	**4250N**	**1.5**	**1.5**	**0.7**
3-Aug-09	Change lines in the morning, moved into middle of open pit. A lot of delays due to machinery, and blasting schedules. Set up for MT readMT	Move line & setup for MT Survey MT	**L2E**	**S2**			**1600N**	**4000N**			**2.4**		
4-Aug-09	Read IP in the morning on Norther part of line, Changed lines to southern portion of line, Read MT	Survey IP Survey MT	**L2E** **L2E**	**S2** **S1**		**0.9**	**1600N** **0N**	**4000N** **2500N**	**1150N**	**4650N**	**1.6**	**2.4**	**1.1**
5-Aug-09	Read IP on Southern spread , change lines to Southern spread of line 300E read MT	Survey IP Survey MT	**L2E** **L3E**	**S1** **S1**	**0.9**		**0N** **0N**	**2500N** **2500N**	**650S**	**3250N**	**2.5**	**1.6**	**1.4**
6-Aug-09	Read IP on Southern spread , change lines to Northern spread read MT	Survey IP Survey MT	**L3E** **L3E**	**S1** **S2**		**0.9**	**0N** **1600N**	**2500N** **4000N**	**650S**	**3250N**	**1.5**	**2.5**	**1.4**
7-Aug-09	Read IP on Northern spread, pack u p gear and roll up Infinite. Pick up remote site	Survey IP Started packing gear	**L3E**	**S2**	**0.9**		**1600N**	**4000N**	**1150N**	**4650N**		**1.5**	**1.1**
8-Aug-09	Demob to Whithorse	Finish packing gear & demob to Whitehorse											
	TOTAL SURVEY COVERAGE (KM) AND				**2.7**	**2.7**					**12**	**12**	**6.4**

APPENDIX C – 2D GEOSOFT SECTION MAPS

List of Figures

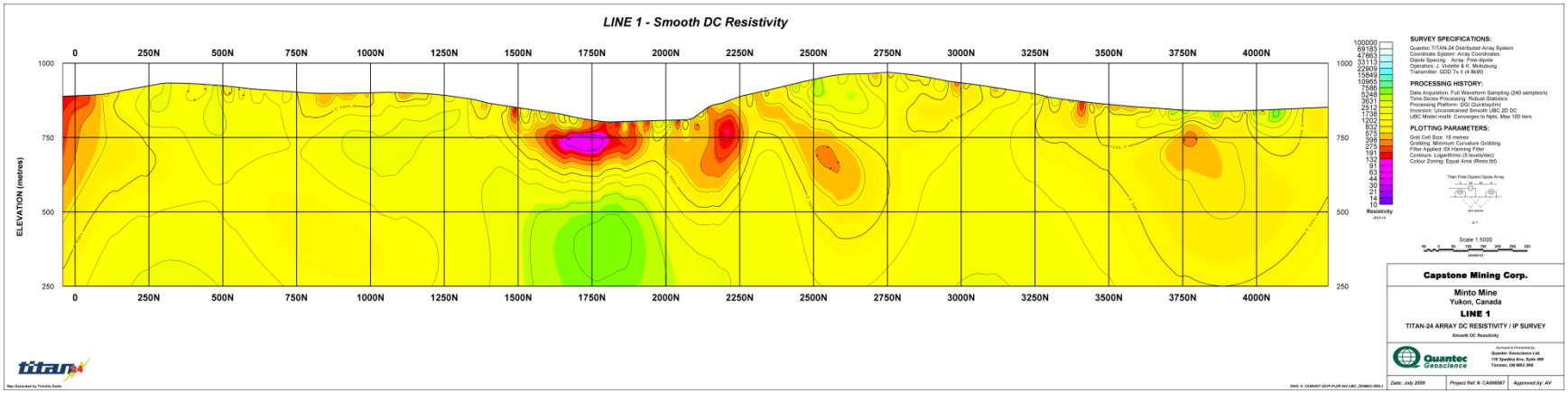

Figure 1: Line 1 Smooth DC Resistivity Model

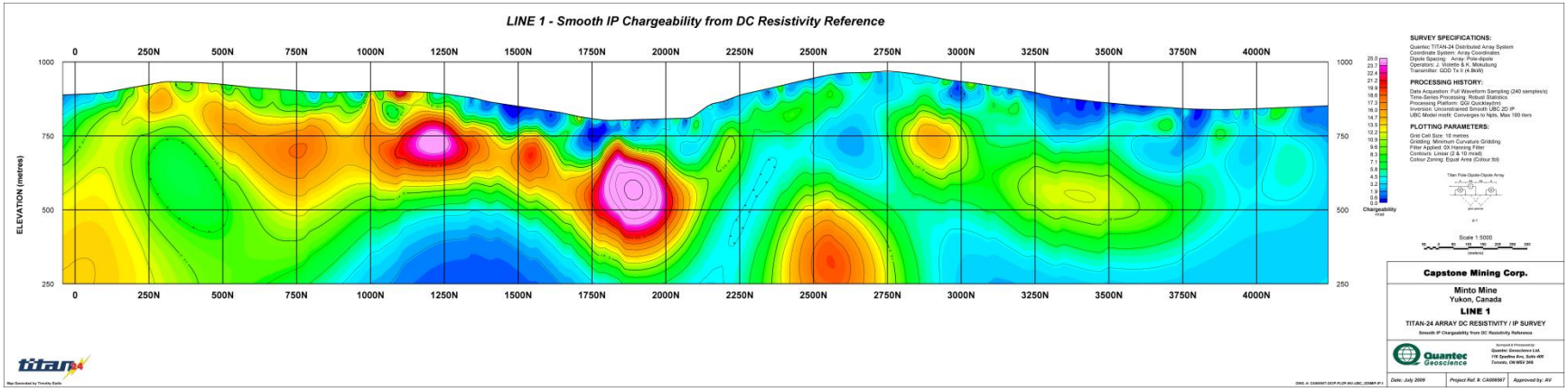

Figure 2: Line 1 Smooth IP Chargeability Model

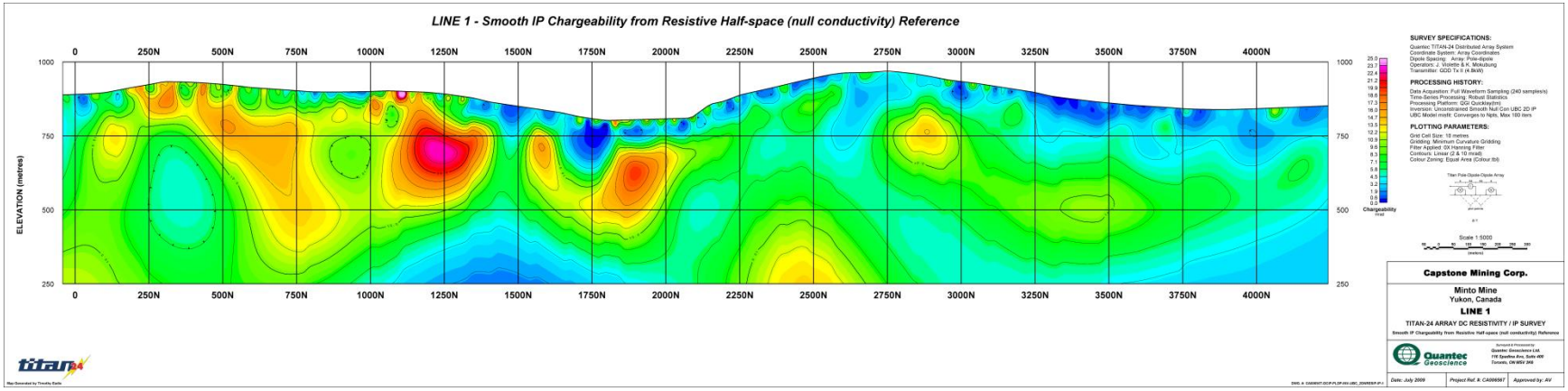

Figure 3: Line 1 Smooth IP (Null Conductivity) Model

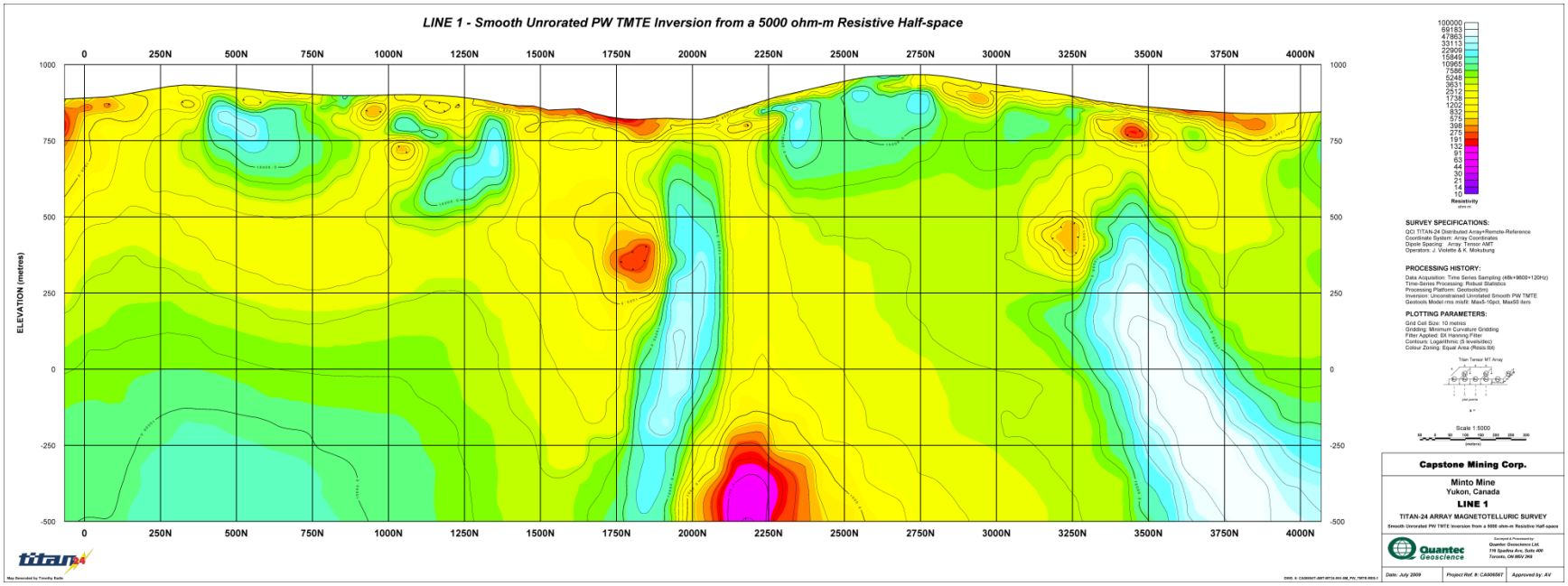

Figure 4: Line 1 Smooth Unrotated PW MT Model

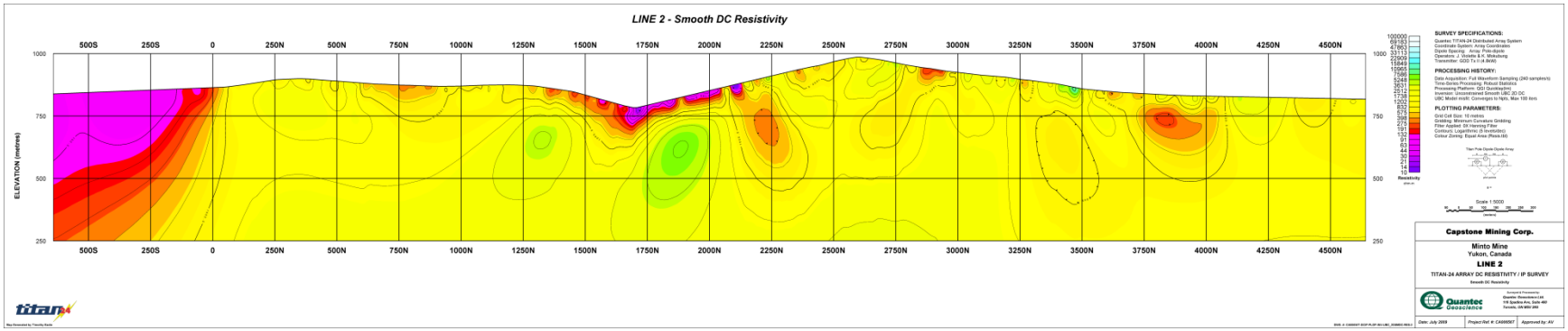

Figure 5: Line 2 Smooth DC Resistivity Model

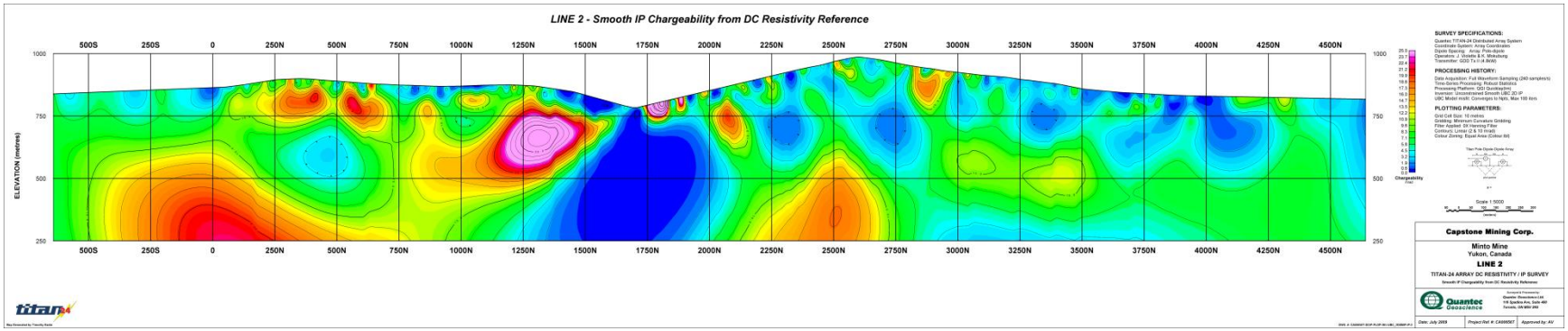

Figure 6: Line 2 Smooth IP Chargeability Model

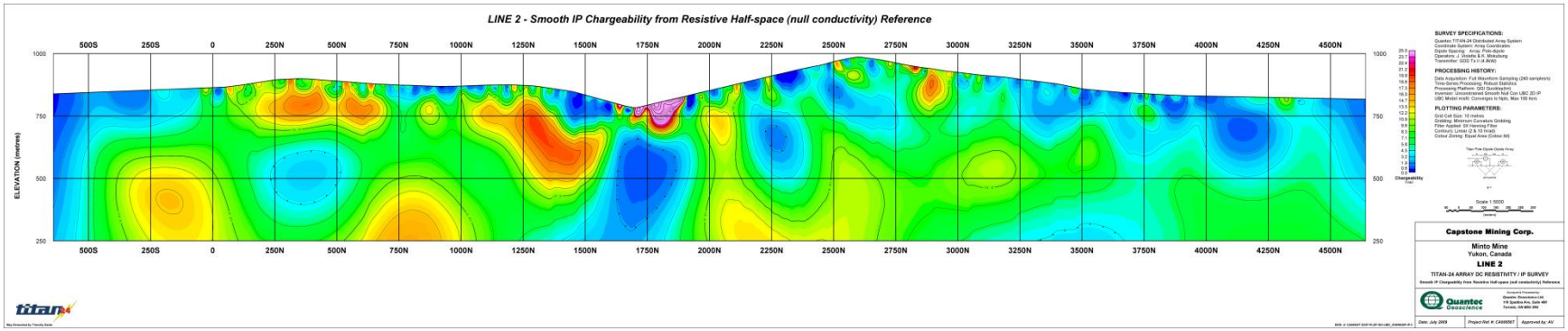

Figure 7: Line 2 Smooth IP (Null Conductivity) Model

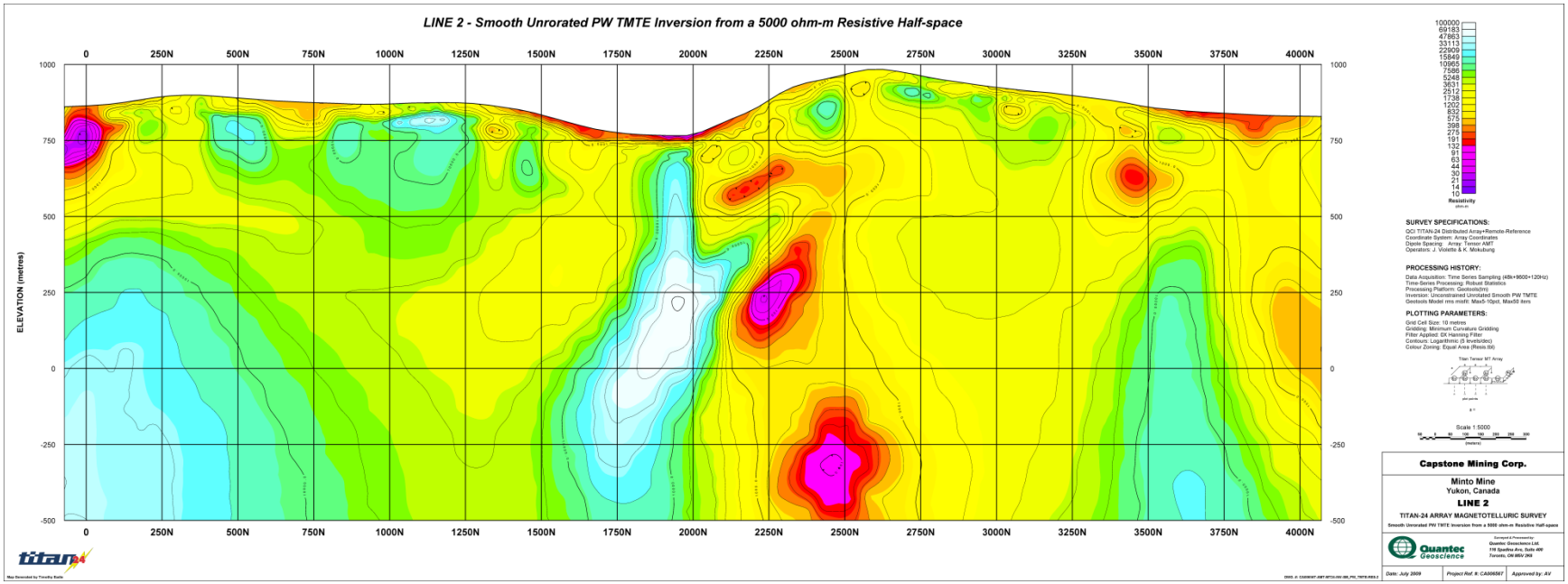

Figure 8: Line 2 Smooth Unrotated PW MT Model

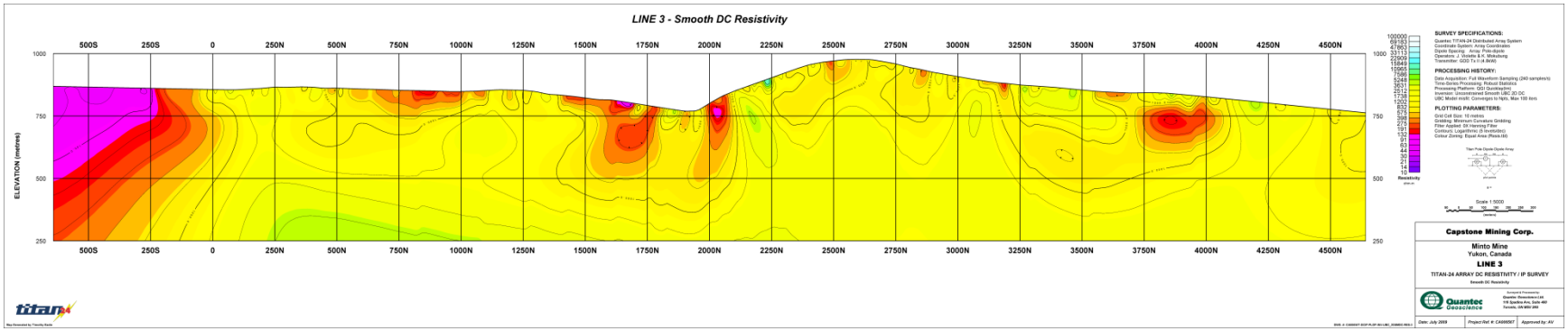

Figure 9: Line 3 Smooth DC Resistivity Model

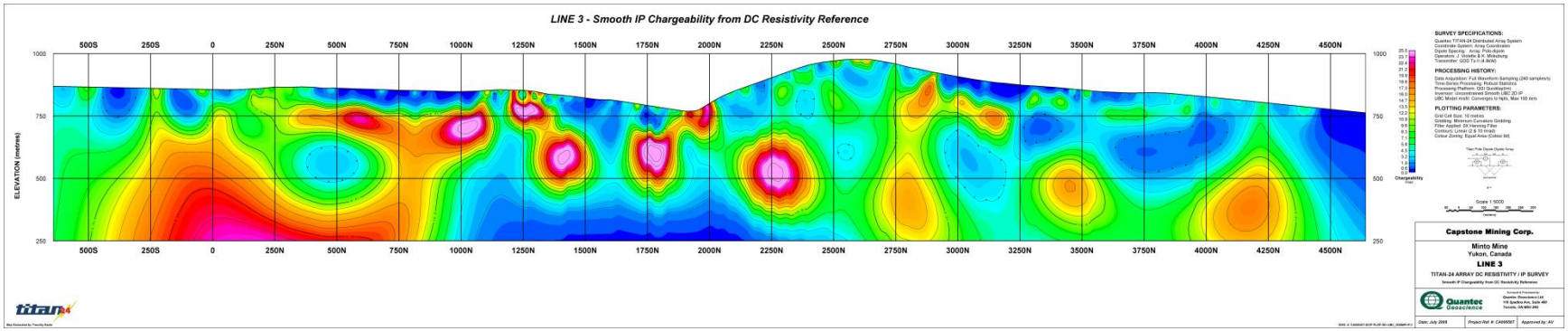

Figure 10: Line 3 Smooth IP Chargeability Model

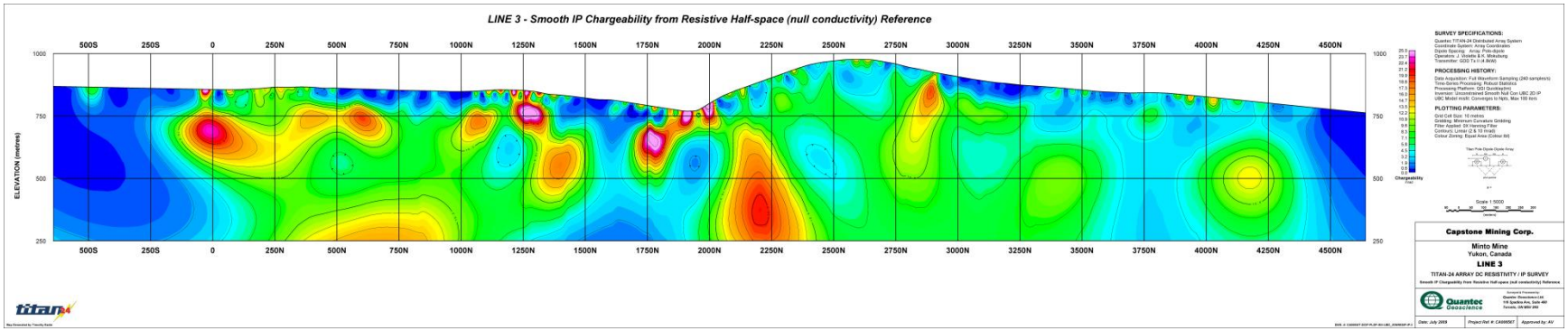

Figure 11: Line 3 Smooth IP (Null Conductivity) Model

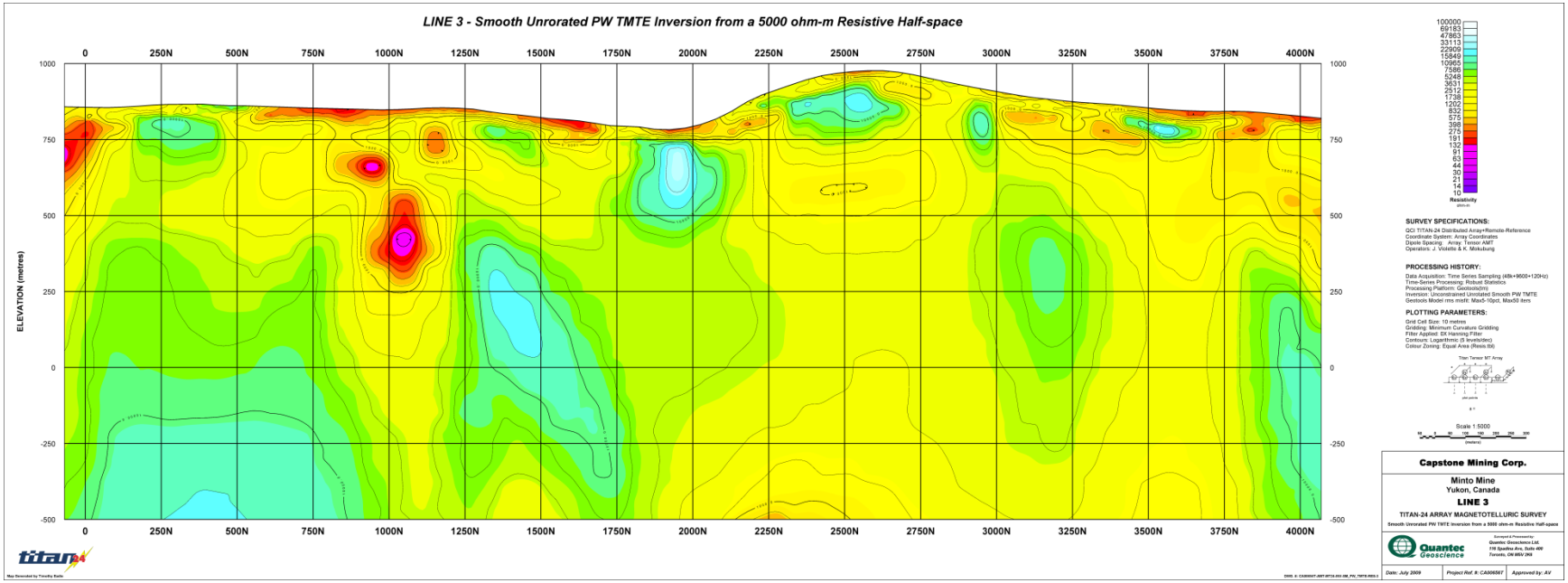

Figure 12: Line 3 Smooth Unrotated PW MT Model

APPENDIX D – 2D GEOSOFT PLAN MAPS

List of Figures

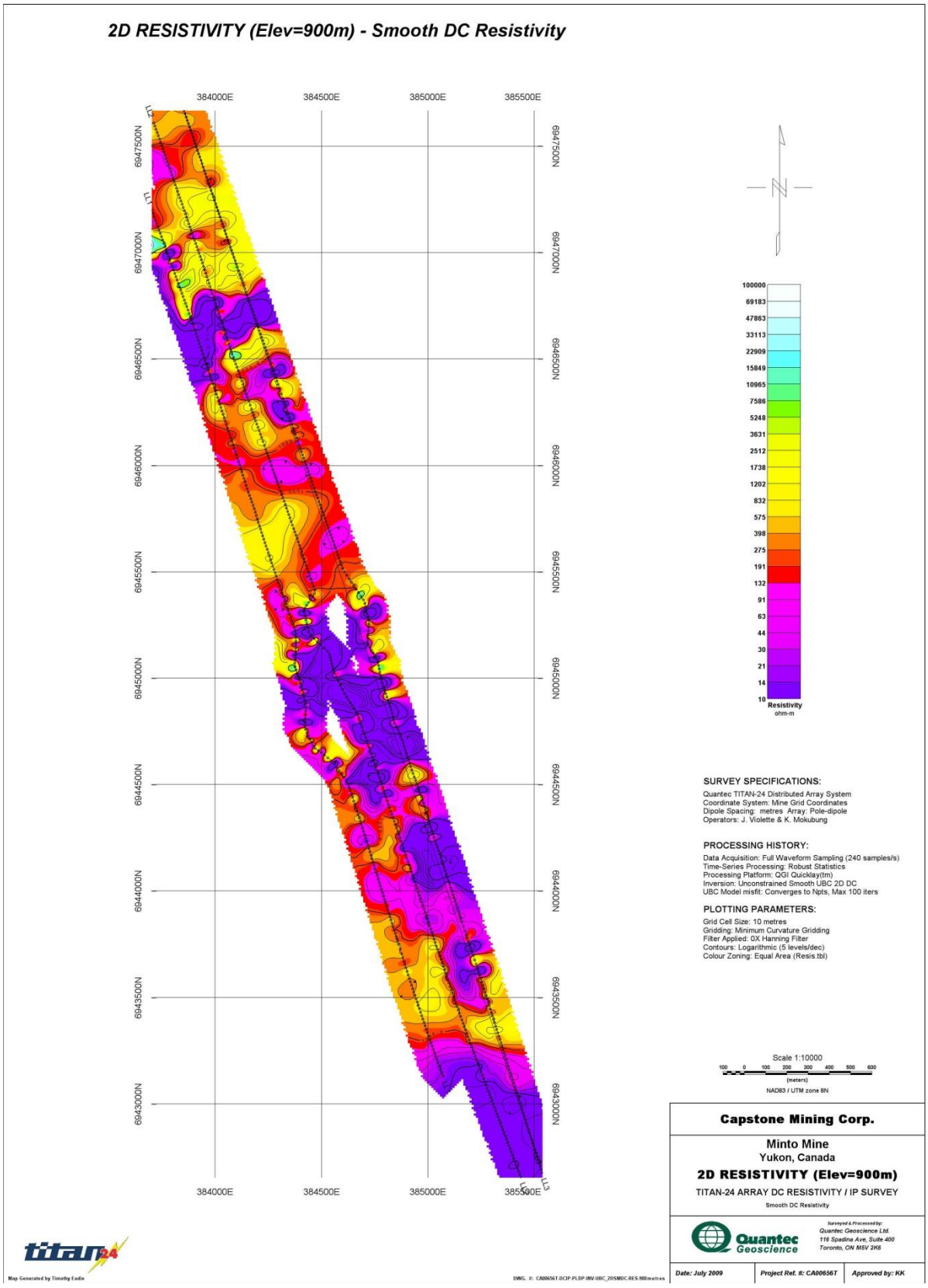

Figure 1: Smooth DC Resistivity Plan Map at 900m Elevation

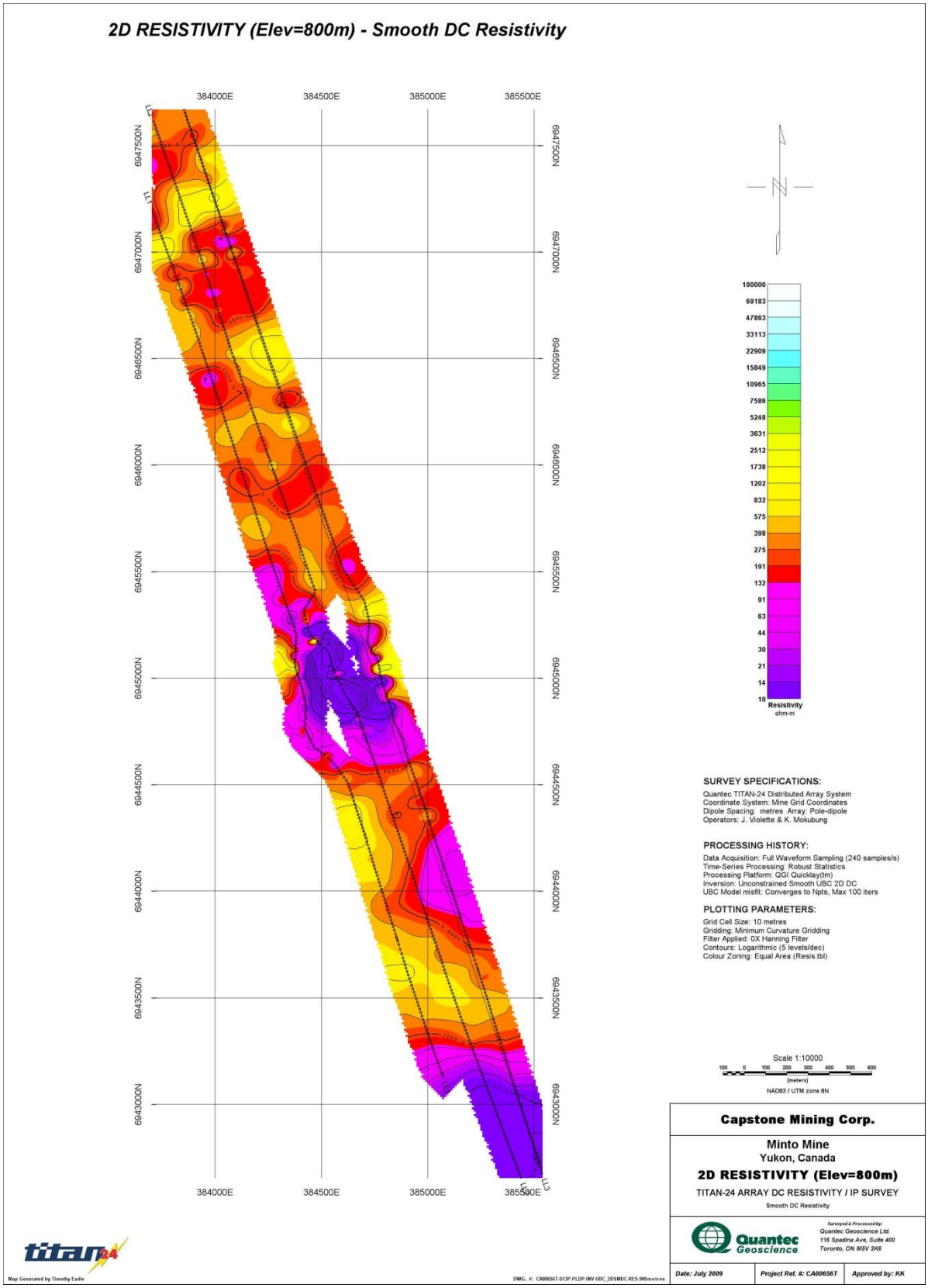

Figure 2: Smooth DC Resistivity Plan Map at 800m Elevation

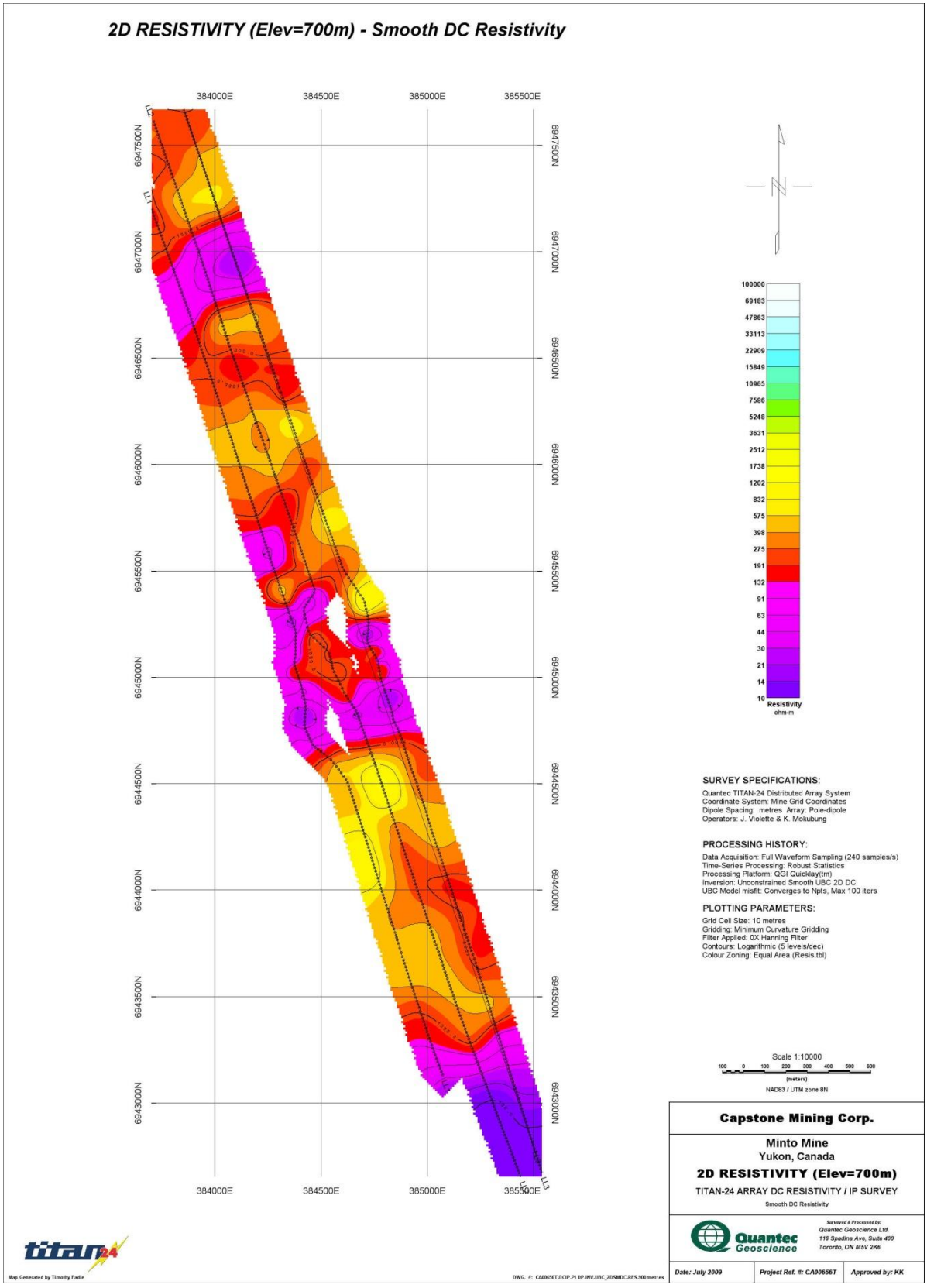

Figure 3: Smooth DC Resistivity Plan Map at 700m Elevation

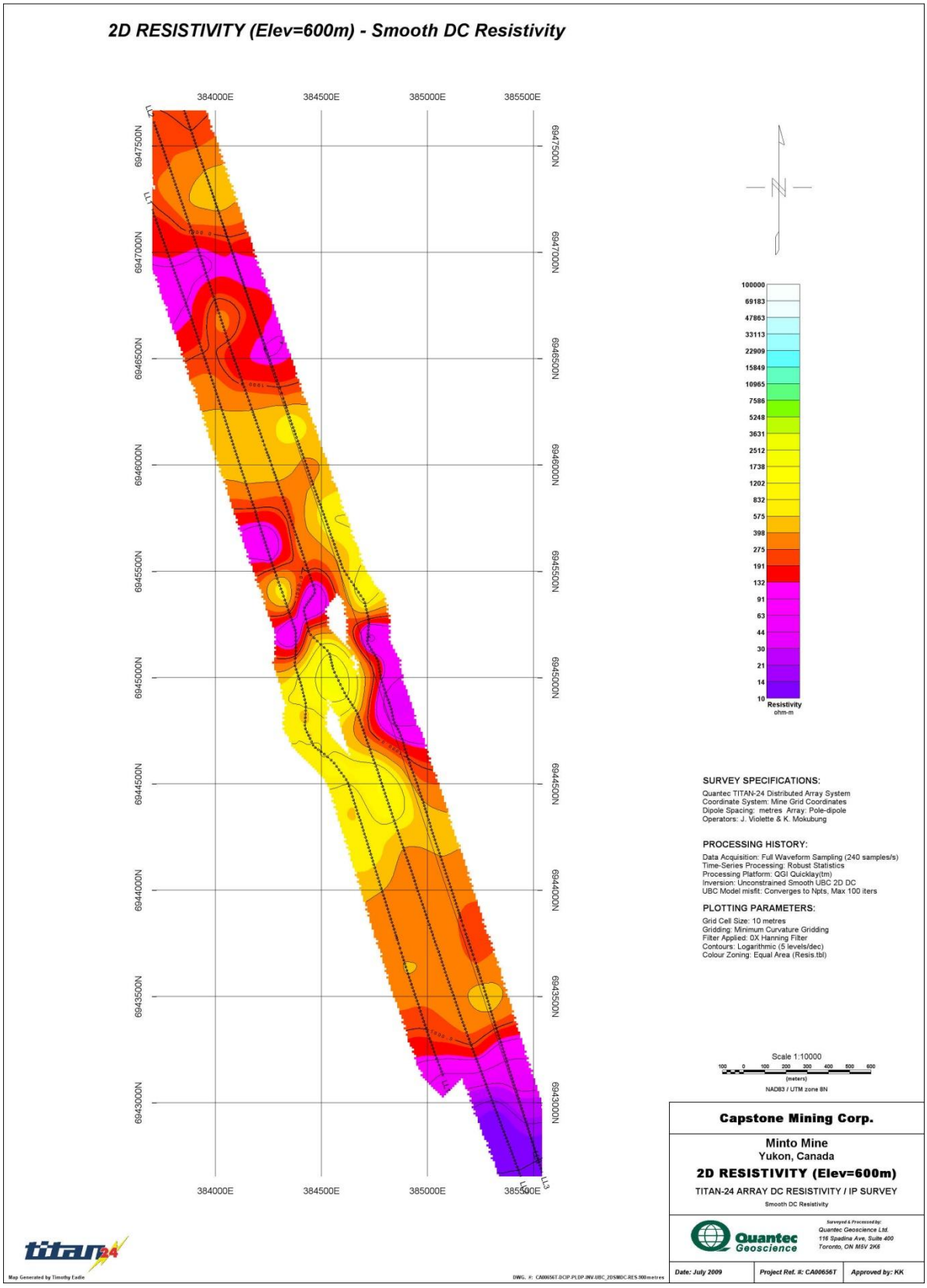

Figure 4: Smooth DC Resistivity Plan Map at 600m Elevation

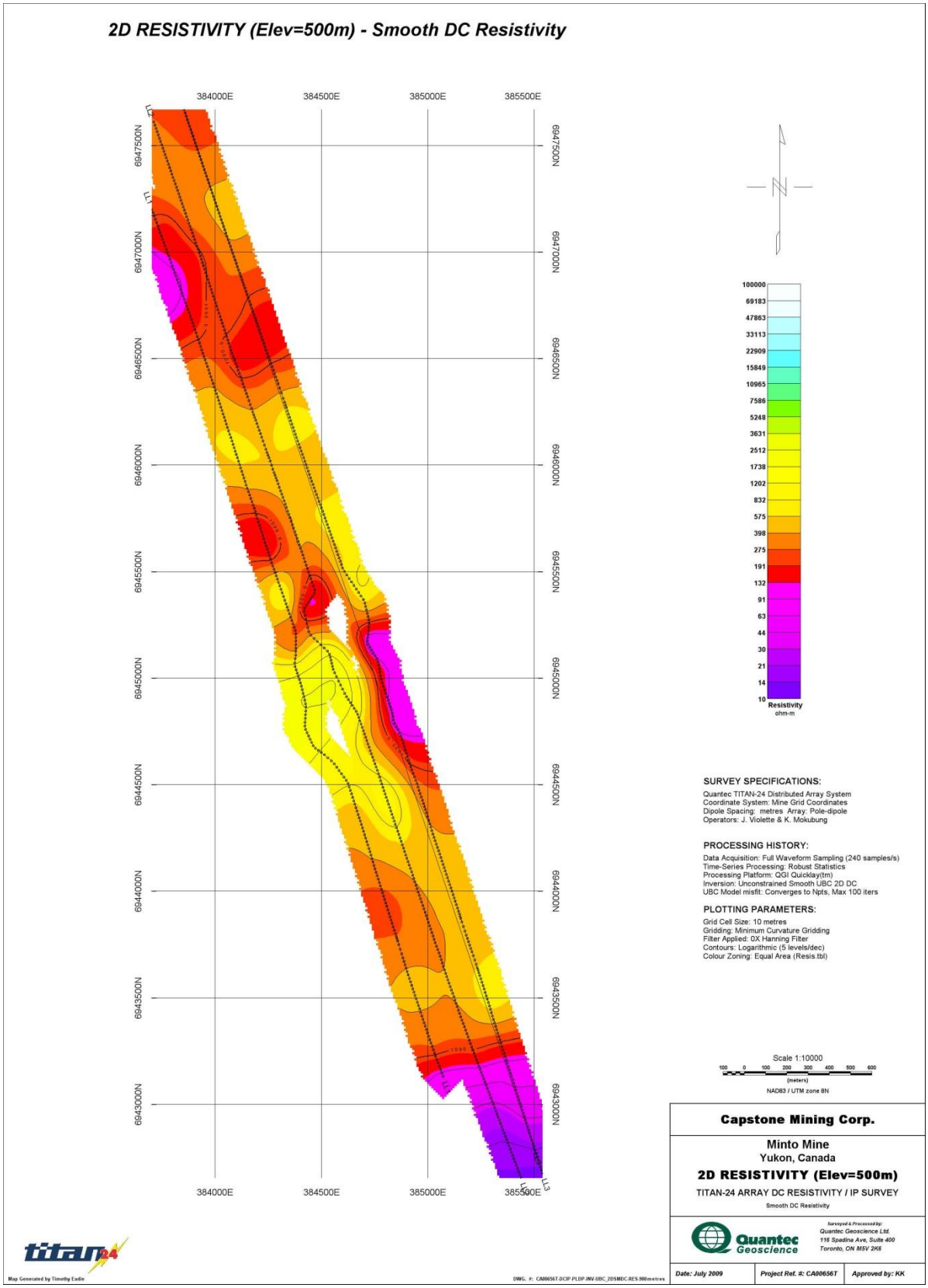

Figure 5: Smooth DC Resistivity Plan Map at 500m Elevation

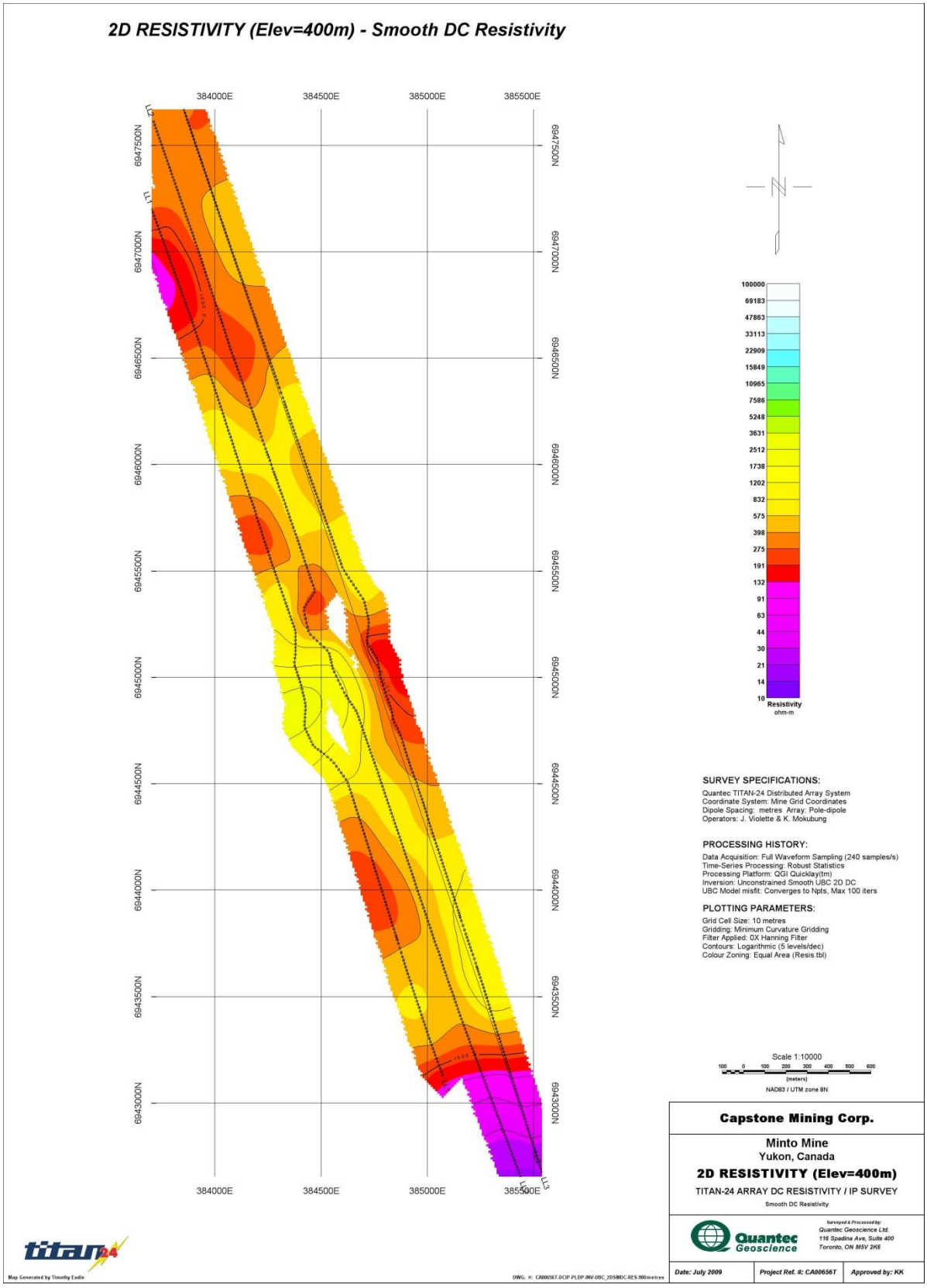

Figure 6: Smooth DC Resistivity Plan Map at 400m Elevation

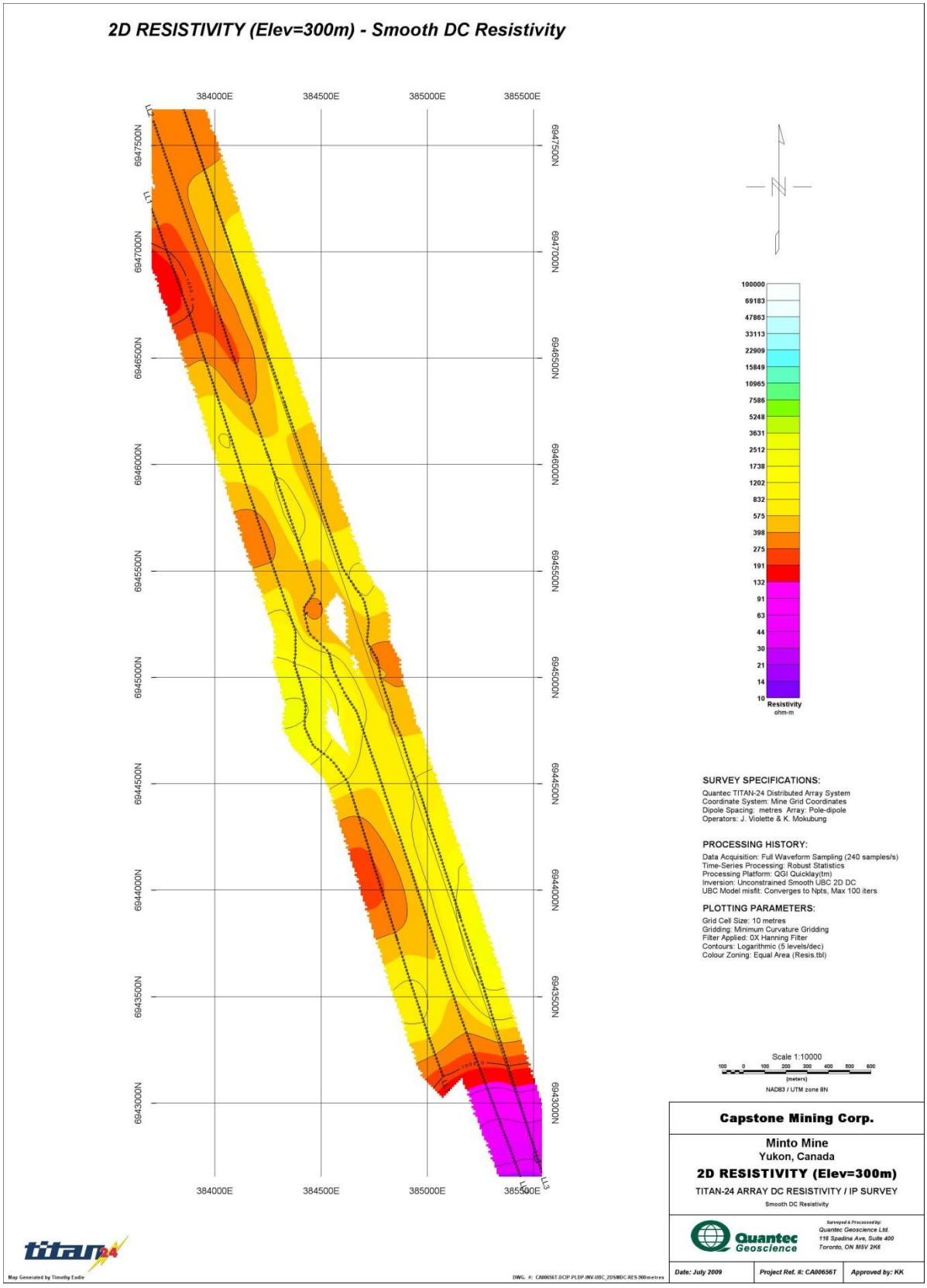

Figure 7: Smooth DC Resistivity Plan Map at 300m Elevation

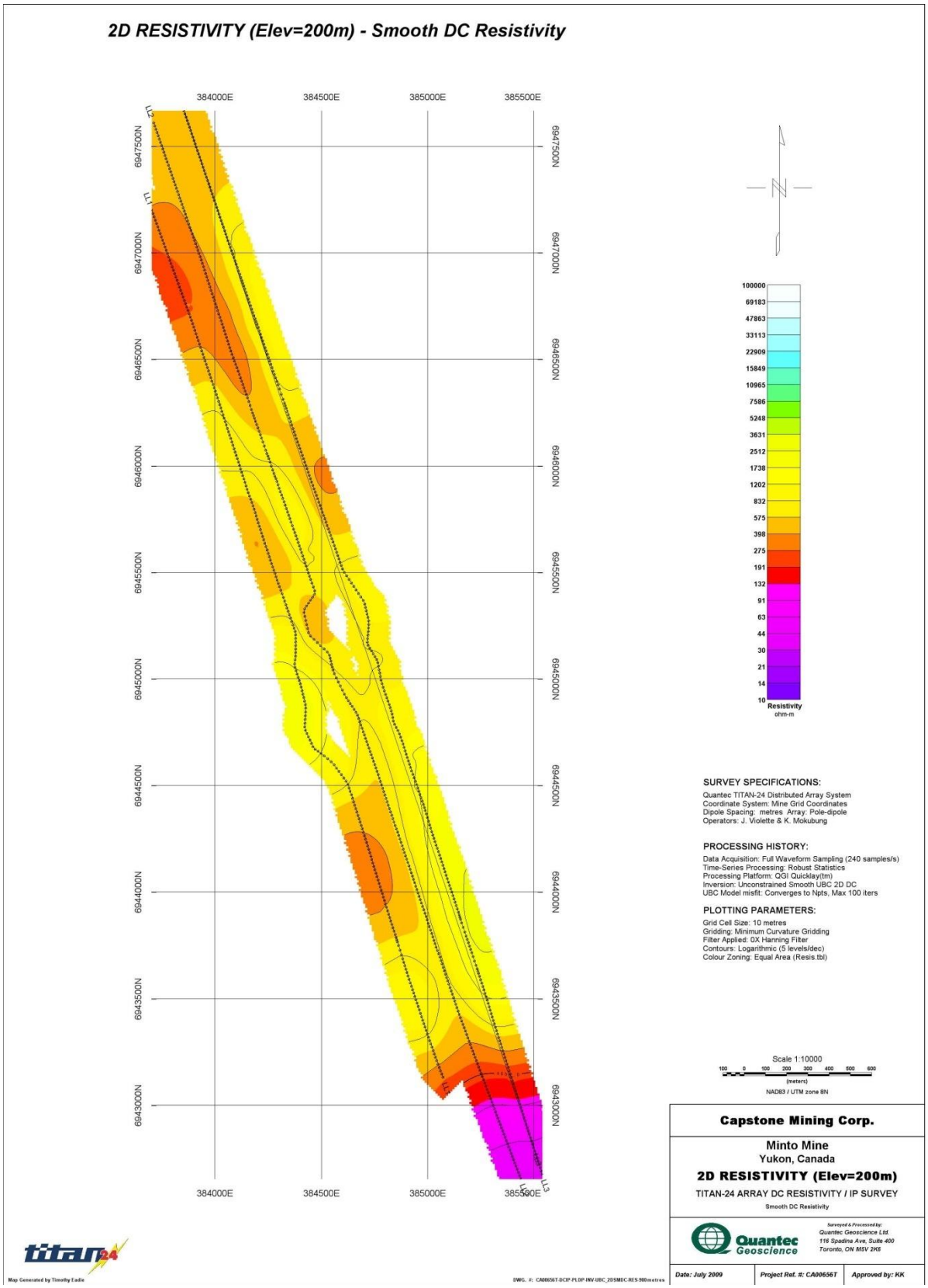

Figure 8: Smooth DC Resistivity Plan Map at 200m Elevation

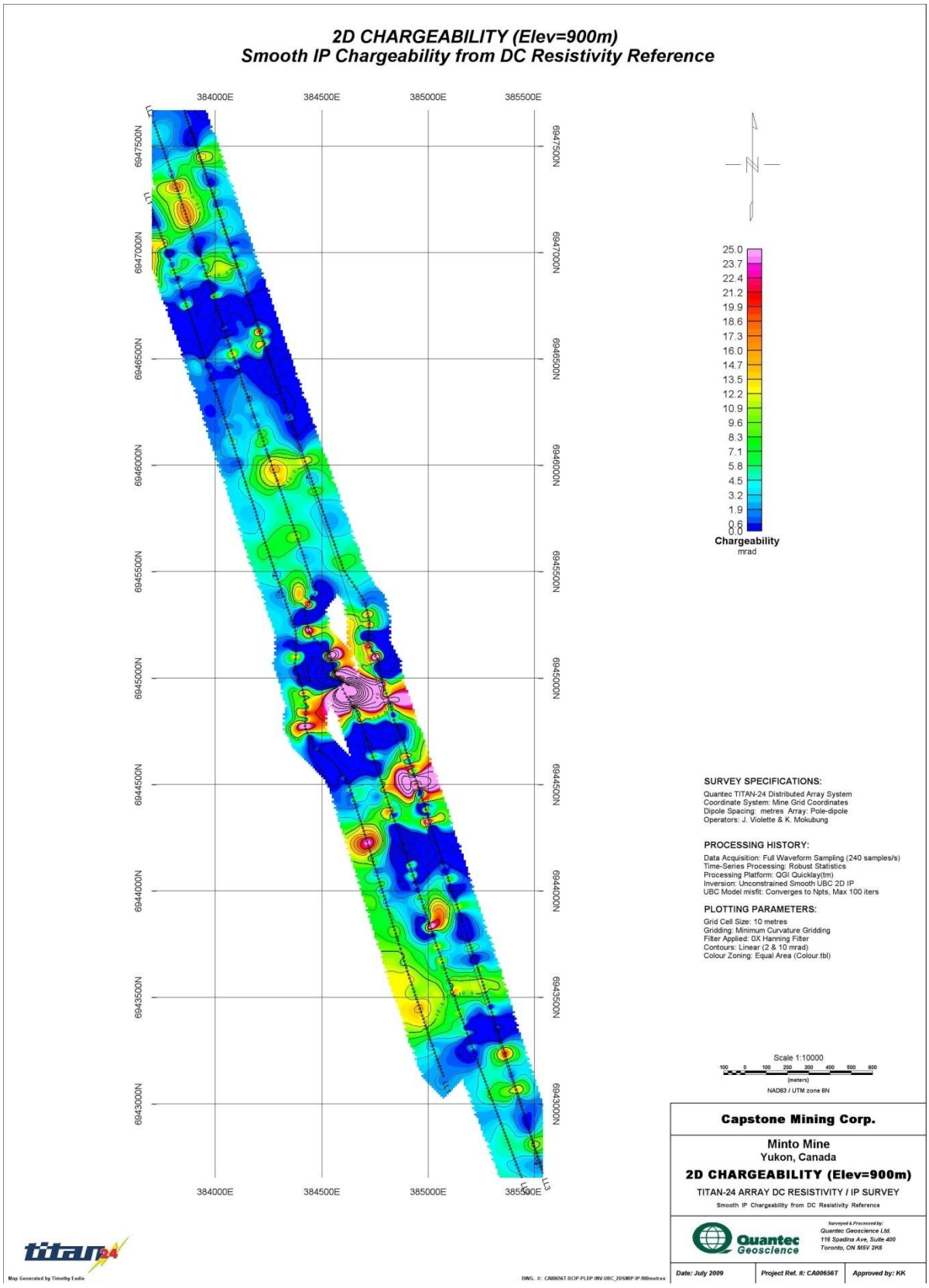

Figure 9: Smooth IP Chargeability from DC Resistivity Reference Plan Map at 900m Elevation

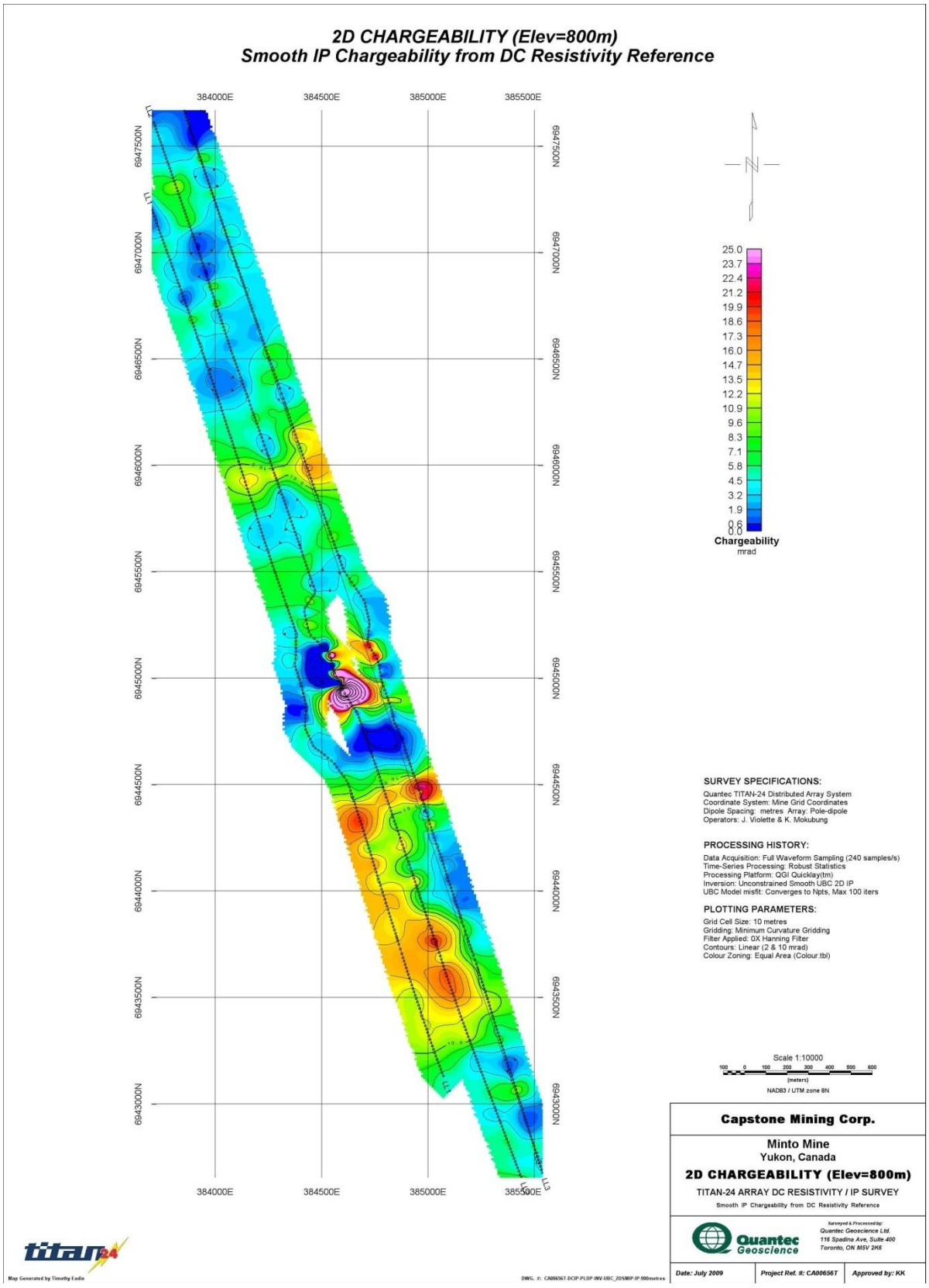

Figure 10: Smooth IP Chargeability from DC Resistivity Reference Plan Map at 800m Elevation

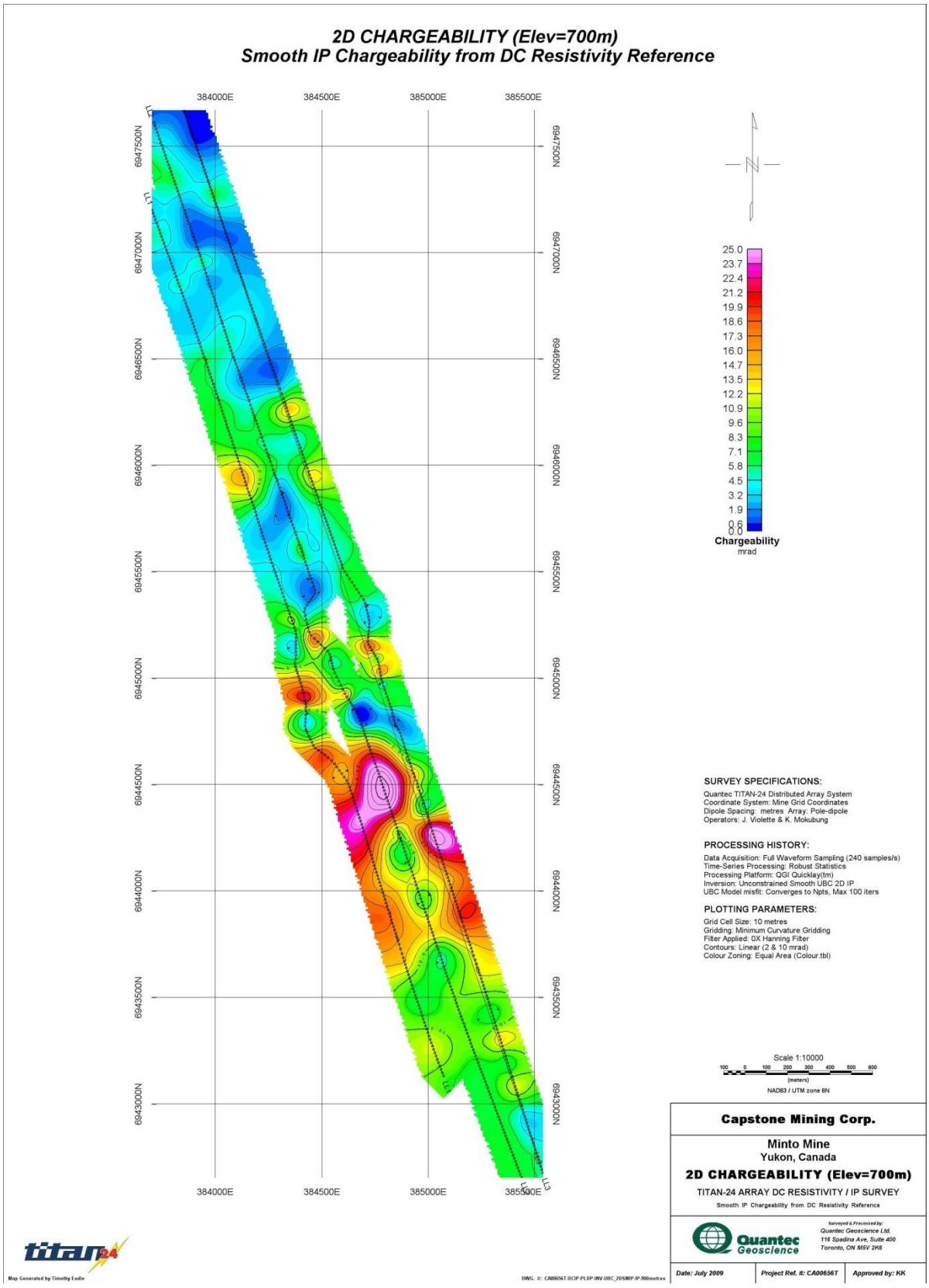

Figure 11: Smooth IP Chargeability from DC Resistivity Reference Plan Map at 700m Elevation

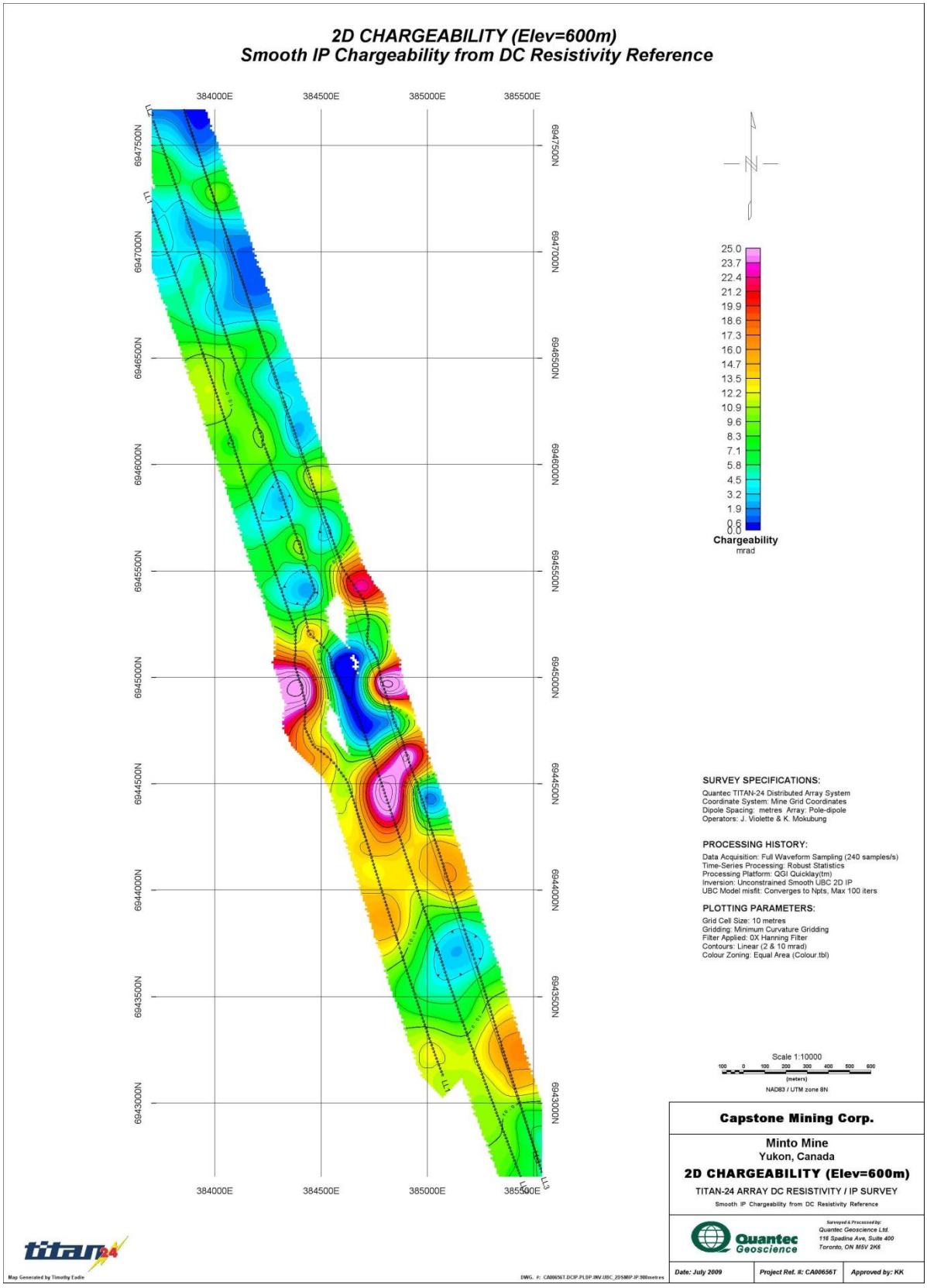

Figure 12: Smooth IP Chargeability from DC Resistivity Reference Plan Map at 600m Elevation

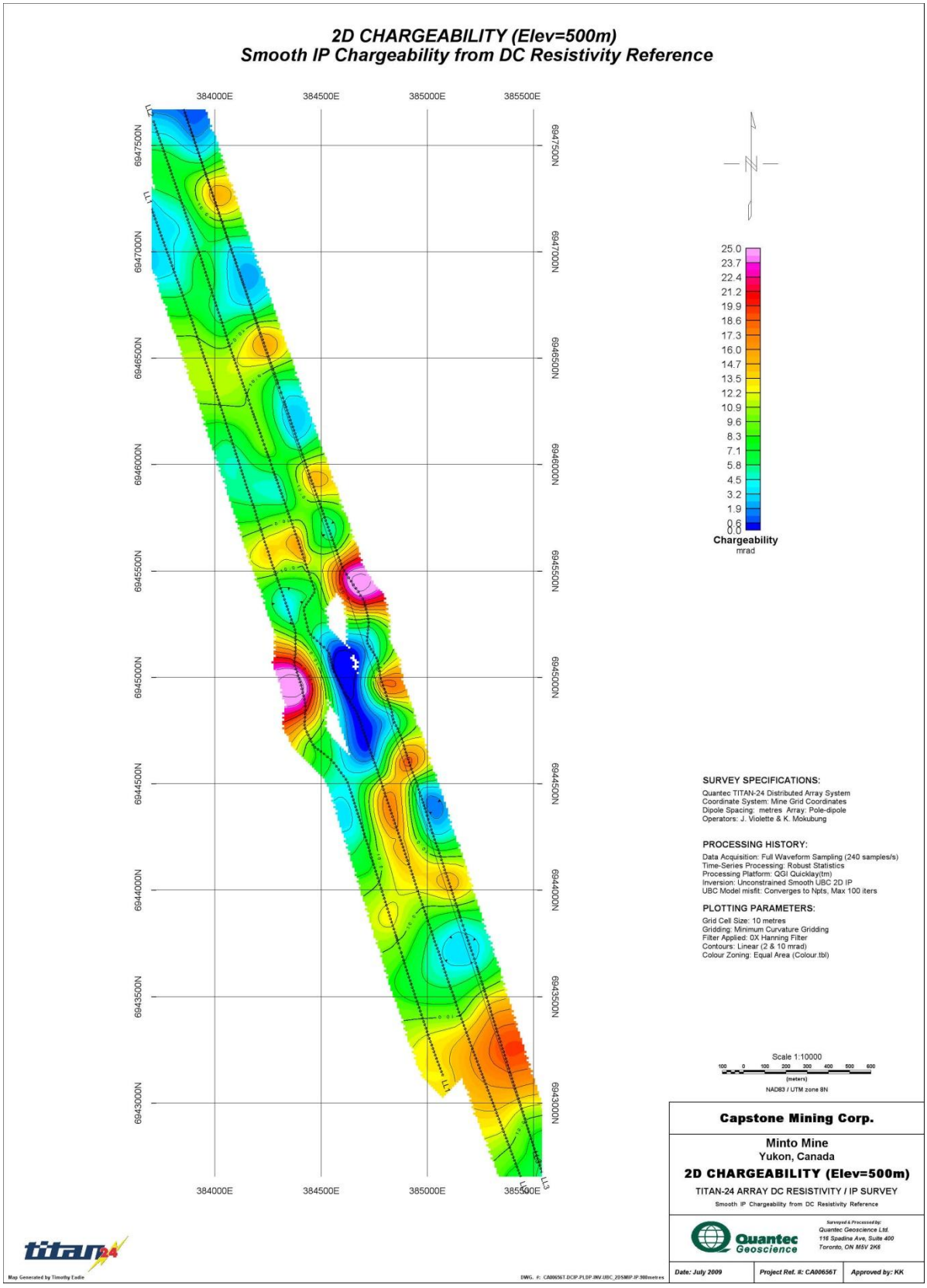

Figure 13: Smooth IP Chargeability from DC Resistivity Reference Plan Map at 500m Elevation

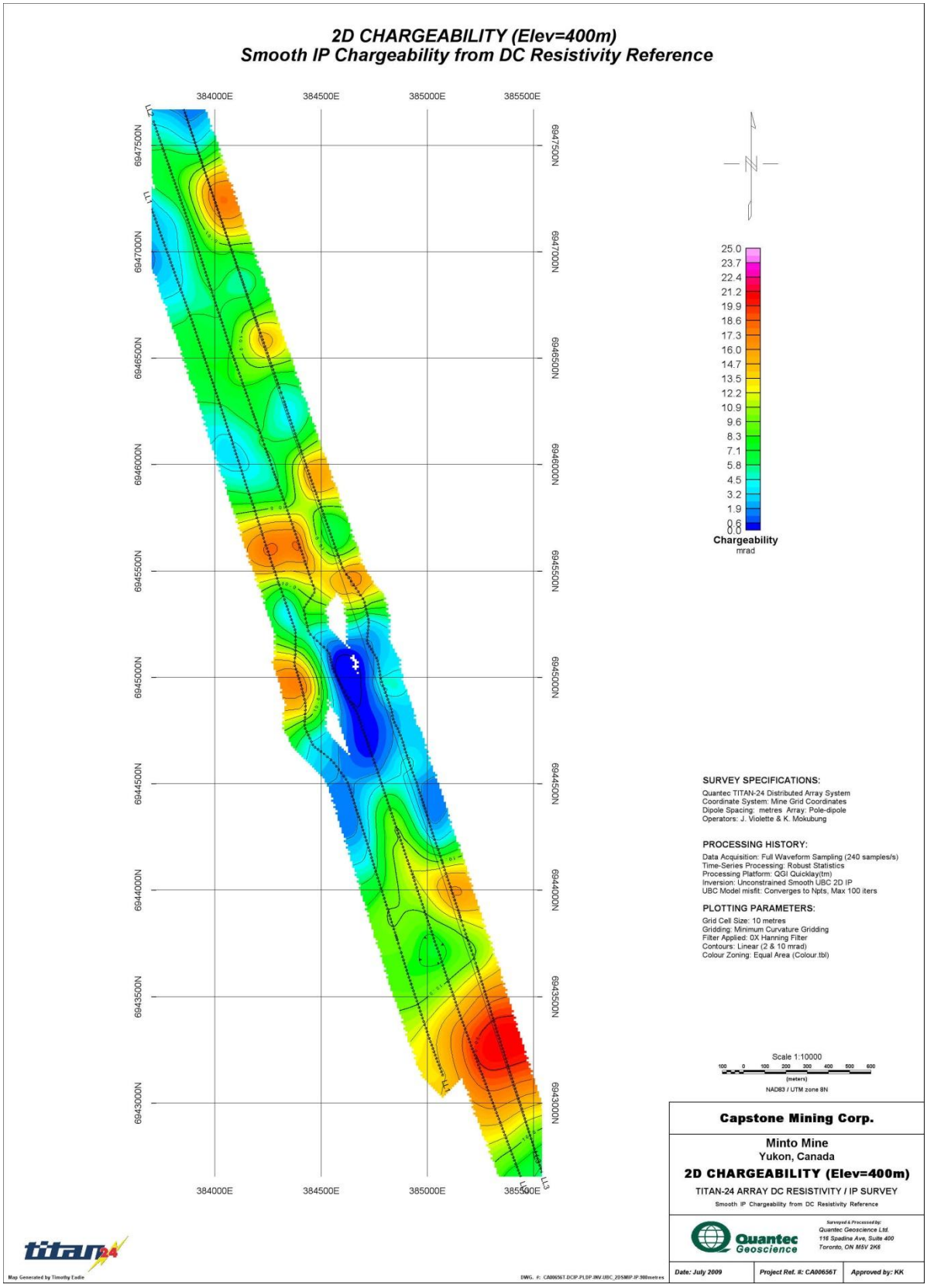

Figure 14: Smooth IP Chargeability from DC Resistivity Reference Plan Map at 400m Elevation

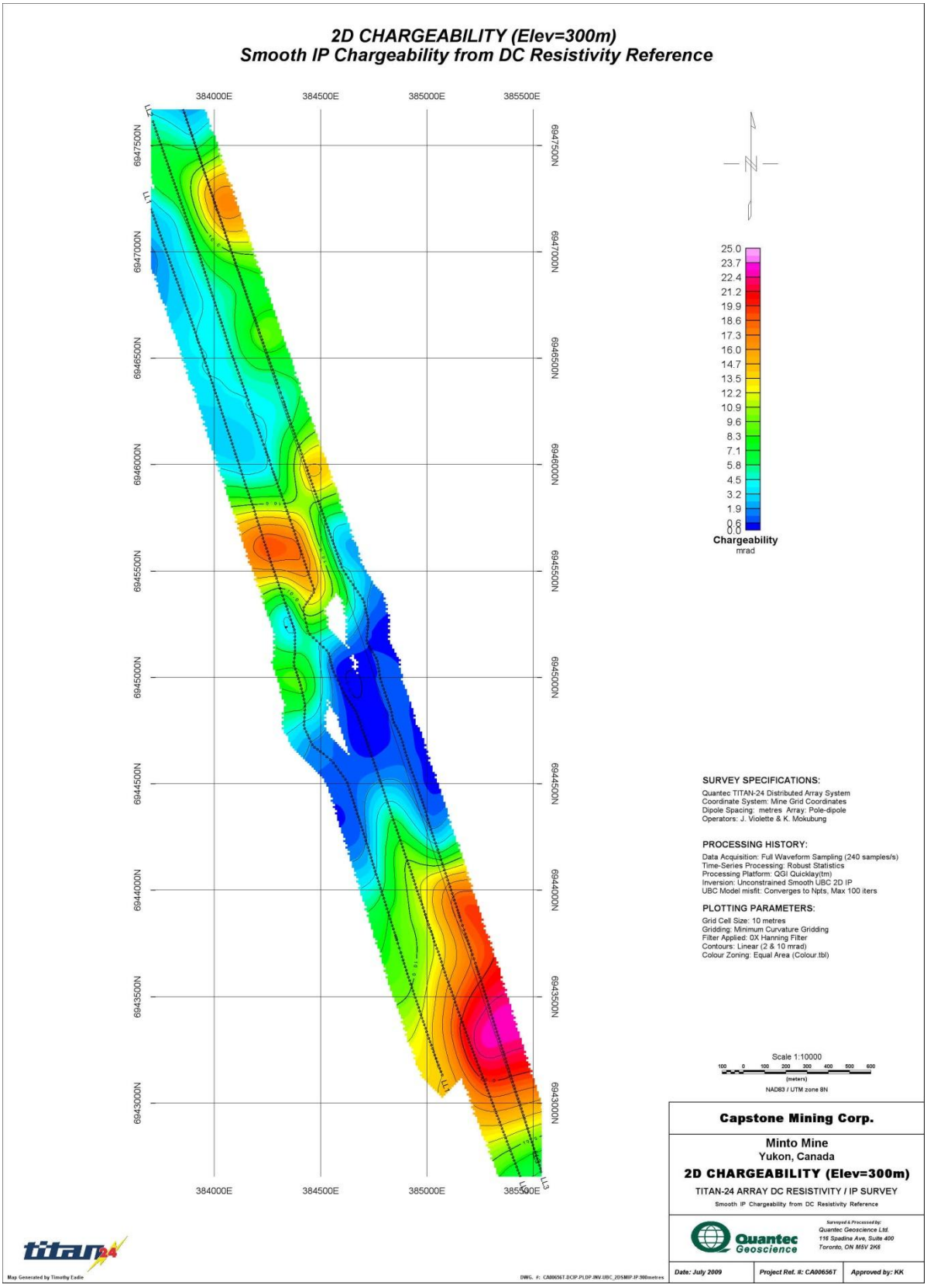

Figure 15: Smooth IP Chargeability from DC Resistivity Reference Plan Map at 300m Elevation

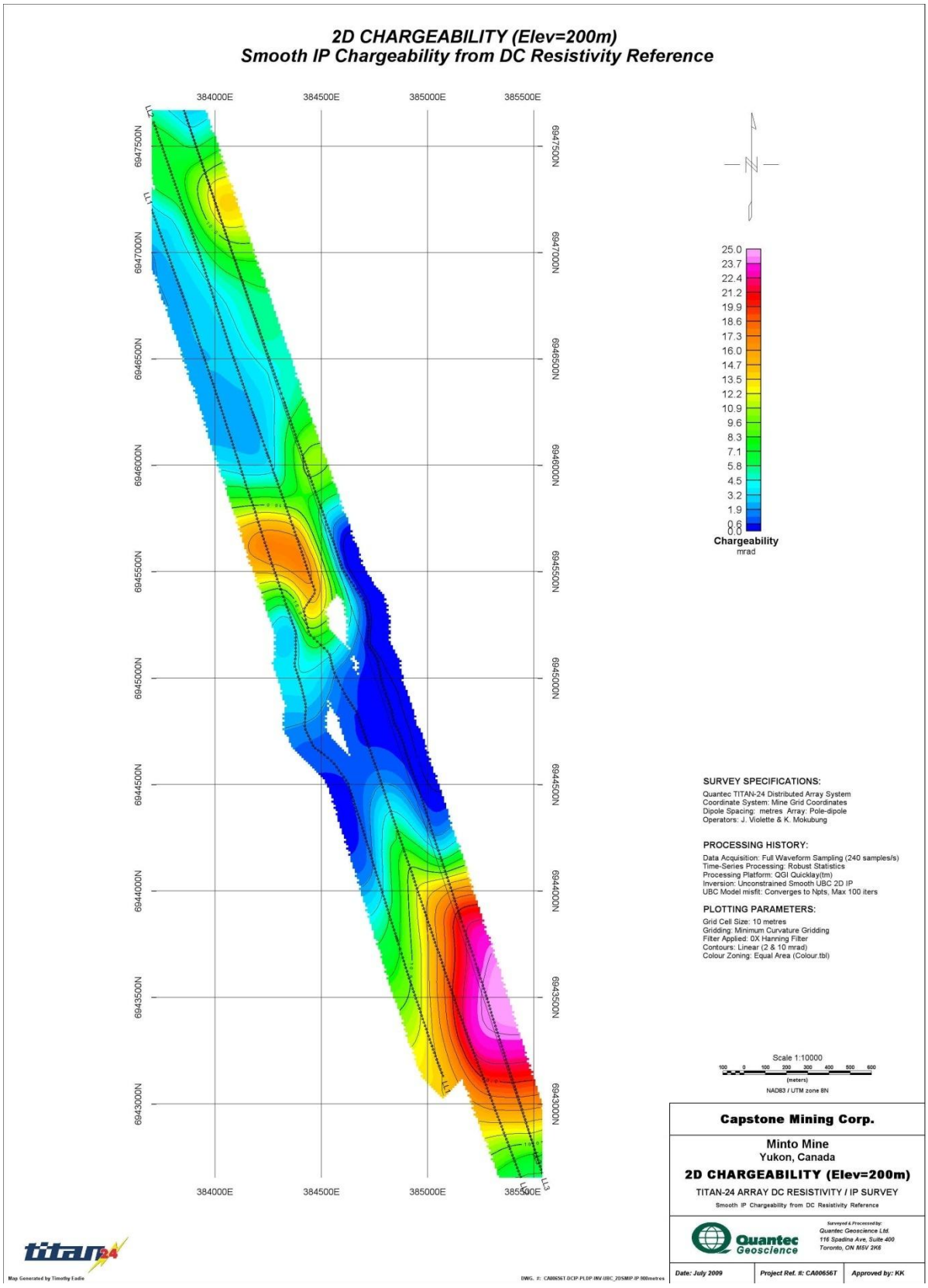

Figure 16: Smooth IP Chargeability from DC Resistivity Reference Plan Map at 200m Elevation

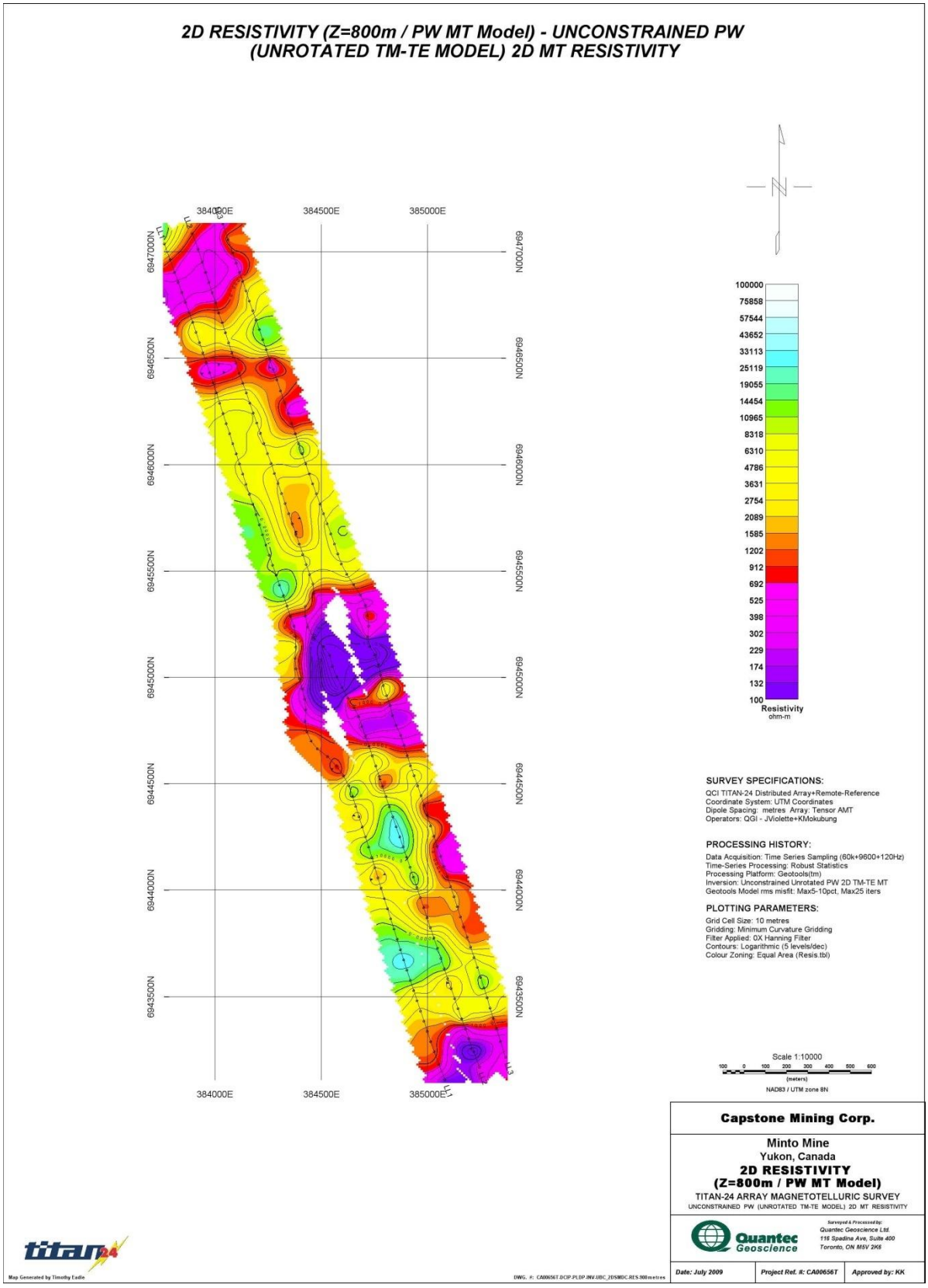

Figure 17: Unconstrained Unrotated TM-TE MT Resistivity Plan Map at 800m Elevation

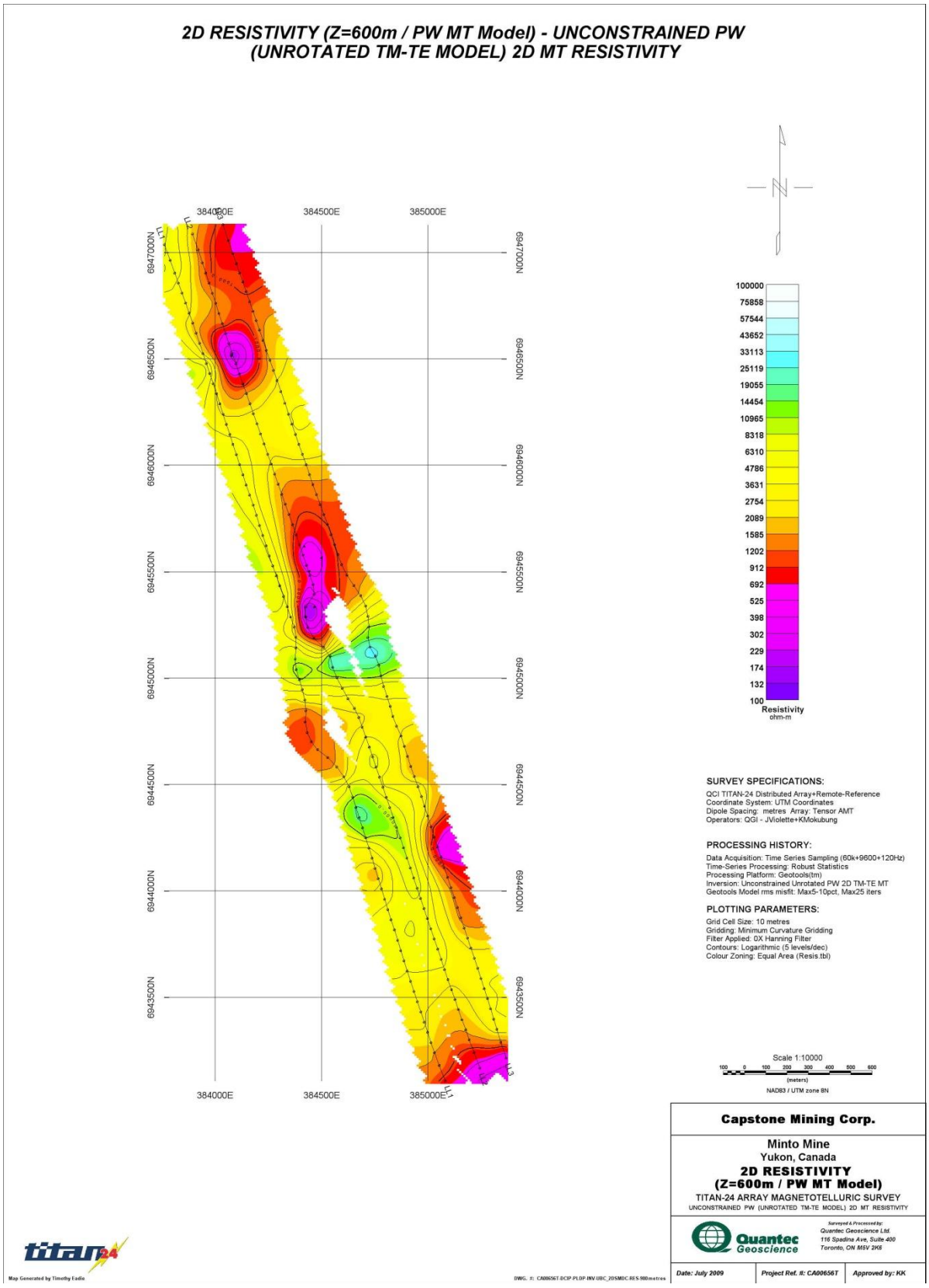

Figure 18: Unconstrained Unrotated TM-TE MT Resistivity Plan Map at 600m Elevation

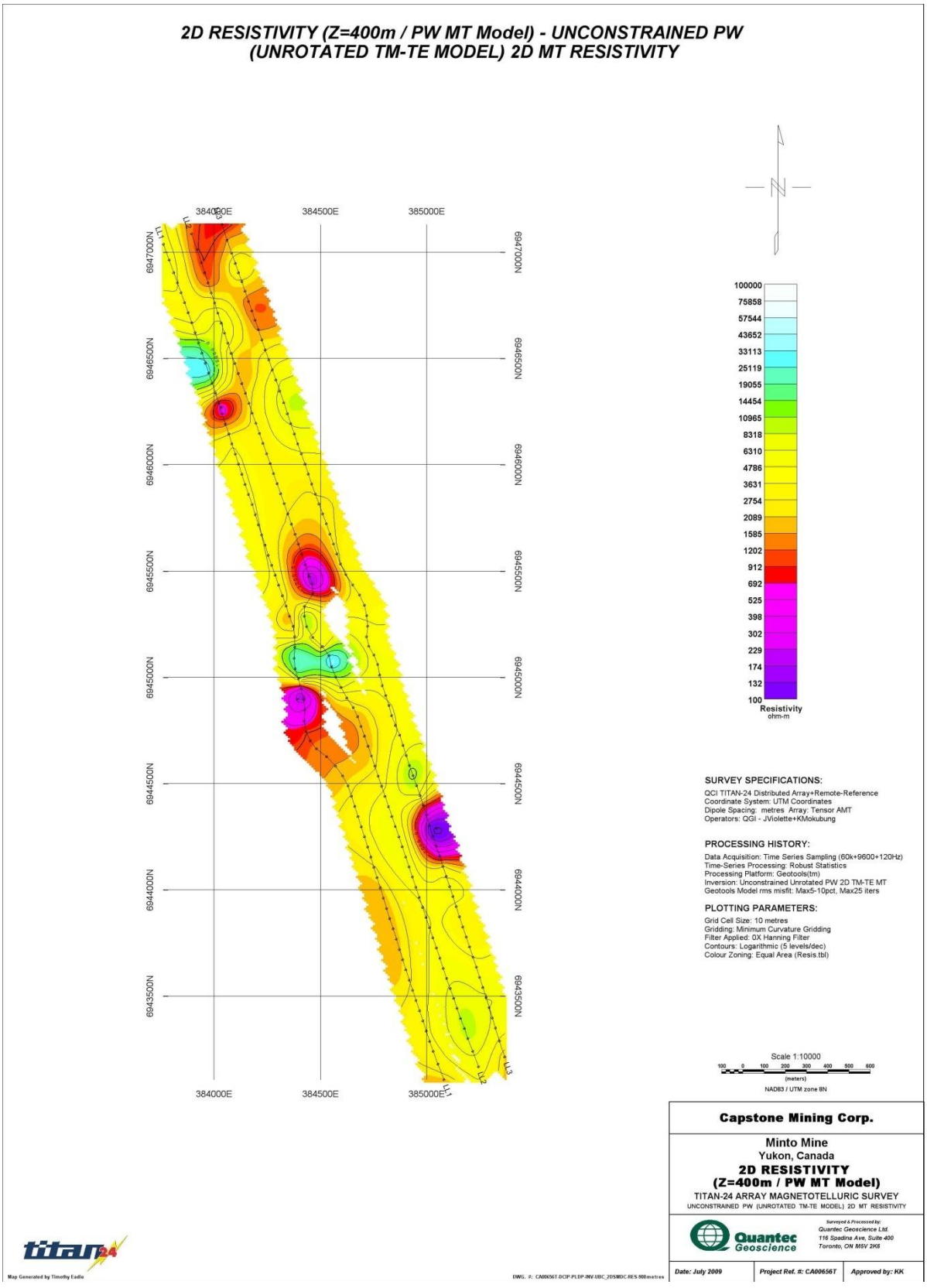

Figure 19: Unconstrained Unrotated TM-TE MT Resistivity Plan Map at 400m Elevation

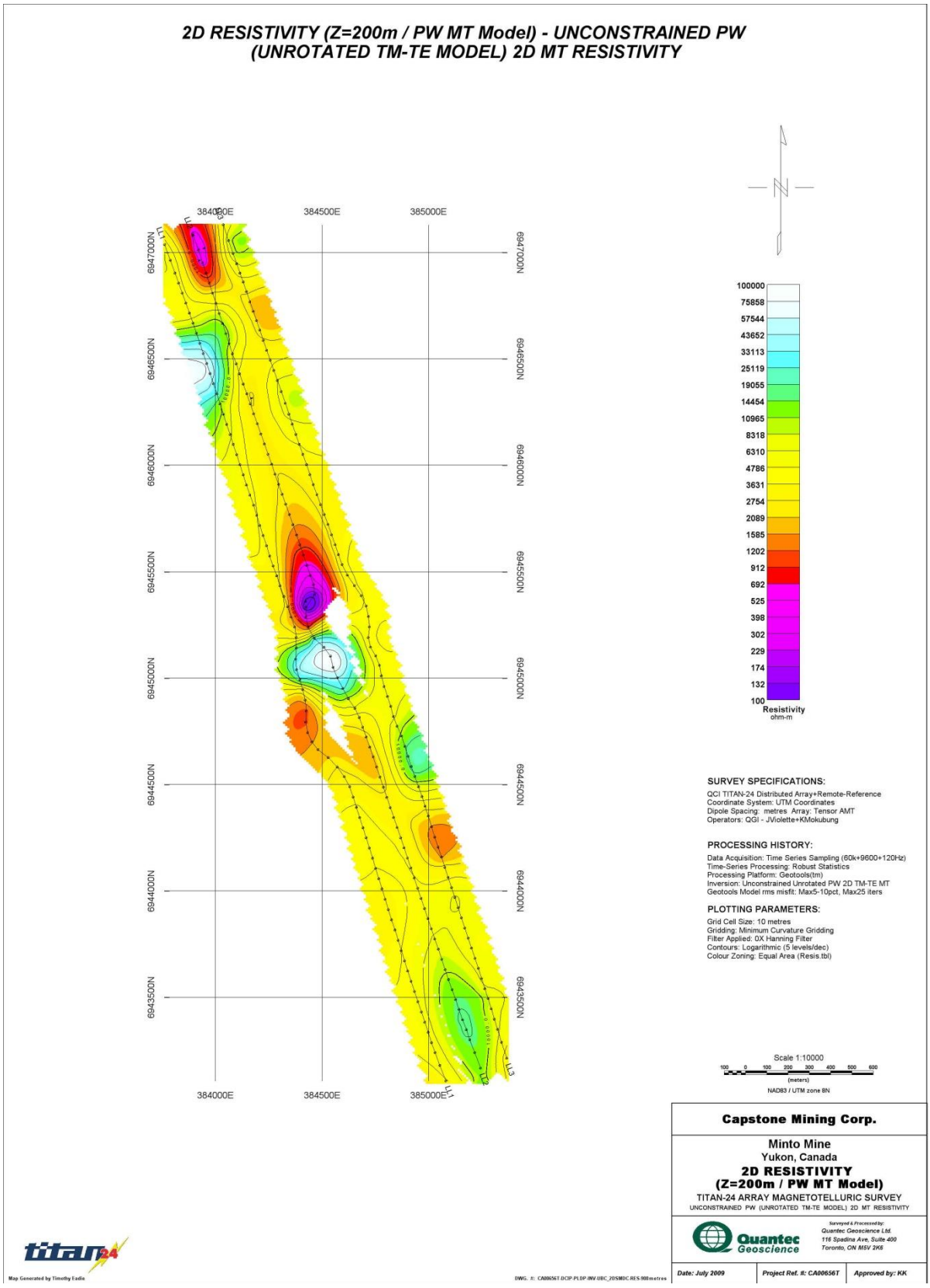

Figure 20: Unconstrained Unrotated TM-TE MT Resistivity Plan Map at 200m Elevation

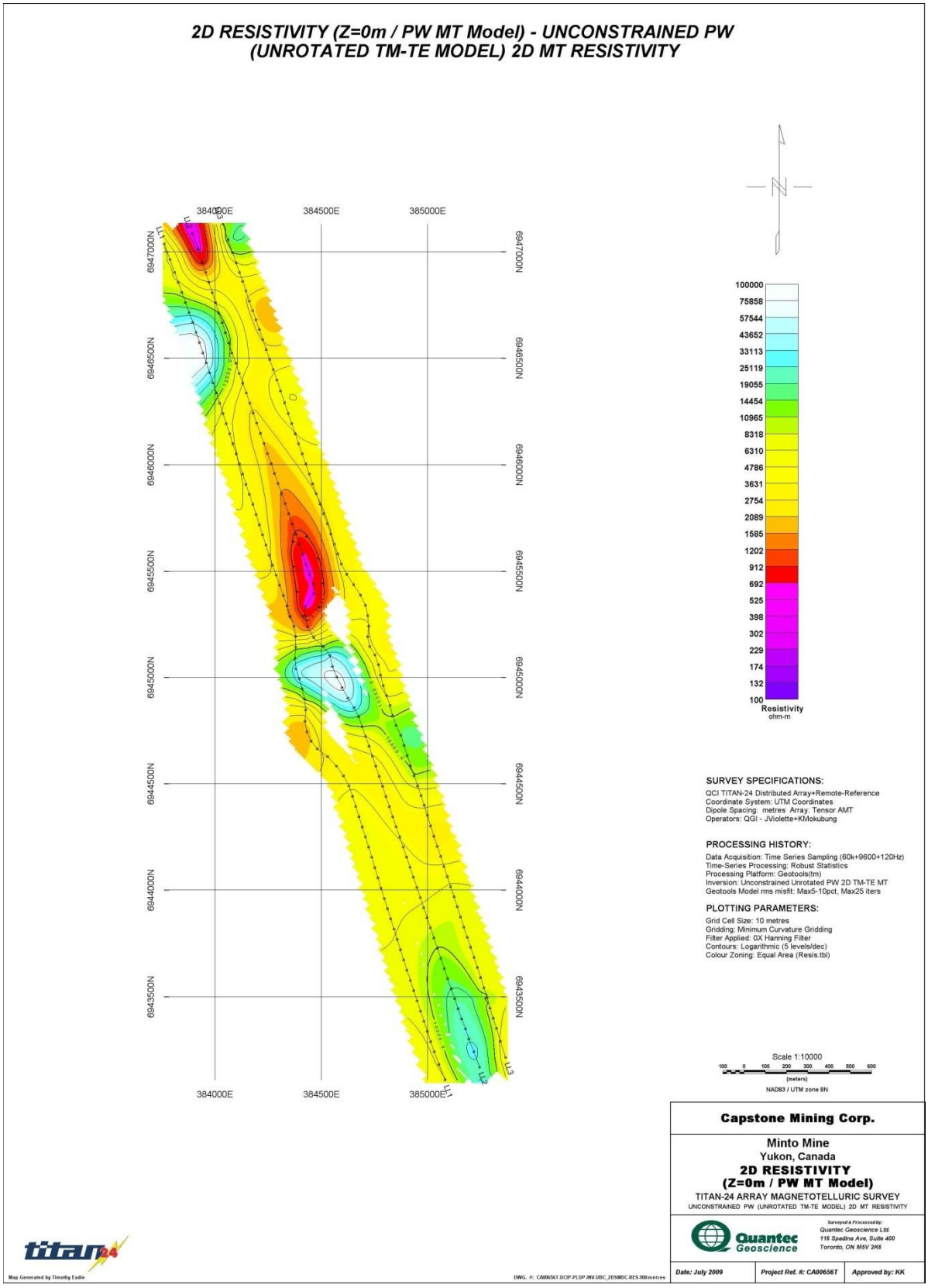

Figure 21: Unconstrained Unrotated TM-TE MT Resistivity Plan Map at 0m Elevation

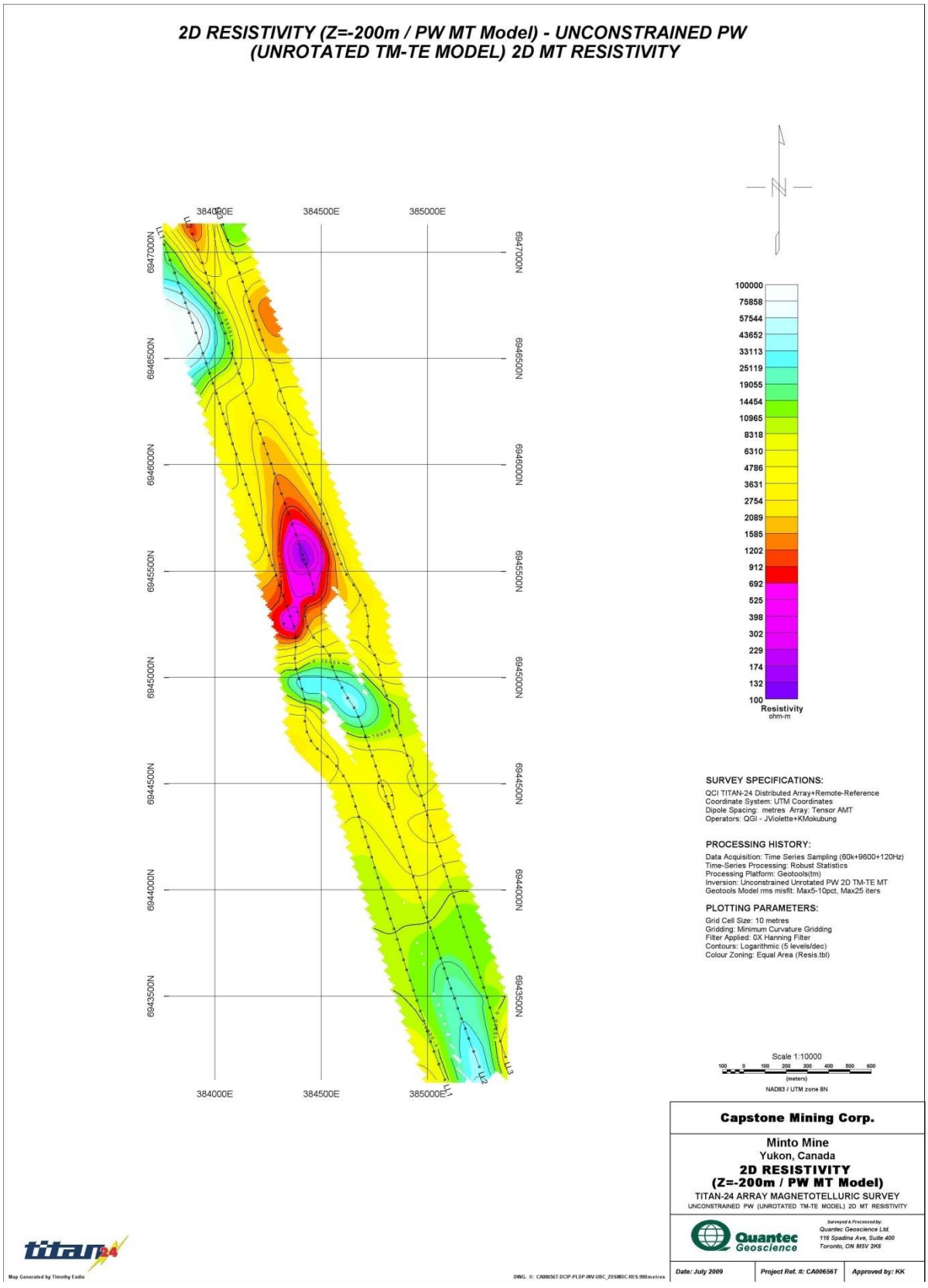

Figure 22: Unconstrained Unrotated TM-TE MT Resistivity Plan Map at -200m Elevation

APPENDIX E: A BRIEF INTRODUCTION TO THE MAGNETOTELLURIC METHOD

The magnetotelluric (MT) method measures time-variations in the Earth's natural electric (E) and magnetic (H) fields to image the subsurface resistivity structure. No source or transmitter is used. These natural fields penetrate much deeper than is practical with a transmitter. At the same time the natural signals are a plane-wave source. The plane-wave source is much simpler to model than complex transmitter geometries and signals.

The E and H fields are measured over a broad range of frequencies. Typically, the frequencies can range from above 10 kHz to below 0.001Hz. High frequency signals are attenuated more rapidly in the subsurface. High frequency data are indicative of shallow resistivity structure while low frequency data are indicative of deep resistivity structure.

At frequencies below 1Hz the signal source is due to oscillations of the Earth's ionosphere as it interacts with the solar wind. At frequencies above 1Hz the signal source is due to worldwide lightning activity. There is a lack of signal around 1Hz, often referred to as the "hole". Modern 24-bit recording hardware and signal processing techniques have largely eliminated the data quality problems that have been traditionally seen around the 1Hz signal hole.

Between about 8Hz and 300Hz the signal from worldwide lightning activity propagates in a "resonant" cavity (the resistive atmosphere) between the conductive ionosphere and the Earth's surface. Above 3 kHz the signal propagates as a ground wave. Between 300Hz and 3 kHz there is a "dead-band" where the signal does not propagate well. Despite hardware and signal processing improvements this dead-band remains problematic. When signal (atmospheric activity) is present within several hundreds of miles of the survey area the data is quite good. When no signal is being generated in the vicinity data quality is poor.

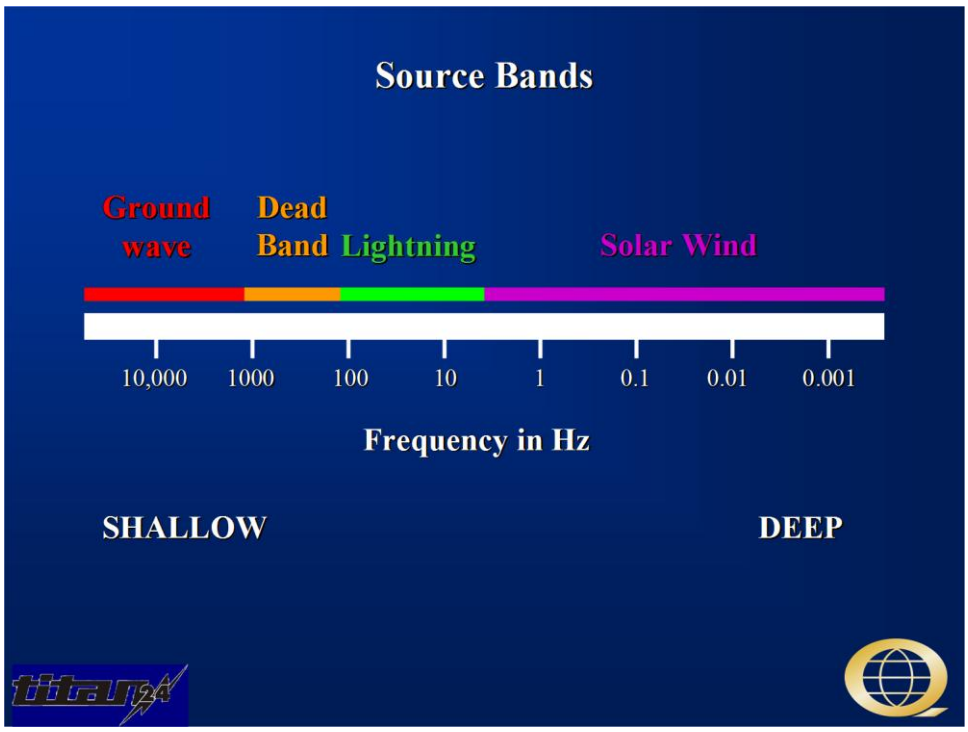

Both the electric and magnetic fields are measured. The measured fields depend on the ionosphere and lightning, and are essentially random. While the E and H fields are random the ratio of the fields depends on the subsurface resistivity structure. Note that it is primarily the orthogonal E and H fields that are related. The magnetic field must be measured perpendicular to the electric field. It is possible for

complex subsurface resistivity structure to rotate the fields, and full tensor data are usually measured.

It is often useful to think of the magnetic field as the source signal and the electric field as the response. Time variations in the magnetic field induce currents to flow in the ground.

In the field the electric and magnetic fields are measured as a function of time. The electric field is measured using two orthogonal dipoles consisting of a wire connecting two grounded electrodes. In essence, the recording system consists of a voltmeter between the electrodes. The voltage measured depends on the electric field strength and the length of the dipole. The magnetic field is measured using an induction coil.

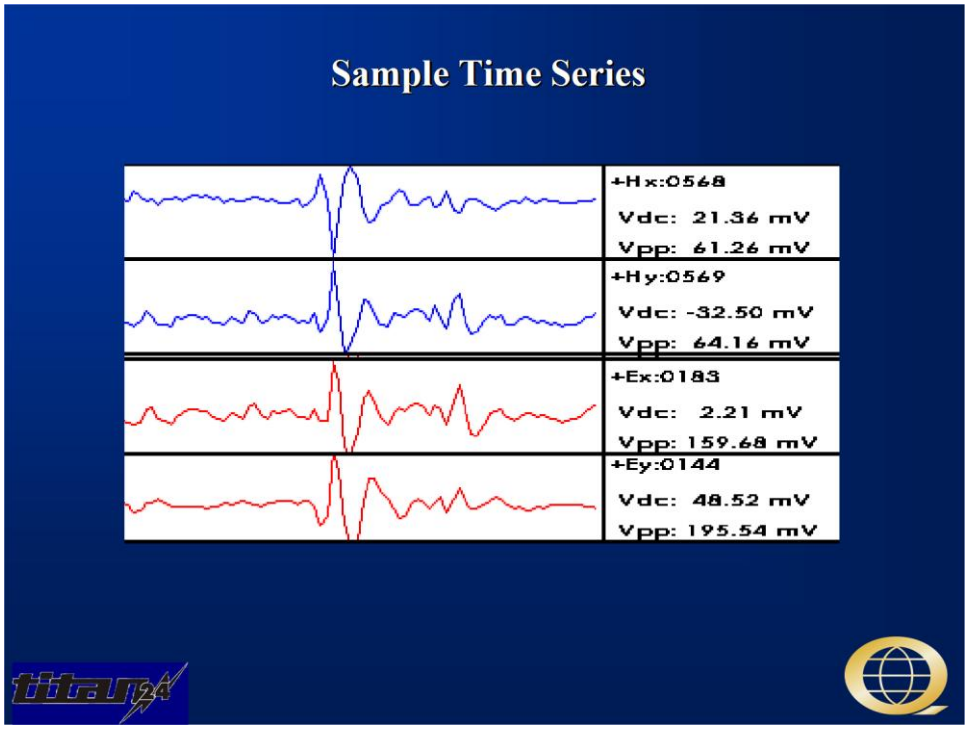

While the actual fields that are measured vary randomly (with solar and lightning activity), the relationship between the measured magnetic and electric fields is constant and depends on the subsurface resistivity structure. Extracting the subsurface resistivity structure from the measured magnetic and electric fields is a multi-step process. First time series processing techniques are used to derive geophysical parameters from the electric and magnetic fields. Then geophysical processing and inversion techniques are used to convert the geophysical parameters to a subsurface resistivity image. Finally, the resistivity image must be interpreted in terms of geologic units.

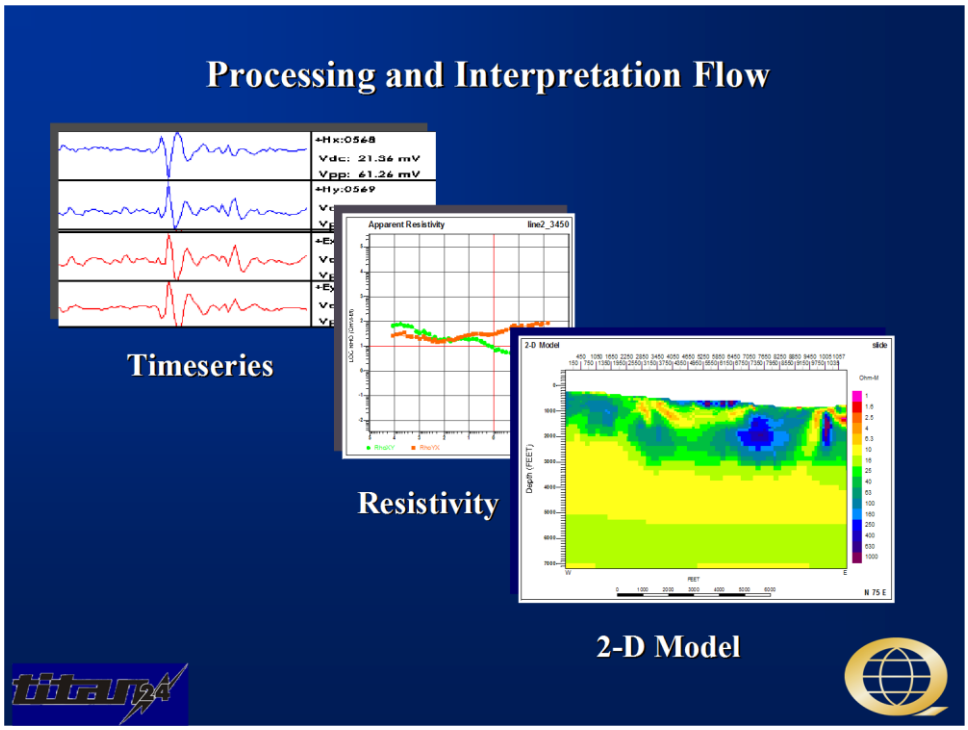

The measured magnetic and electric fields are Fourier transformed into the frequency domain. The system response is removed from the data (making the measurement independent of the hardware system). The Fourier coefficients represent the amplitude and phase of the electric and magnetic fields as a function of frequency.

A variety of signal processing techniques are used to minimize noise and bias in the estimation of geophysical parameters from the measured fields. The details are complex, but the approach is easily understood. Philosophically, the idea is to use multiple approaches to noise and bias reduction, not letting any one statistical approach have too much impact on the data, but relying on the combination of approaches to produce good estimates. The approaches include:

1. Spatial isolation of noise. A remote reference magnetic station is used to separate widely distributed signal from local noise.
2. Coherency sieves to find coherent signal. First the local and remote magnetic field measurements are compared and coherent signal kept. Then the local magnetic and electric fields are compared for coherency.
3. Frequency isolation of noise. Long Fourier transforms are used to provide extremely sharp isolation of noise in frequency.
4. Time isolation of noise. Short Fourier transforms are used to remove noise that is isolated in time (noise spikes, or noise that is randomly turning off and on).
5. Robust statistics that minimize biasing effects of a few isolated measurements.

Once the time series processing is complete geophysical parameters can be estimated. The primary geophysical parameters for MT are typically the apparent resistivity versus frequency and phase versus frequency.

The depth of penetration of the signal depends on its frequency and the resistivity of the rocks. The depth at which the signal amplitude has been attenuated to 37% (1/e) is called the skin depth and is defined:

$$\delta = \sqrt{\frac{2}{\mu\omega\sigma}} = 503\left(\sqrt{\frac{\rho}{f}}\right)(m)$$

where

δ = skin depth

μ = magnetic permeability

σ = conductivity=1/resistivity

ω = angular frequency=2πf

ρ=resistivity=1/conductivity

The ratio between the two measured components (E and H) is the electrical impedance. The impedance (denoted Z) is defined as $|Z| = |E/H|$. The impedance is a complex number because the E and H fields are out of phase. Note that Z, E, and H are all functions of frequency.

The complex impedance is used to calculate an apparent resistivity as follows:

$$\rho_a = \frac{1}{\mu\omega}|Z|^2 (ohm.m)$$

The apparent resistivity is also a function of frequency. At any frequency the fields must travel through the overlying geology. The apparent resistivity depends on the integrated (weighted) conductance of the rocks being sampled. It is a smoothly varying function of frequency because it represents the average resistivity of a progressively larger volume of the subsurface. On a log resistivity-log frequency plot the apparent resistivity generally can not exceed a slope of +/- 45 degrees.

The phrase “apparent resistivity” arises from the volume averaging. At a single frequency the electric and magnetic fields measurements can be used to calculate an impedance. This impedance depends on the resistivity of a large volume of the subsurface. The impedance can be thought of as the impedance of a half-space that would provide identical measurements to the actual subsurface.

The calculated phase or apparent phase is the difference between the measured E field phase and the measured H field phase. If the subsurface is one-dimensional (1D) or two-dimensional (2D) the phase is related to the resistivity. The Hilbert formula (minimum phase wavelet) relates the phase to the slope of the apparent resistivity curve. If the slope of the resistivity curve (on a log-log plot) is 0 the phase is 45 degrees. If the resistivity is increasing with decreasing frequency the phase is less than 45 degrees. If the resistivity is decreasing with decreasing frequency the phase is more than 45 degrees. As the apparent resistivities are constrained to a slope of no more than 45 degrees on a log-log plot, the phases are constrained to remain in a quadrant, between 0 and 90 degrees.

The phase measurement is largely independent of the apparent resistivity measurement. The Hilbert relationship provides an independent way to calculate the apparent resistivity curve from the phase data. There are effectively two independent measurements of the resistivity curve, providing a powerful check on data quality.

The apparent resistivity and phase curves are the primary parameters used in the interpretation of MT data. For a layered (1D) earth the apparent resistivity and phase data can be converted into intrinsic resistivity versus depth simply by accounting for the volume averaging nature of the method. There are a variety of algorithms for doing the conversion. The conversion is not unique. Some algorithms provide

smoothly varying intrinsic resistivity versus depth functions (Occam inversion, Bostick transform). Others provide distinct layered solutions (Marquardt inversion).

1D modeling and inversion raises the following points:

- A single MT site provides information about resistivity versus depth. This is a major distinction from potential fields techniques that only provide information about relative variations along a profile.
- The conversion from apparent resistivity versus frequency to intrinsic resistivity versus depth is not unique. It is susceptible to equivalence. In particular any sharp resistivity contrast can be replaced by an equivalent transition zone.
- In a layered model the thickness of a resistive layer is well resolved. The resistivity of a resistive layer is poorly resolved.
- In a layered model the conductance (conductivity*thickness) of a layer is resolved. Neither the thickness nor the conductivity is uniquely resolved.
- Once the constraint that the subsurface is composed of distinct, resolvable, units is imposed the 1D inversion of MT data is essentially unique. Resolution is excellent (better than 5% of depth).

Apparent resistivity versus frequency is the most fundamental way of looking at the data in the interpretation phase. While the overall process is complex, with advanced processing techniques and inversions, it is important to keep in mind that the subsurface structures are apparent in the raw data – the apparent resistivity plots.

The following sequence of illustrations is intended to introduce the apparent resistivity versus frequency sounding curves. But it is also intended to highlight the relatively complex, but understandable, relationships between the observed data and subsurface structure.

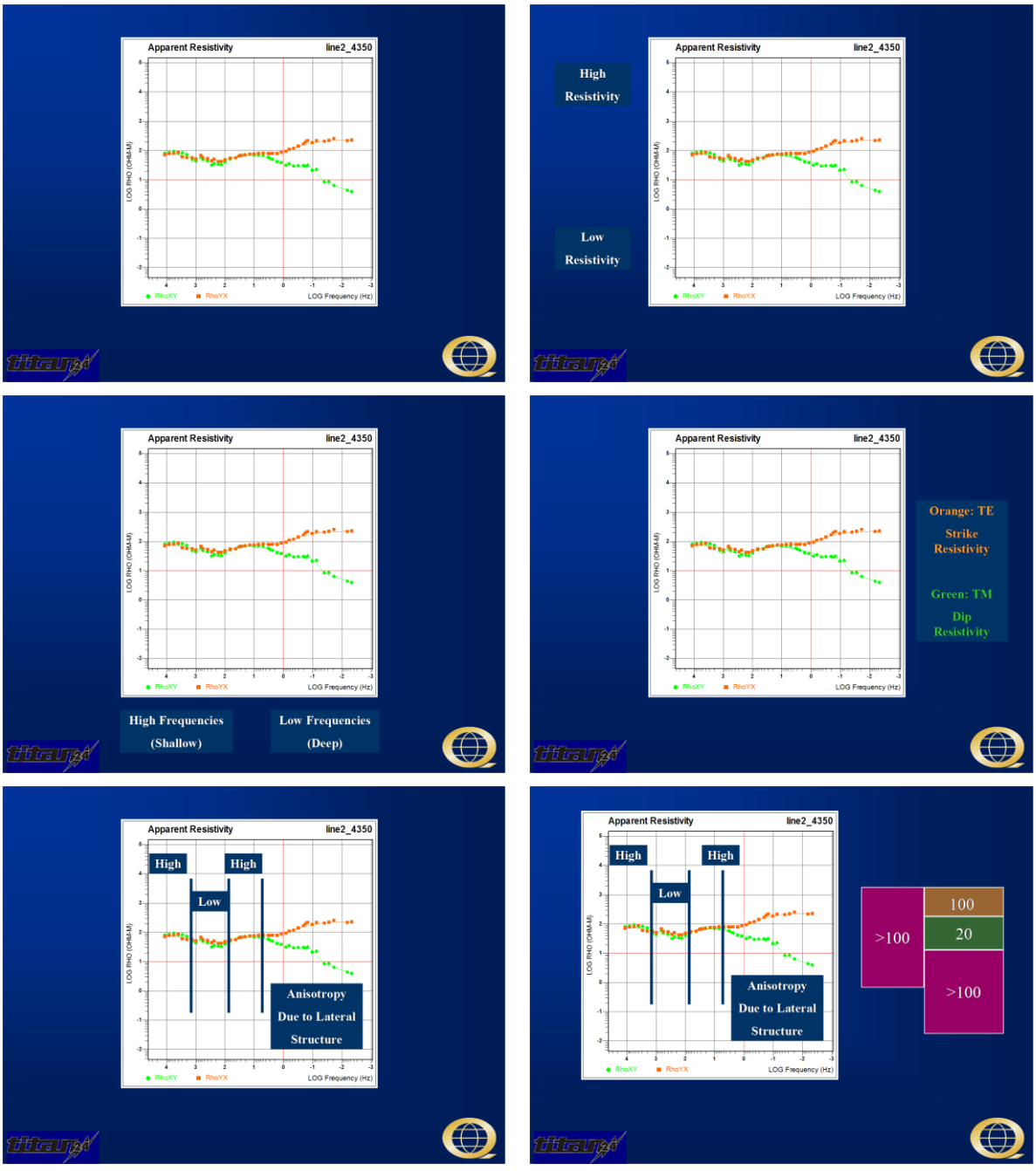

A simple layered subsurface structure is not generally the problem of immediate interest in exploration. In the case of more complex two-dimensional (2D) or three-dimensional (3D) structure the MT response will be affected by lateral resistivity variations.

The MT measurement relies on natural, plane-wave, source signals. The measured response depends on lateral resistivity variations as much as (or more than) resistivity variations below the immediate sounding site.

Full tensor measurements of the E and H fields are made at every site. For each site there are two apparent resistivity sounding curves (or modes) and phase curves. These two modes are arbitrarily labeled Rho-XY and Rho-YX. The first, Rho-XY, refers to the apparent resistivity (Rho) calculated from Ex and Hy.

Once full tensor measurements are made in the field it is possible to mathematically rotate the fields to any arbitrary coordinate system. Traditionally, the data are rotated independently at each frequency to maximize the difference between the two apparent resistivity sounding curves. This puts the data into “geologic” or “principal” coordinates.

One sounding curve will have the electric field in the geologic strike direction and is referred to as “Transverse Electric” or TE. The other mode will have the electric field in the geologic dip direction and is referred to as “Transverse Magnetic” or TM. Note that TE and TM are interpretive designations, and refer to geologic strike. XY and YX were simply geometric designation.

For a layered (1D) earth the two measurements are identical. When the structure is 2D or 3D the lateral resistivity variations will distort (often severely) the simple 1D response. The distortion of the fields by complex structure is realized in the apparent resistivity data as “anisotropy”. This is a divergence between the two apparent resistivity sounding curves.

The measurement of two orthogonal apparent resistivity sounding curves provides valuable information. Both curves reflect the resistivity structure underlying the site. Both curves will show increasing or decreasing resistivity at a frequency in response to resistivity structure under a site. The two apparent resistivity curves will diverge in response to lateral resistivity variations.

If the site is located on the resistive side of a lateral resistivity contrast the TE mode will be slightly suppressed due to the contact and the TM mode will be significantly biased up by the contact. If the site is located on the conductive side of a lateral resistivity contrast the TE mode will be slightly biased up while the TM mode will be significantly biased down by the contact.

For a 2D resistivity structure the TE mode is always providing an indication of the integrated conductance of the volume being sampled. It will always be a slowly varying function of position. The TM mode is responding dramatically to the presence of charges on the lateral resistivity boundaries, and will dramatically overshoot on the resistive side of a contact and undershoot on the conductive side. The anisotropy (divergence of the two sounding curves) is diagnostic of a lateral resistivity contrast.

The following simple model demonstrates most of the critical 2D behaviours. The model consists of a 100 Ohm-m host with a 10 Ohm-m basin on the right. There is a 1 Ohm-m layer buried within the host and below the basin. The response is shown at two sites, one immediately on the resistive side of the basin contact and the other immediately on the conductive side of the contact.

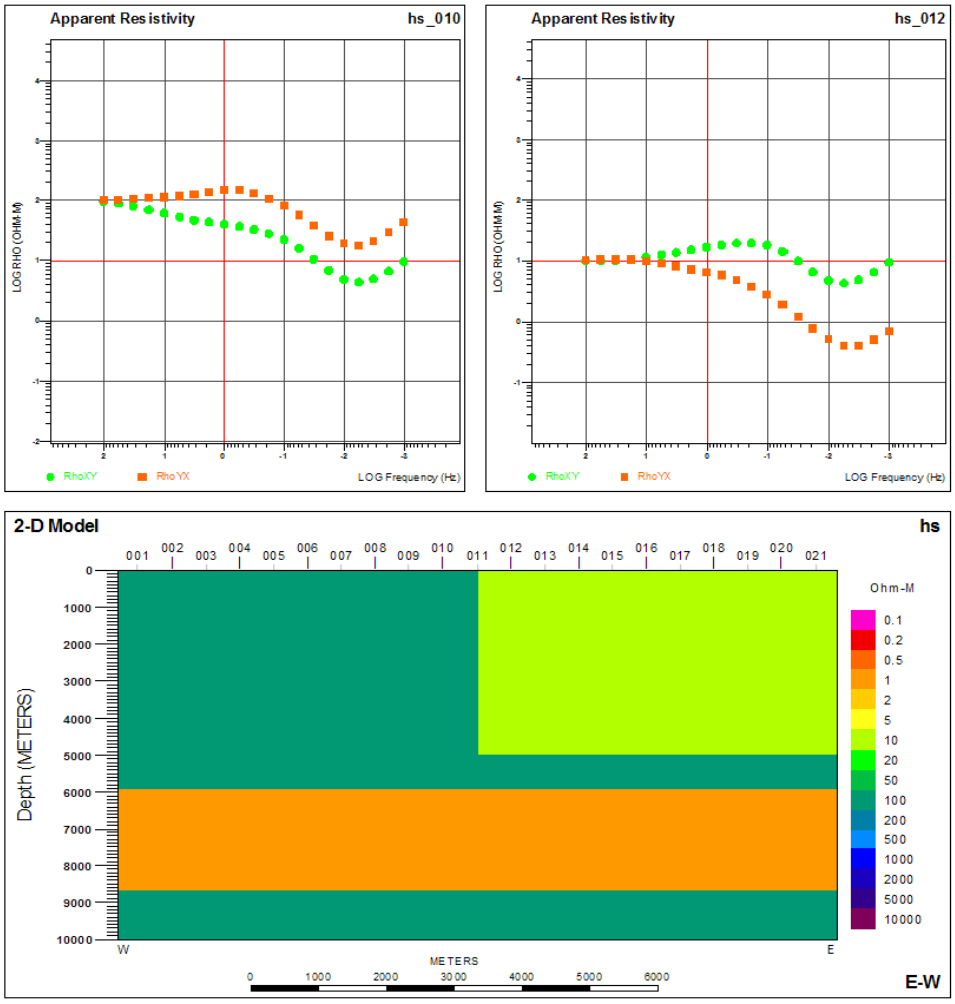

The following observations summarize the behaviour of 2D MT responses:

- The apparent resistivity at high frequencies reflects the true shallow resistivity.
- The apparent resistivities converge at high frequencies to the true shallow resistivity.
- The divergence in apparent resistivities occurs at a higher frequency for the site on the resistive side of the contact. Because the skin depth is larger in the resistive media the site on the resistive side of the contact is effectively “closer” to the contact than the site on the conductive side of the contact. The TE mode is constrained to the range of physical resistivities actually present in the model
- The TE mode “volume averages” the intrinsic resistivity. The TM mode exhibits apparent resistivities outside the range of physical resistivities in the model. Note that for the site on the right the TM mode indicates resistivities below 1 Ohm-m.
- Both the TE and TM modes respond in tandem, at the same frequency, to resistivity structure under the site. At both sites both the TE and TM modes indicate the top and bottom of the 1 Ohm-m layer. While 1D inversion of the TE and TM modes would place different apparent depths to the 1 Ohm-m layer the response is at the same frequency in both modes indicating it is the response of one layer.
- The intrinsic resistivity of the 1 Ohm-m layer is difficult or impossible to discern.

Without physical property data only the conductance of the layer can be resolved.

These effects can also be clearly seen in pseudo-sections of the TE and TM apparent resistivity response of the model:

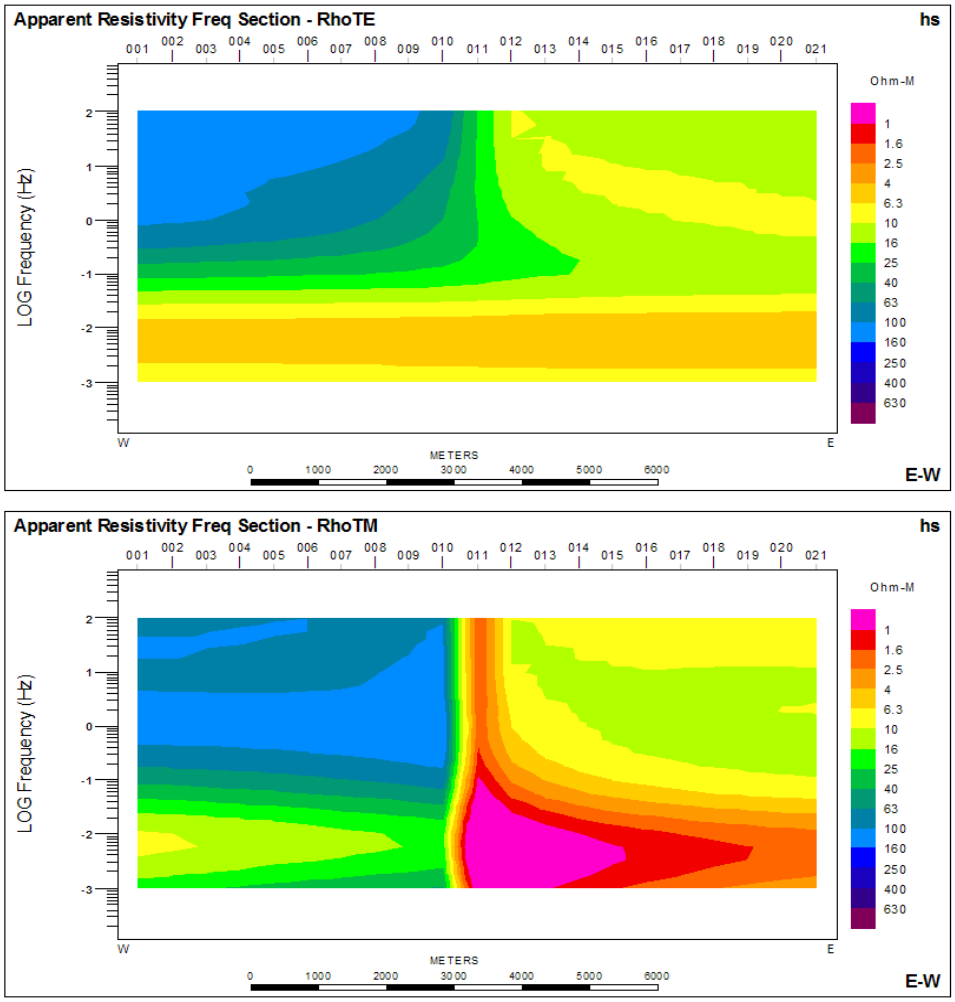

The apparent resistivity data at each site have been contoured, as a function of frequency. The inherent smoothness of the TE section can be clearly discerned. The distinctive “undershoot” of the TM response on the conductive side of the contact can be clearly seen.

One of the key factors in multidimensional MT data is “static shifts”. The apparent resistivity sounding curves can be biased, up or down, by lateral resistivity contrasts too small to be resolved by the MT data. The curve is essentially DC shifted on the log-log apparent resistivity plot. This can be seen by examining the sounding curves from the previous 2D model. Assuming data had not been acquired above 1Hz the two sounding modes would be seen to be separated in the highest frequency data. Note that there are no static shift effects in the phase data.

Inversions and forward modeling are used to derive the subsurface resistivity structure from the data. The primary interpretation tools are 2D inversions. Problems emerge when the real world, complex, data are not consistent with the simplistic 2D assumptions. In a perfect world we would use modeling and inversion programs capable of reflecting the full complexity of the subsurface. However, in practice incorporating too much complexity in the modeling and inversion programs results in very coarse models

which are incapable of resolving exploration targets. Instead, we must find ways to remove some of the complexity from the actual data. To this end, we have developed the Titan "EVA" data processing stream:

- Rotation to principal coordinates. The inversion algorithms presume that we have acquired a true geologic dip profile. In reality, geologic dip is often difficult to define, and seldom known prior to acquisition. However, because we have acquired full tensor data we can rotate our data to the geologic dip direction after acquisition.
- Eigenvector processing. 3D structures can introduce complex "rotations" of the electrical currents. These rotations produce effects, such as excessively steep resistivity curves and out-of-range phases, which would be impossible to fit with 2D modeling programs. By relaxing the assumption that the electric and magnetic fields are orthogonal, eigenvector analysis provides a unique and trivial methodology for simplifying complex 3D data.
- 1D inversion for curve fitting. Real data are often noisy, and inconsistent. Out-of-range phases are a typical example of features seen in real data that can not be fit using 2D inversion. It is often best to make use 1D inversion to make interpretative decisions about how to "best" fit the data, rather than letting the 2D inversion thrash trying to fit inconsistent data.

Once these data processing techniques have been completed the data are inverted. Generally, two inversions of the MT data are done. The first inversion uses an approach (a model norm) that explicitly looks for the "smoothest" model consistent with the data. This approach essentially finds the minimal subsurface structure consistent with the data. The second inversion uses an approach (a model norm) that looks for a model most consistent with the known geology.

For the geologically constrained inversion we use a proprietary approach developed by Dr. Phil Wannamaker. This approach uses the geologic constraints as a target, while not imposing any intrinsic smoothing on the inversion. The approach finds the maximum structural information, at the risk of sometimes including structure not required by the data. It represents an effort to extract the maximum exploration information from the data.

Both approaches are valid, and important. A smooth model approach to inversion can be viewed as finding the least possible useful exploration information. However, it does provide an independent assessment of what the data actually require. The geologically constrained inversion will provide a much sharper subsurface image. But it will also reproduce the known geology where the data does not require a change to the model. Without an independent smooth model inversion it can be hard to determine whether a geologically constrained inversion has confirmed the geologic interpretation, or simply doesn't have any information either way.

REFERENCES

Orange, A. S, 1989. Magnetotelluric exploration for hydrocarbons: Proceedings of the IEEE, 77, 287–317.

Vozoff, K., 1972. The Magnetotelluric method in the Exploration of Sedimentary basins. Geophysics, 37, 98-141.

APPENDIX F: DC/IP THEORY

INTRODUCTION

The resistivity is among the most variable of all geophysical parameters, with a range exceeding 10^6. Because most minerals are fundamentally insulators, with the exception of massive accumulations of metallic and submetallic ores (electronic conductors) which are rare occurrences, the resistivity of rocks depends primarily on their porosity, permeability and particularly the salinity of fluids contained (ionic conduction), according to Archie's Law. In contrast, the chargeability responds to the presence of polarizeable minerals (metals, submetallic sulphides and oxides, and graphite), in amounts as minute as parts per hundred. Both the quantity of individual chargeable grains present, and their distribution within subsurface current flow paths are significant in controlling the level of response. The relationship of chargeability to metallic content is straightforward, while the influence of mineral distribution can be understood in geologic terms by considering two similar, hypothetical volumes of rock in which fractures constitute the primary current flow paths. In one, sulphides occur predominantly along fracture surfaces. In the second, the same volume percent of sulphides are disseminated throughout the rock. The second example will, in general, have significantly lower intrinsic chargeability.

More detailed descriptions on the theory and application of the IP/Resistivity method can be found in Van Blaricom (1992) and Telford et al. (1976).

HALVERSON-WAIT CHARGEABILITY

The Titan-24 DCIP chargeability decays are described using the Halverson-Wait spectral model (Halverson et al., 1981), which is not well known, but is similar to the Cole-Cole model proposed by Pelton et al. (1978) which is a simple relaxation model that fits complex (frequency-dependant) resistivity results.

The time domain chargeability, originally proposed by Siegel (1959), is defined (Telford et al., 1976) as

$$M = \frac{1}{V_C} \int_{t1}^{t2} V(t)\,dt$$

Where $V(t)$ is the residual or secondary voltage at a time t, that is decaying after the current is cut off, between time t_1 and t_2, with the steady voltage V_C during the current flow interval. The ratio $V(t)/V_C$ is expressed in millivolts per volt.

In the frequency domain, the "frequency effect" is defined as:

$$fe = (\rho_{DC} - \rho_{AC}) / \rho_{AC}$$

Where ρ_{DC} and ρ_{AC} are apparent resistivities measured at d.c. and "very high" frequency, usually in the 0.1 to 10 Hz range.

The Cole-Cole model for the chargeability m, as defined by Pelton et al. (1978) is given by the following:

$$Z(\omega) = R_0\left[1 - m\left(1 - \frac{1}{1+(i\omega\tau)^C}\right)\right]$$

Where ***Z(ω)*** is the complex impedance, R_0 is the DC resistivity, ***m*** is the chargeability in volts per volt, ***ω*** is the angular frequency in Hz, τ is the time constant in seconds, and ***c*** is the frequency dependence (unitless). The latter two physical properties describe the shape of the decay curve in time domain or the phase spectrum in frequency domain, and commonly range between 0.01s to +100s and 0.1 to +0.5, respectively (Johnson, 1984).

The Halverson-Wait model was proposed by Halverson et al. (1981) as an extension to the Wait (1959) model of the impedance of "volume loading" of spheres, given by:

$$Z(\omega) = \frac{\rho}{G}\left[1 - 3v\left(1 - \frac{3\delta}{1+2\delta}\right)\right]$$

Where ***G*** is a geometric factor, ***ρ*** is the resistivity of the media, ***v*** is the volume loading (the volume fraction of chargeable "spheres"), δ is the sphere surface impedance. The Wait model was designed to provide an explanation of the differences in the shape of decay curves from different polarizeable targets, but does not describe very well the physical attributes of the rocks.

The Halverson-Wait model expands the Wait coated sphere IP model to include a new formulation of the sulphide-rock interface impedance, based on field studies and laboratory tests on samples. It is closely correlated to the Pelton et al. (1978) Cole-Cole model and is given by:

$$Z(\omega) = \frac{\rho}{G}\left[1 - 3v\left(1 - \frac{3/2}{1+r[i\omega]^K}\right)\right]$$

Where ***r*** is the sphere radius and is equivalent to τ - the Cole-Cole time constant ($r = \tau^K$). The ***v*** volume loading compares well to ***m*** – the Cole-Cole chargeability (see equation below) – and the exponent ***k*** is equal to ***c*** - the Cole-Cole frequency dependence (Halverson et al., 1983). For sulphide systems, the *r*-factor reflects the size or interconnection of the sulphide grains and the *k*-factor reflects the electrical characteristics of the sulphide surfaces. An example of time domain Halverson-Wait model responses is shown in Figure G.1.

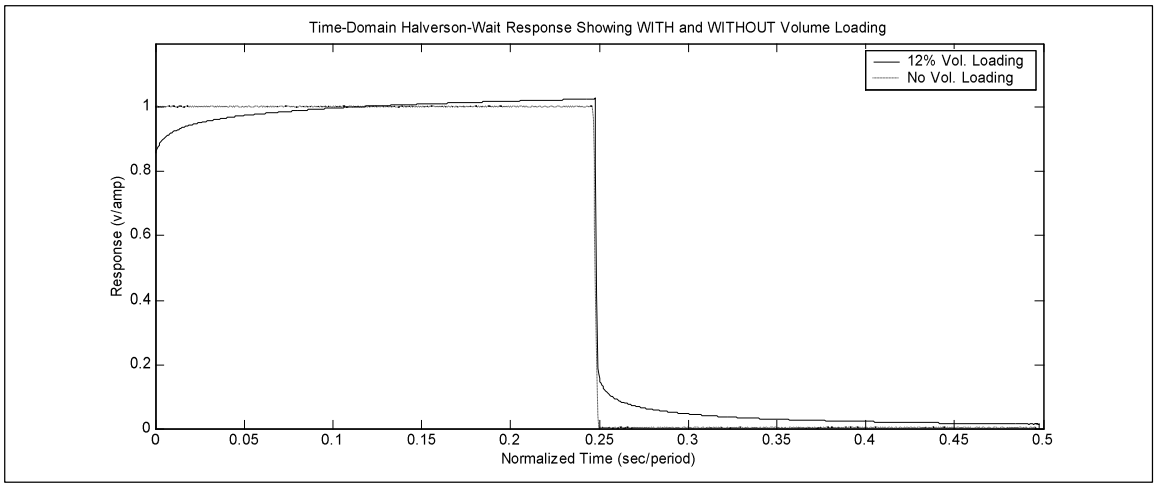

Figure G.1: Polarizeable versus Non-Polarizeable TDIP Response using Halverson-Wait Model

In practice the Titan chargeability decays are fit to a Halverson-Wait model. In order to solve for the volume loading *v*, the *r*-factor and *k*-factor are set to the standard (typical) Halverson-Wait values of 1.0 and 0.2, respectively. In the Halverson-Wait model the theoretical PFE (for infinite bandwidth), which equates to the theoretical chargeability in the Cole-Cole equation, is thereby defined by the volume loading:

$$PFE_0 = m_0 = \frac{9v}{(2+3v)}$$

and ***m*** is output in units of milliradians.

INVERSION THEORY

An excellent overview and introduction to both the philosophy and use of inversions in geophysics is available on the University of British Columbia (UBC) website (http://www.geop.ubc.ca/ubcgif/; Oldenburg et al., 1998).

Several points, detailed on the website, are crucial to understanding the Titan-24 approach to exploration:

- Inversion is a powerful 'tool', not a 'solution'.
- Inversion is not normally "unique". Given noisy and incomplete data of inherently limited resolution there are usually an 'infinite' range of models that 'fit' the data equally well. Recognition of this inherent non-uniqueness is why inversion must be viewed as a tool rather than a solution. Understanding and exploration of this non-uniqueness is an important part of the interpretive process.
- Inversion finds a model that 'fits' the data. The precise definition of 'fit' can be critical in the actual model that is found.
- The inversion depends on the data, and the data errors. The importance of the data errors is often overlooked.
- Inversion depends on a "model norm" – the mathematical definition of which model the inversion should try to find. This definition is almost as important as the actual data in

determining the final inversion model.

Mathematically, inversion is the process of minimizing a function. The choice of which function to minimize ultimately defines the inversion model. Schematically, this function might be expressed:

$$\phi = \phi_d + \beta \phi_m = \text{(misfit)} + \beta\,\text{(model norm)}$$

$$0 < \beta < \infty \quad \beta \text{ is a constant}$$

This defines a function to be minimized that consists of some function that minimizes the data misfit, combined with some function that finds a "smooth" model. Beta represents a relative weighting between fitting the data and smoothing the model.

Clearly, the data misfit function must be defined in more detail. One approach might be:

$$\phi_d = \sum_{i=1}^{N} \left(\frac{F_i[m] - d_i^{obs}}{\varepsilon_i} \right)^2$$

This function defines the data misfit as the sum of the individual misfits squared, normalized by the errors associated with each data point. It is a very common, and stable, definition of the data misfit.

An important point not made on the UBC website is that the errors depend on many factors. The most common measure of data errors is simply the repeatability of the voltage and current measurements in the field. This may be misleading as there are also "errors" associated with electrode positioning, geologic complexity (2D vs 3D, but also coupling of shallow and deeper structure), and errors in the numerical calculation of model responses and inversion.

Another point not sufficiently detailed on the UBC site is the importance of not overestimating the data errors and fitting the data as closely as possible. Most geophysical techniques, but particularly electrical techniques, have large responses to shallow structure. This is expressed as "pant legs" in DC/IP, or "statics" in MT. The response to deep structure is generally a very subtle component of the data, compared to the sensitivity to shallow structure. Without excellent data, and an excellent match between the data and model response, the deep structure will not be imaged to the degree necessary for commercial exploration.

The model misfit function must also be defined in more detail. One of the most flexible definitions is the one used by UBC:

$$\phi_m(m,m_0) = \alpha_s \int_{vol} (m-m_0)^2 dv + \alpha_x \int_{vol} \left(\frac{\partial (m-m_0)}{\partial x} \right)^2 dv + \alpha_z \int_{vol} \left(\frac{\partial (m-m_0)}{\partial z} \right)^2 dv$$

In this definition there are three components to the "model norm" (or "smoothness" constraint, or "regularization"), each of which contains an α constant (α_S, α_X, α_Z) that are commonly referred to as "alpha parameters". The first component is simply an overall difference between the model and a "target" model, the second component is a horizontal smoothness, and the third component is a vertical smoothness. The three "alpha" parameters (α_S, α_X, α_Z) represent a relative weighting of each component. A fourth variable, m_0, refers to the starting or reference model – either a half-space or geophysical constraint – that also has a profound influence on the model-misfit.

The UBC website provides an excellent example of the importance of selecting an appropriate "model norm", reproduced in Figure G.2

In this example the expected response of the top figure was computed. These 'data' were then inverted six times, using different "model norms" (α_S, α_X, α_Z, m_0). The lower six figures show the range of valid inversion models that can be produced. Note that six of these models are essentially mathematically equivalent, they all "fit" the data.

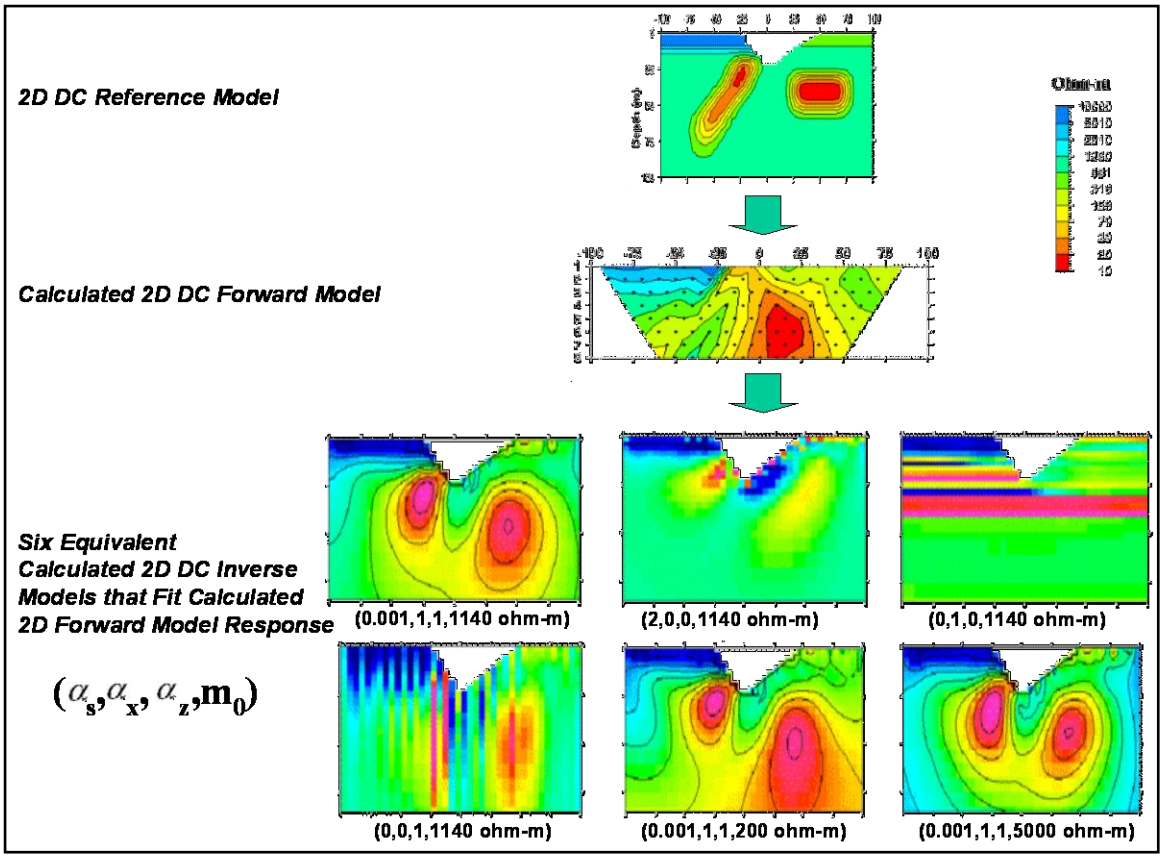

Figure G.2: Effects of Model Norm and Starting Model on Inversion Results (modified after Oldenburg, et al.,1998).

An important philosophy, driving much of the academic communities approach to inversion for the last two decades, is that the "best" model is the "smoothest" model consistent with the data. There are good reasons for taking this approach. However, from an exploration viewpoint this philosophy can be rephrased to "find the model with the least exploration value" – perhaps not reflecting the real goal of an exploration program.

Recently, several groups have taken major steps towards developing inversion approaches more tuned to exploration needs. Instead of using "smooth" model norms, they are being replaced with "focused (minimum transition zone) inversion, or smoothing to a geologic "target" model.

For exploration smoothing to a geologic target model makes sense. It requires good geologic control, and some understanding of the rock physical properties. There are three drawbacks to the geologic target approach:

- The geologic information is incomplete or inaccurate.

- Physical property data are incomplete.
- It is difficult to determine whether the geophysical data support the geologic model, or simply provide no information.

The most sensible approach is to combine smooth model inversion with geologic target inversion. For now, we are focusing on providing inversions using both approaches. It is up to the project geologist and geophysicist to review these inversions and develop a final interpretation.

REFERENCES

1. Halverson, M., Zinn, W.G., McAlister, E., Ellis, R., and Yates, W. (1981). Assessment of results of broad-band spectral IP field tests. In: Advances in Induced Polarization and Complex Resistivity, pp. 295–346, University of Arizona.
2. Johnson, I. (1984). Spectral induced polarization parameters as determined through time-domain measurements. Geophysics, v. 49, pp. 1993-2003.
3. Oldenburg, D., and Li, Y. (1999). Estimating depth of investigation in DC and IP surveys. Geophysics, v. 64, pp. 403-416.
4. Oldenburg, D., and Li, Y. (1994). Inversion of induced polarization data. Geophysics, v. 59, pp. 1327-1341.
5. Oldenburg, D., Li, Y., and Jones, F. (1998). Tutorial: Inversion (Res/IP) Methodology. In: The UBC Geophysical Inversion Facility Tutorials. [On line]. http://www.geop.ubc.ca/ubcgif/tutorials/invtutorial/index.html.
6. Pelton, W., Ward, S., Hallof, P., Sill, W. and Nelson, P. (1978). Mineral discrimination and removal of inductive coupling with multifrequency IP. Geophysics, v. 43, pp. 588-609.
7. Seigel, H. (1959). Mathematical formulation and type curves for induced polarization. Geophysics, v. 24, pp. 547-565.
8. Telford., W.M., Geldart, L., Sheriff, R., and Keys, D. (1976). Applied Geophysics. Cambridge University Press, New York, NY, 860 pp.
9. Van Blaricom, R. (1992). Practical Geophysics for the Exploration Geologist. Nortwest Mining Association, Spokane, WA, 570 pp.
10. Wait, J. (1959). Overvoltage Research and Geophysical Applications. Pergammon Press.

APPENDIX G: PRELIMINARY 2D INVERSIONS

LINE L1 spread 1
TITAN-24 Survey
Minto Mine Project
Capstone Mining Corp - Minto Explorations

Preliminary 2D Inversion

Quantec Geoscience Ltd.
Toronto, Canada

A. Verweerd, Dr. Rer. Nat.

Preliminary
02.08.09

Capstone Mining Corp.
Minto Mine Project

2D DC/IP inversion

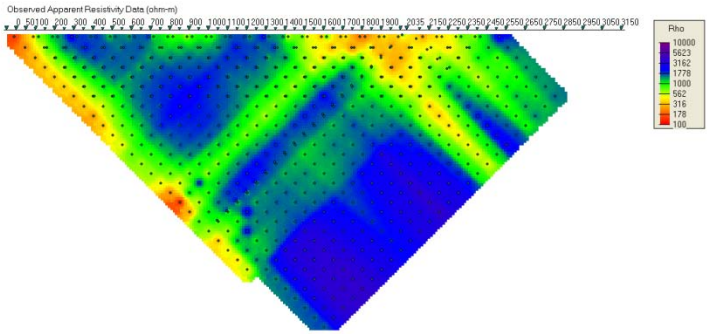

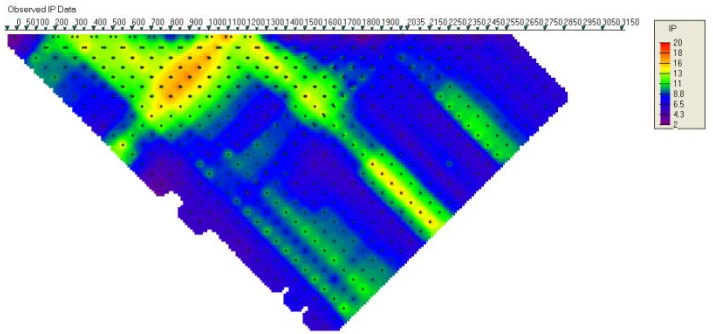

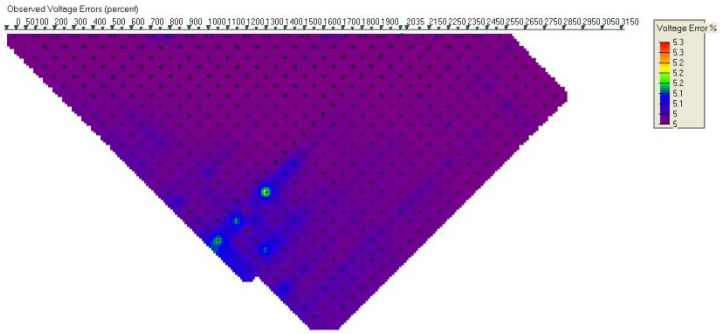

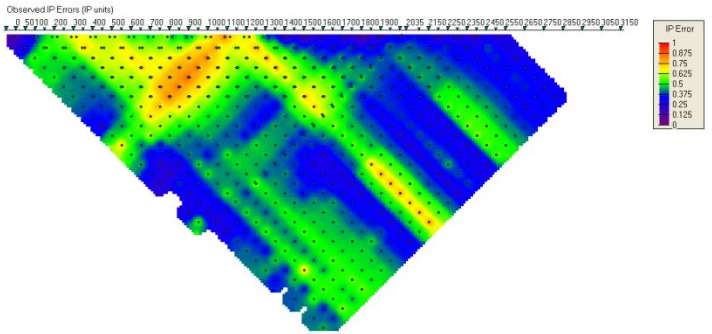

Error assignment:

DC data: Acquisition error + 5%

IP data: Remove acquisition error>25%

if error < 5%, set at 5%, else keep error, outlier rejection

titan24

Quantec Geoscience

Preliminary
02.08.09

Capstone Mining Corp.
Minto Mine Project

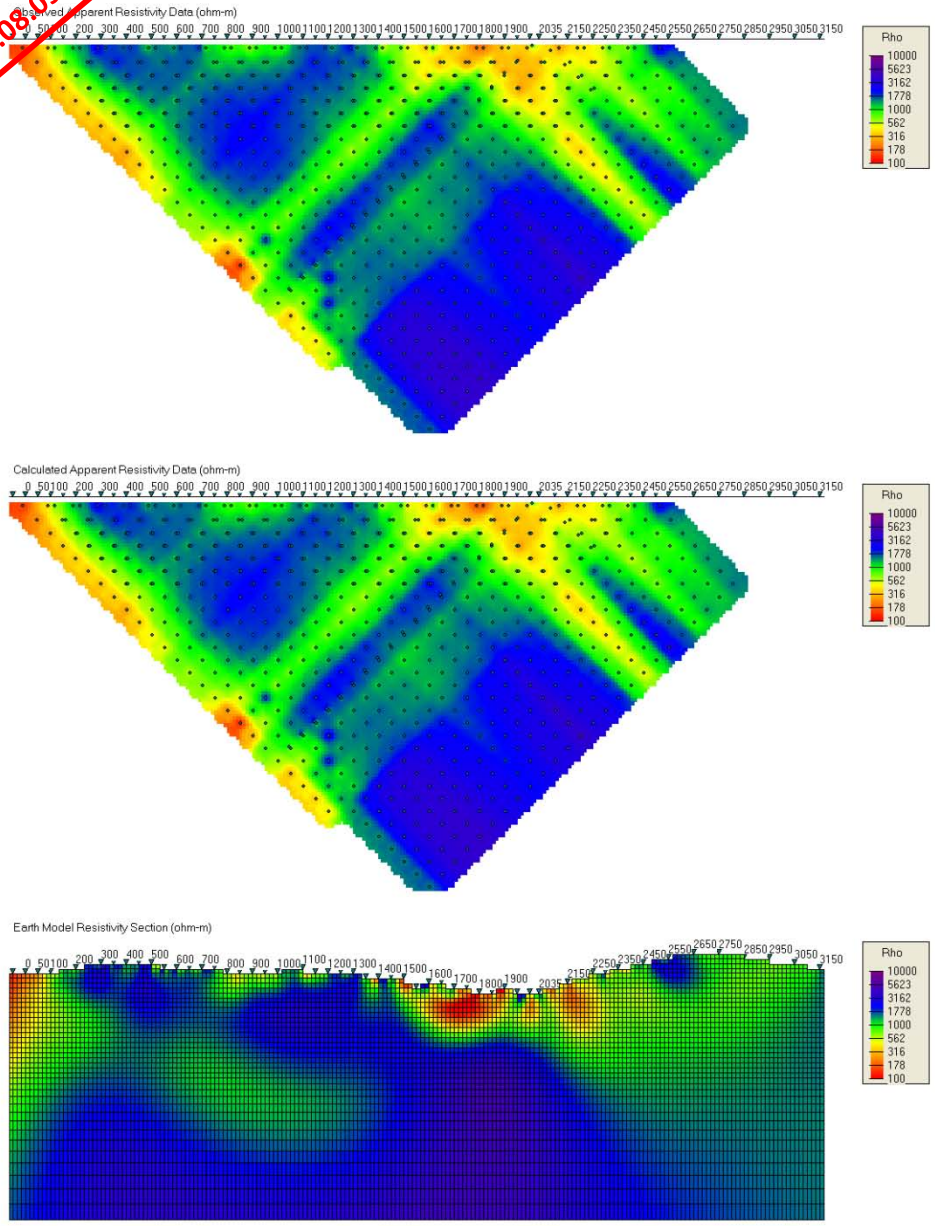

2D DC resistivity inversion results:
N data = 793
Misfit = 7.92998E+02
N iterations = 18

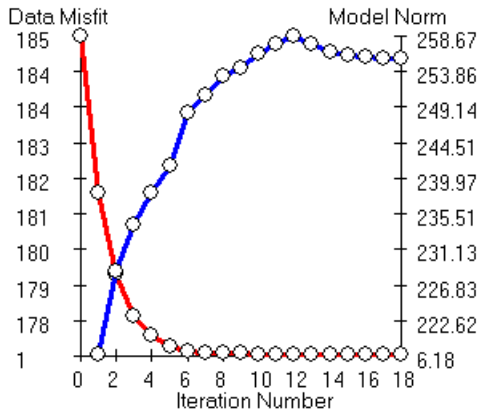

Note: Depth indications are approximate

Preliminary
02.08.09

Capstone Mining Corp.
Minto Mine Project

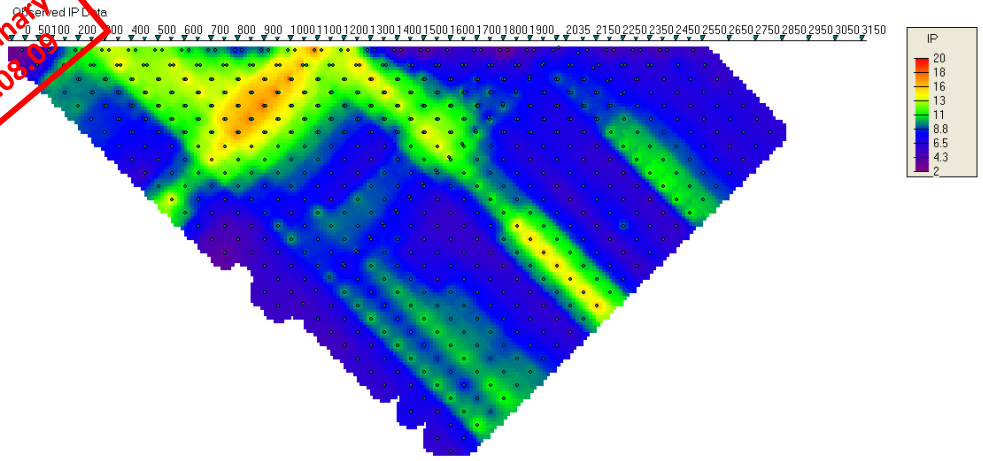

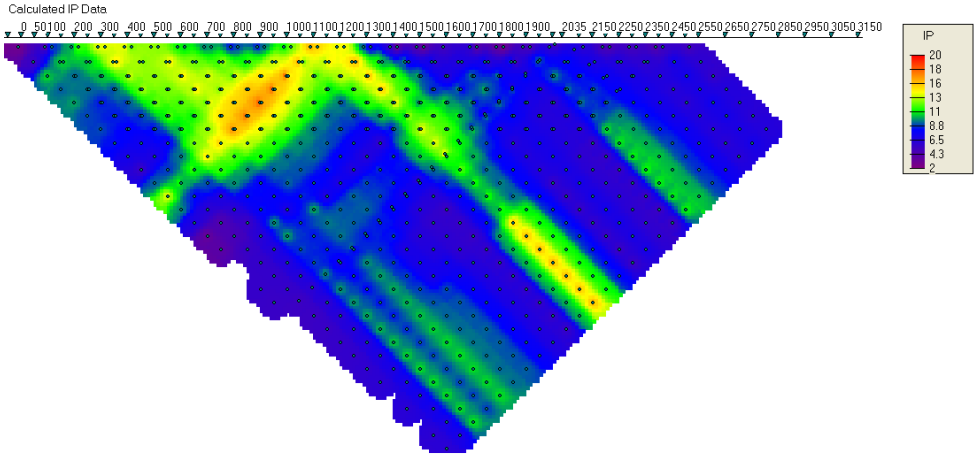

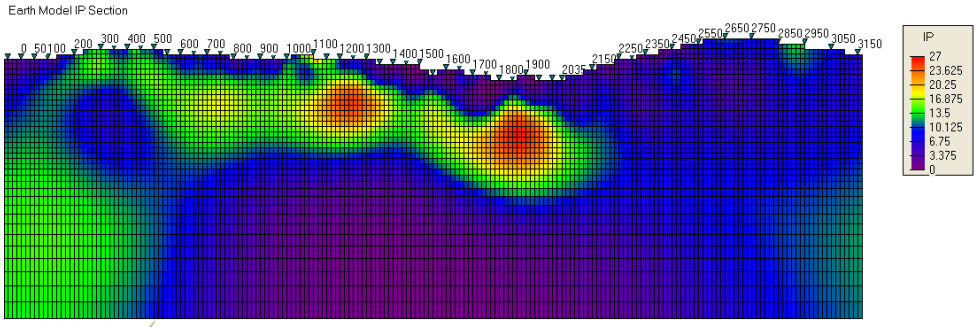

0

500 m

1000m

2D IP chargeability inversion results
smooth model:
data = 746
Misfit = 7.45967E+02
N iterations = 19

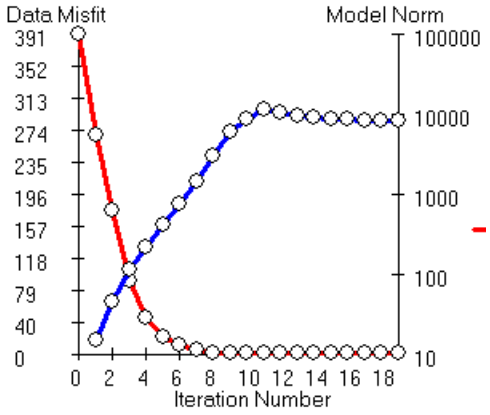

titan24

Note: Depth indications are approximate

Quantec Geoscience

Preliminary
02.08.09

Capstone Mining Corp.
Minto Mine Project

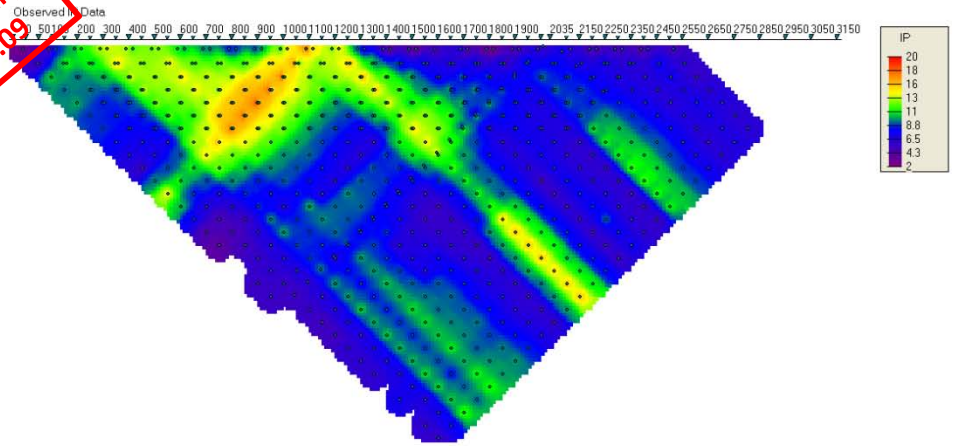

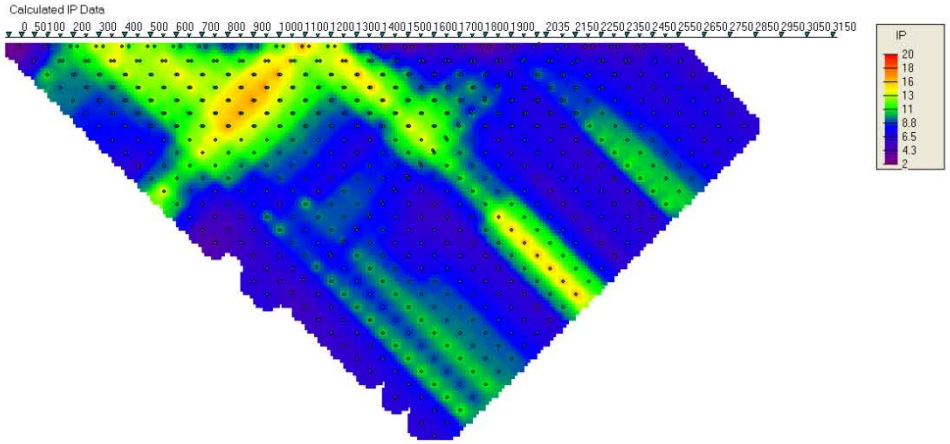

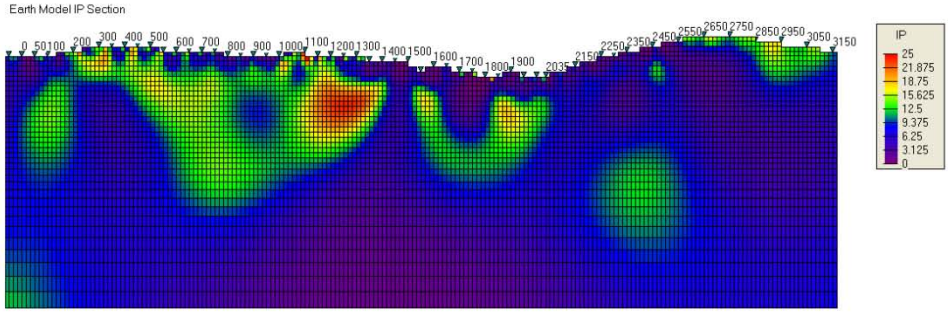

0

500 m

1000m

2D IP chargeability inversion results
Null Conductivity model:
N data = 746
Misfit = 7.46005E+02
N iterations = 40

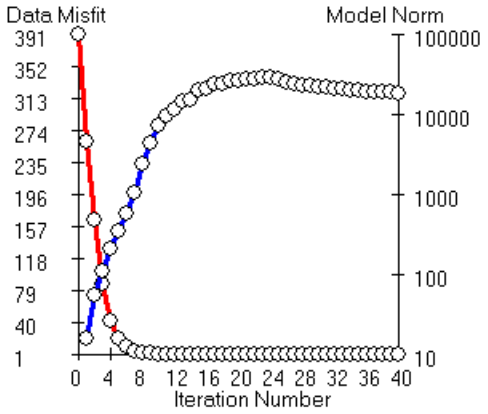

titan24

Note: Depth indications are approximate

Quantec Geoscience

DOI Investigation

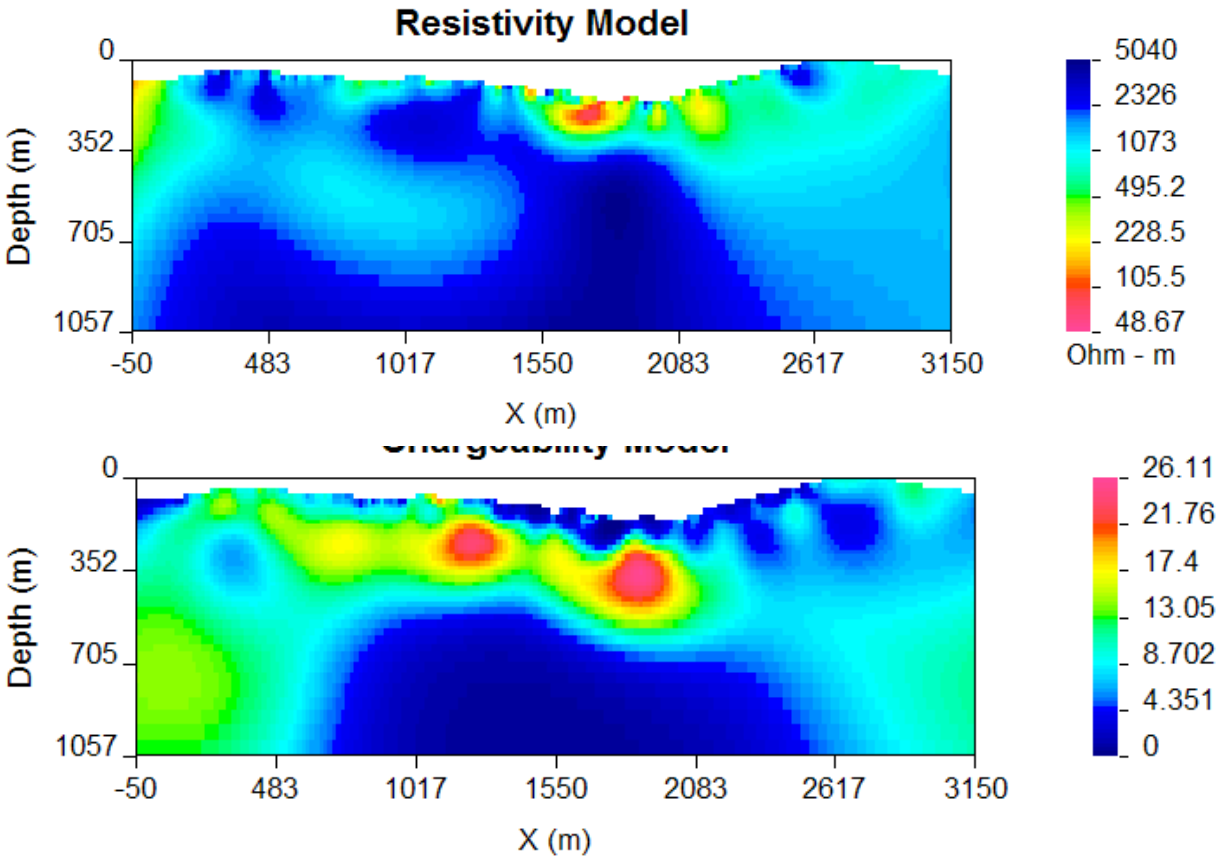

DOI (depth of investigation) is a Tool designed by the UBC-GIF to image the validity of inversion models. It compares two models calculated with different reference models.

Thus creating an image of how regions in the model which are influenced by the choice of reference model and not the actual data.

These zones are indicated with the hatched colours.

For the DC model a 10 kOhm-m and the default reference (average resistivity of the line) was used, in the IP the smooth and null con. Models were compared, a 0.1 cut off value was chosen

See: Oldenburg & Li, "**Estimating depth of investigation in dc resistivity and IP surveys**" GEOPHYSICS, VOL. 64, NO. 2 (MARCH-APRIL 1999); P. 403–416

titan24

Quantec Geoscience

Preliminary
02.08.09

Capstone Mining Corp.
Minto Mine Project

Geosoft Images

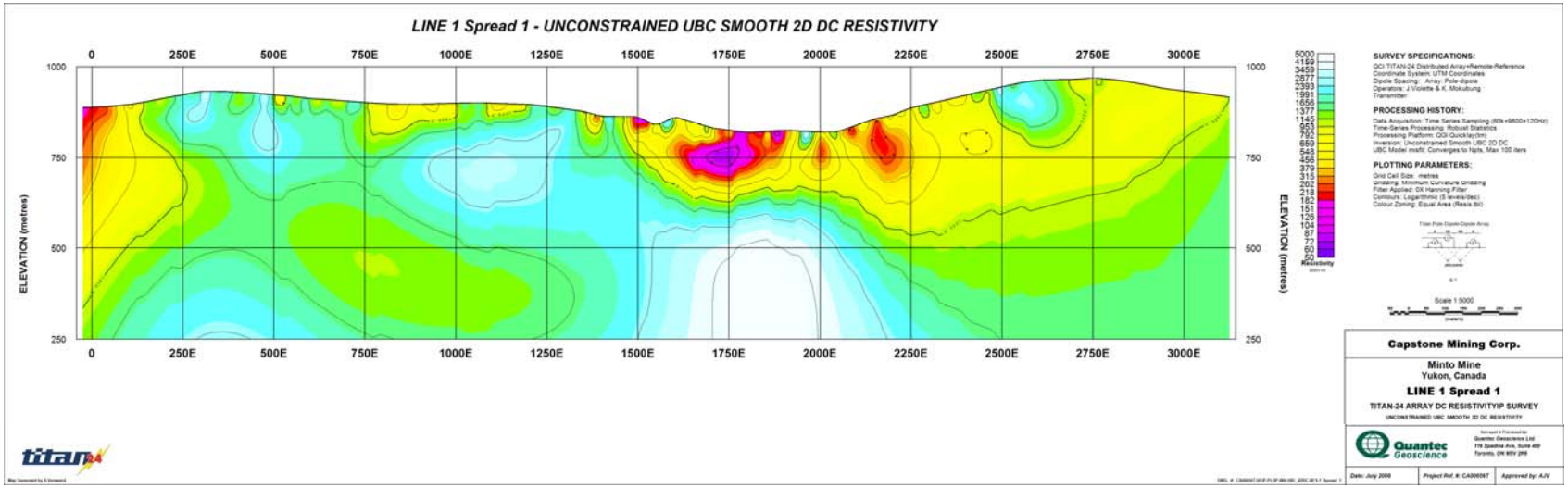

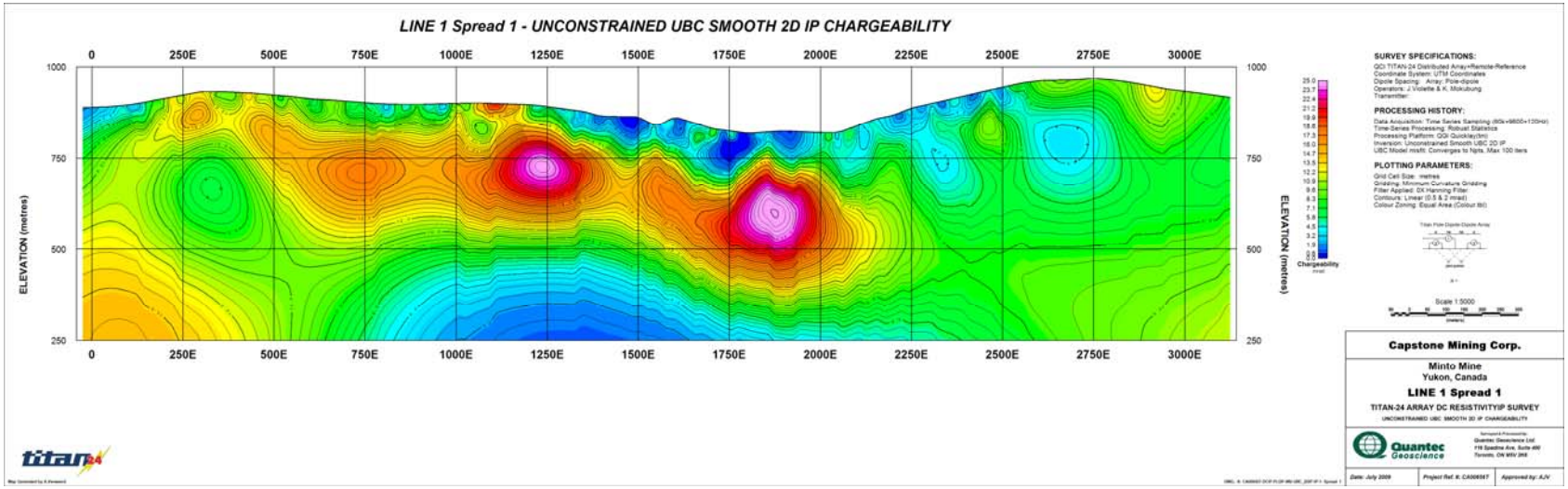

Preliminary
02.08.09

Capstone Mining Corp.
Minto Mine Project

Geosoft Images

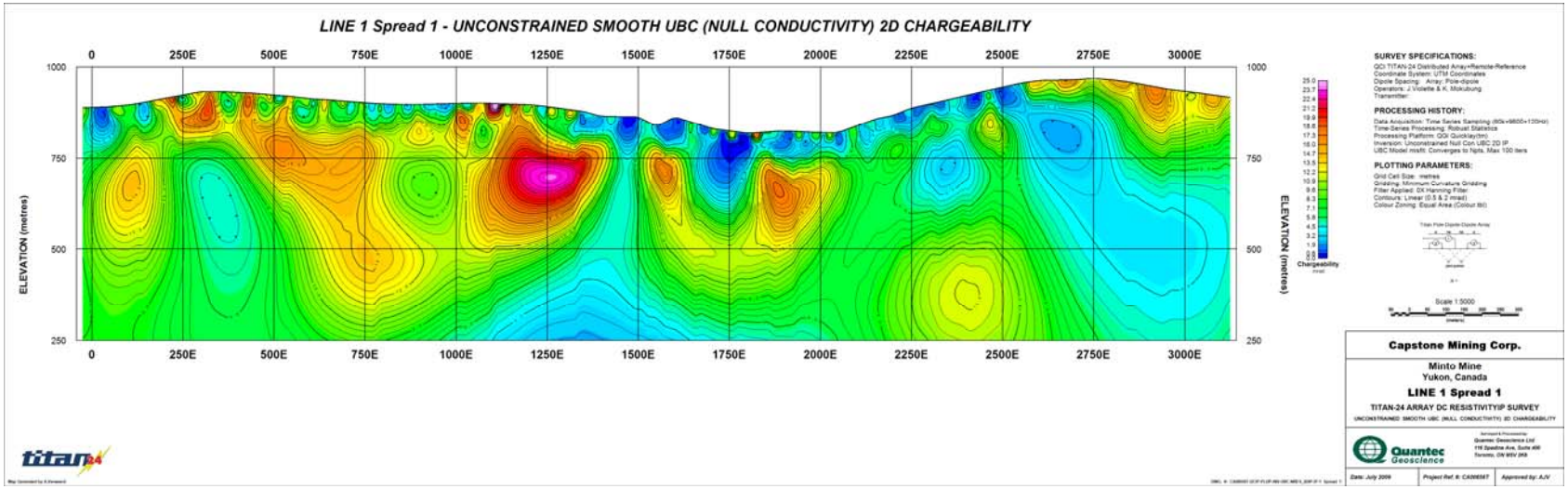

Preliminary
02.08.09

Capstone Mining Corp.
Minto Mine Project

MT inversion

Observed data

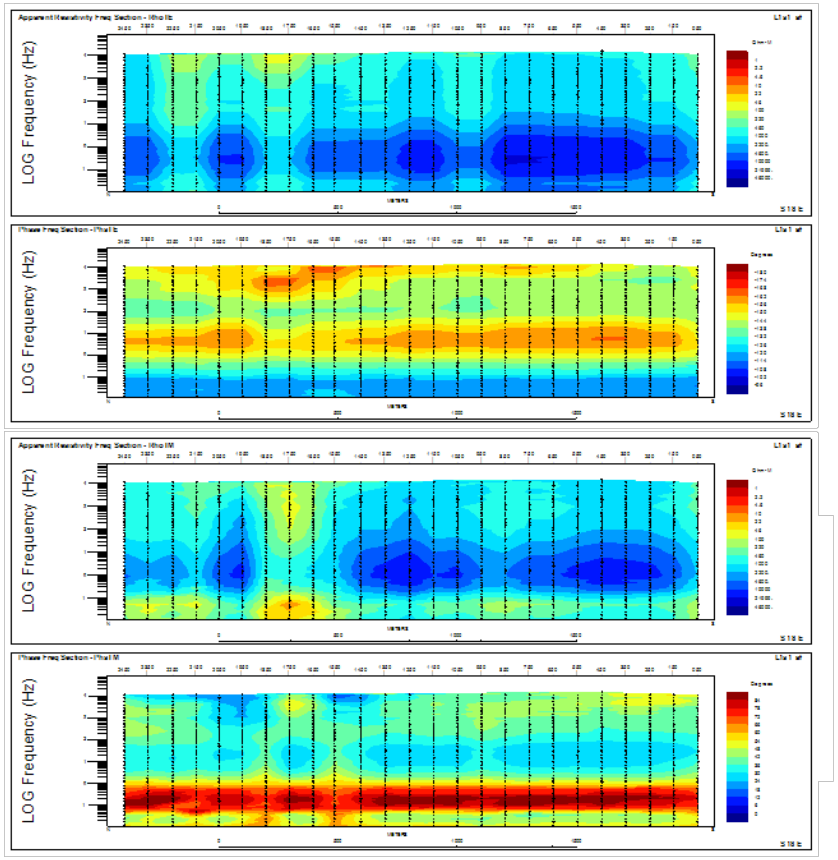

Interpolated data

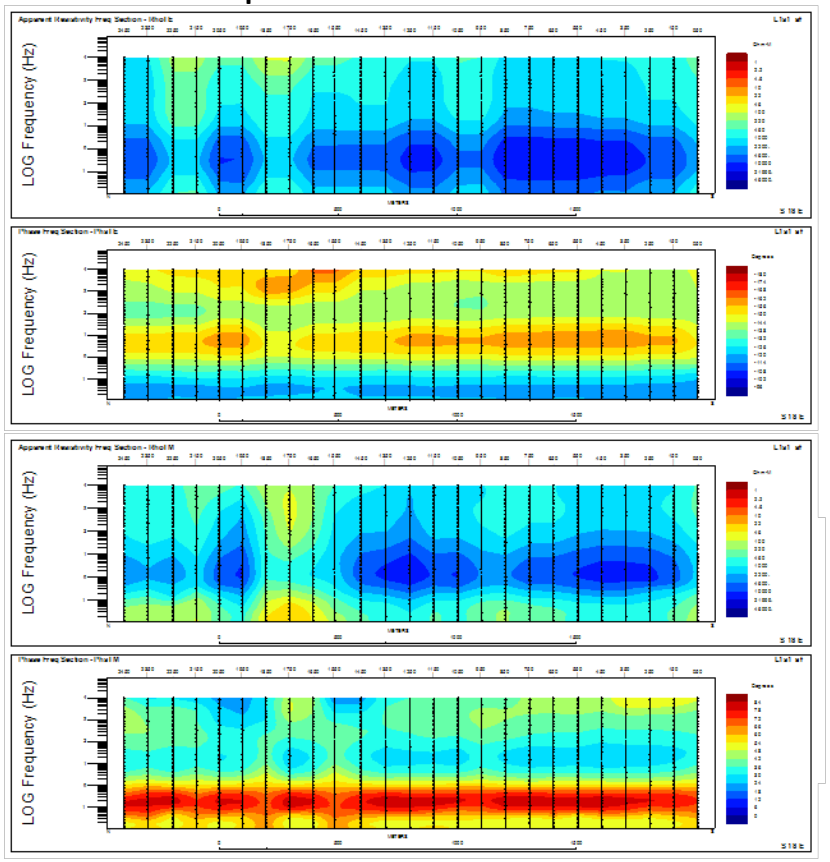

Note: The MT inversion program (GEOTOOLS), has a different plotting convention than the DC/IP inversion program (DCIP2D). Low station numbers are located on the lefts side in the DC/IP images and on the right side in the MT images.

titan24

Quantec Geoscience

Preliminary
02.08.09

Capstone Mining Corp.
Minto Mine Project

1D inversion results

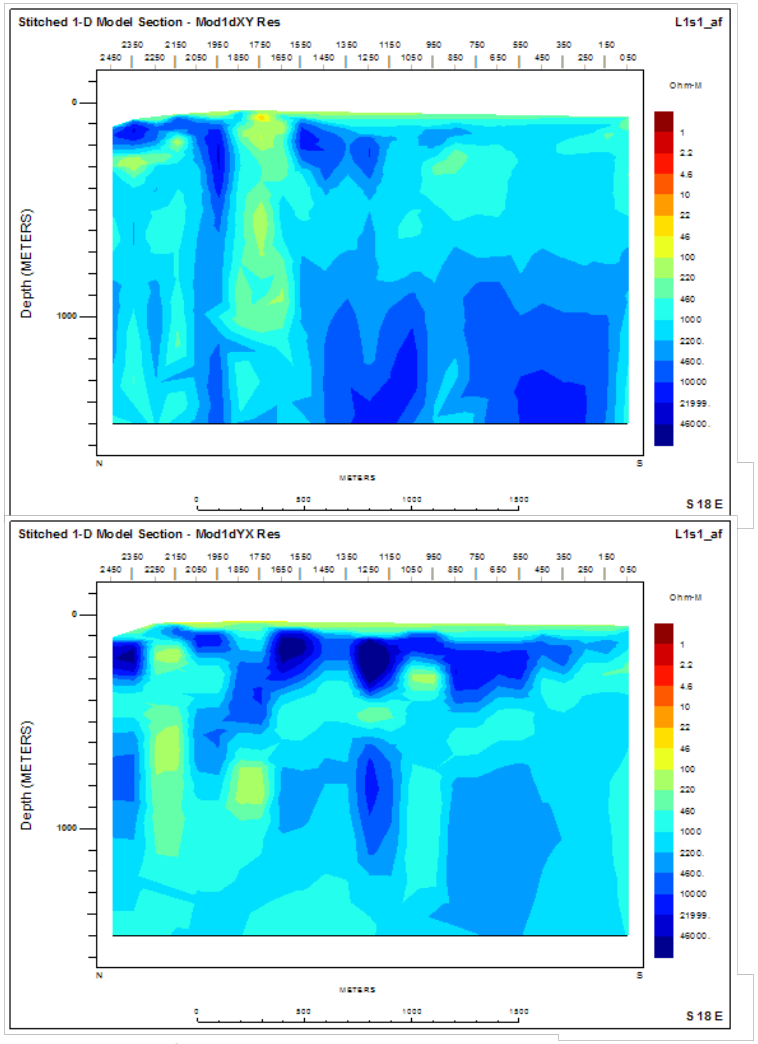

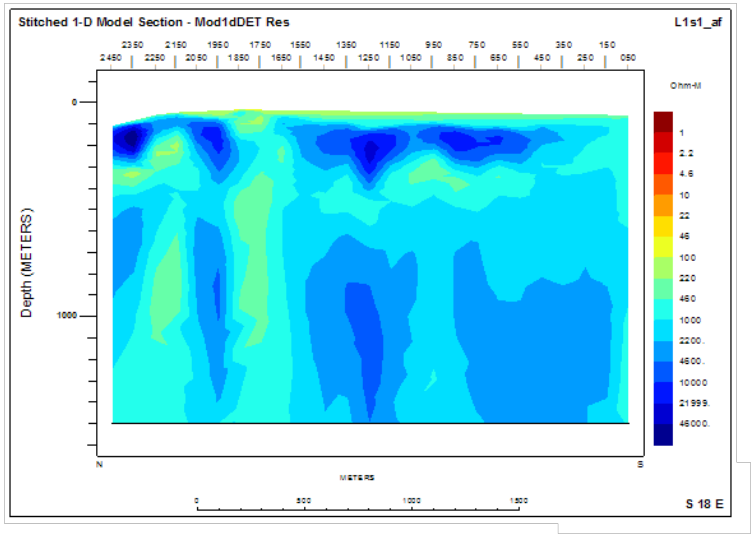

Left top: 1D stitched TE resistivity
Left bottom: 1D stitched TM resistivity
Right top: 1D stitched DET resistivity

titan24

Quantec Geoscience

Preliminary
02.08.09

Capstone Mining Corp.
Minto Mine Project

2D RLM Inversion

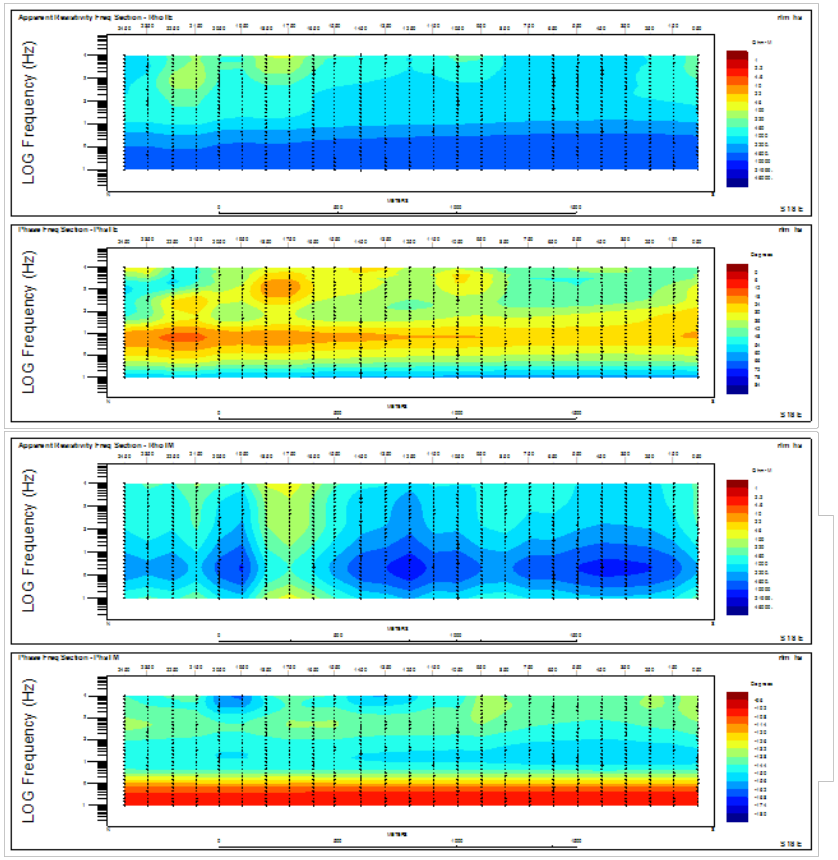

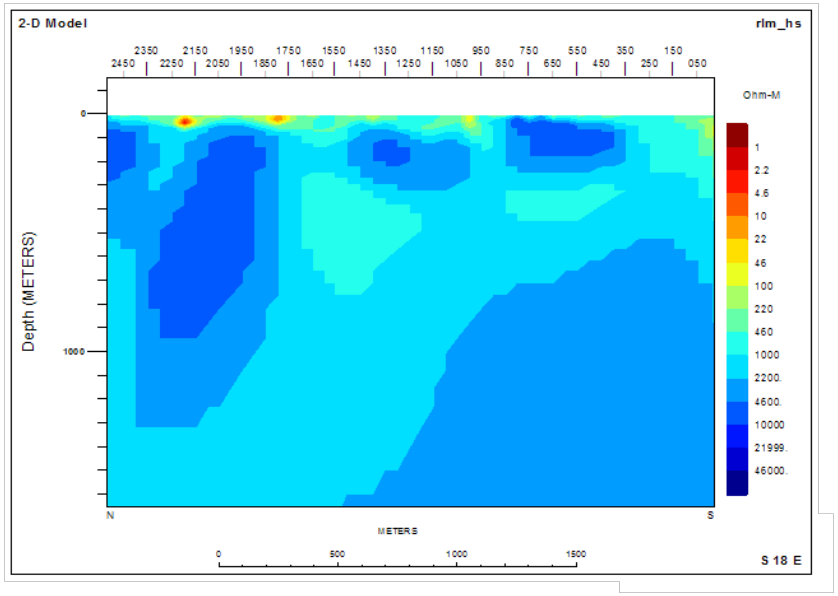

2D RLM TM,TE inversion results:
Starting model: 5000 Ohm-m halfspace
RMS misfit: 0.5609E+01
N iteration: 48

titan24

Quantec Geoscience

Preliminary
02.08.09

Capstone Mining Corp.
Minto Mine Project

2D PW inversion

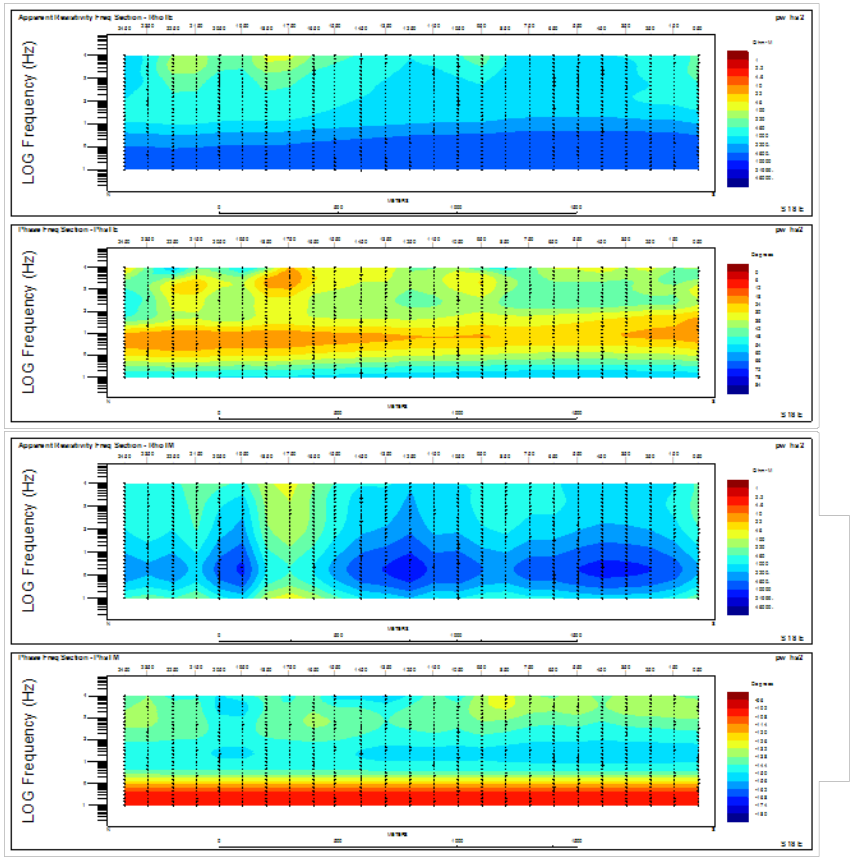

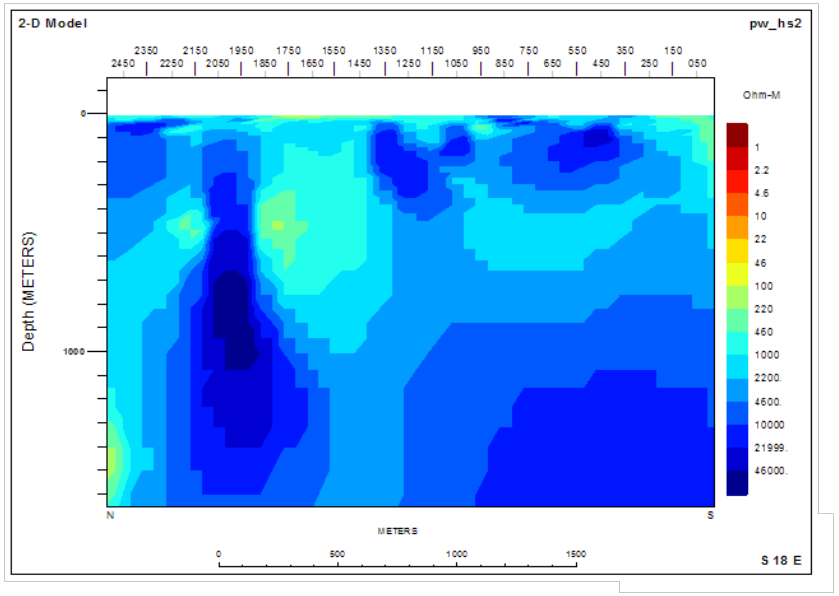

2D PW TM,TE inversion results:
Starting model: 5000 Ohm-m halfspace
RMS misfit: 0.5312E+01
N iteration: 34

titan24

Quantec Geoscience

Preliminary
02.08.09

Capstone Mining Corp.
Minto Mine Project

2D PW inversion

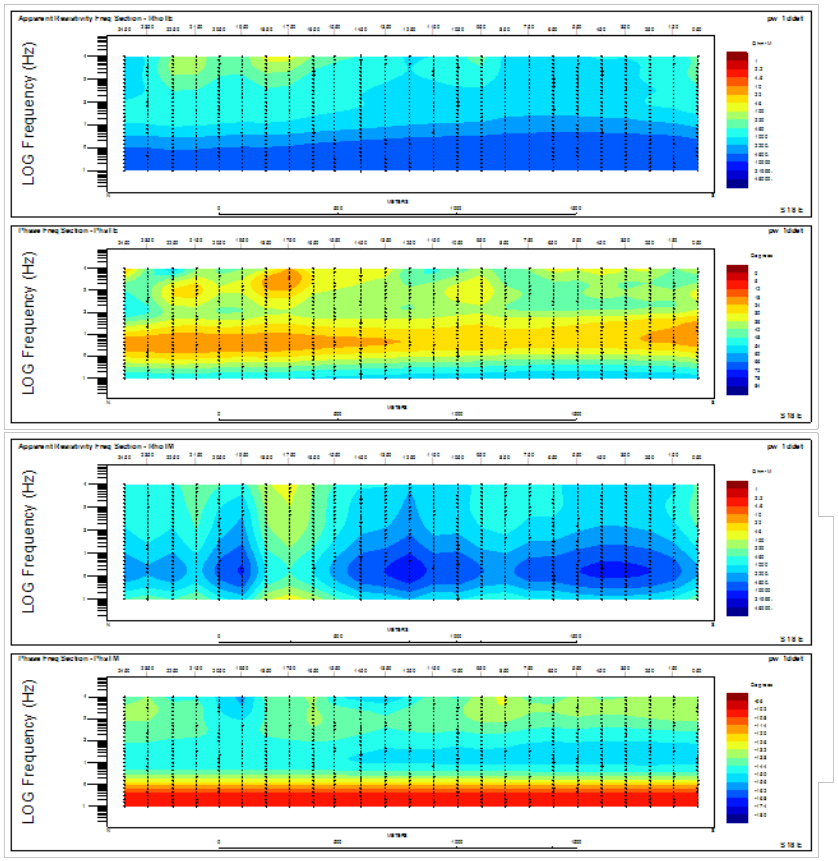

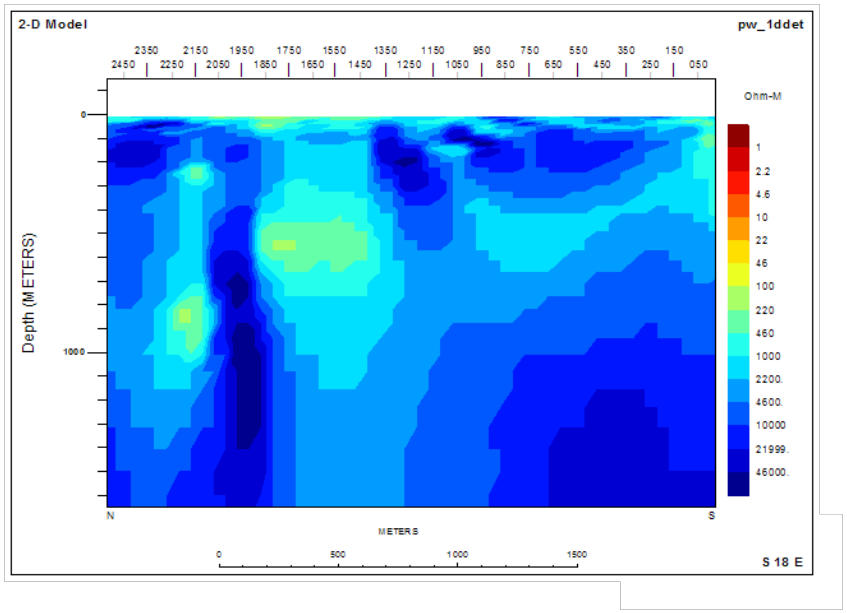

2D PW TM,TE inversion results:
Starting model: Stitched 1D DET
RMS misfit: 0.5207E+01
N iteration: 48

titan24

Quantec Geoscience

Preliminary
02.08.09

Capstone Mining Corp.
Minto Mine Project

Geosoft Images

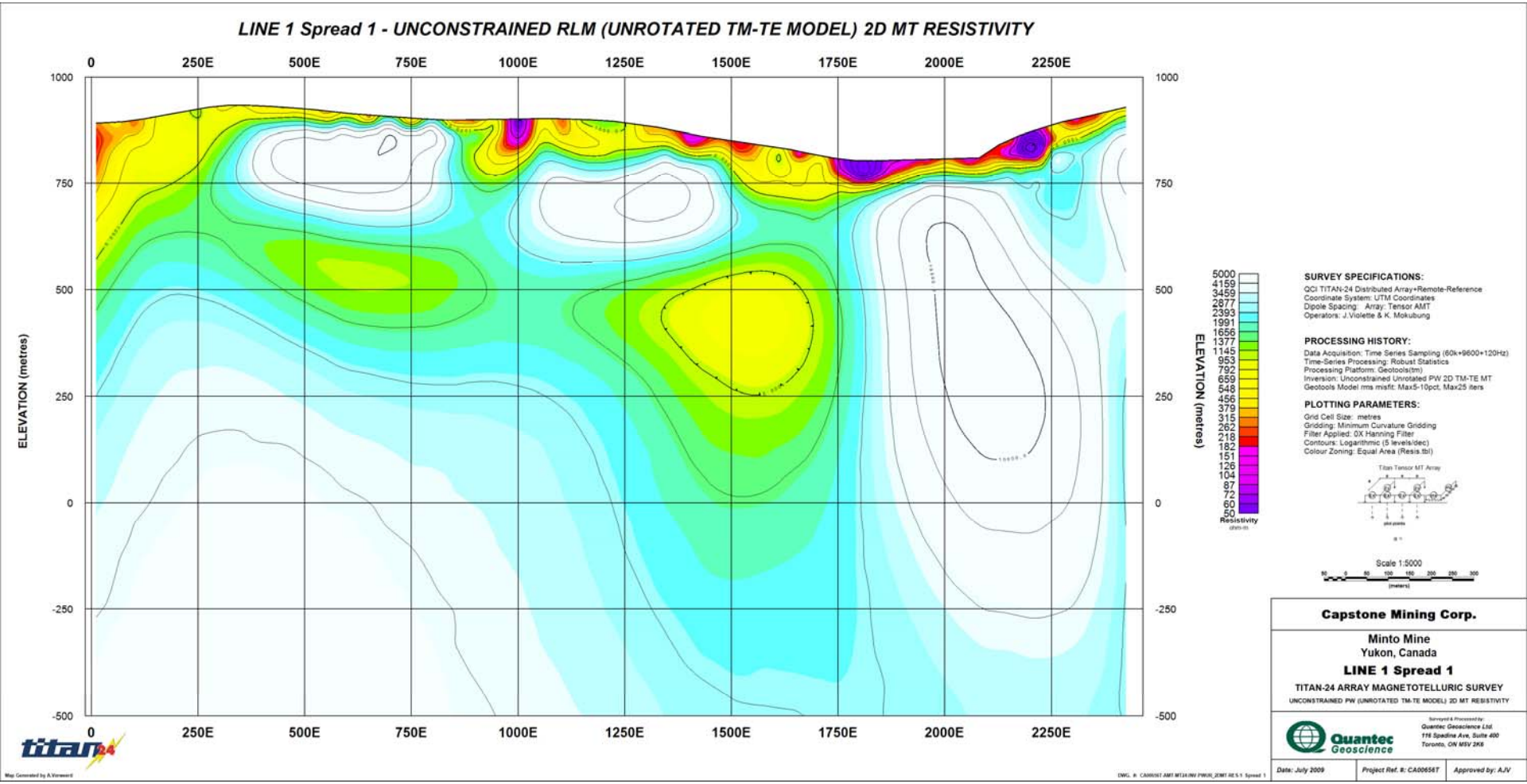

Preliminary
02.08.09

Capstone Mining Corp.
Minto Mine Project

Geosoft Images

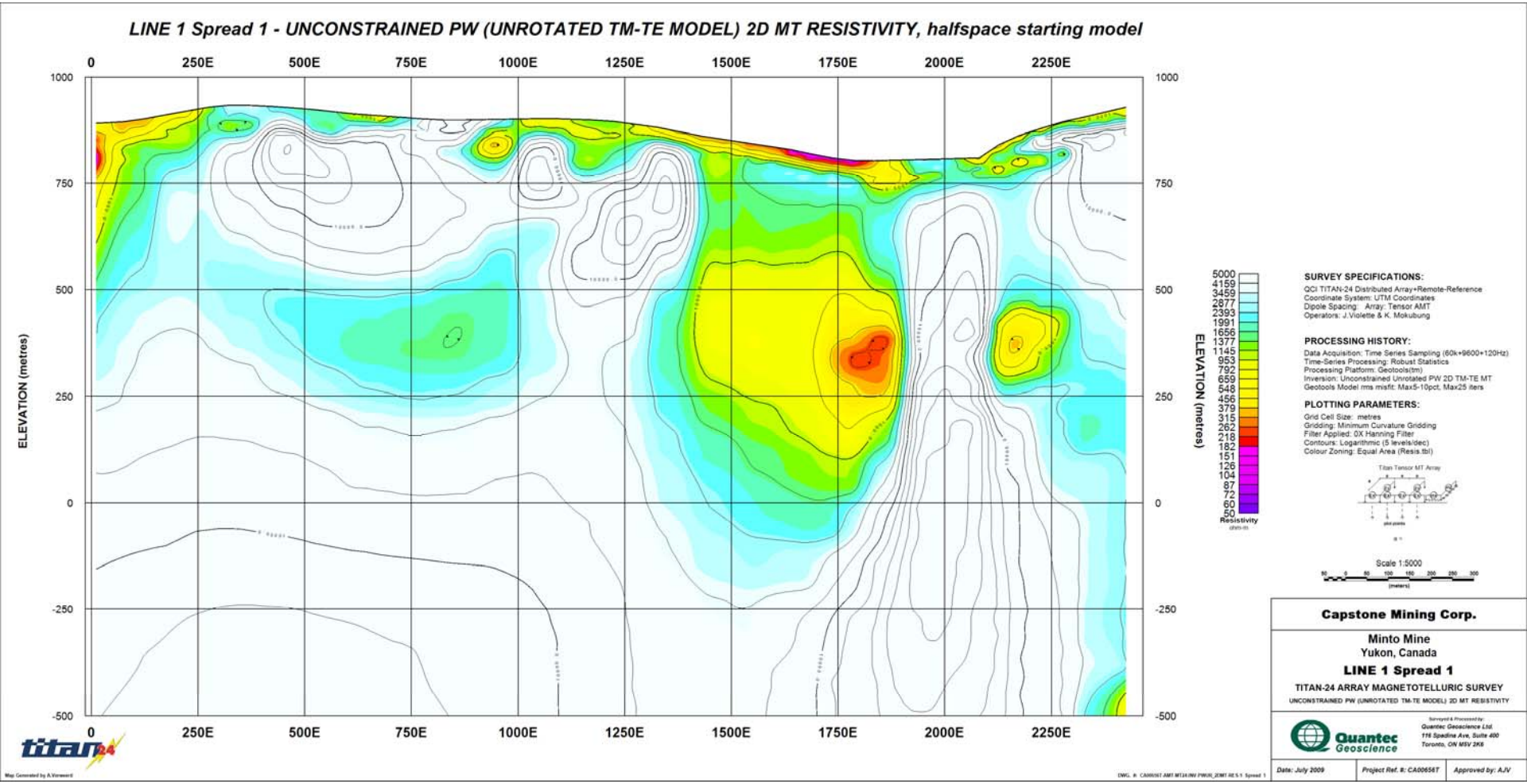

Preliminary
02.08.09

Capstone Mining Corp.
Minto Mine Project

Geosoft Images

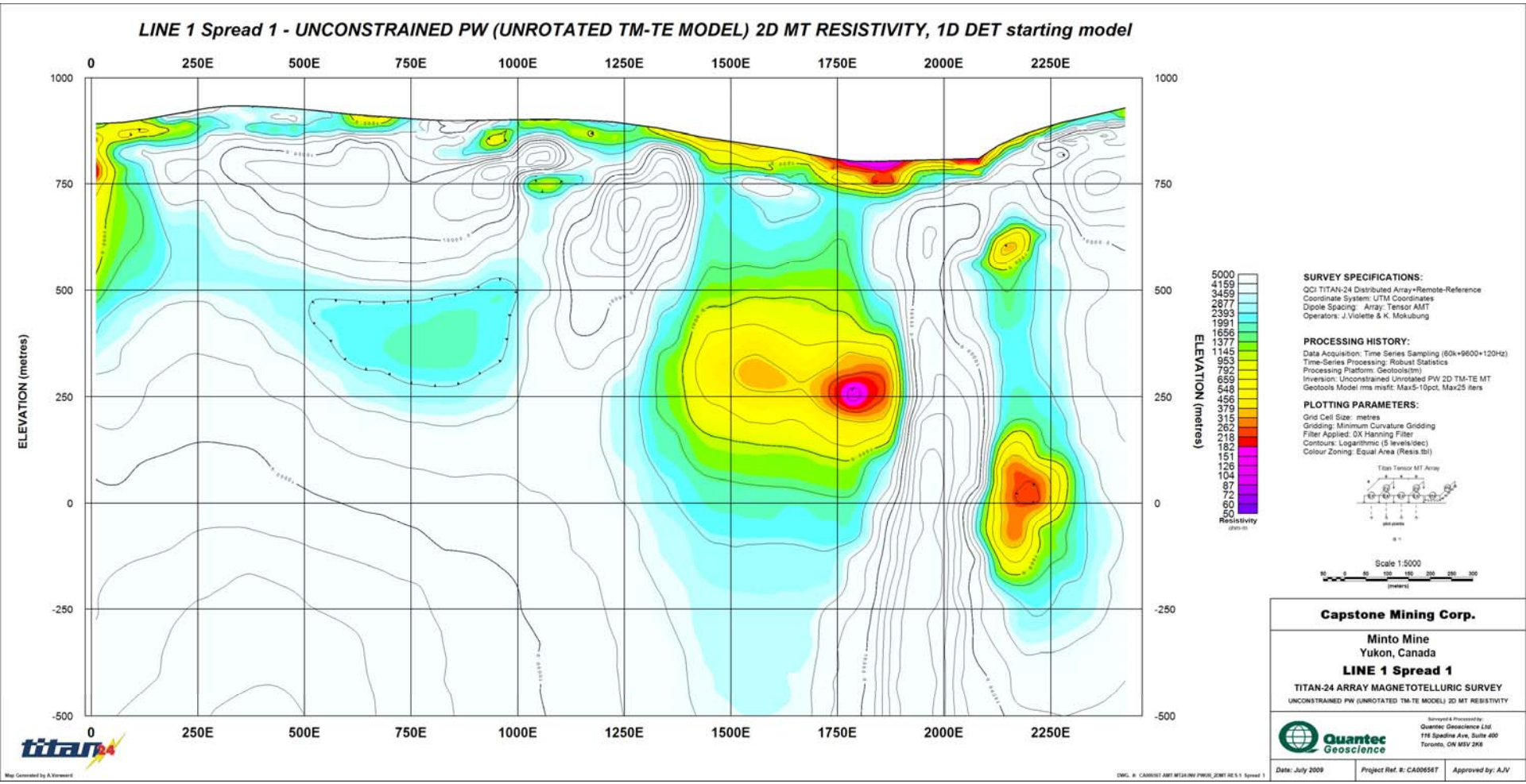

LINE 1 spread 2
TITAN-24 Survey
Minto Mine Project
Capstone Mining Corp - Minto Explorations

Preliminary 2D Inversion

Quantec Geoscience Ltd.
Toronto, Canada

A. Verweerd, Dr. Rer. Nat.

Preliminary
03.08.09

Capstone Mining Corp.
Minto Mine Project

2D DC/IP inversion

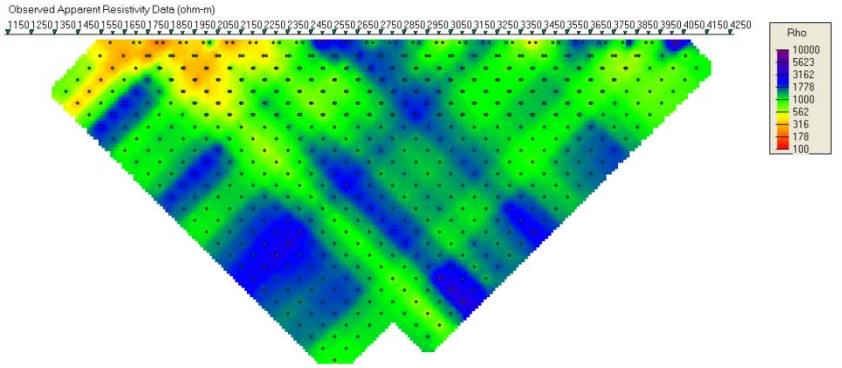

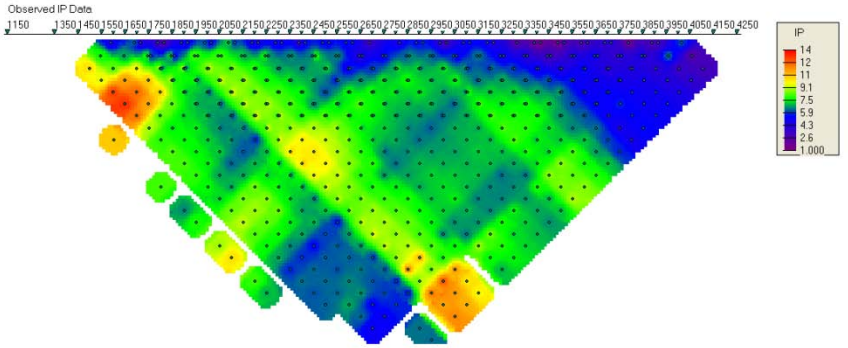

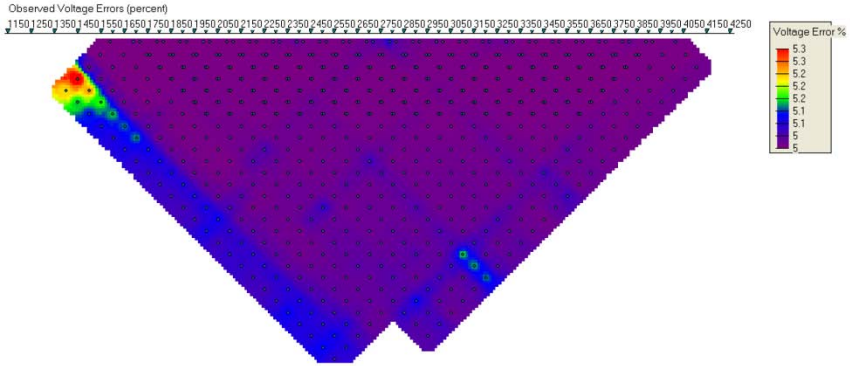

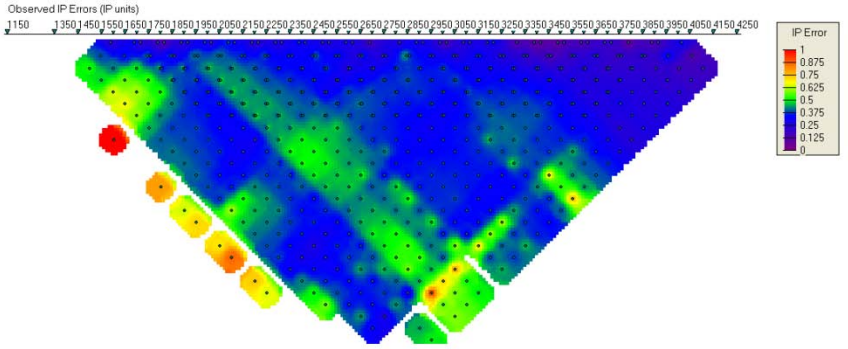

Error assignment:

DC data: Acquisition error + 5%

IP data: Remove acquisition error>25%

if error < 5%, set at 5%, else keep error, outlier rejection

titan24

Quantec Geoscience

Preliminary
03.08.09

Capstone Mining Corp.
Minto Mine Project

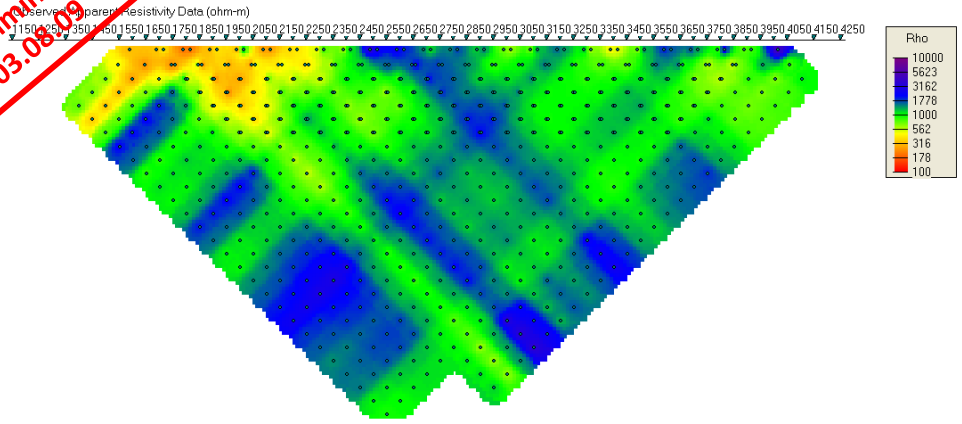

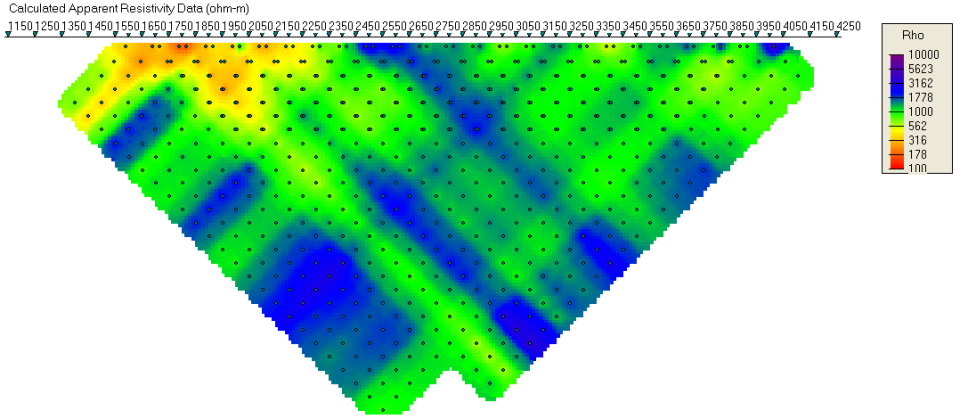

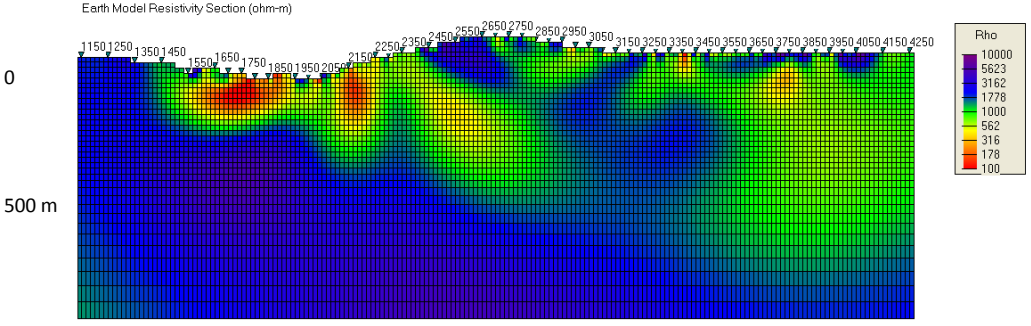

2D DC resistivity inversion results:
N data = 744
Misfit = 7.43564E+02
N iterations = 16

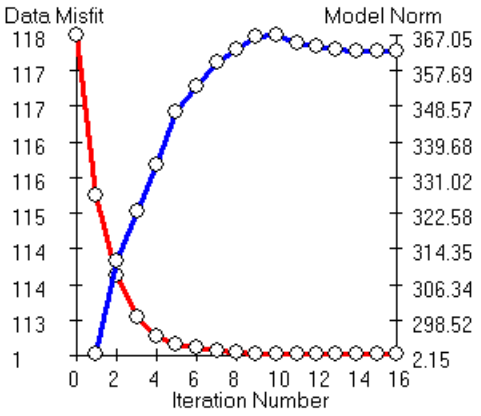

Note: Depth indications are approximate

Capstone Mining Corp.
Minto Mine Project

Preliminary
03.08.09

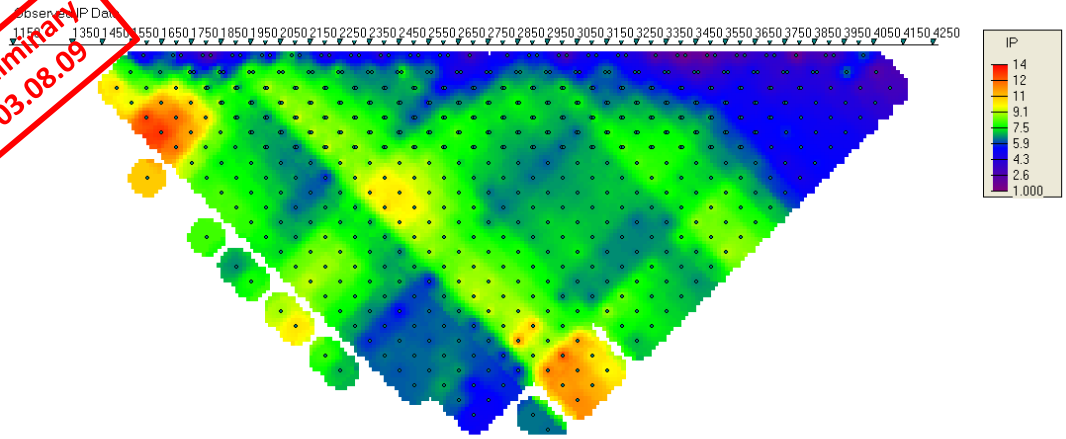

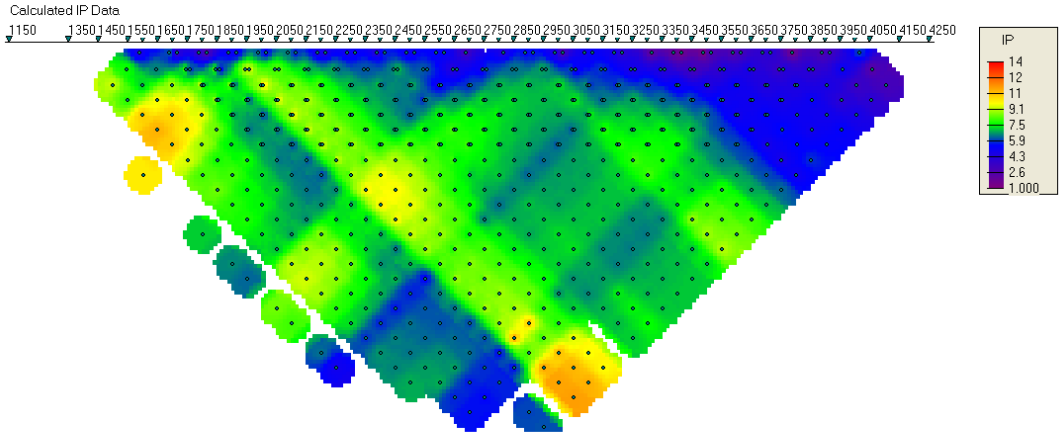

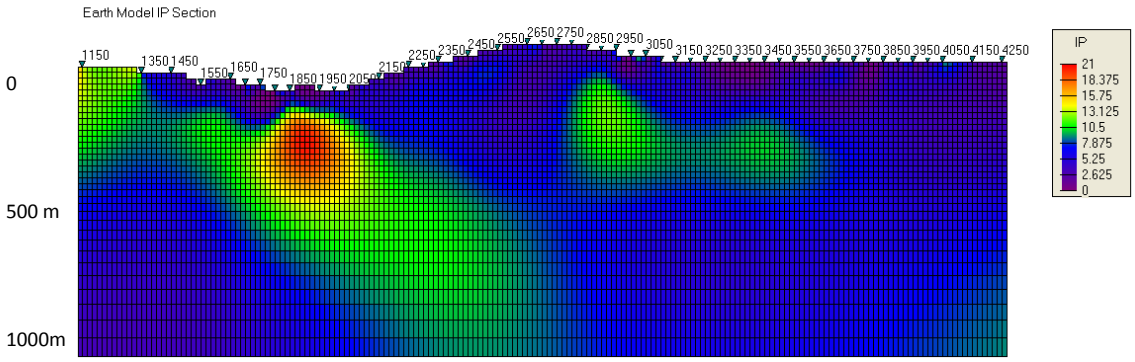

2D IP chargeability inversion results
smooth model:
data = 676
Misfit = 6.76044E+02
N iterations = 17

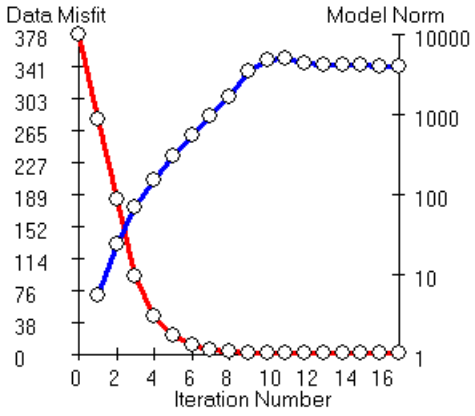

titan24

Note: Depth indications are approximate

Quantec Geoscience

Capstone Mining Corp.
Minto Mine Project

Preliminary
03.08.09

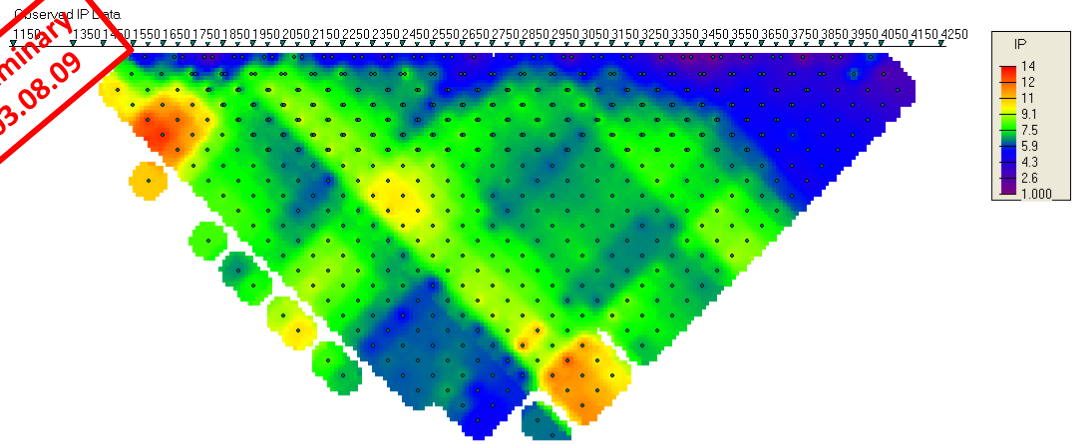

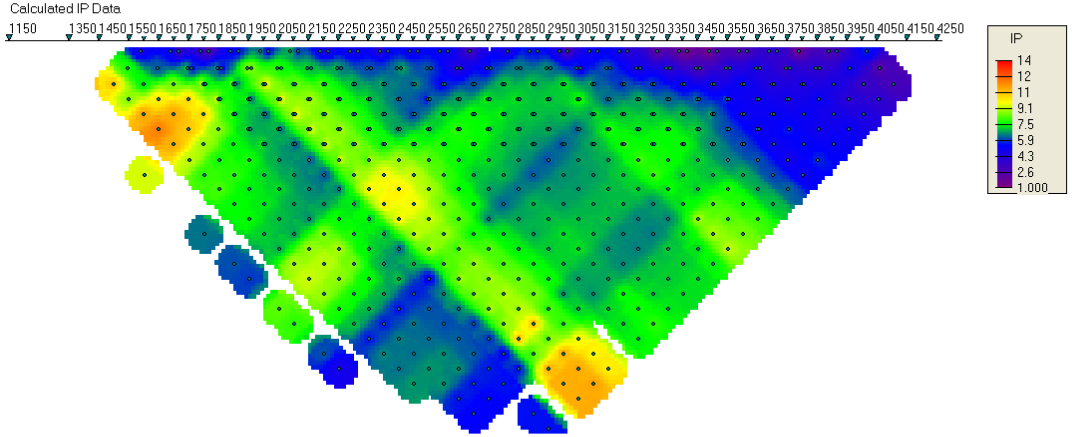

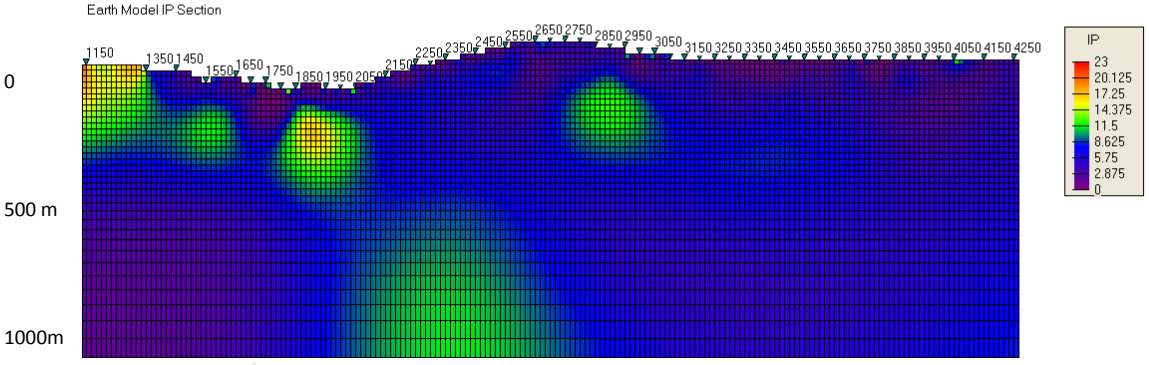

2D IP chargeability inversion results
Null Conductivity model:
N data = 676
Misfit = 6.76071E+02
N iterations = 22

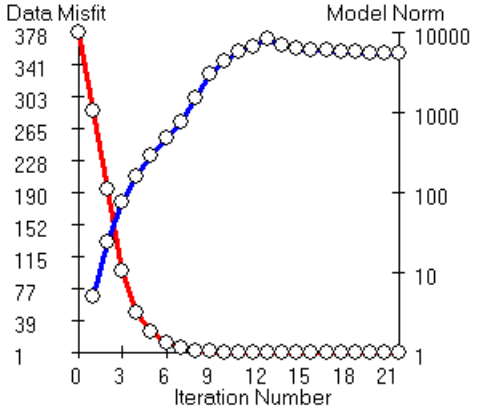

titan24

Note: Depth indications are approximate

Quantec Geoscience

Preliminary
03.08.09

DOI Investigation

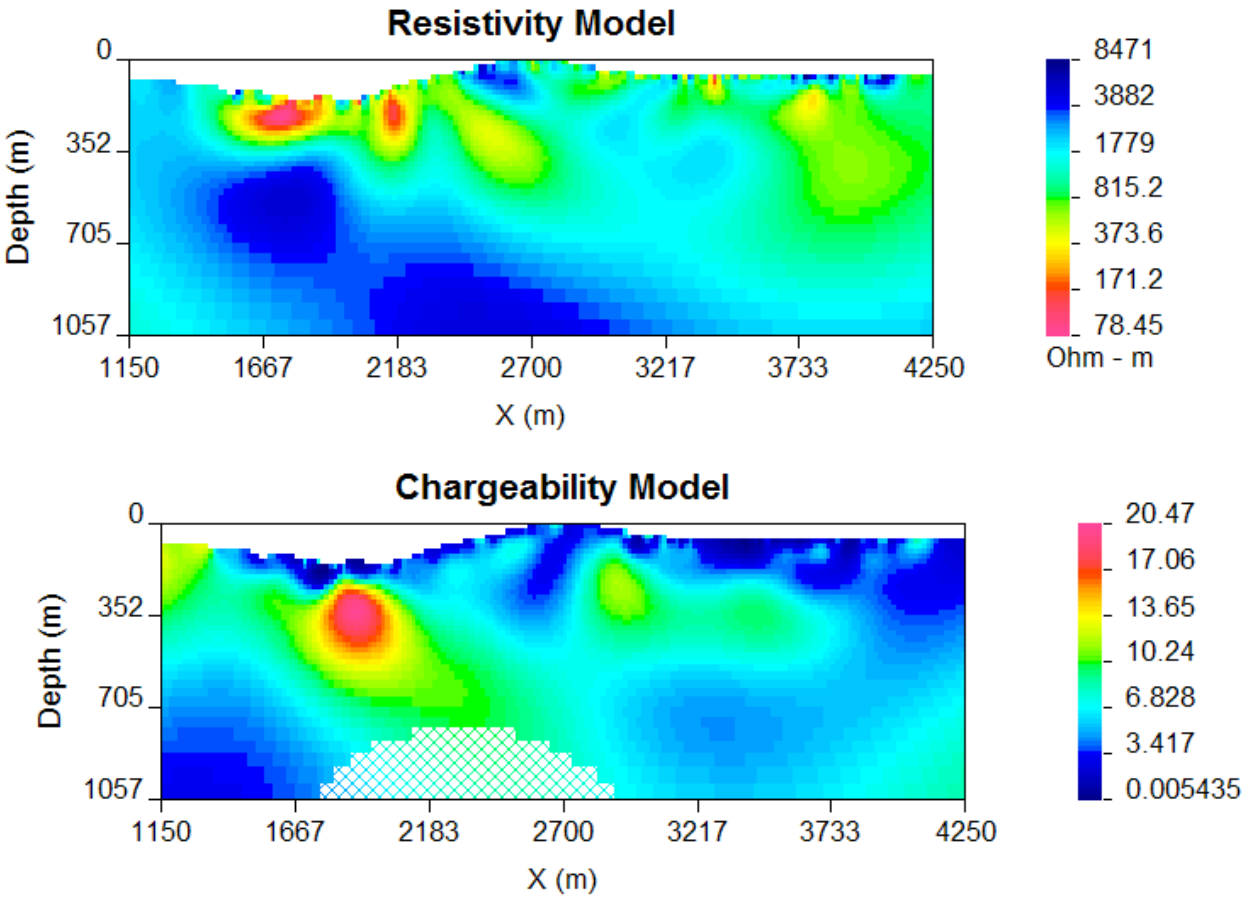

DOI (depth of investigation) is a Tool designed by the UBC-GIF to image the validity of inversion models. It compares two models calculated with different reference models.

Thus creating an image of how regions in the model which are influenced by the choice of reference model and not the actual data.

These zones are indicated with the hatched colours.

For the DC model a 10 kOhm-m and the default reference (average resistivity of the line) was used, and in the IP the smooth and null con. models were compared, a 0.1 cut off value was chosen

See: Oldenburg & Li, "**Estimating depth of investigation in dc resistivity and IP surveys**" GEOPHYSICS, VOL. 64, NO. 2 (MARCH-APRIL 1999); P. 403–416

titan24

Quantec Geoscience

Preliminary
03.08.09

Capstone Mining Corp.
Minto Mine Project

Geosoft Images

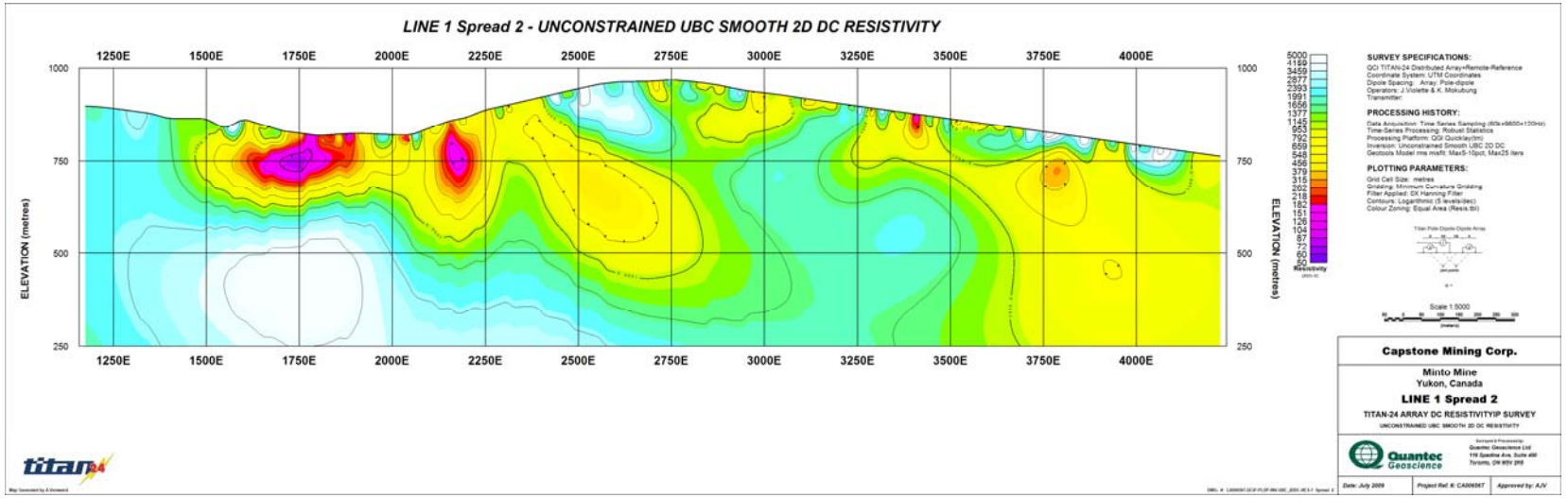

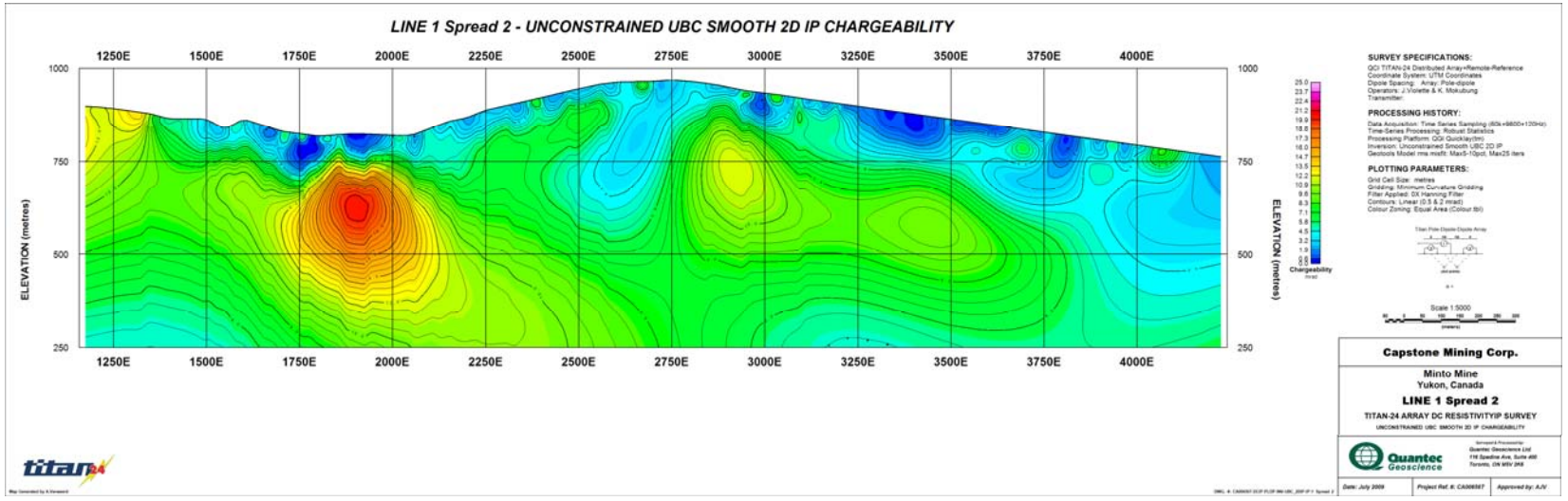

Preliminary
03.08.09

Capstone Mining Corp.
Minto Mine Project

Geosoft Images

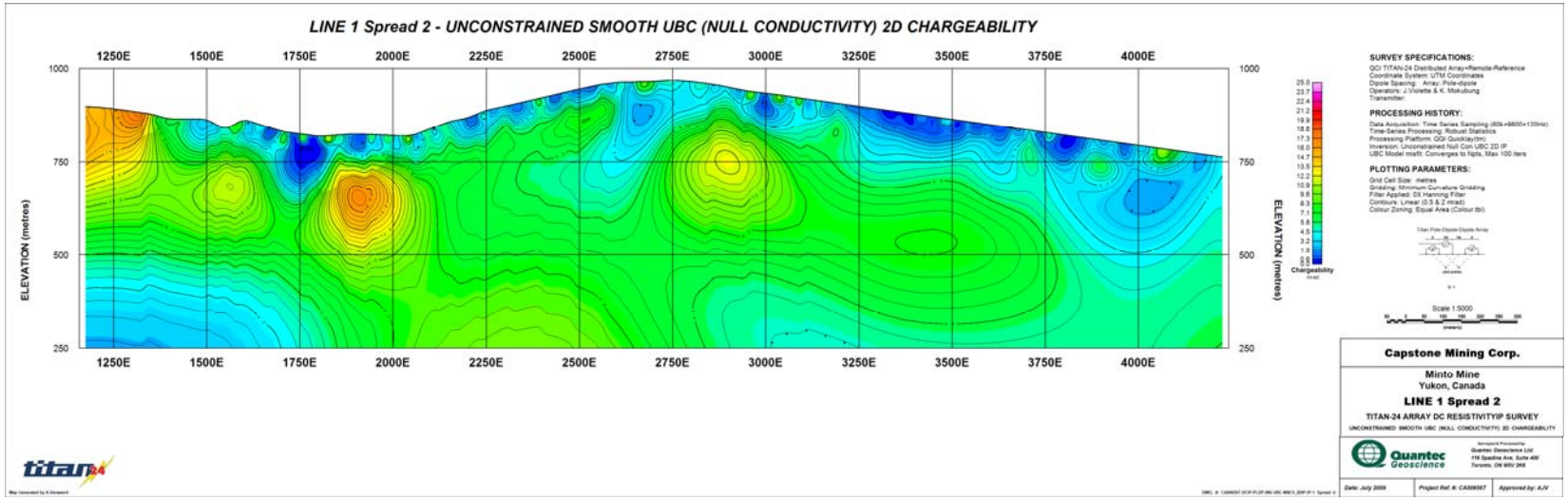

Preliminary
03.08.09

Capstone Mining Corp.
Minto Mine Project

MT inversion

Observed data

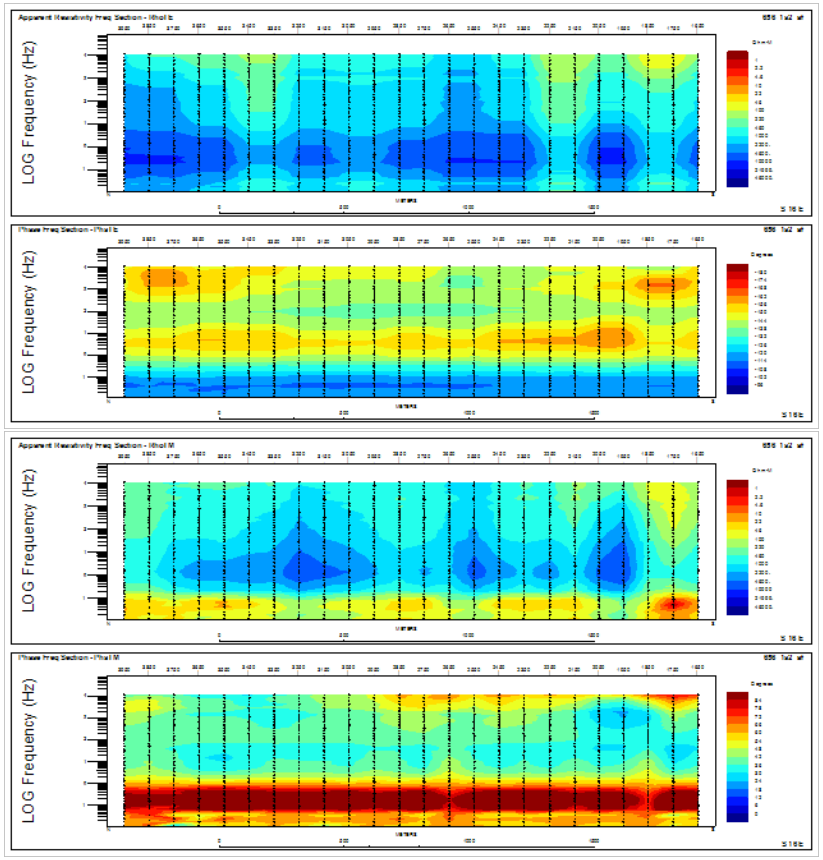

Interpolated data

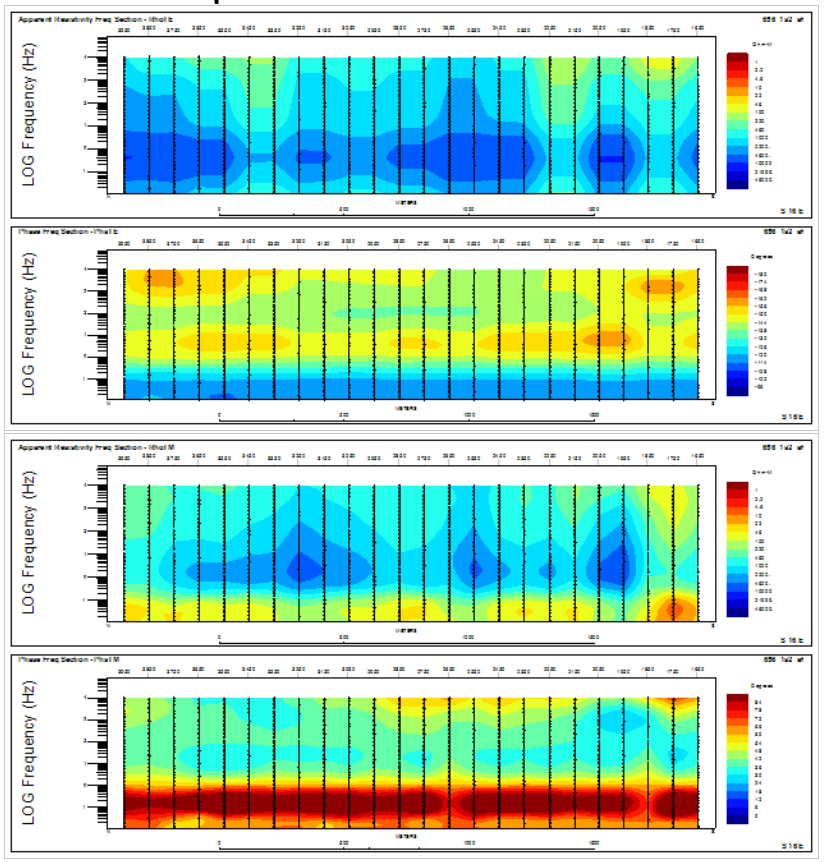

Note: The MT inversion program (GEOTOOLS), has a different plotting convention than the DC/IP inversion program (DCIP2D). Low station numbers are located on the lefts side in the DC/IP images and on the right side in the MT images.

titan24

Quantec Geoscience

Preliminary
03.08.09

Capstone Mining Corp.
Minto Mine Project

1D inversion results

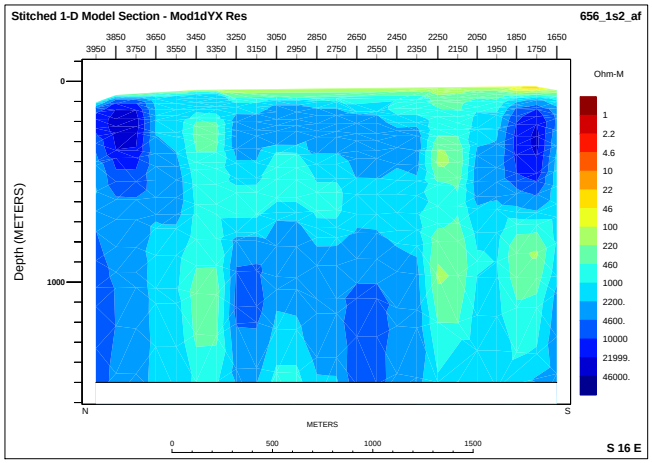

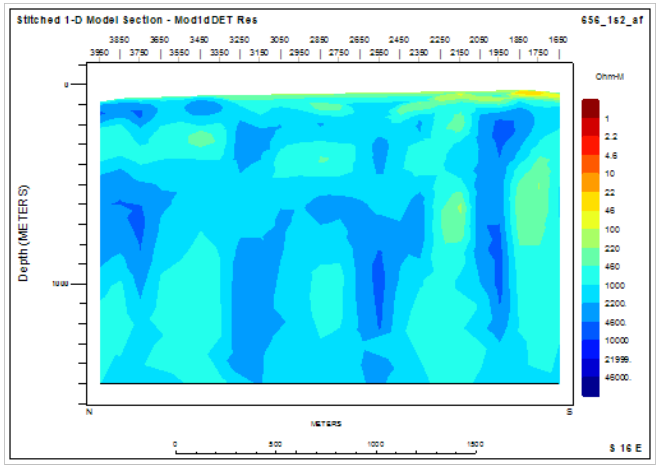

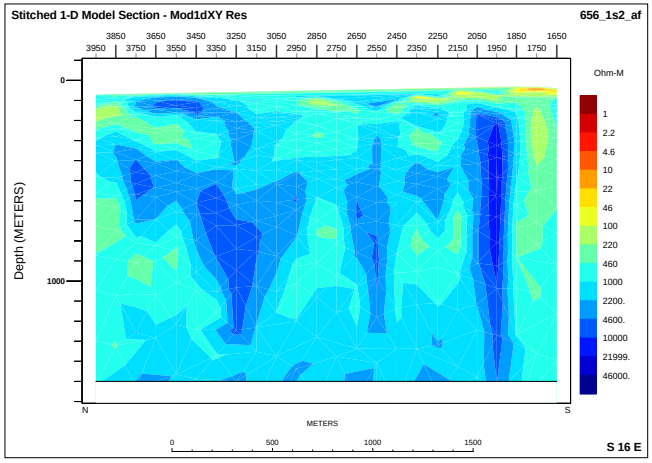

Left top: 1D stitched TE resistivity
Left bottom: 1D stitched TM resistivity
Right top: 1D stitched DET resistivity

titan24

Quantec Geoscience

Preliminary
03.08.09

Capstone Mining Corp.
Minto Mine Project

2D RLM Inversion

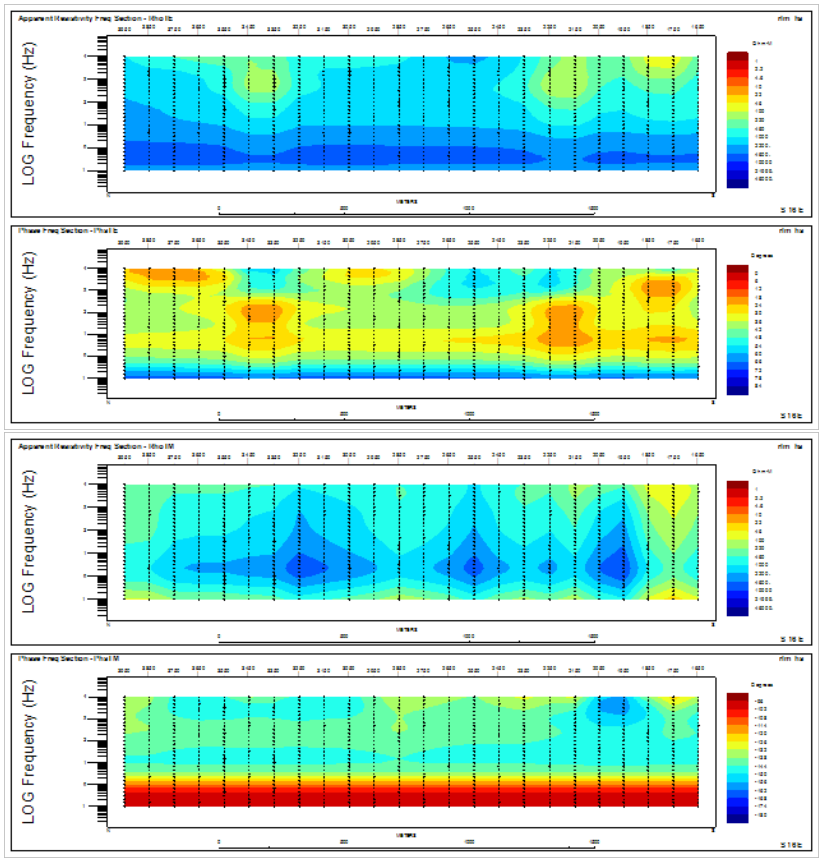

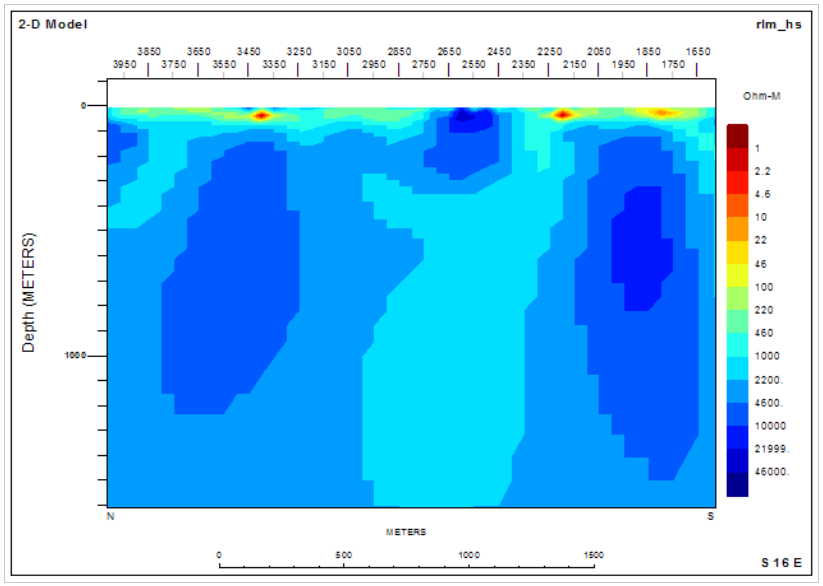

2D RLM TM,TE inversion results:
Starting model: 5000 Ohm-m halfspace
RMS misfit: 0.5609E+01
N iteration: 48

Preliminary
03.08.09

Capstone Mining Corp.
Minto Mine Project

2D PW inversion

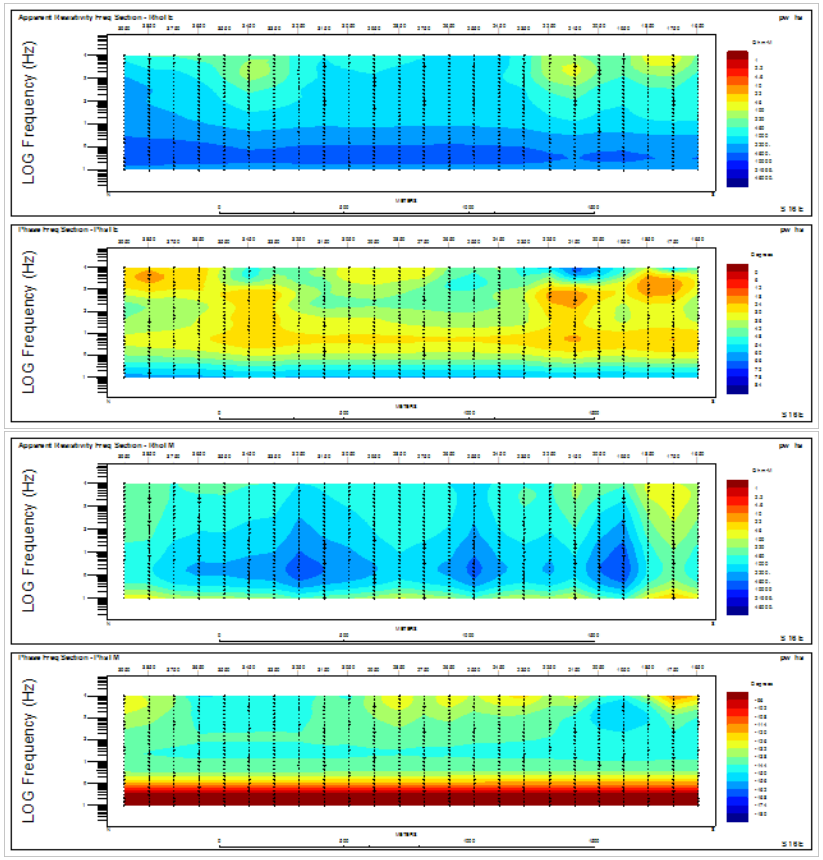

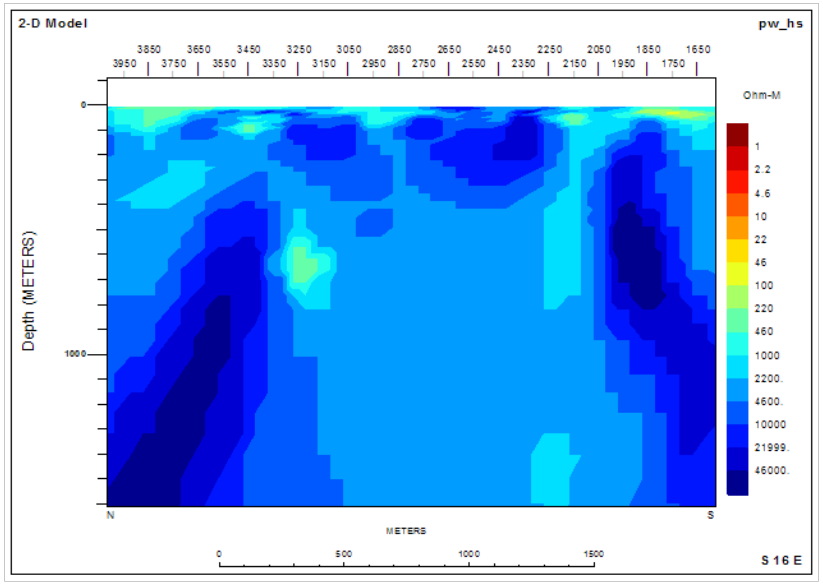

2D PW TM,TE inversion results:
Starting model: 5000 Ohm-m halfspace
RMS misfit: 0.5312E+01
N iteration: 34

titan24

Quantec Geoscience

Preliminary
03.08.09

Capstone Mining Corp.
Minto Mine Project

2D PW inversion

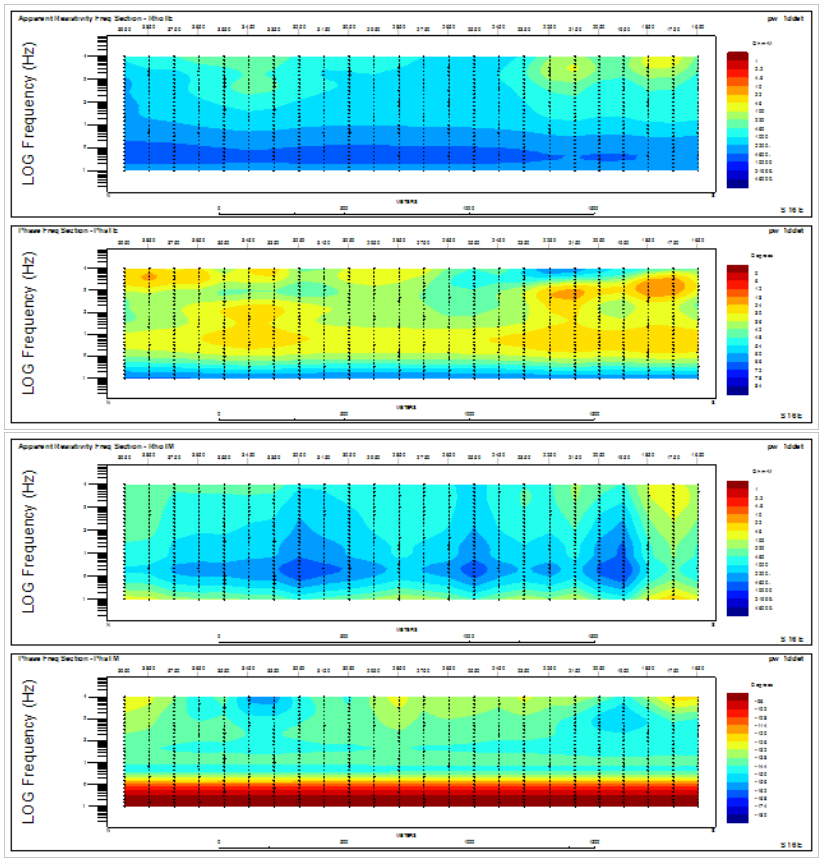

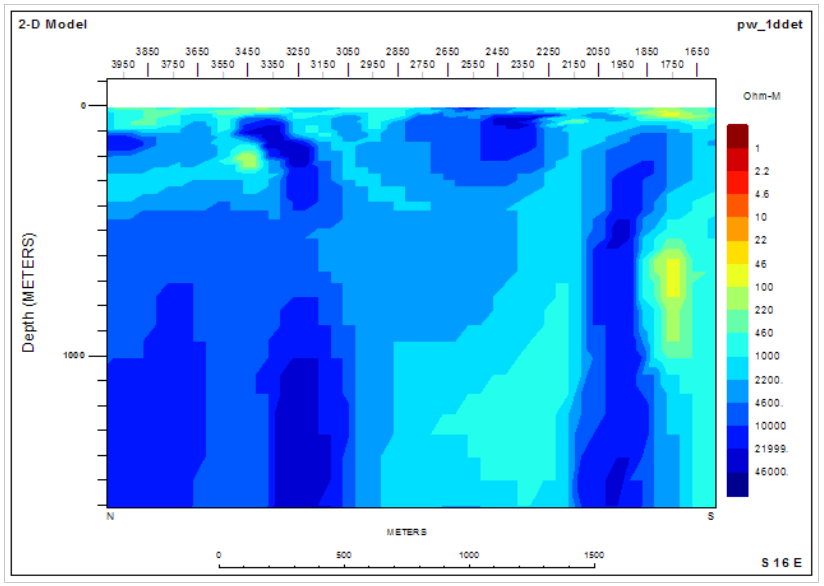

2D PW TM,TE inversion results:
Starting model: Stitched 1D DET
RMS misfit: 0.5207E+01
N iteration: 48

titan24

Quantec Geoscience

Preliminary
03.08.09

Capstone Mining Corp.
Minto Mine Project

Geosoft Images

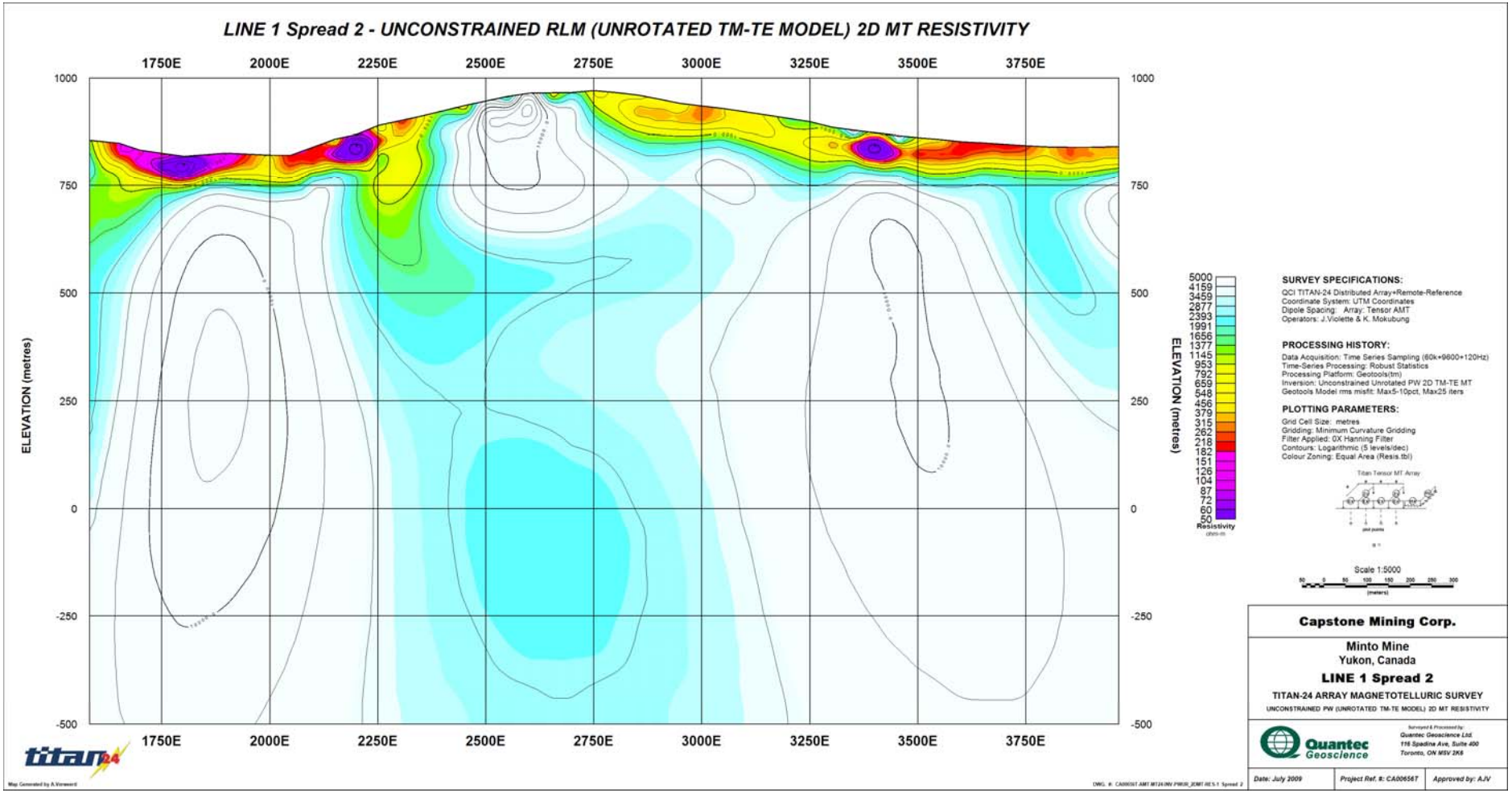

Preliminary
03.08.09

Capstone Mining Corp.
Minto Mine Project

Geosoft Images

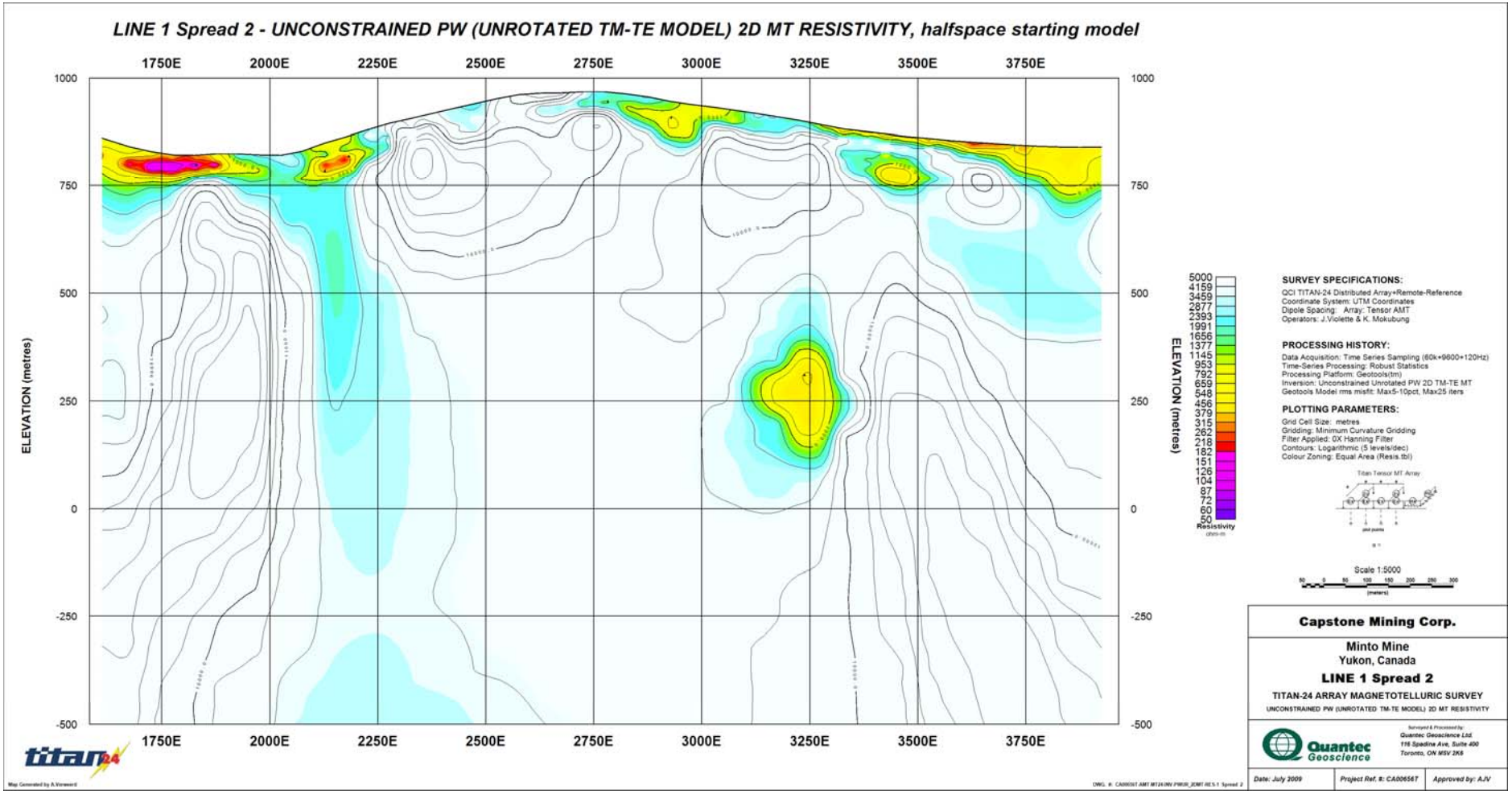

Preliminary
03.08.09

Capstone Mining Corp.
Minto Mine Project

Geosoft Images

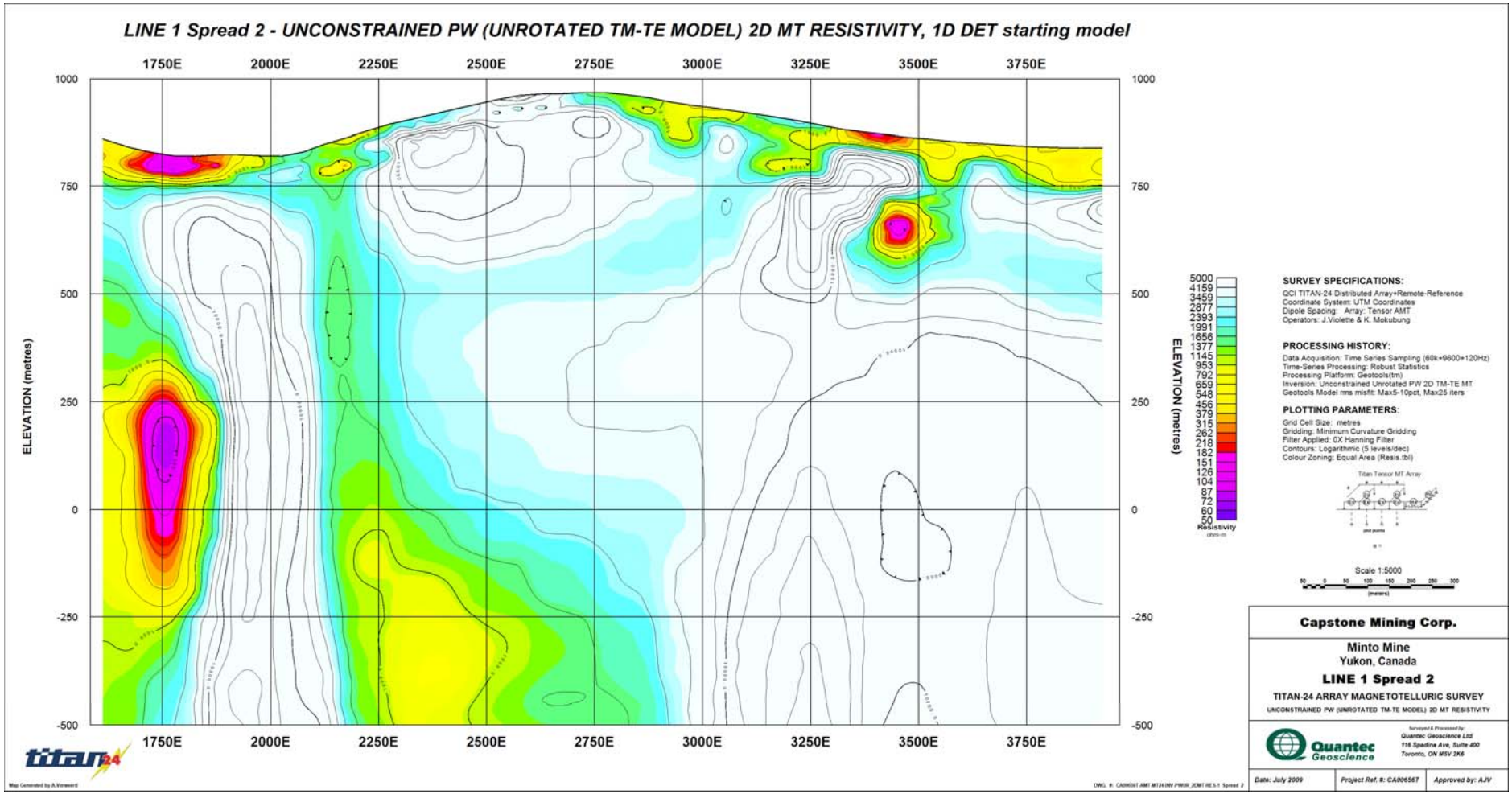

LINE L2 spread 1
TITAN-24 Survey
Minto Mine Project
Capstone Mining Corp - Minto Explorations

Preliminary 2D Inversion

Quantec Geoscience Ltd.
Toronto, Canada

A. Verweerd, Dr. Rer. Nat.

2D DC/IP inversion

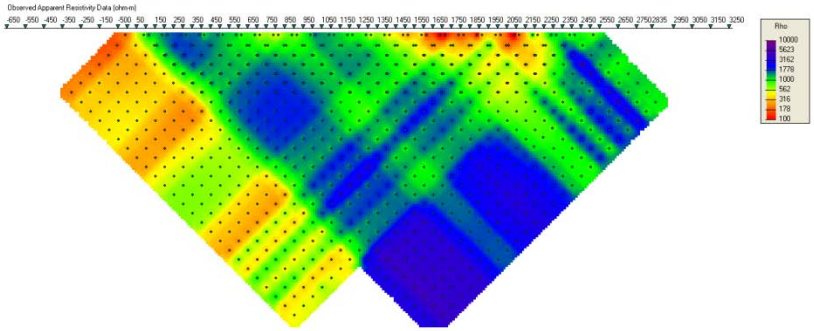

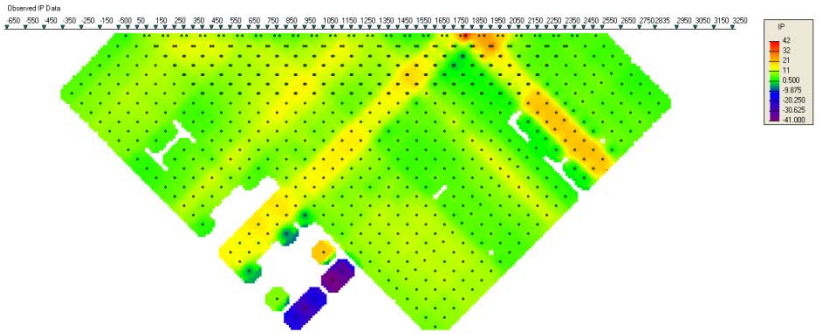

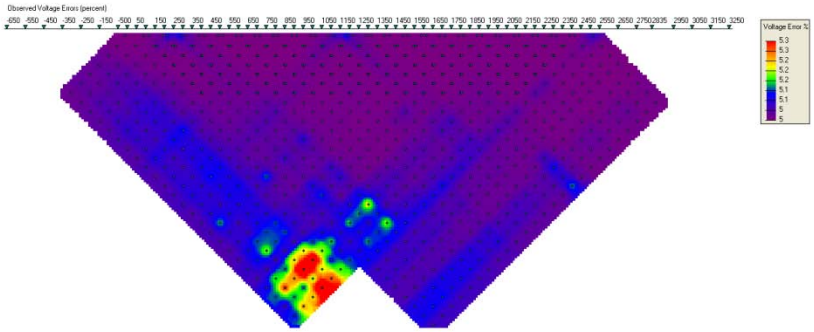

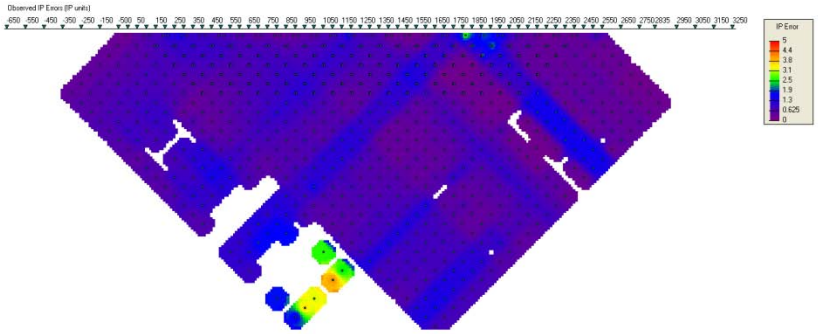

Error assignment:

DC data: Acquisition error + 5%

IP data: Remove acquisition error>25%

if error < 7%, set at 7%, else keep error, outlier rejection

Preliminary
06.08.09

Capstone Mining Corp.
Minto Mine Project

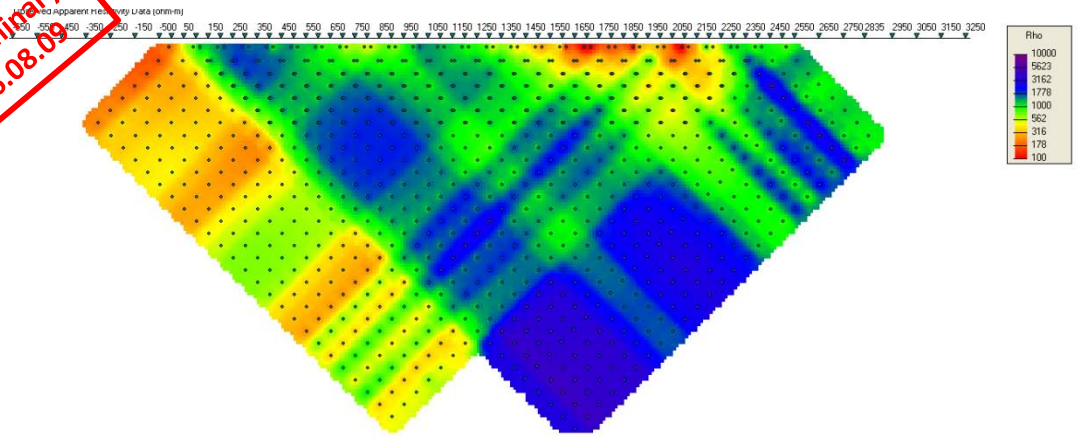

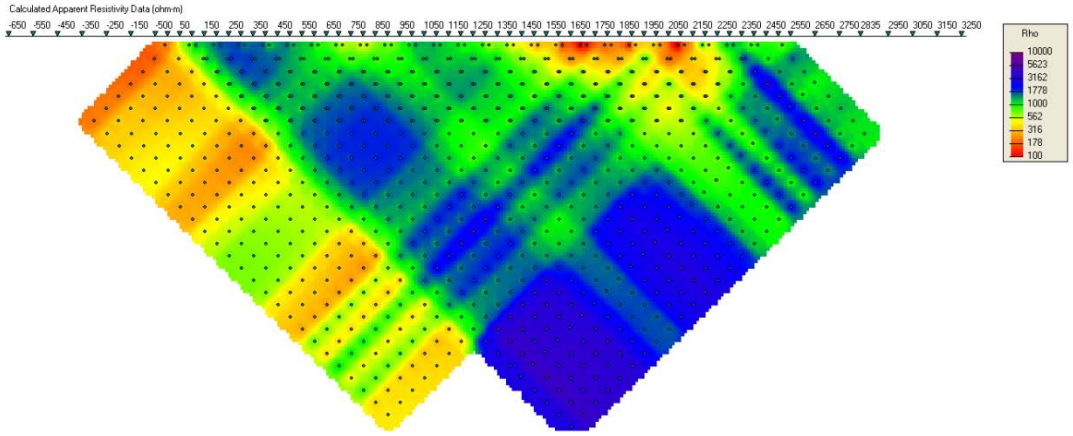

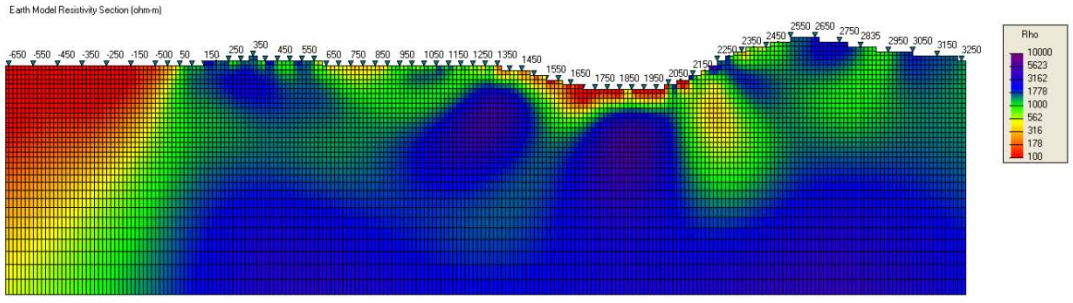

0

500 m

1000m

2D DC resistivity inversion results:
N data = 975
Misfit = 9.74998E+02
N iterations = 17

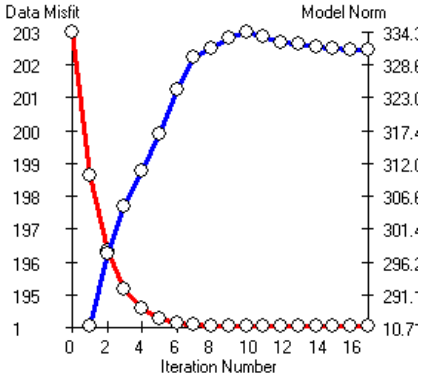

titan24

Note: Depth indications are approximate

Quantec Geoscience

Capstone Mining Corp.
Minto Mine Project

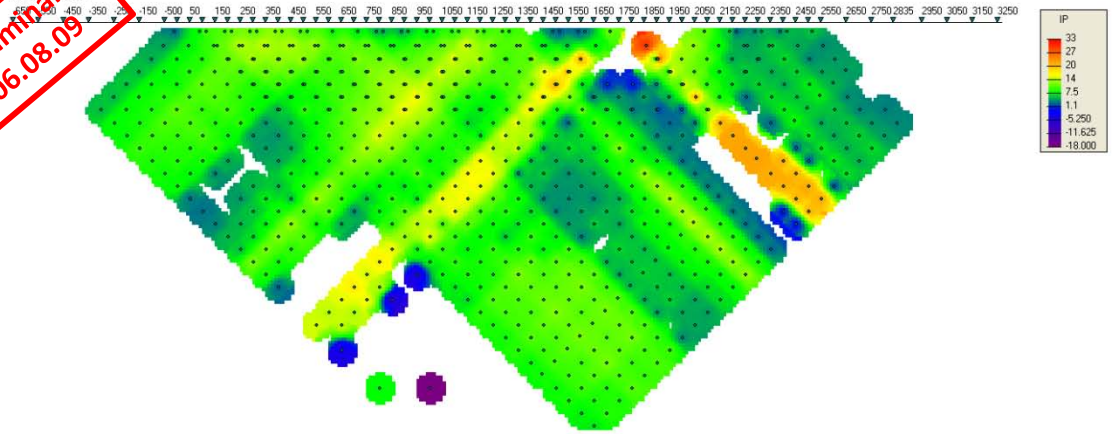

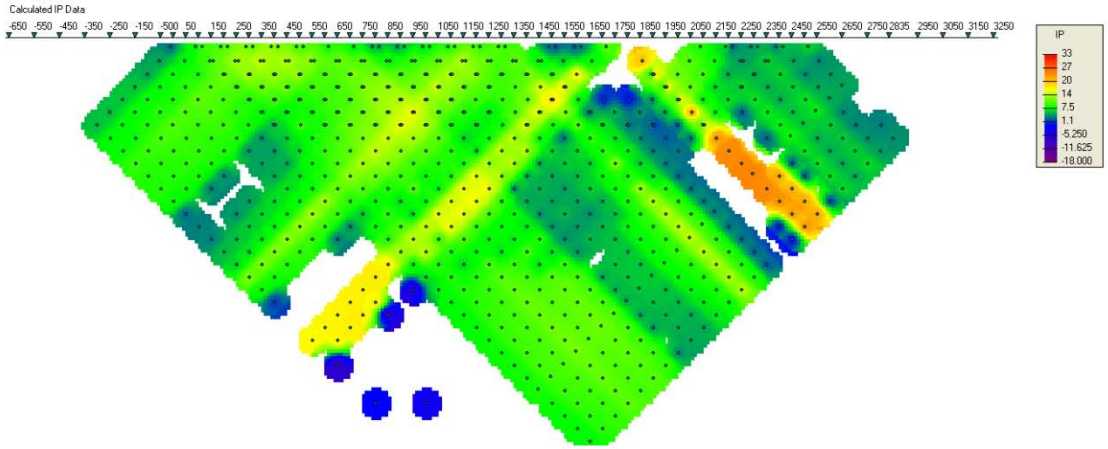

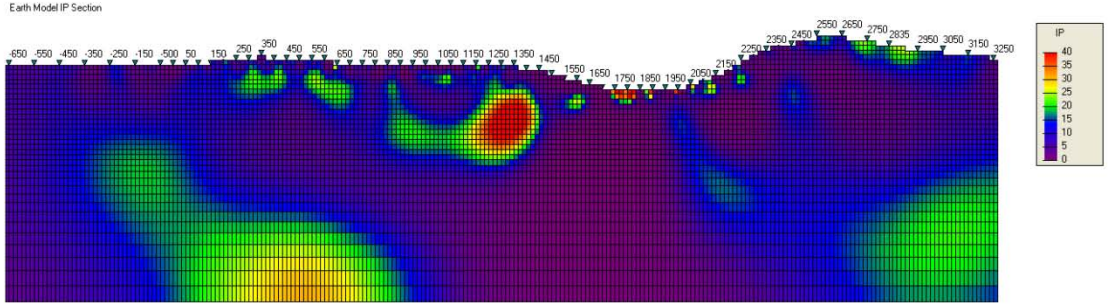

2D IP chargeability inversion results
smooth model:
data = 763
Misfit = 7.63057E+02
iterations = 30

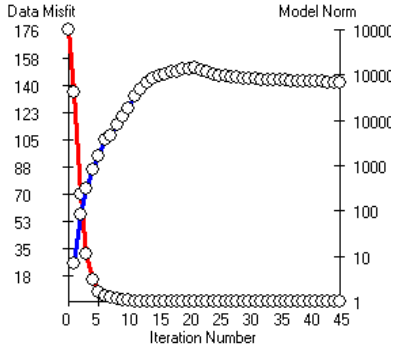

titan24

Note: Depth indications are approximate

Quantec Geoscience

Preliminary
06.08.09

Capstone Mining Corp.
Minto Mine Project

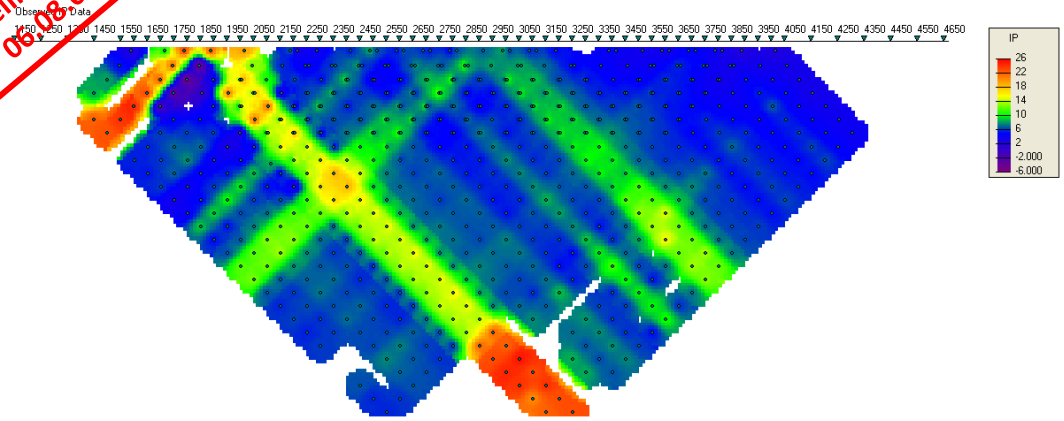

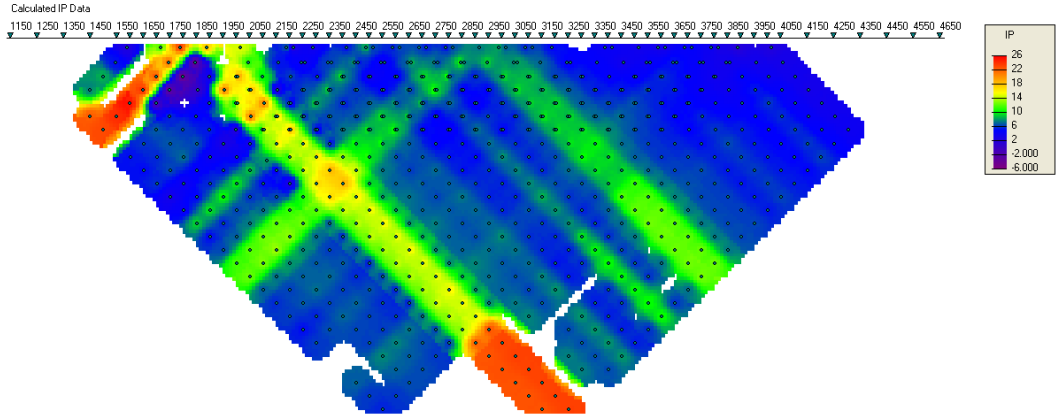

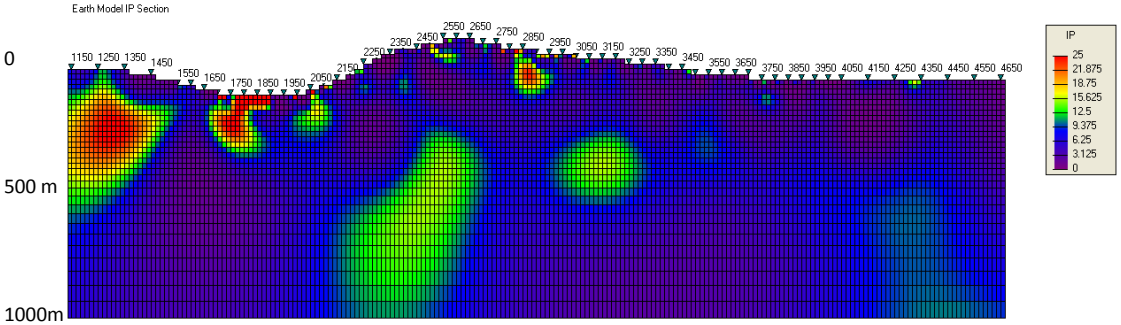

2D IP chargeability inversion results
Null Conductivity model:
N data = 763
Misfit = 7.63057E+02
N iterations = 30

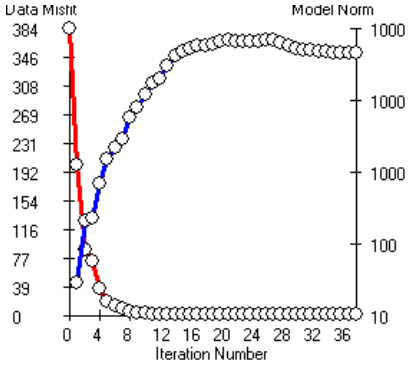

titan24

Note: Depth indications are approximate

Quantec Geoscience

DOI Investigation

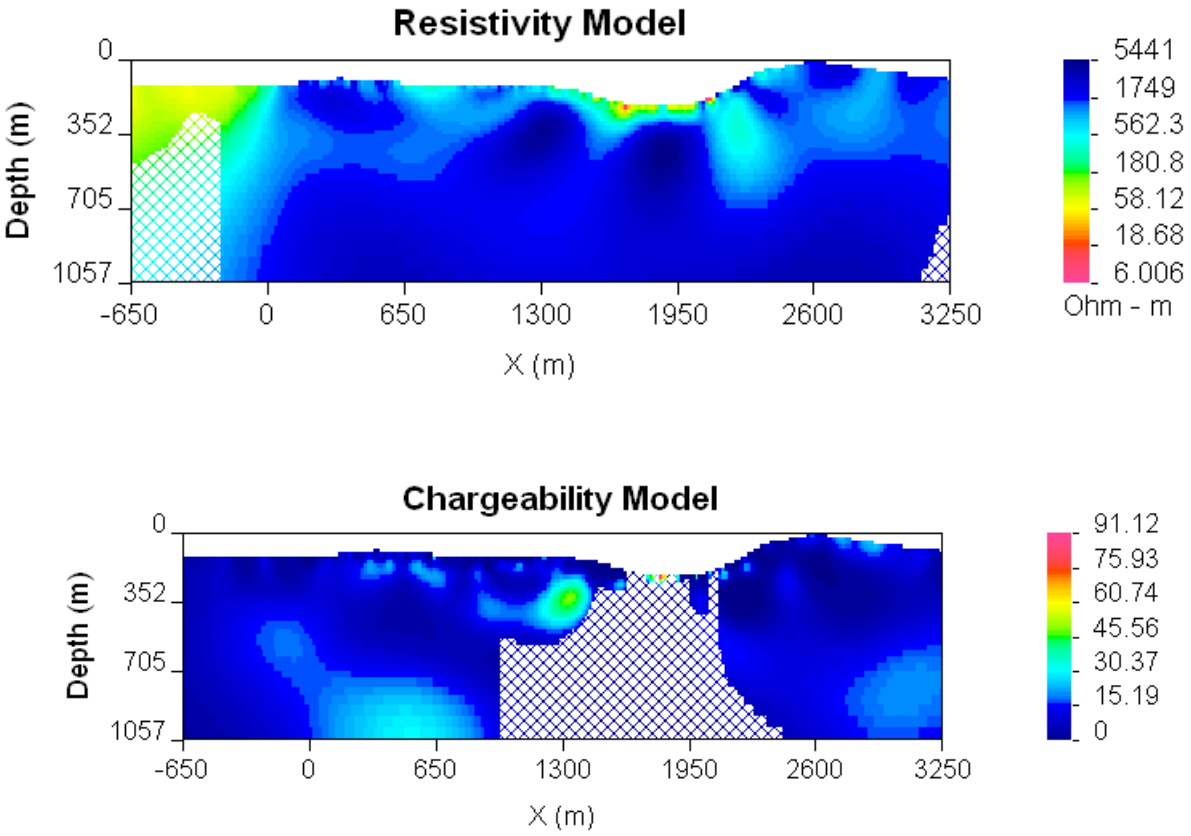

DOI (depth of investigation) is a Tool designed by the UBC-GIF to image the validity of inversion models. It compares two models calculated with different reference models.

Thus creating an image of how regions in the model which are influenced by the choice of reference model and not the actual data.

These zones are indicated with the hatched colours.

For the DC model a 10 kOhm-m and the default reference (average resistivity of the line) was used, in the IP the smooth and null con. Models were compared, a 0.1 cut off value was chosen

See: Oldenburg & Li, "**Estimating depth of investigation in dc resistivity and IP surveys**" GEOPHYSICS, VOL. 64, NO. 2 (MARCH-APRIL 1999); P. 403–416

titan24

Quantec Geoscience

Preliminary
06.08.09

Capstone Mining Corp.
Minto Mine Project

Geosoft Images

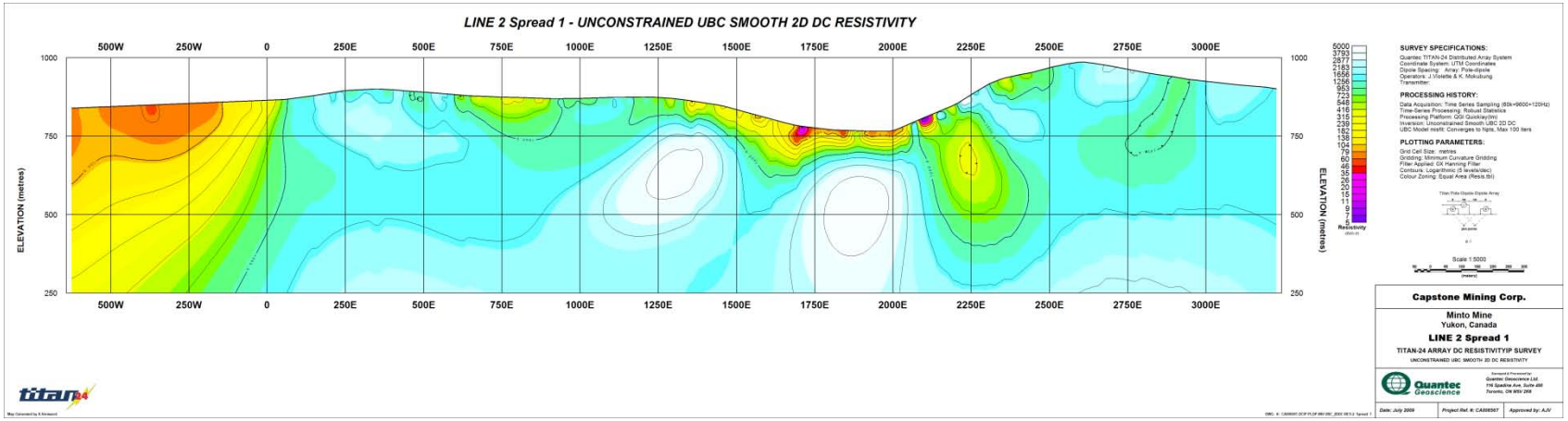

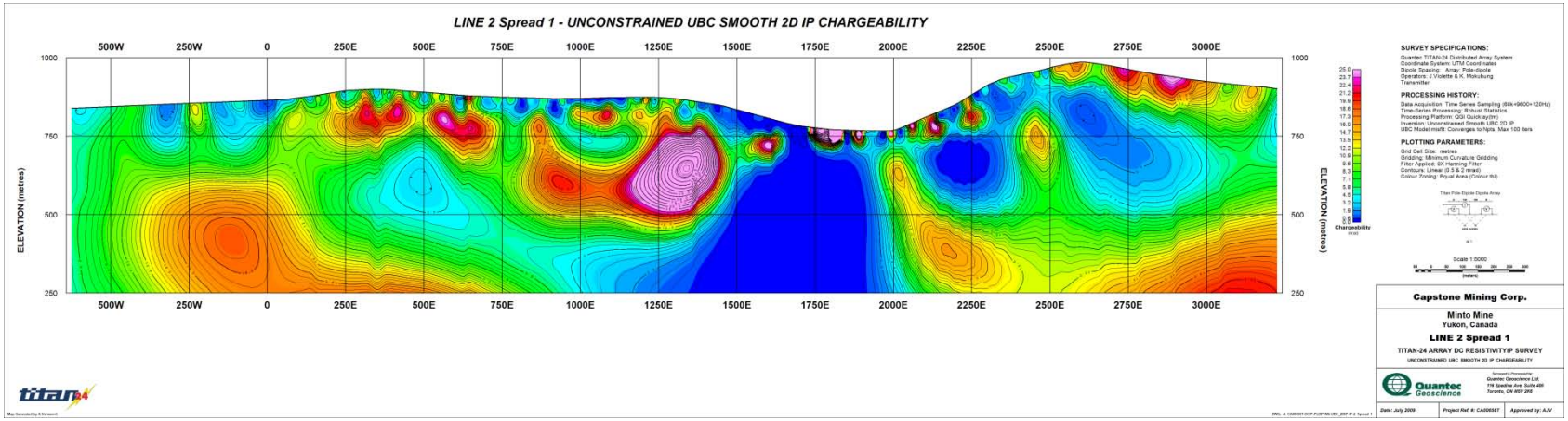

Preliminary
06.08.09

Capstone Mining Corp.
Minto Mine Project

Geosoft Images

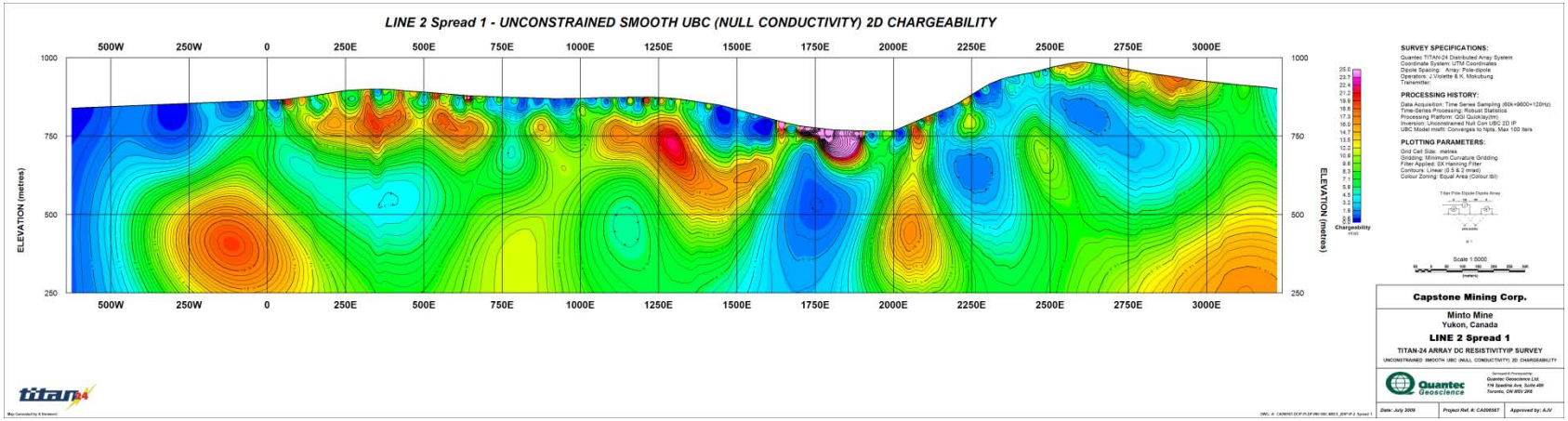

Preliminary
06.08.09

Capstone Mining Corp.
Minto Mine Project

MT inversion

Observed data

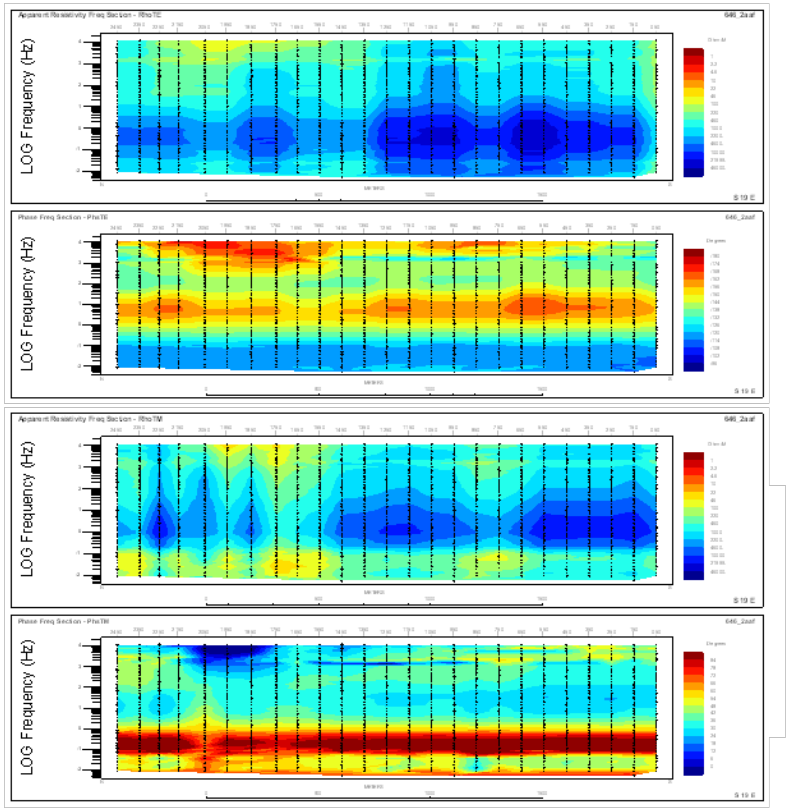

Interpolated data

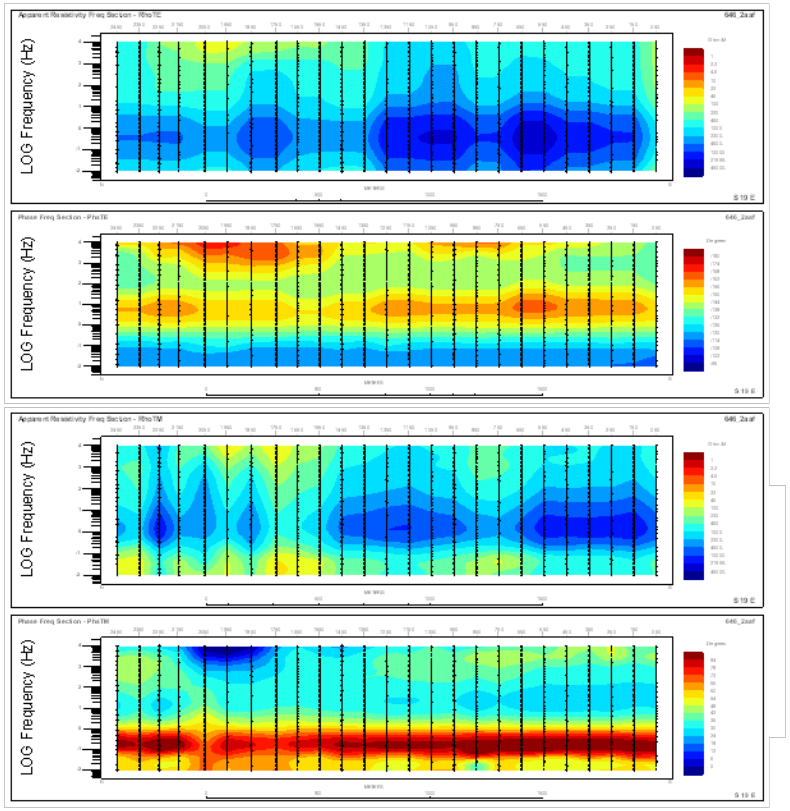

Note: The MT inversion program (GEOTOOLS), has a different plotting convention than the DC/IP inversion program (DCIP2D). Low station numbers are located on the lefts side in the DC/IP images and on the right side in the MT images.

titan24

Quantec Geoscience

Preliminary
06.08.09

Capstone Mining Corp.
Minto Mine Project

1D inversion results

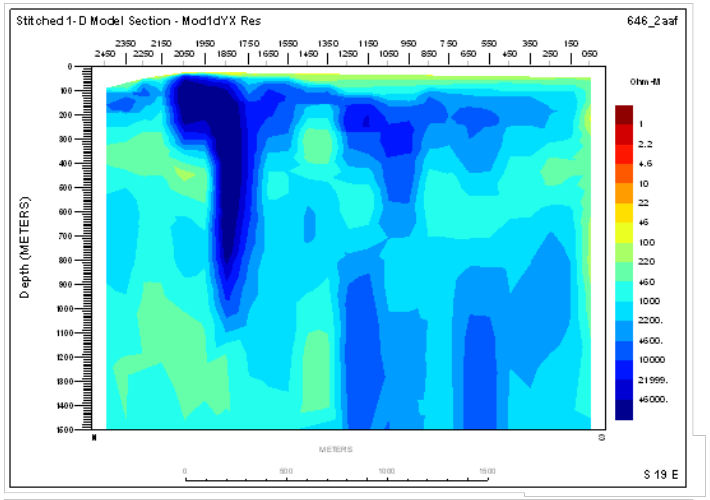

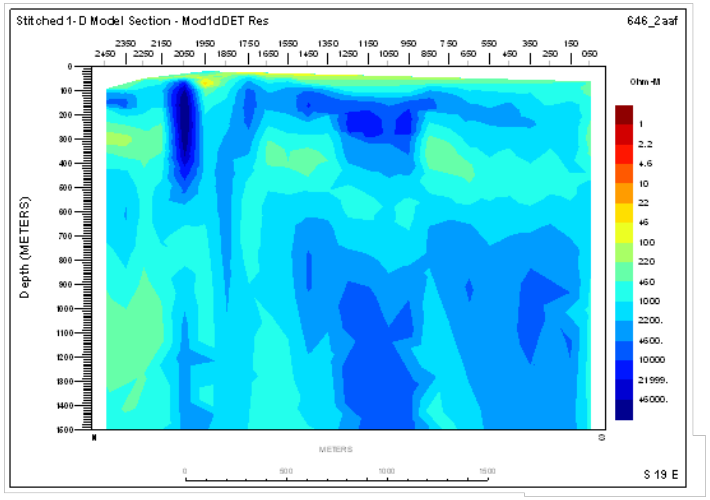

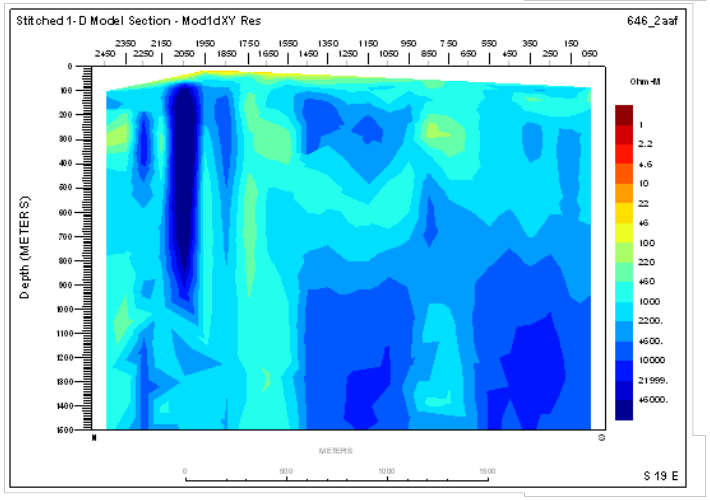

Left top: 1D stitched TE resistivity
Left bottom: 1D stitched TM resistivity
Right top: 1D stitched DET resistivity

titan24

Quantec Geoscience

Preliminary
06.08.09

Capstone Mining Corp.
Minto Mine Project

2D RLM Inversion

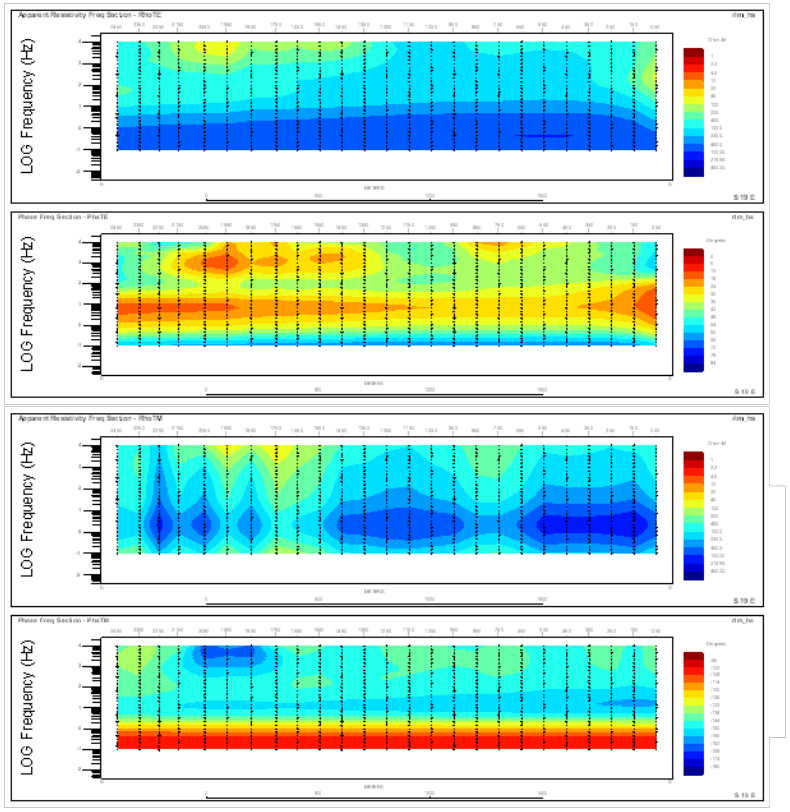

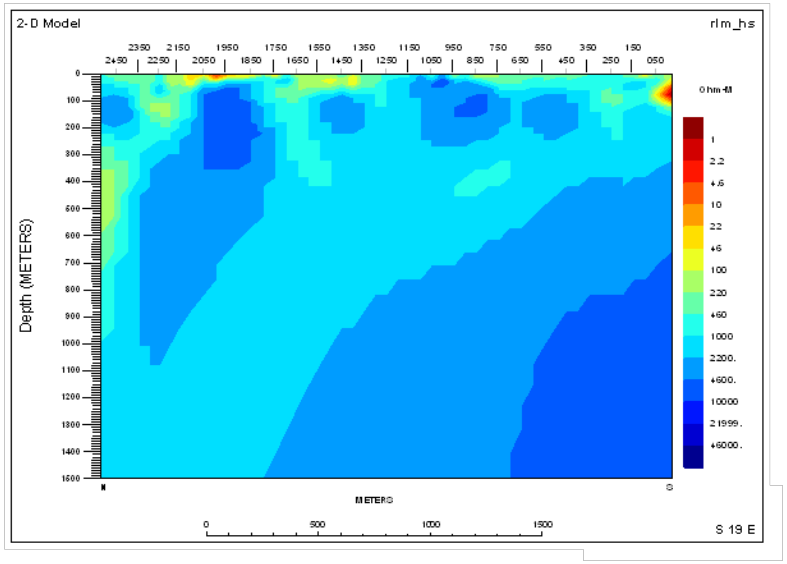

2D RLM TM,TE inversion results:
Starting model: 5000 Ohm-m halfspace
RMS misfit: 0.5776E+01
N iteration: 50(max)

Preliminary
06.08.09

Capstone Mining Corp.
Minto Mine Project

2D PW inversion

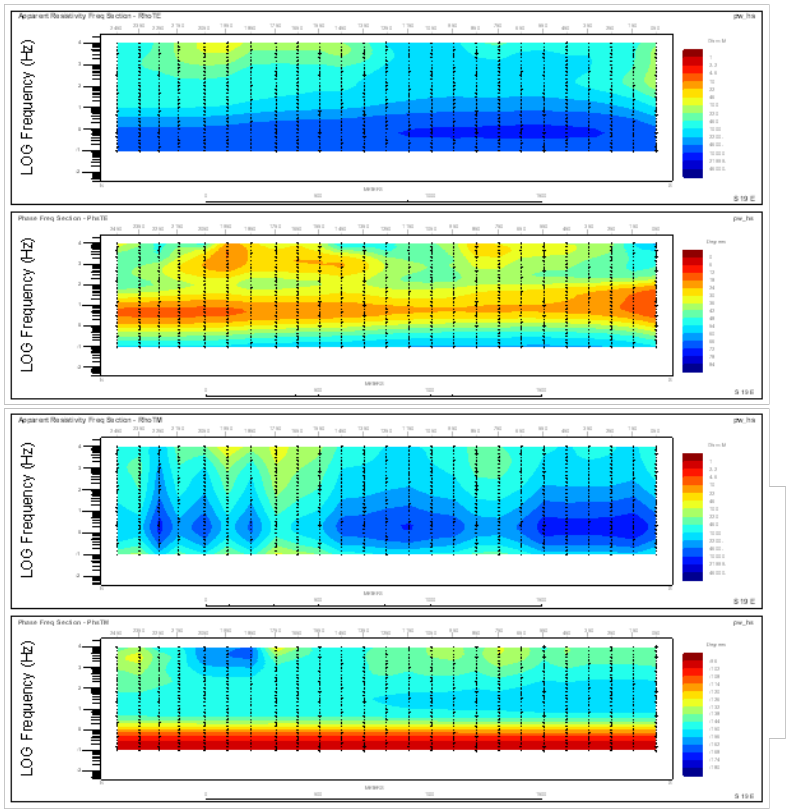

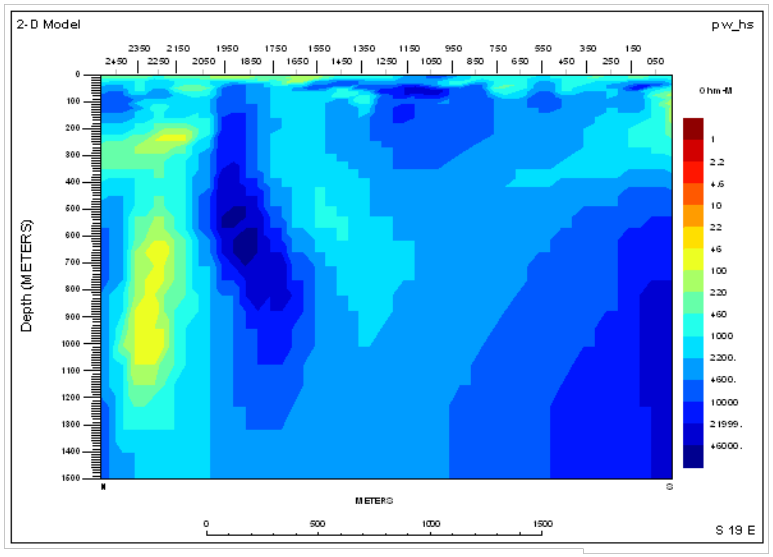

2D PW TM,TE inversion results:
Starting model: 5000 Ohm-m halfspace
RMS misfit: 0.5436E+01
N iteration: 29

titan24

Quantec Geoscience

Preliminary
06.08.09

Capstone Mining Corp.
Minto Mine Project

2D PW inversion

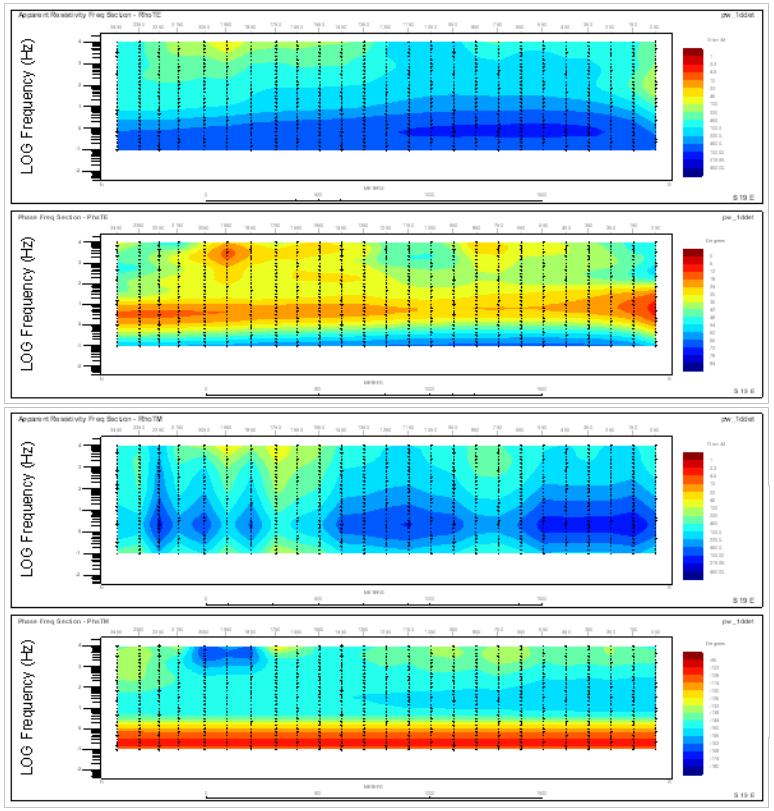

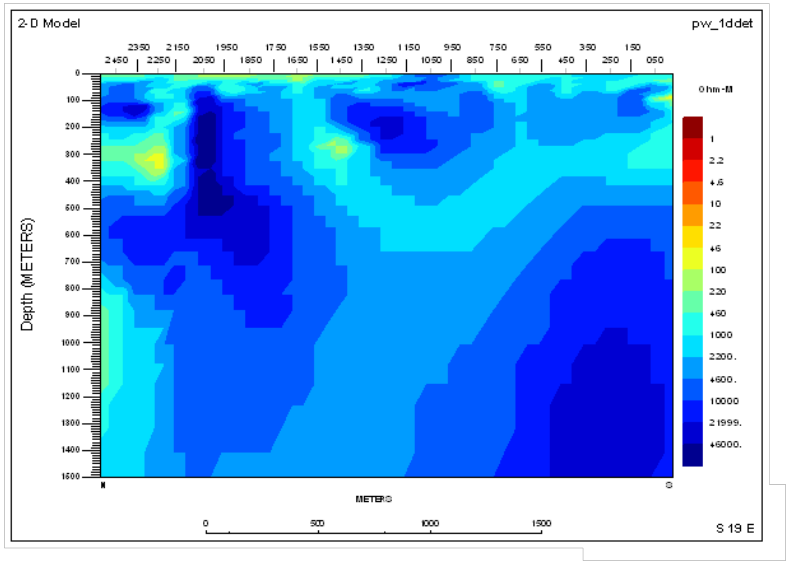

2D PW TM,TE inversion results:
Starting model: Stitched 1D DET
RMS misfit: 0.5425E+01
N iteration: 45

titan24

Quantec Geoscience

Preliminary
06.08.09

Capstone Mining Corp.
Minto Mine Project

Geosoft Images

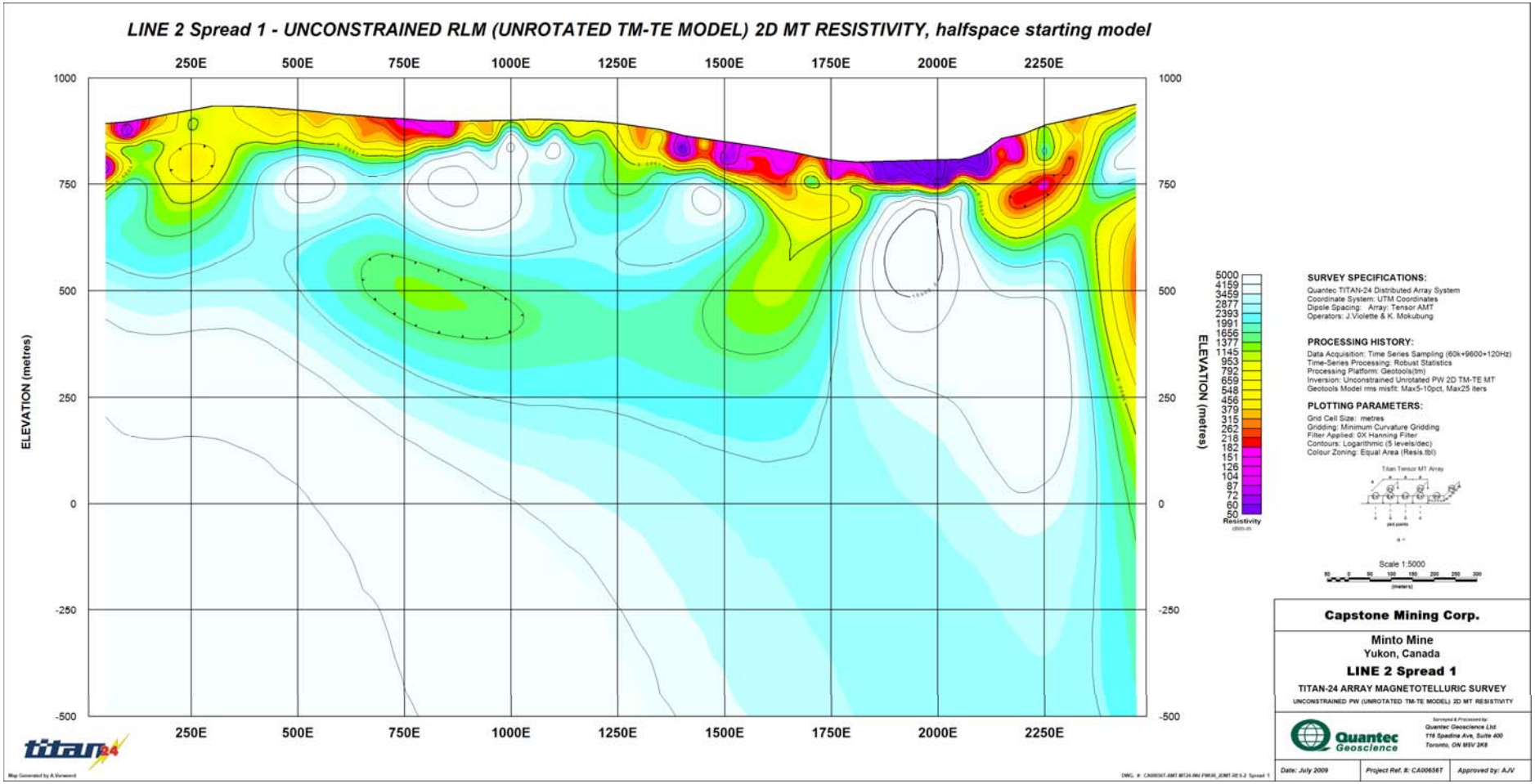

Preliminary
06.08.09

Capstone Mining Corp.
Minto Mine Project

Geosoft Images

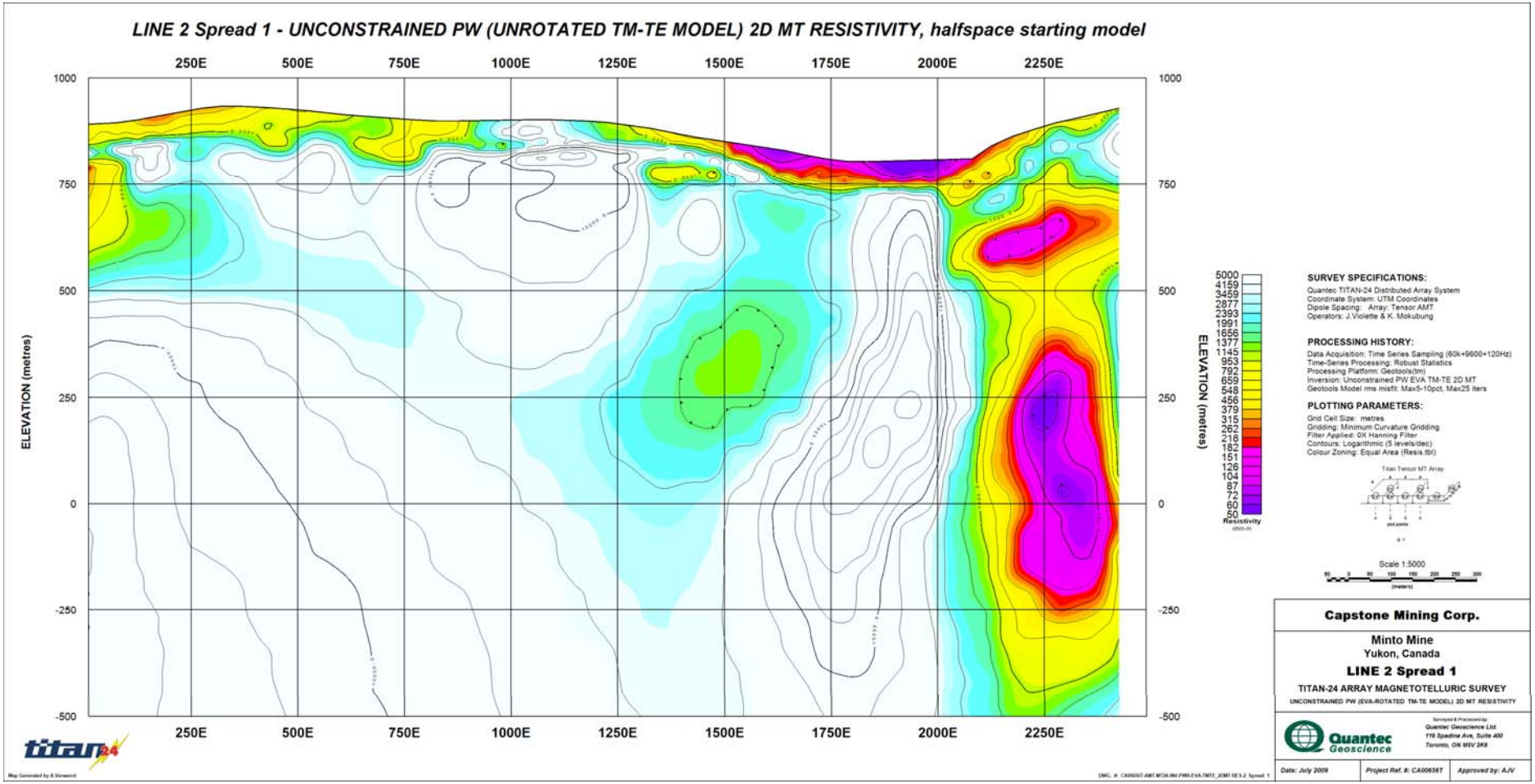

Preliminary
06.08.09

Capstone Mining Corp.
Minto Mine Project

Geosoft Images

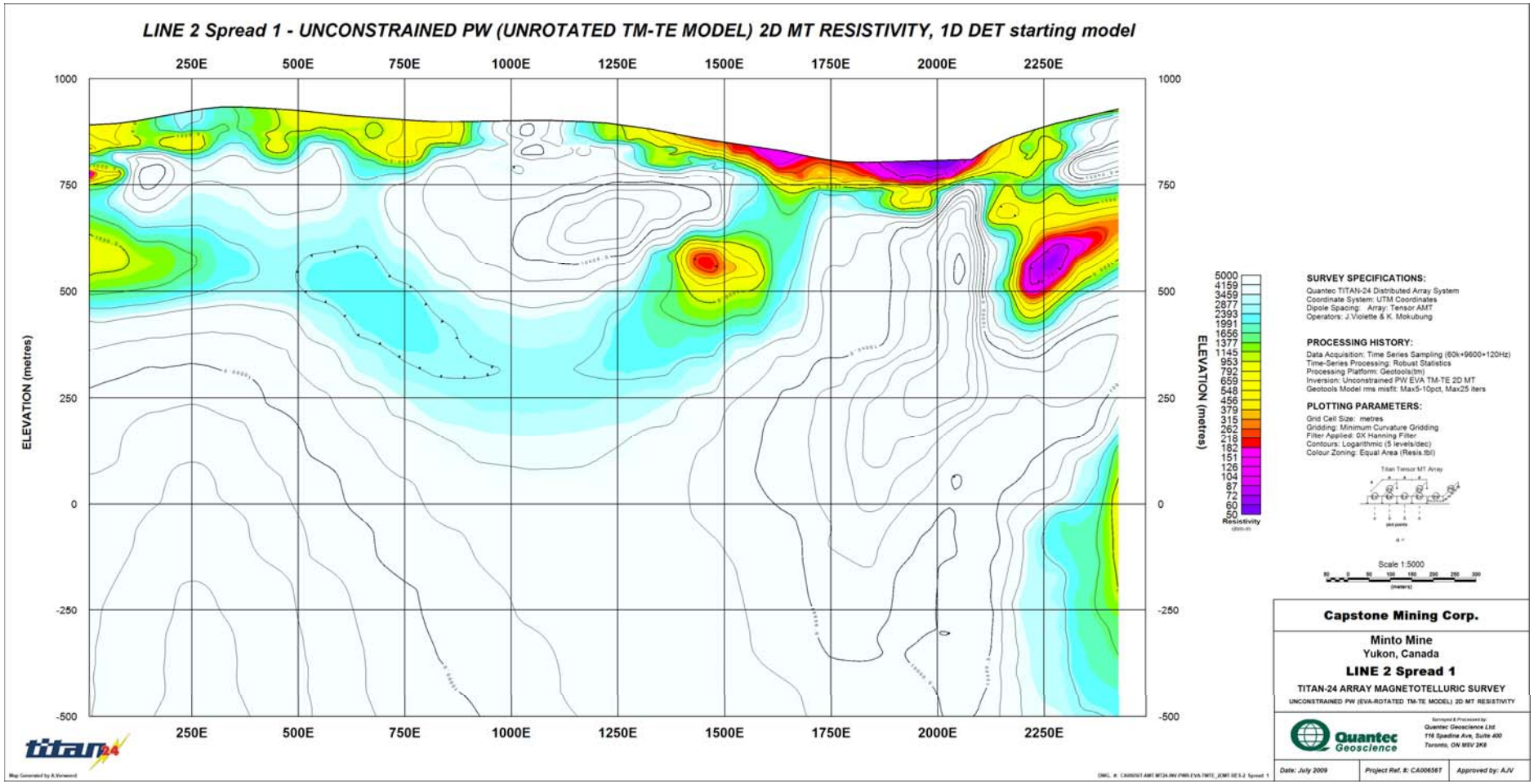

LINE L2 spread 2
TITAN-24 Survey
Minto Mine Project
Capstone Mining Corp - Minto Explorations

Preliminary 2D Inversion

Quantec Geoscience Ltd.
Toronto, Canada

A. Verweerd, Dr. Rer. Nat.

Preliminary
05.08.09

Capstone Mining Corp.
Minto Mine Project

2D DC/IP inversion

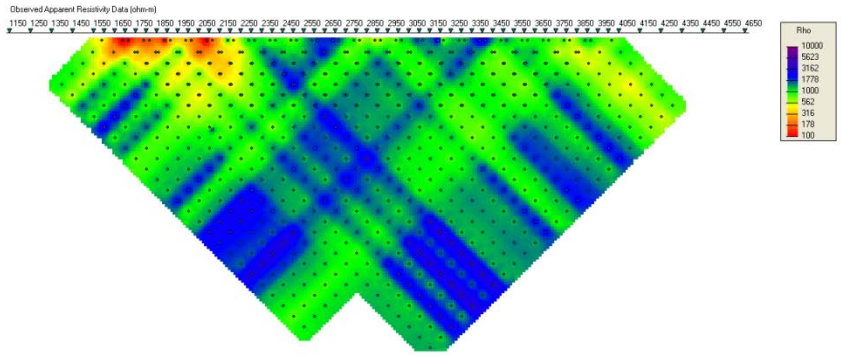

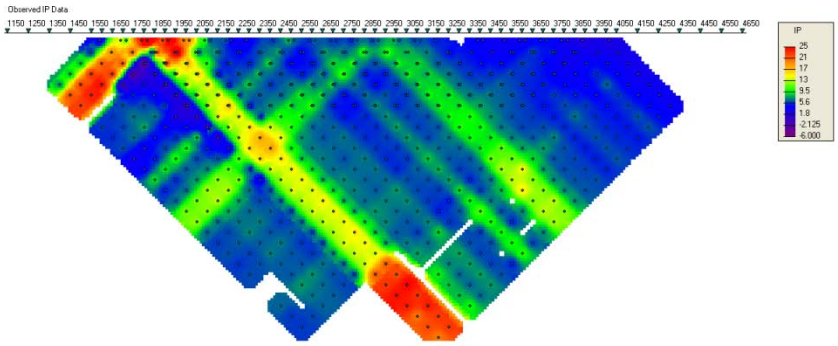

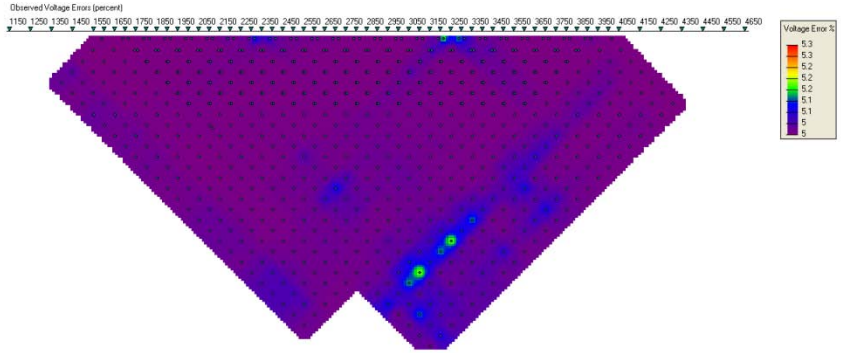

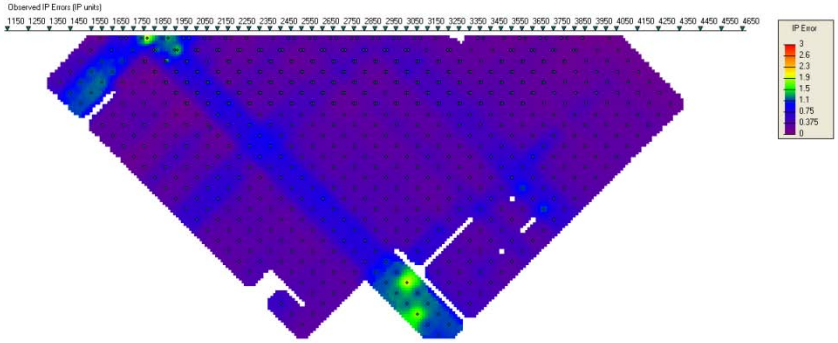

Error assignment:

DC data: Acquisition error + 5%

IP data: Remove acquisition error>10%
if error < 5%, set at 5%, else keep error, outlier rejection

titan24

Quantec Geoscience

Preliminary
05.08.09

Capstone Mining Corp.
Minto Mine Project

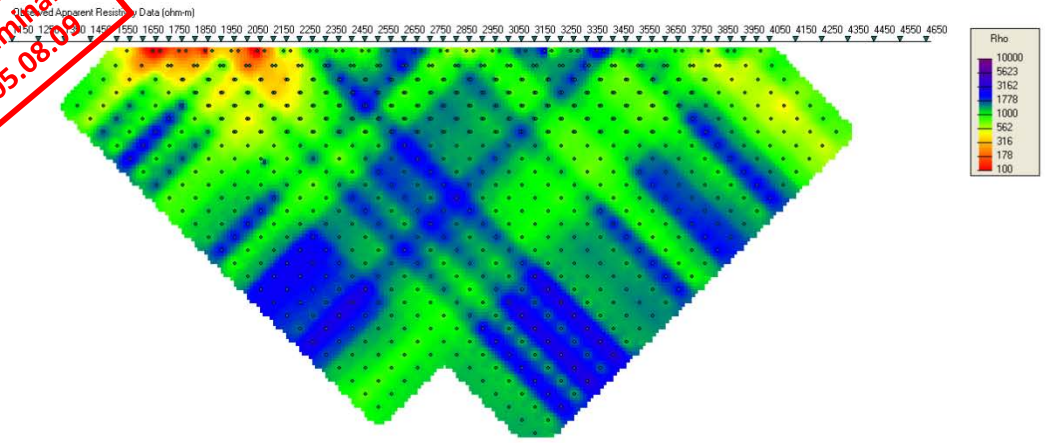

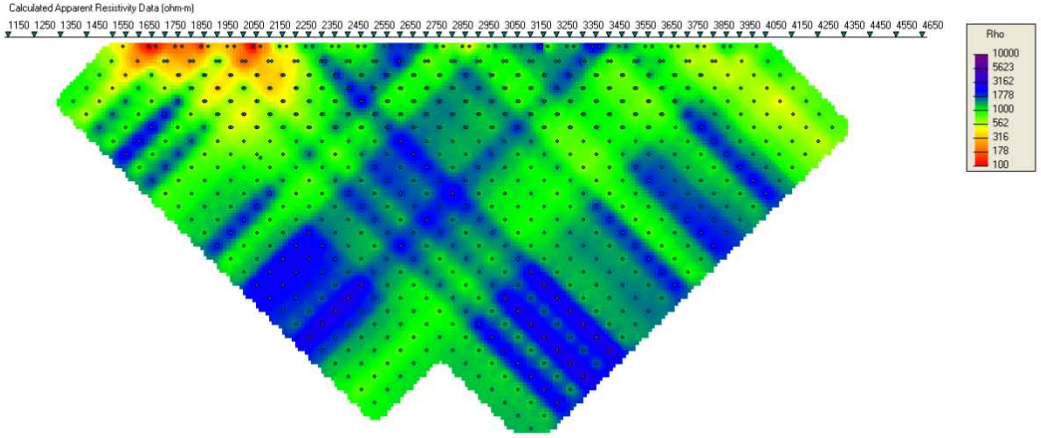

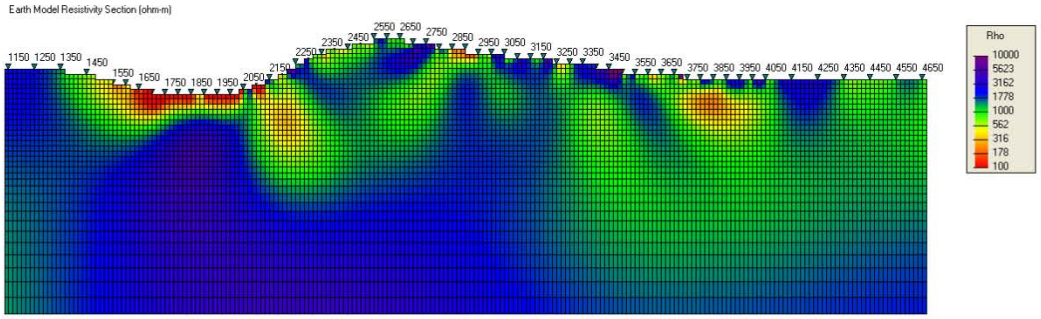

2D DC resistivity inversion results:
N data = 840
Misfit = 8.39967E+02
N iterations = 15

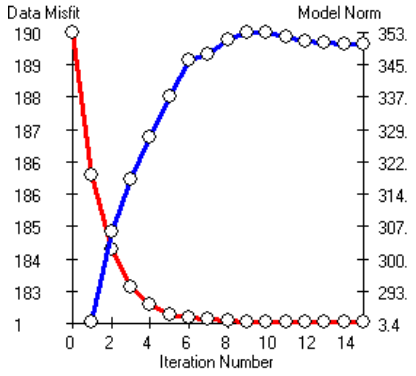

titan24

Note: Depth indications are approximate

Quantec Geoscience

Preliminary
05.08.09

Capstone Mining Corp.
Minto Mine Project

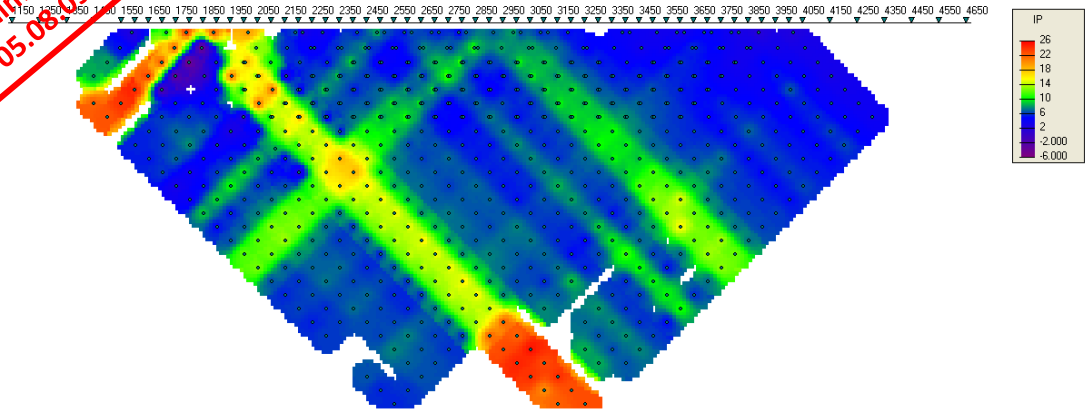

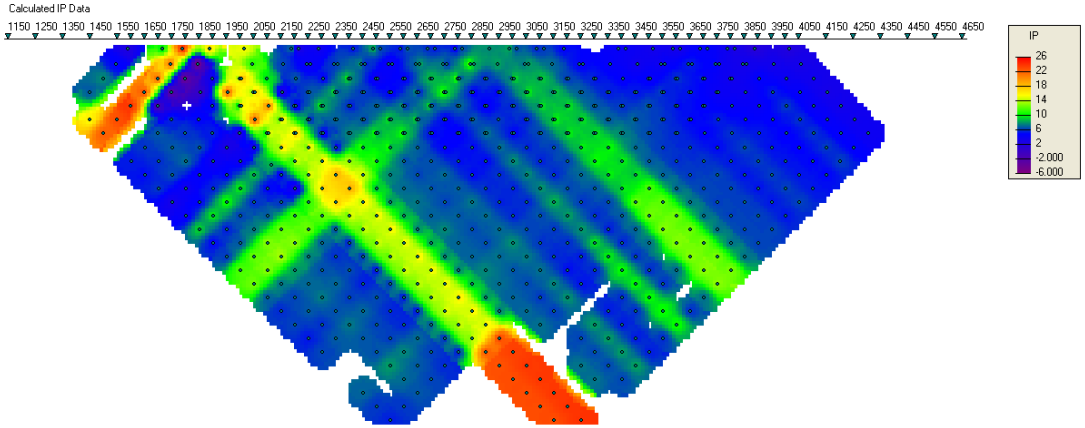

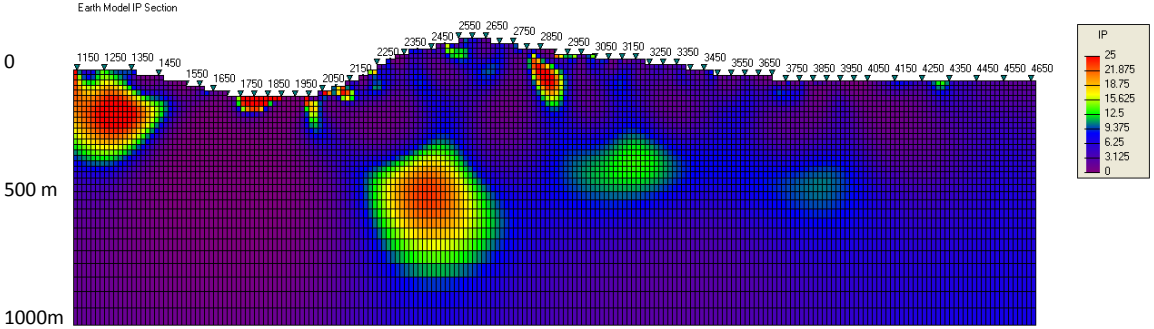

2D IP chargeability inversion results
smooth model:
data = 731
Misfit = 7.31012E+02
N iterations = 33

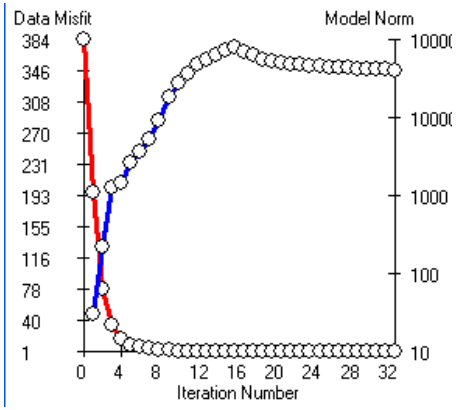

titan24

Note: Depth indications are approximate

Quantec Geoscience

Preliminary
05.08.09

Capstone Mining Corp.
Minto Mine Project

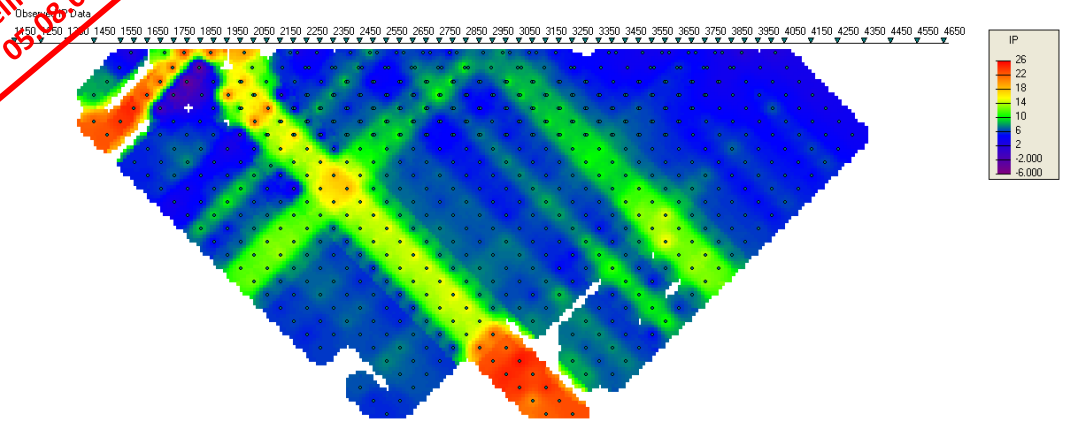

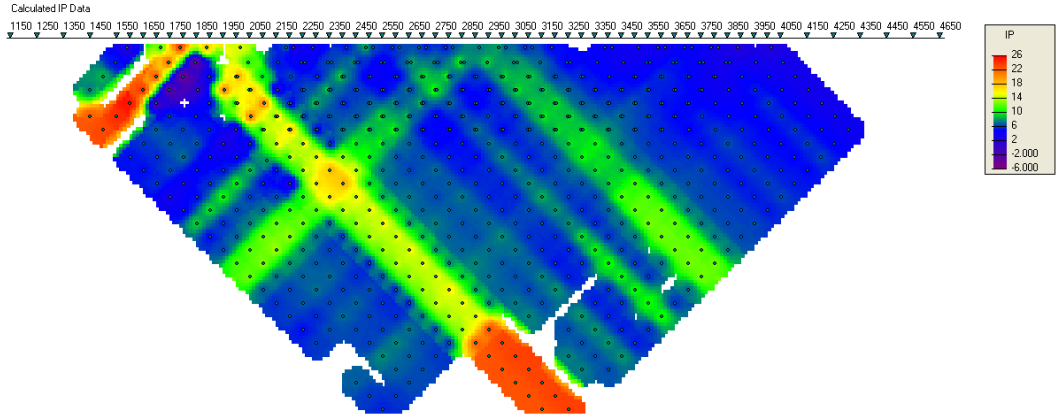

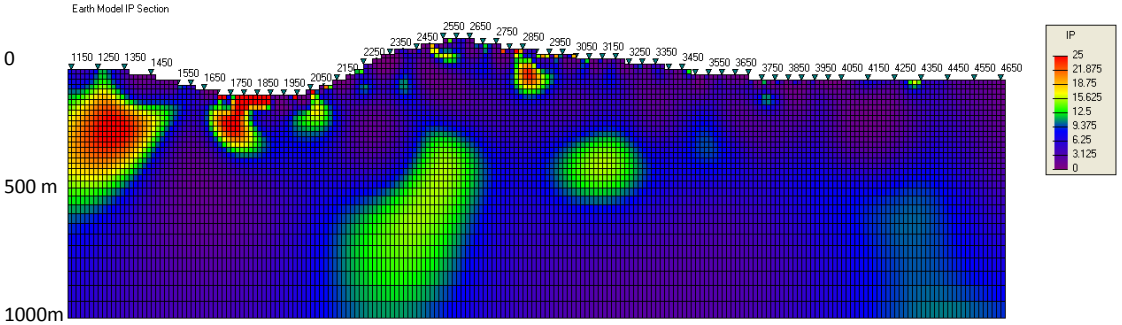

2D IP chargeability inversion results
Null Conductivity model:
N data = 731
Misfit = 7.31048E+02
N iterations = 37

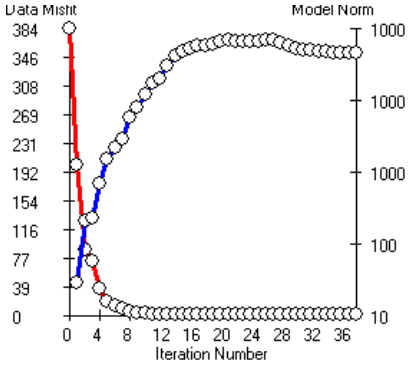

titan24

Note: Depth indications are approximate

Quantec Geoscience

DOI Investigation

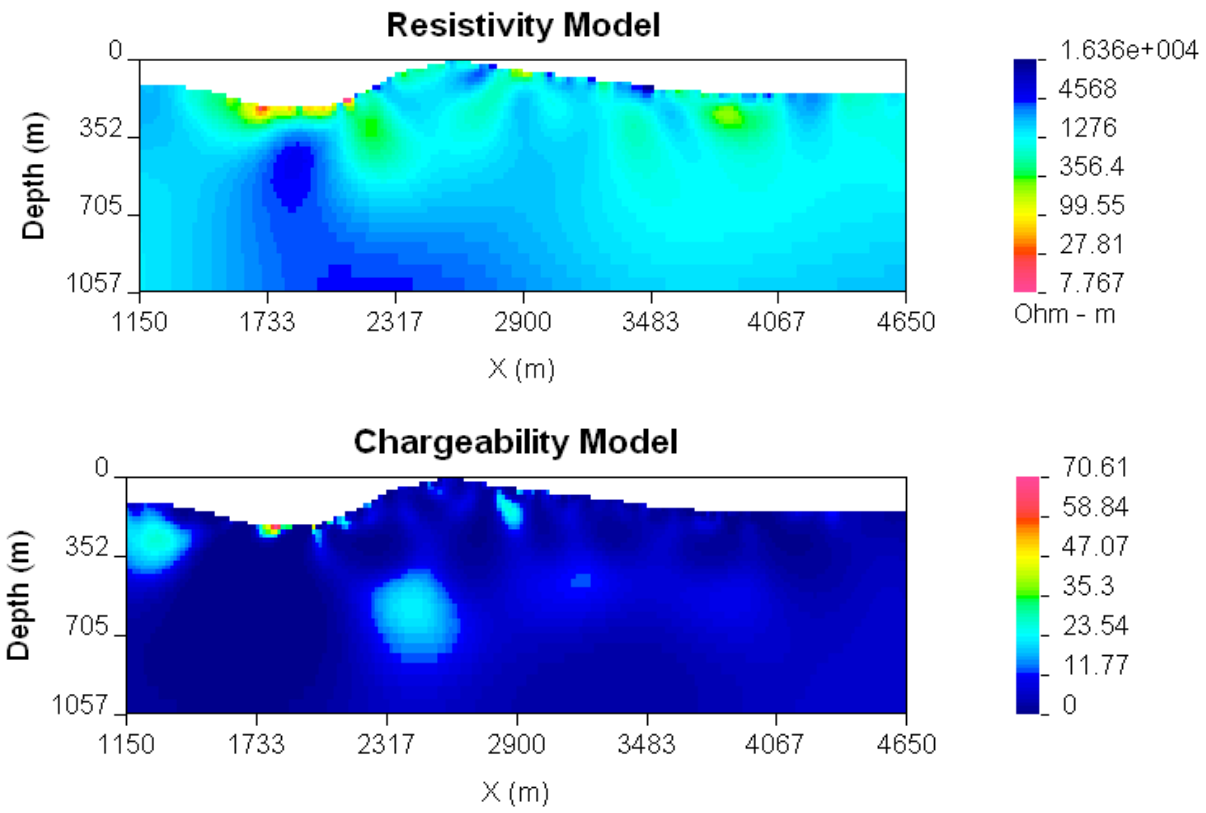

DOI (depth of investigation) is a Tool designed by the UBC-GIF to image the validity of inversion models. It compares two models calculated with different reference models.

Thus creating an image of how regions in the model which are influenced by the choice of reference model and not the actual data.

These zones are indicated with the hatched colours.

For the DC model a 10 kOhm-m and the default reference (average resistivity of the line) was used, in the IP the smooth and null con. Models were compared, a 0.1 cut off value was chosen

See: Oldenburg & Li, "**Estimating depth of investigation in dc resistivity and IP surveys**" GEOPHYSICS, VOL. 64, NO. 2 (MARCH-APRIL 1999); P. 403–416

titan24

Quantec Geoscience

Preliminary
05.08.09

Capstone Mining Corp.
Minto Mine Project

Geosoft Images

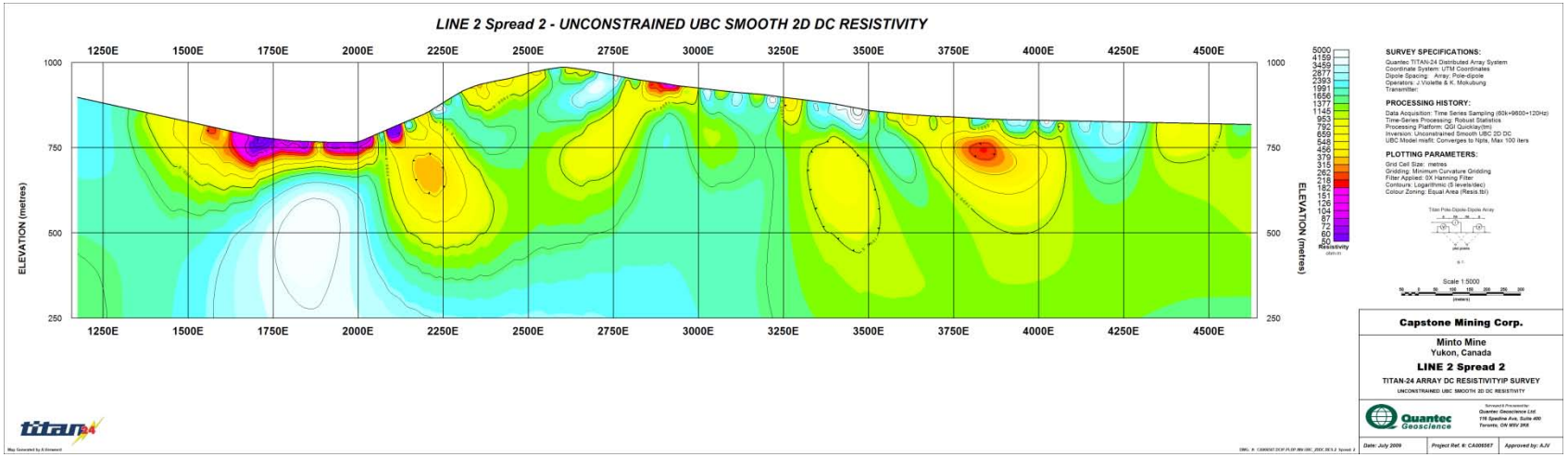

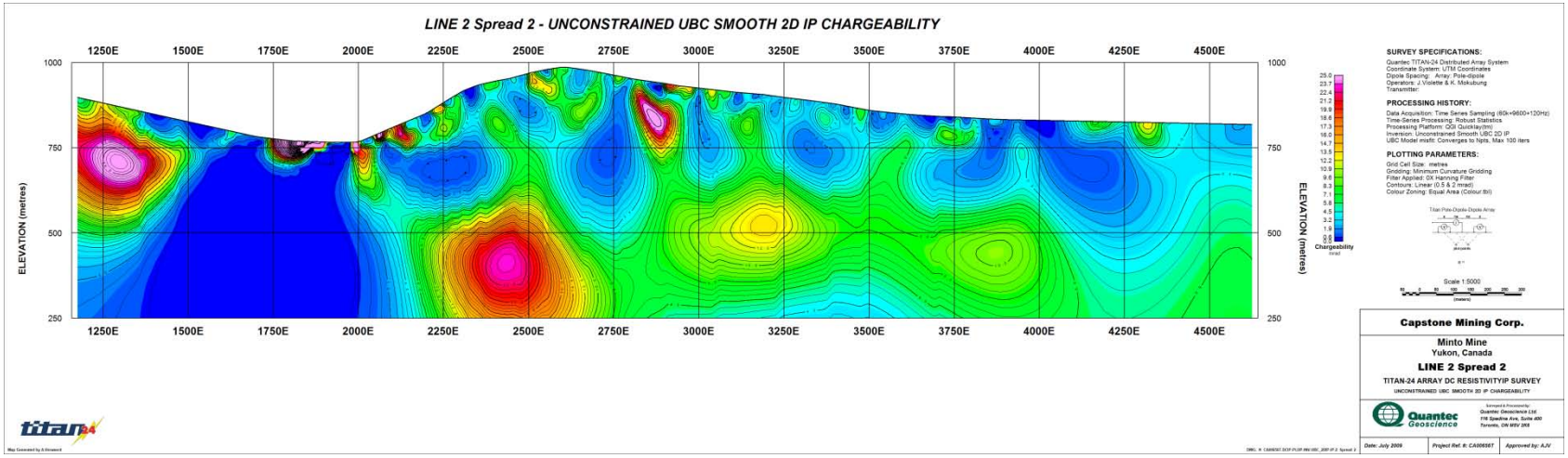

Preliminary
05.08.09

Capstone Mining Corp.
Minto Mine Project

Geosoft Images

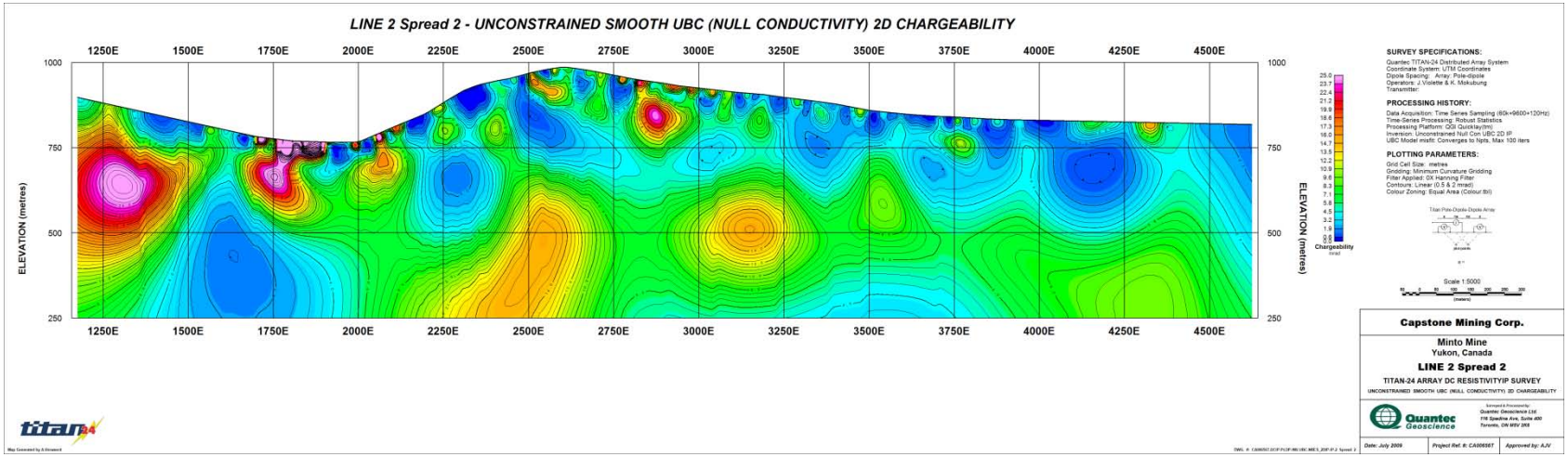

Preliminary
02.08.09

Capstone Mining Corp.
Minto Mine Project

MT inversion

Observed data

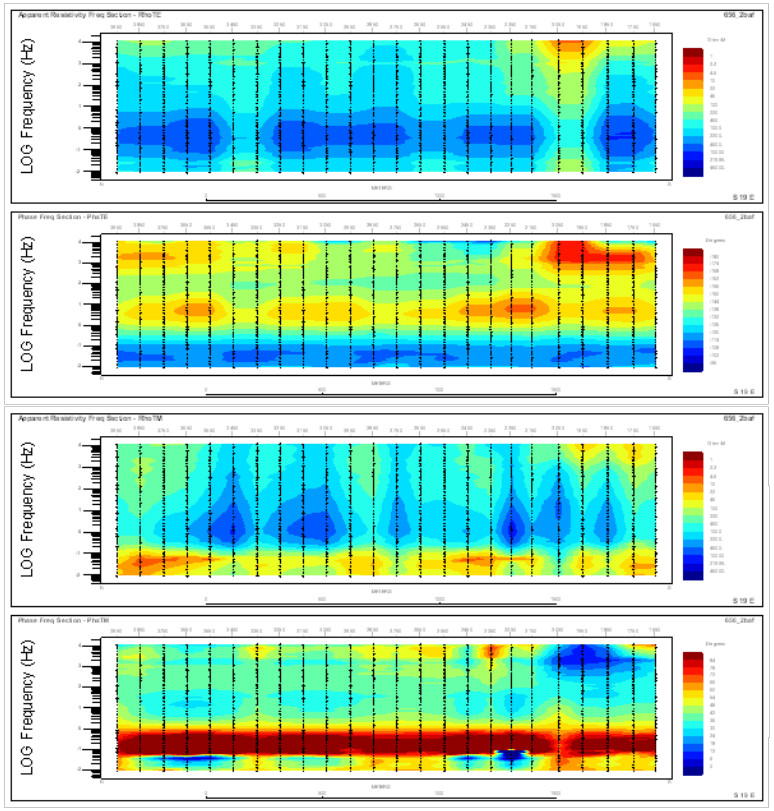

Interpolated data

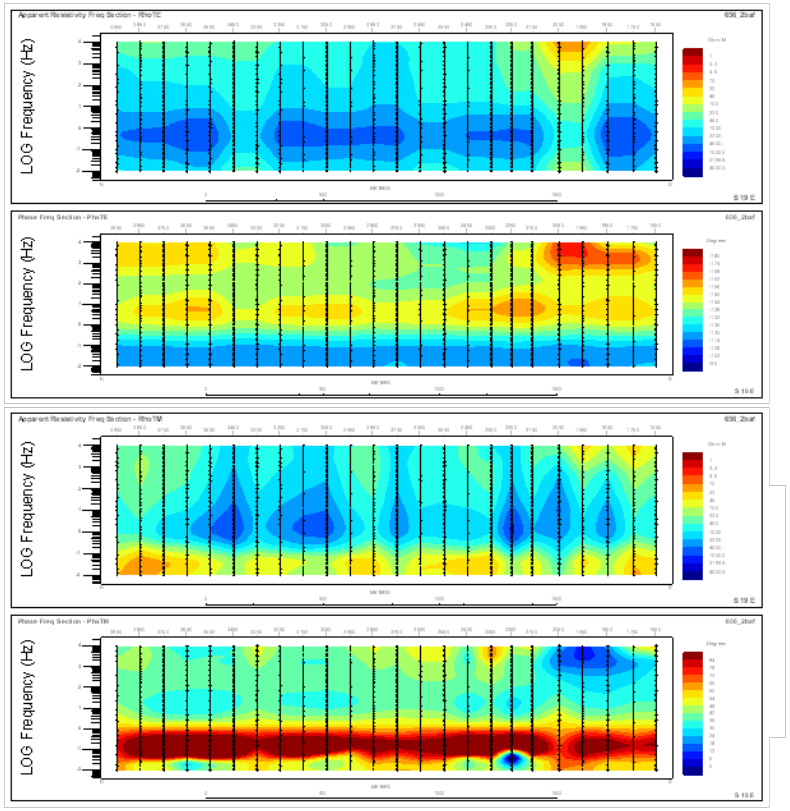

Note: The MT inversion program (GEOTOOLS), has a different plotting convention than the DC/IP inversion program (DCIP2D). Low station numbers are located on the lefts side in the DC/IP images and on the right side in the MT images.

titan24

Quantec Geoscience

Preliminary
02.08.09

Capstone Mining Corp.
Minto Mine Project

1D inversion results

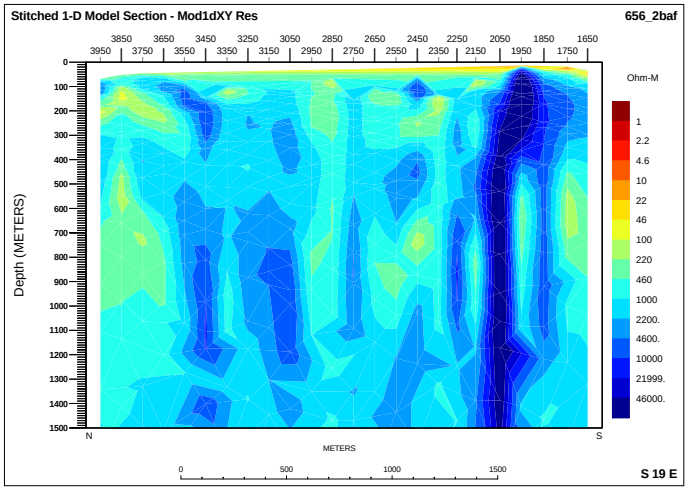

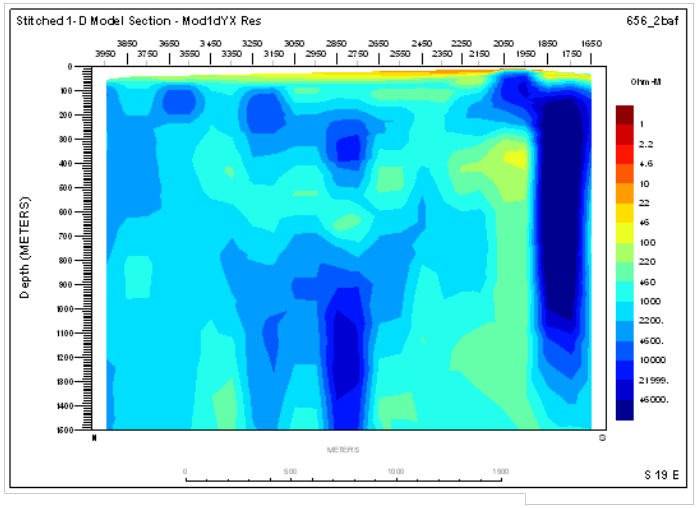

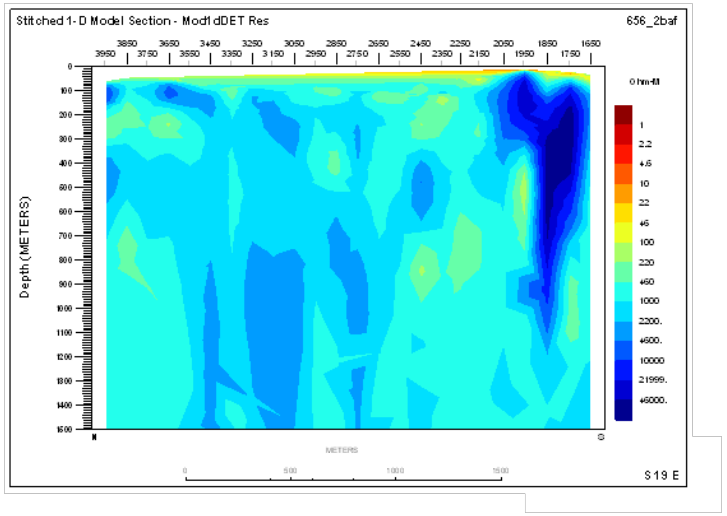

Left top: 1D stitched TE resistivity
Left bottom: 1D stitched TM resistivity
Right top: 1D stitched DET resistivity

titan24

Quantec Geoscience

Preliminary
05.08.09

Capstone Mining Corp.
Minto Mine Project

2D RLM Inversion

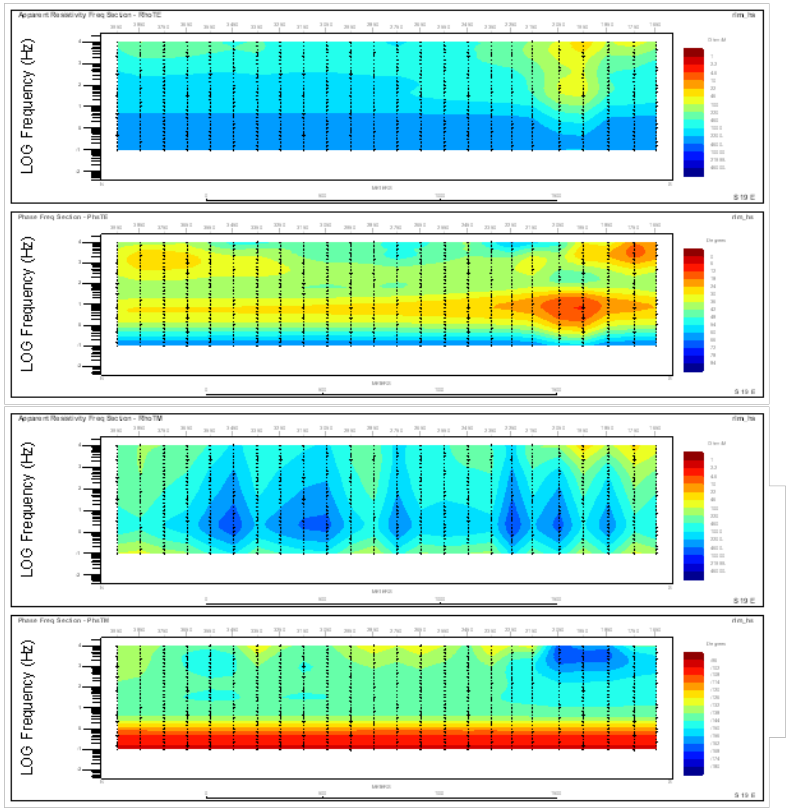

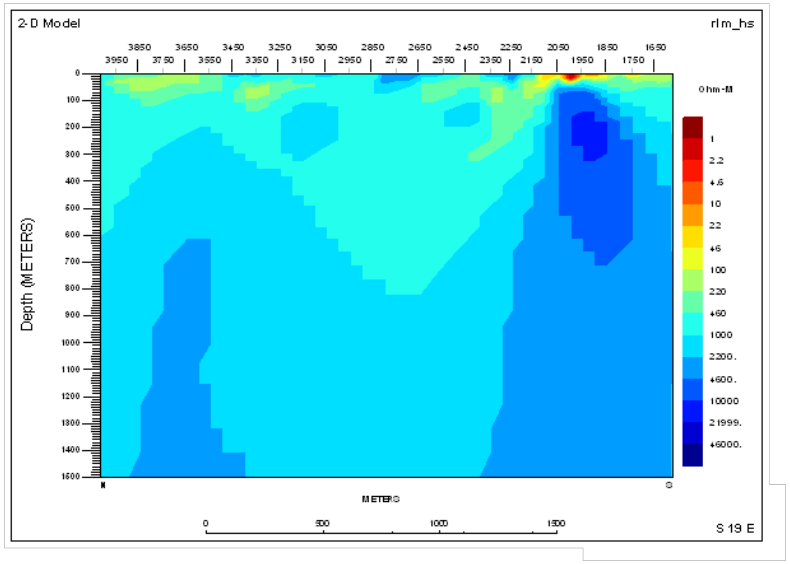

2D RLM TM,TE inversion results:
Starting model: 5000 Ohm-m halfspace
RMS misfit: 0.5049E+01
N iteration: 49

titan24

Quantec Geoscience

Preliminary
05.08.09

Capstone Mining Corp.
Minto Mine Project

2D PW inversion

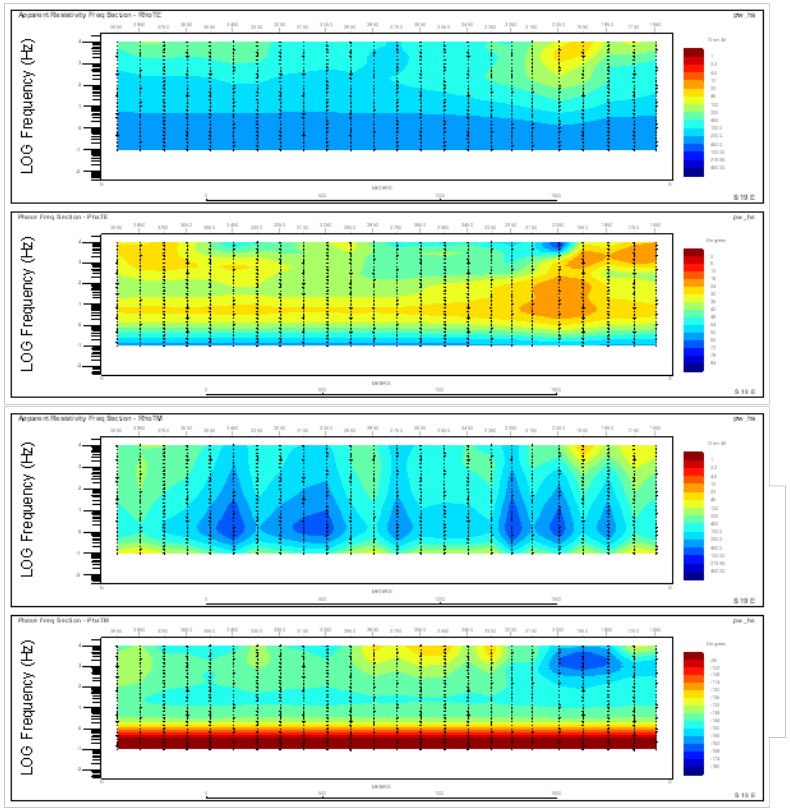

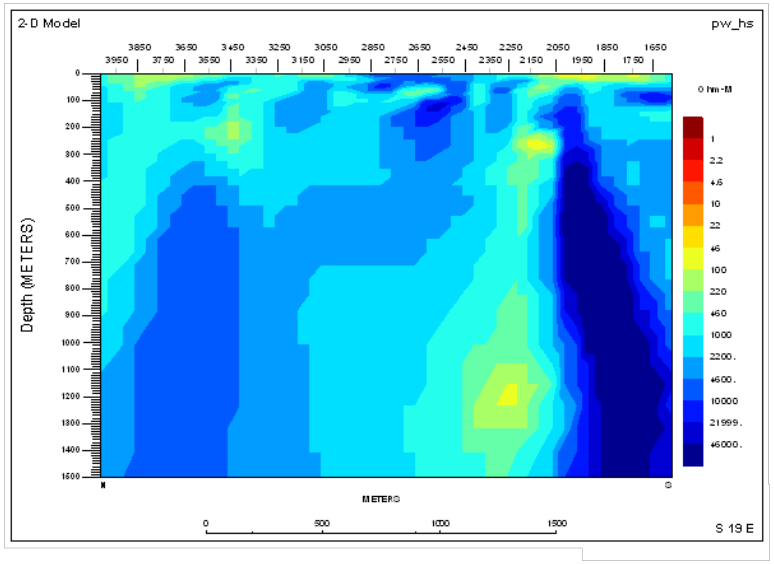

2D PW TM,TE inversion results:
Starting model: 5000 Ohm-m halfspace
RMS misfit: 0.5091E+01
N iteration: 45

titan24

Quantec Geoscience

2D PW inversion

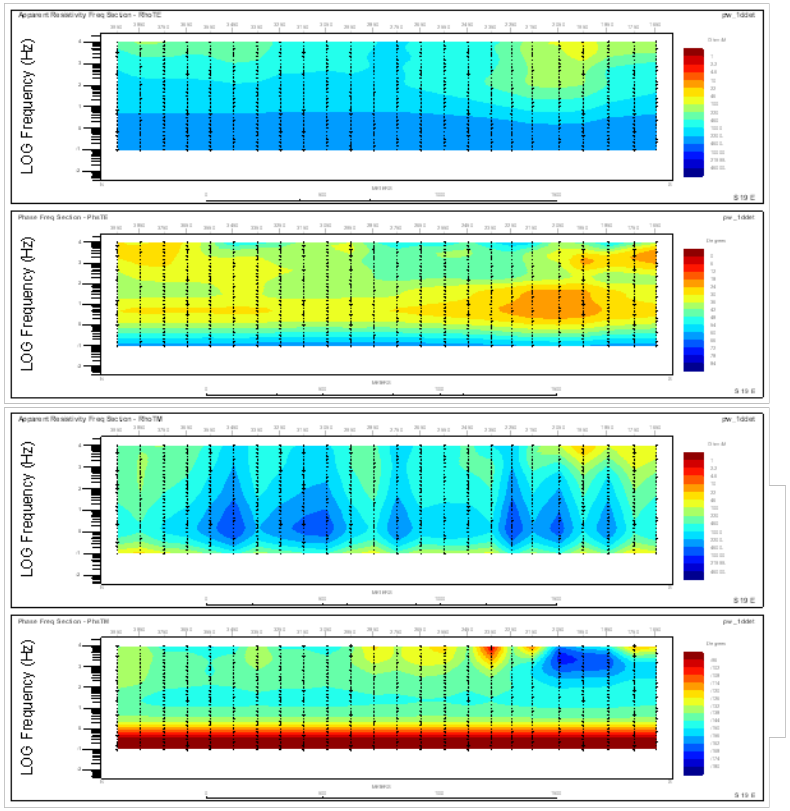

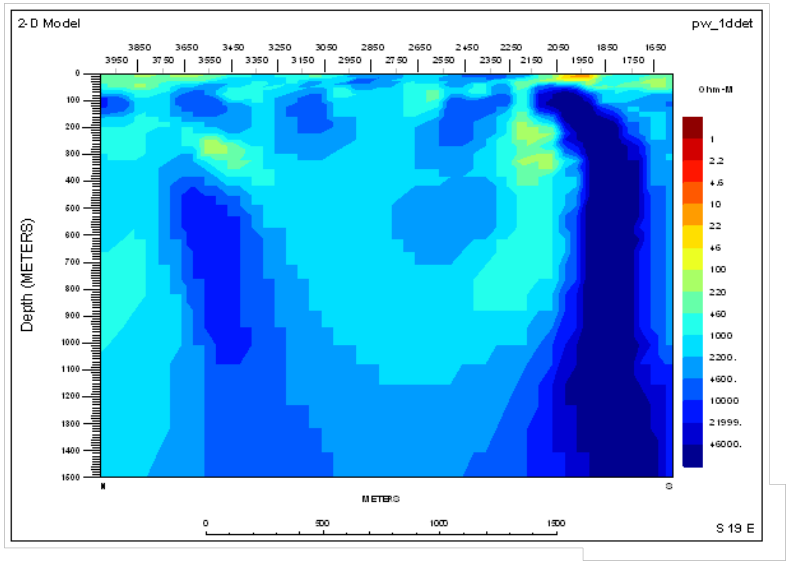

2D PW TM,TE inversion results:
Starting model: Stitched 1D DET
RMS misfit: 0.5402E+01
N iteration: 39

Preliminary
05.08.09

Capstone Mining Corp.
Minto Mine Project

Geosoft Images

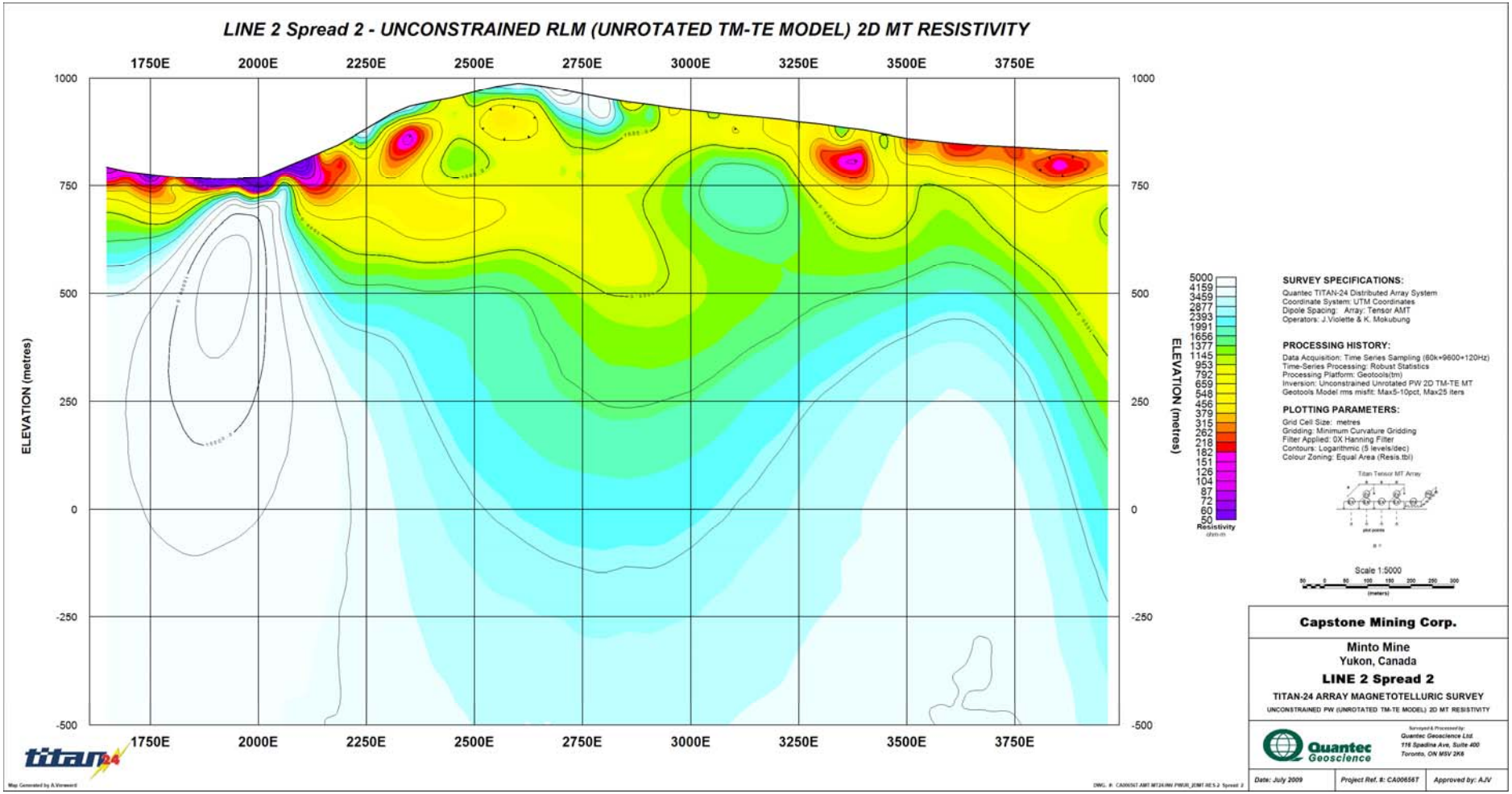

Preliminary
05.08.09

Capstone Mining Corp.
Minto Mine Project

Geosoft Images

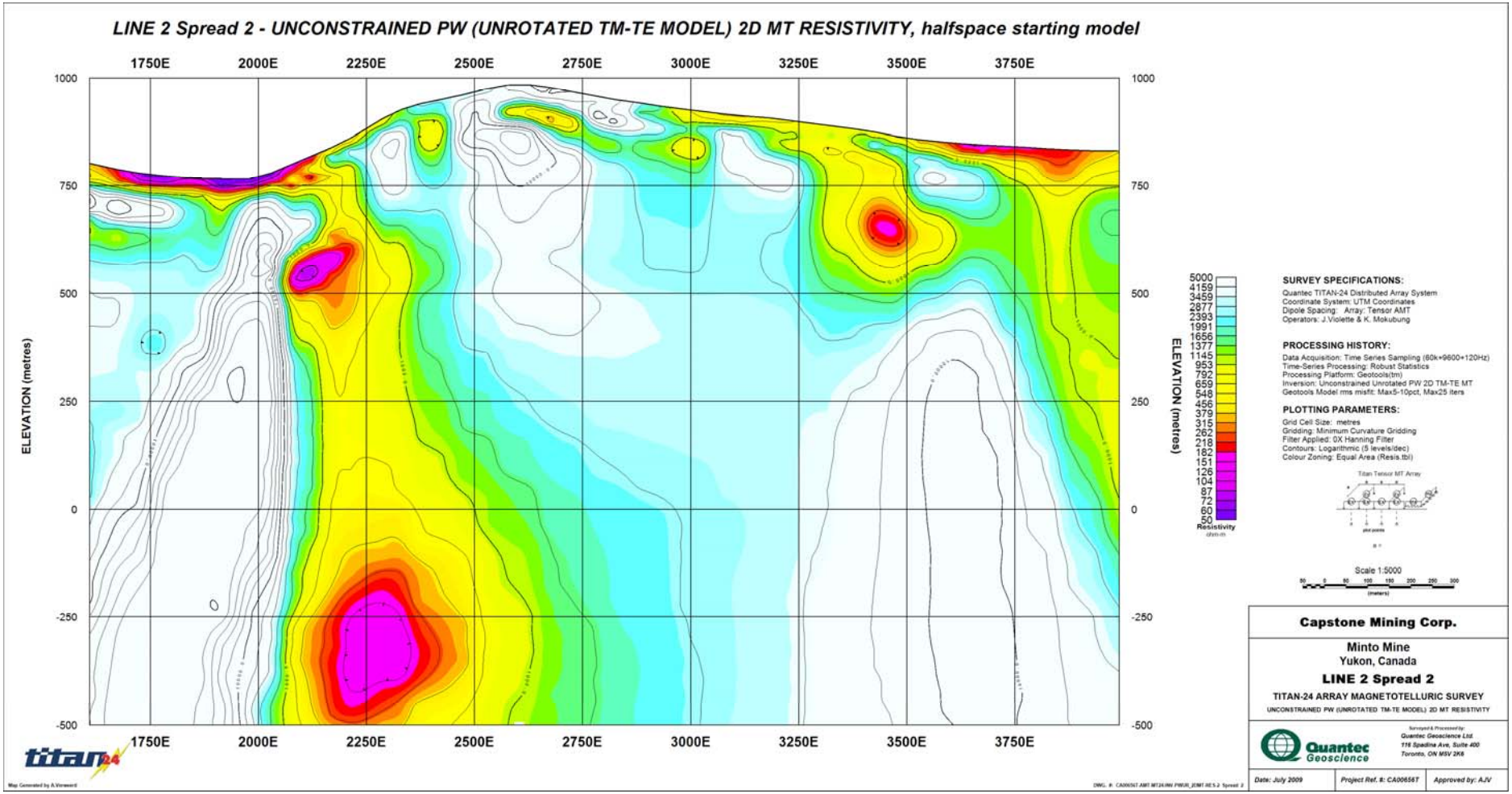

Preliminary
05.08.09

Capstone Mining Corp.
Minto Mine Project

Geosoft Images

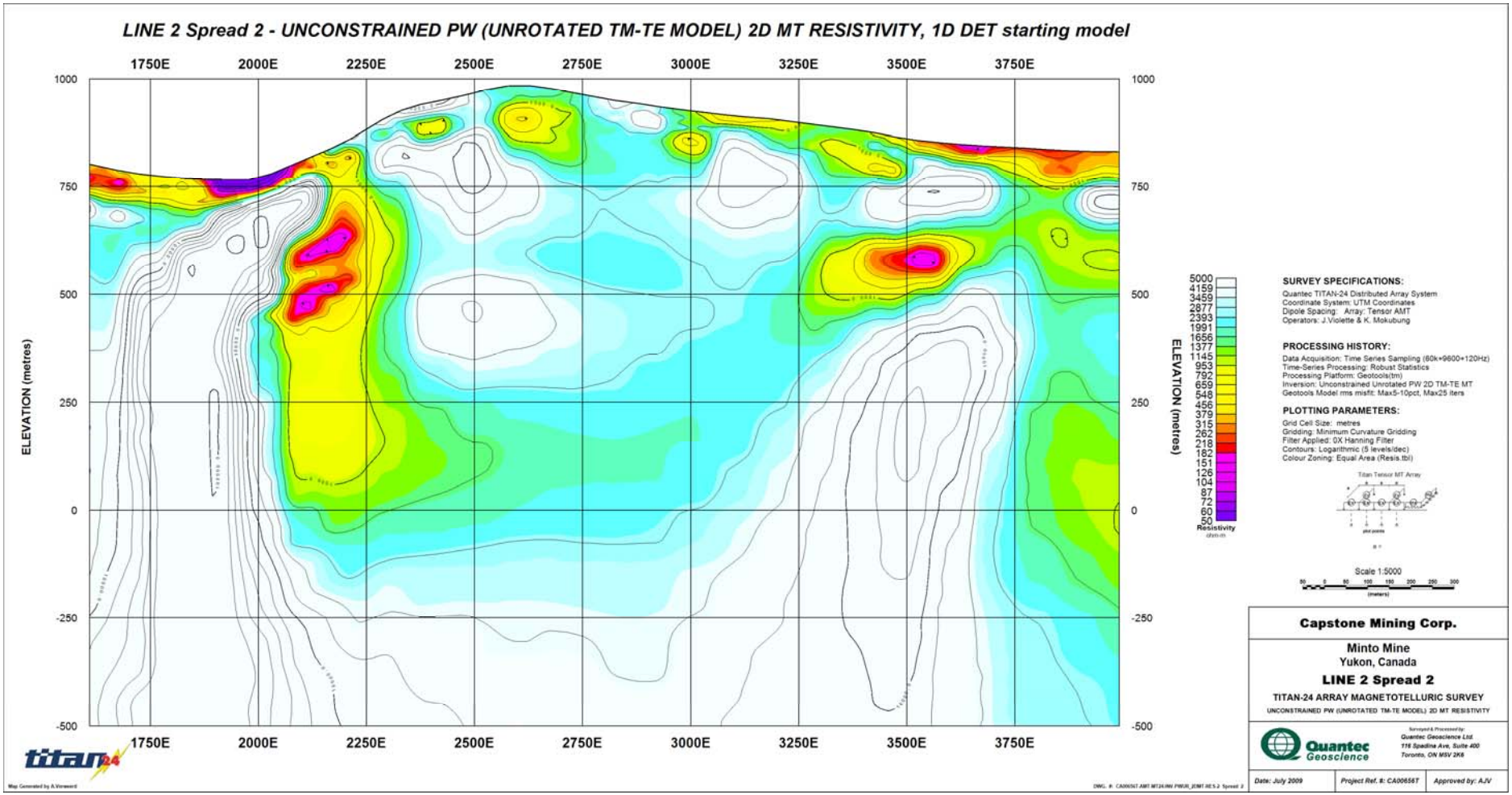

LINE L3 spread 1
TITAN-24 Survey
Minto Mine Project
Capstone Mining Corp - Minto Explorations

Preliminary 2D Inversion

Quantec Geoscience Ltd.
Toronto, Canada

A. Verweerd, Dr. Rer. Nat.

Preliminary
07.08.09

Capstone Mining Corp.
Minto Mine Project

2D DC/IP inversion

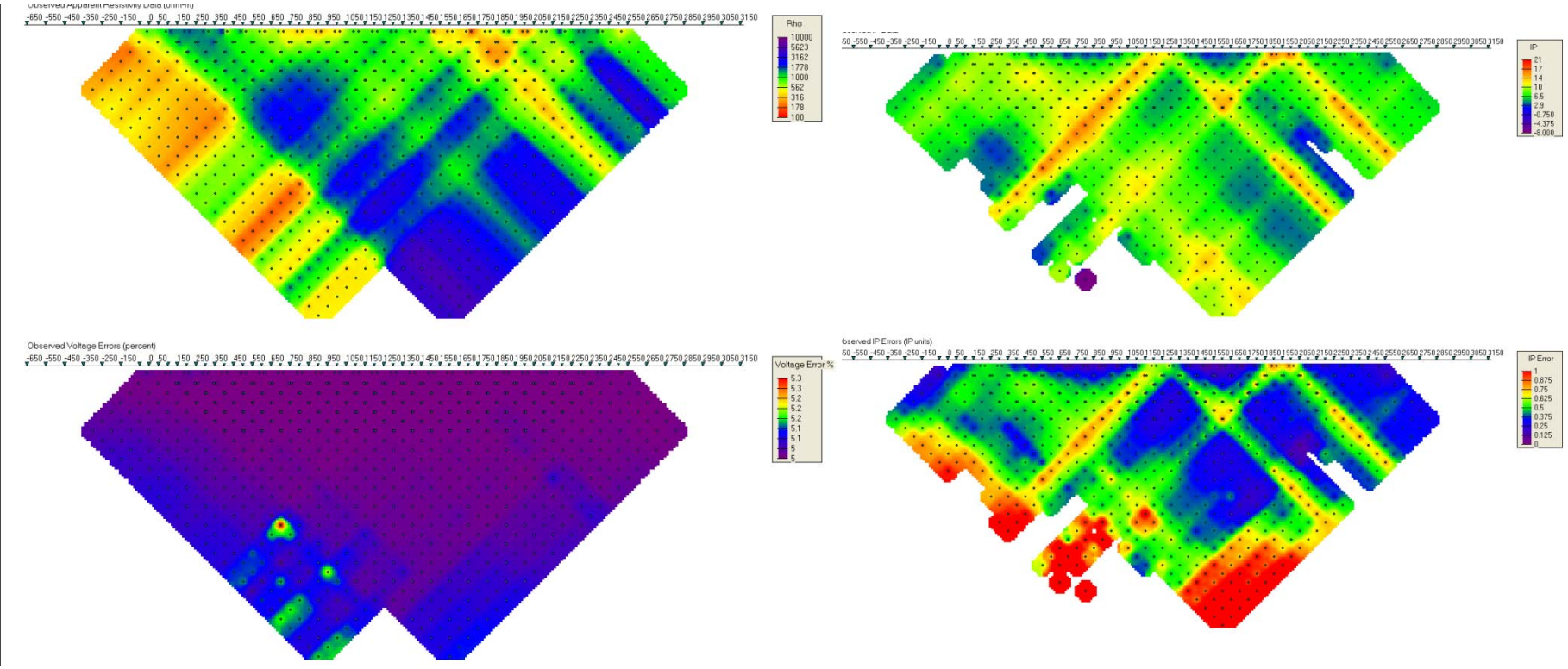

DC data: Acquisition error + 5%

IP data: Remove acquisition error>25%

if error < 7%, set at 7%, else keep error, outlier rejection

titan24

Quantec Geoscience

Preliminary
07.08.09

Capstone Mining Corp.
Minto Mine Project

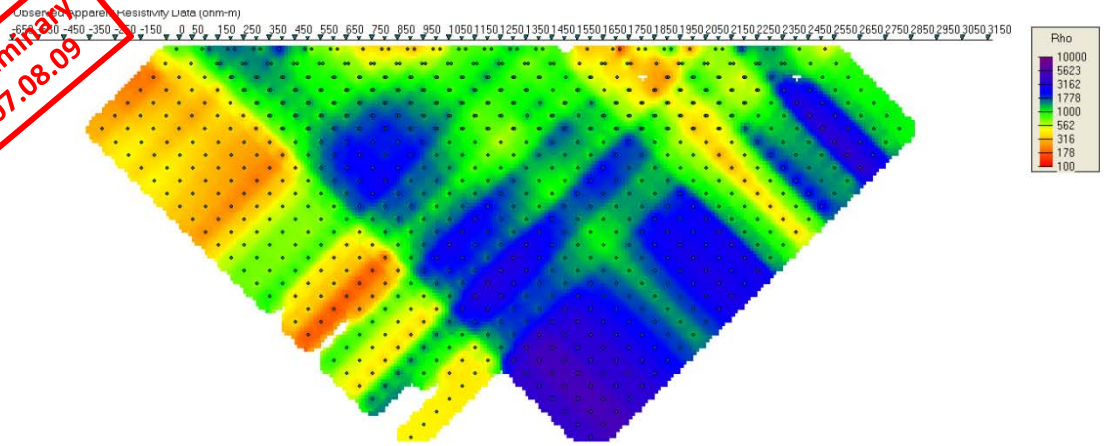

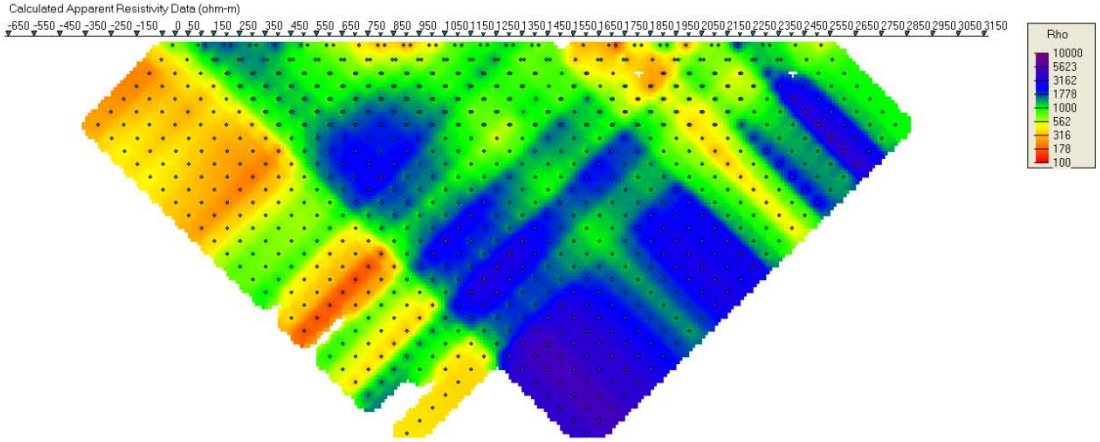

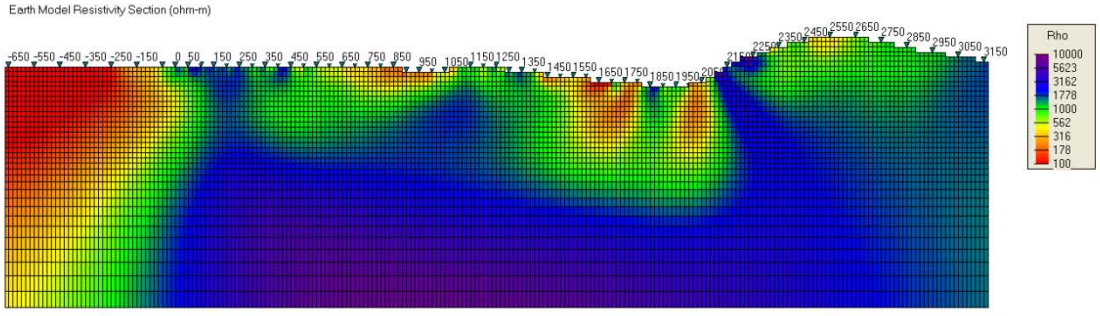

0

500 m

1000m

2D DC resistivity inversion results:
N data = 917
Misfit = 9.16773E+02
N iterations = 12

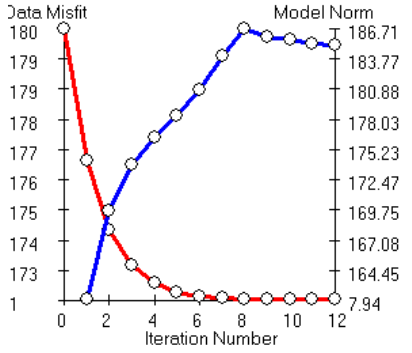

Note: Depth indications are approximate

Quantec Geoscience

Preliminary
07.08.09

Capstone Mining Corp.
Minto Mine Project

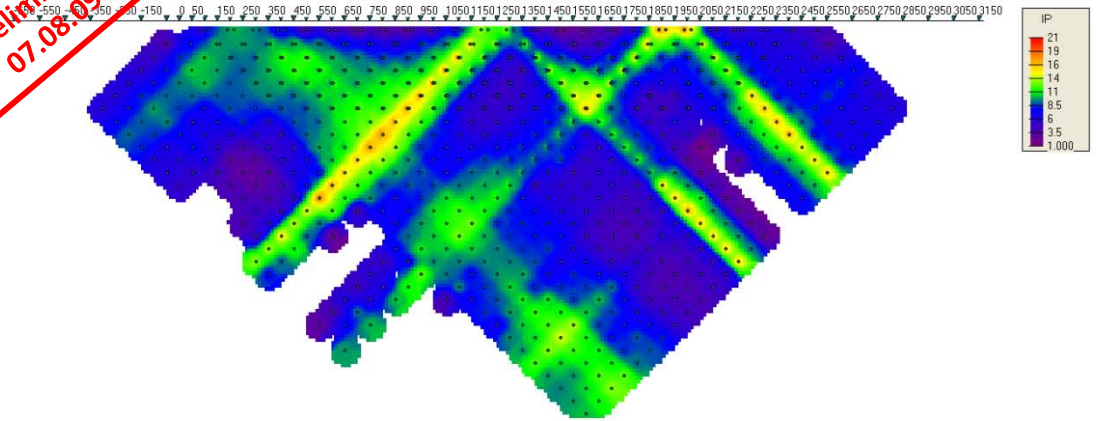

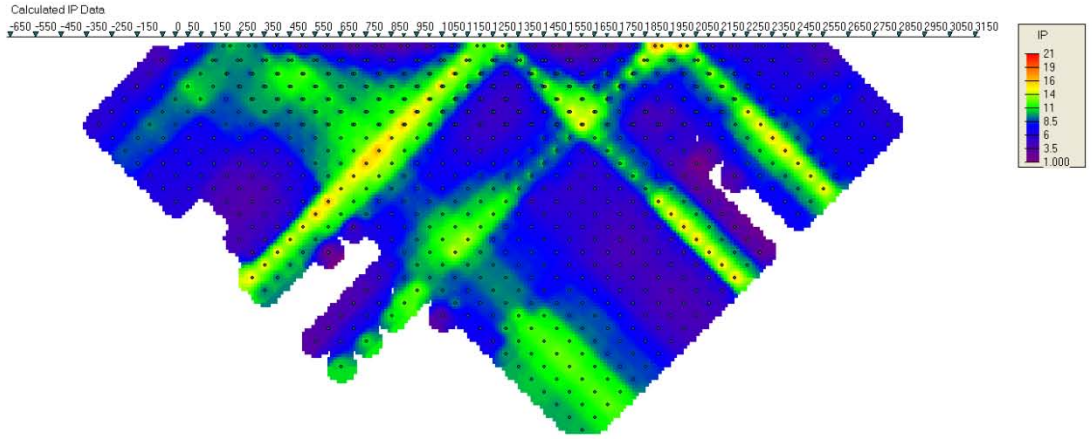

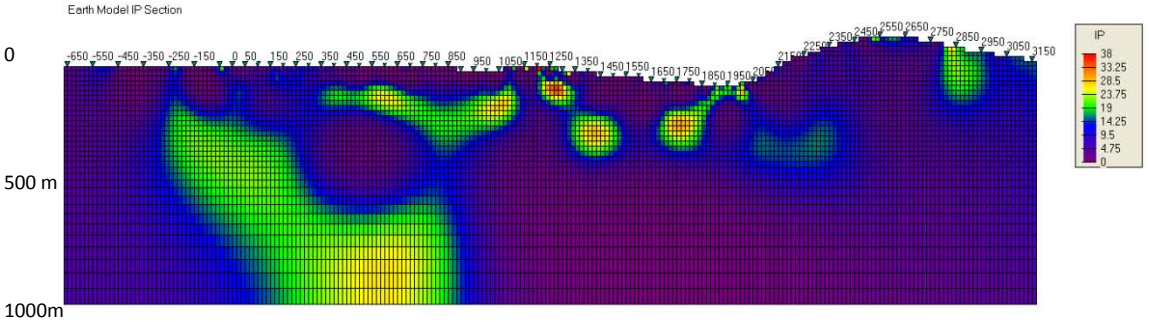

2D IP chargeability inversion results
smooth model:
data = 848
Misfit = 8.48056E+02
iterations = 34

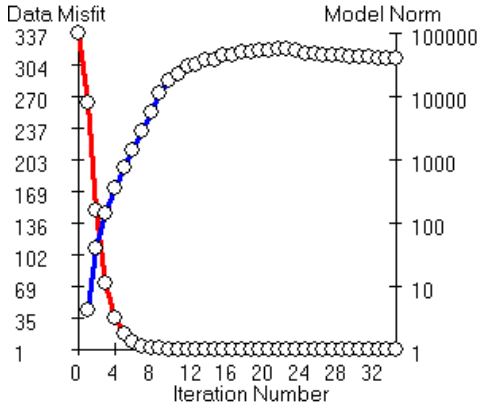

Note: Depth indications are approximate

Preliminary
07.08.09

Capstone Mining Corp.
Minto Mine Project

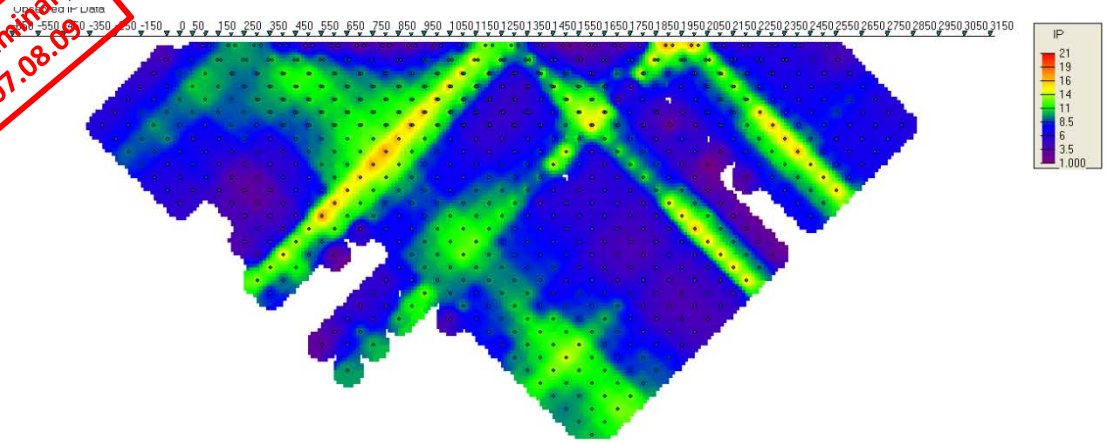

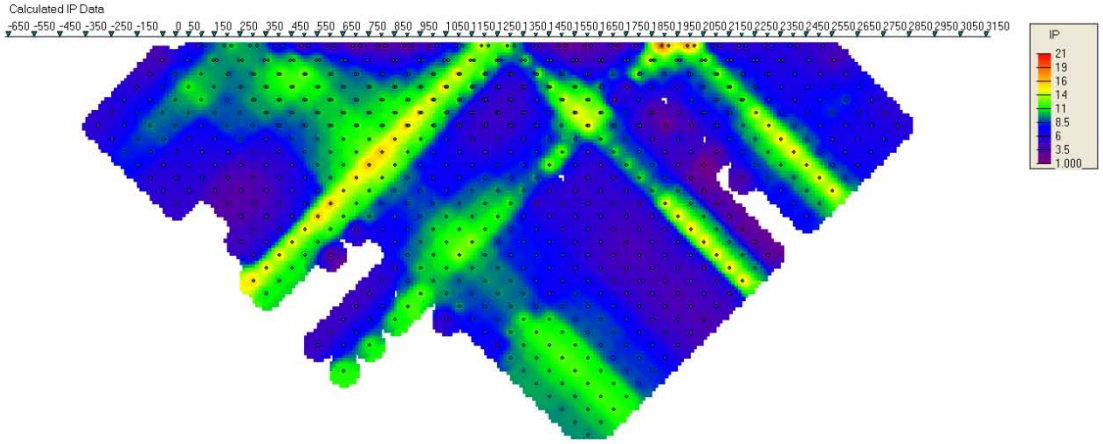

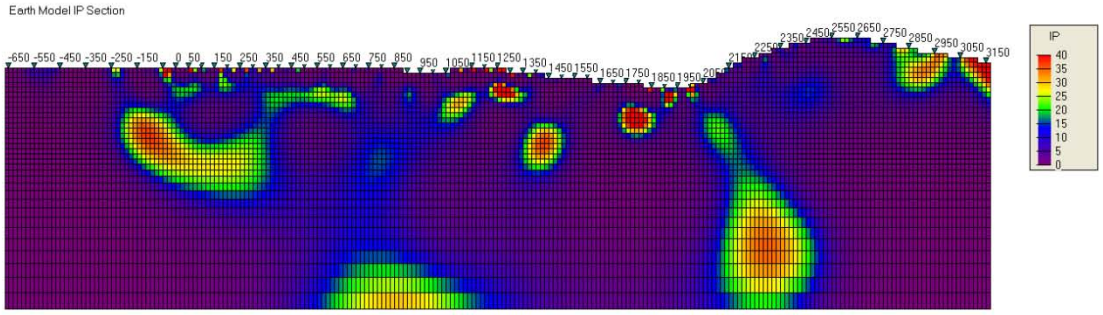

0

500 m

1000m

2D IP chargeability inversion results
Null Conductivity model:
N data = 833
Misfit = 8.33057E+02
N iterations = 33

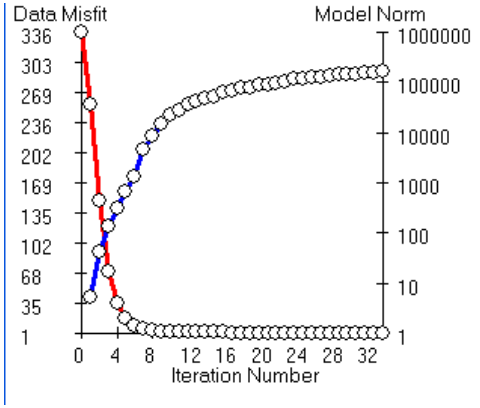

titan24

Note: Depth indications are approximate

Quantec Geoscience

DOI Investigation

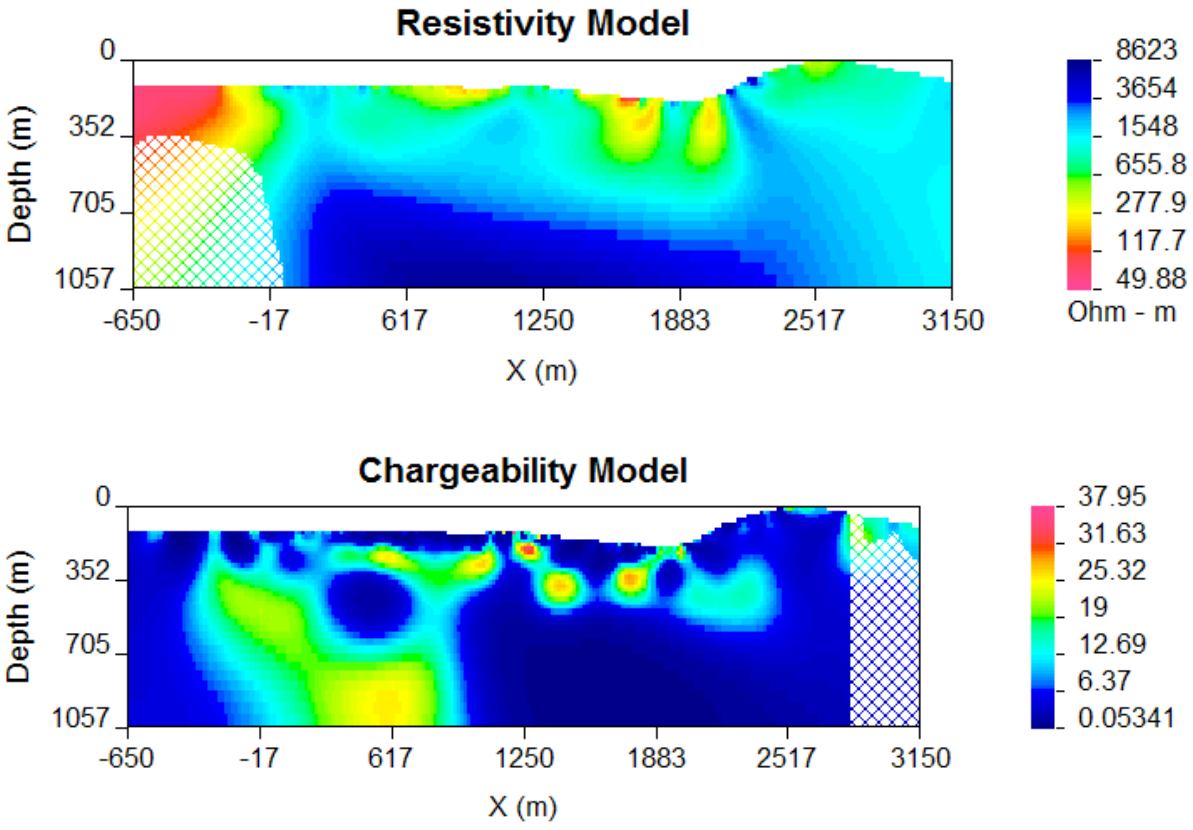

DOI (depth of investigation) is a Tool designed by the UBC-GIF to image the validity of inversion models. It compares two models calculated with different reference models.

Thus creating an image of how regions in the model which are influenced by the choice of reference model and not the actual data.

These zones are indicated with the hatched colours.

For the DC model a 10 kOhm-m and the default reference (average resistivity of the line) was used, in the IP the smooth and null con. Models were compared, a 0.1 cut off value was chosen

See: Oldenburg & Li, "**Estimating depth of investigation in dc resistivity and IP surveys**" GEOPHYSICS, VOL. 64, NO. 2 (MARCH-APRIL 1999); P. 403–416

titan24

Quantec Geoscience

Preliminary
07.08.09

Capstone Mining Corp.
Minto Mine Project

Geosoft Images

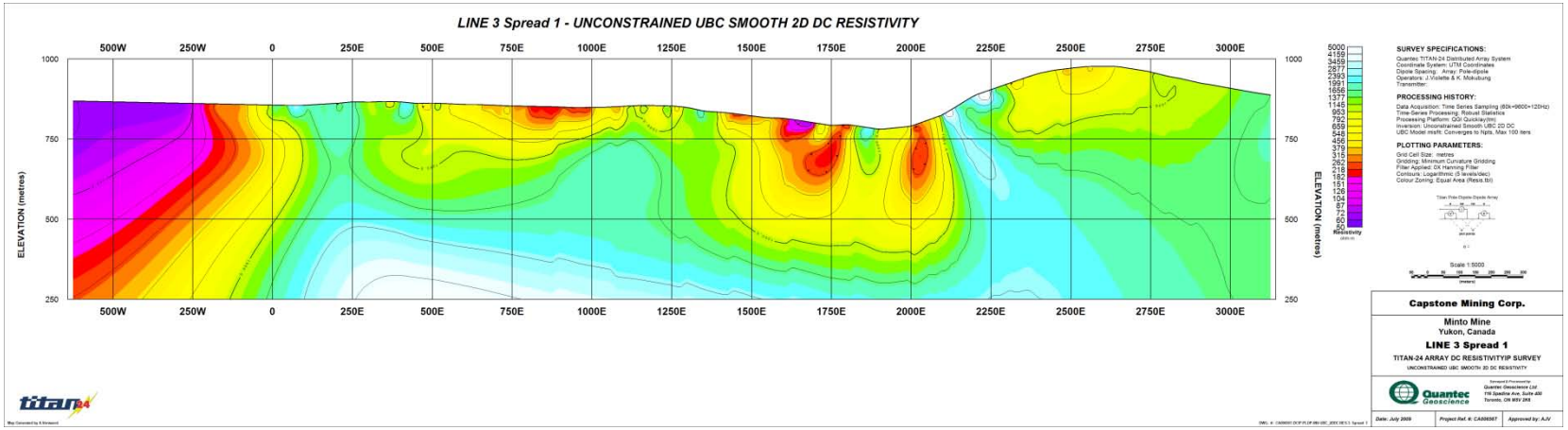

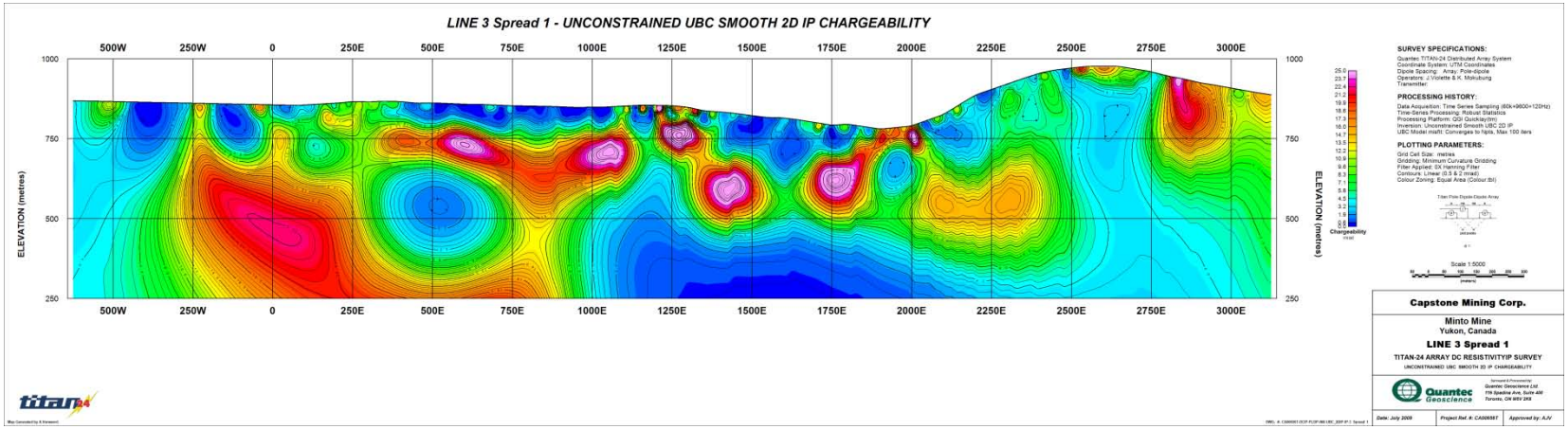

Preliminary
07.08.09

Capstone Mining Corp.
Minto Mine Project

Geosoft Images

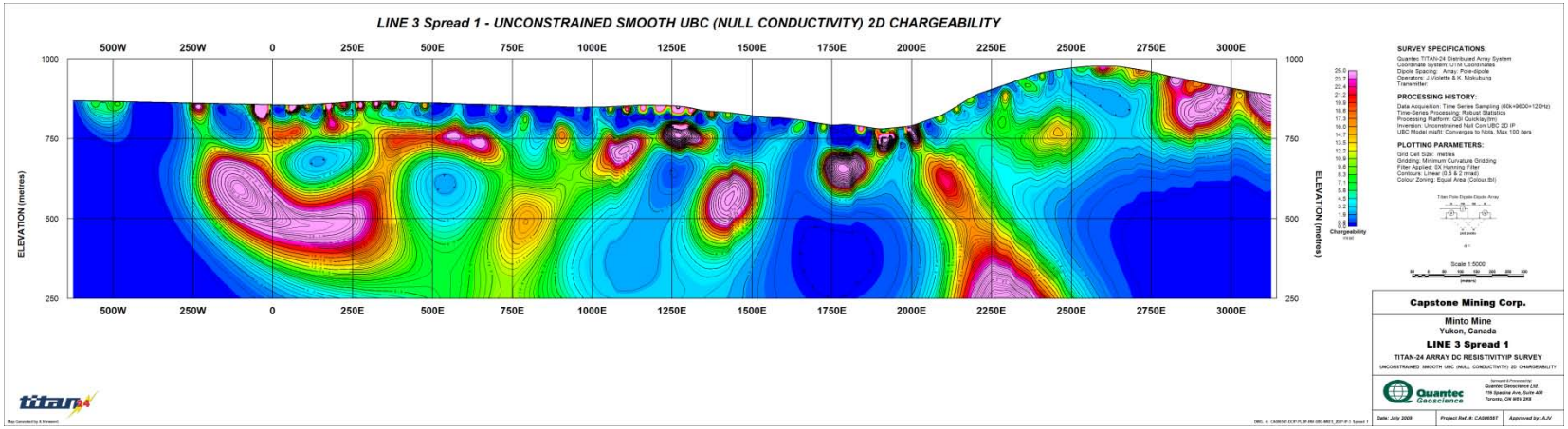

Preliminary
07.08.09

Capstone Mining Corp.
Minto Mine Project

MT inversion

Observed data

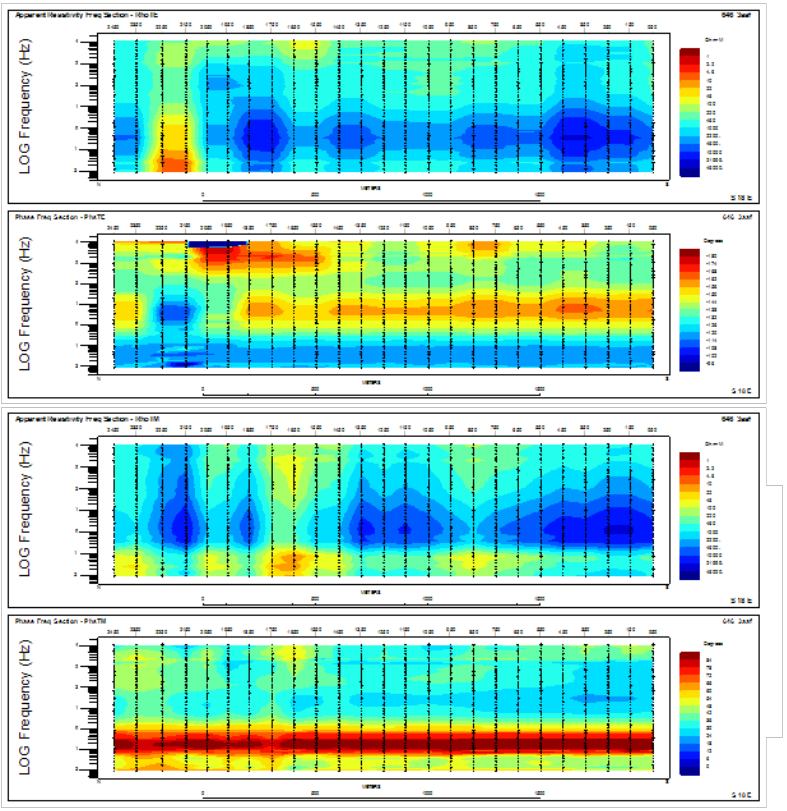

Interpolated data

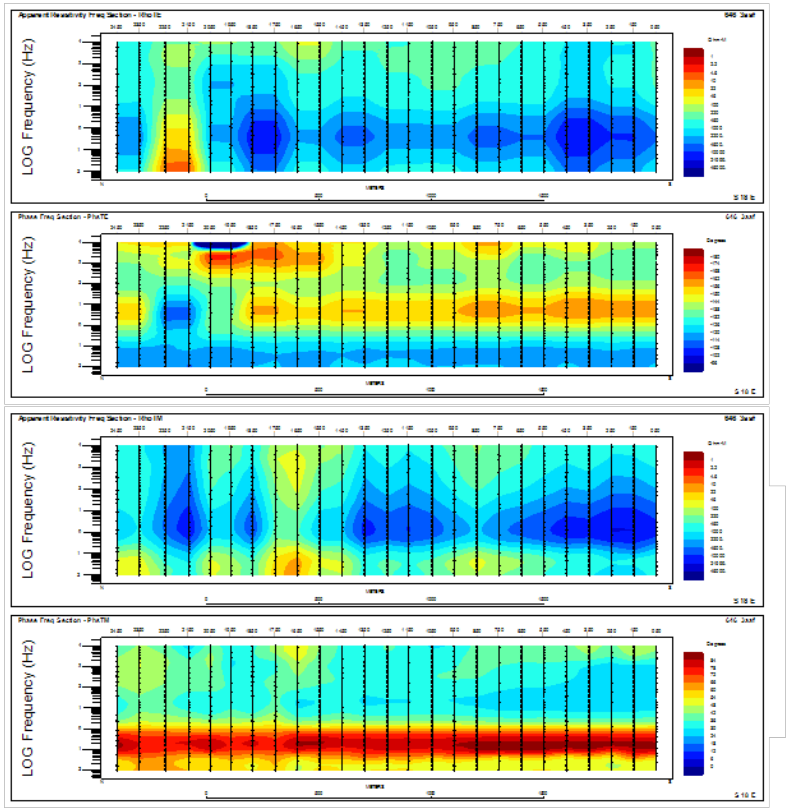

Note: The MT inversion program (GEOTOOLS), has a different plotting convention than the DC/IP inversion program (DCIP2D). Low station numbers are located on the lefts side in the DC/IP images and on the right side in the MT images.

titan24

Quantec Geoscience

Preliminary
07.08.09

Capstone Mining Corp.
Minto Mine Project

1D inversion results

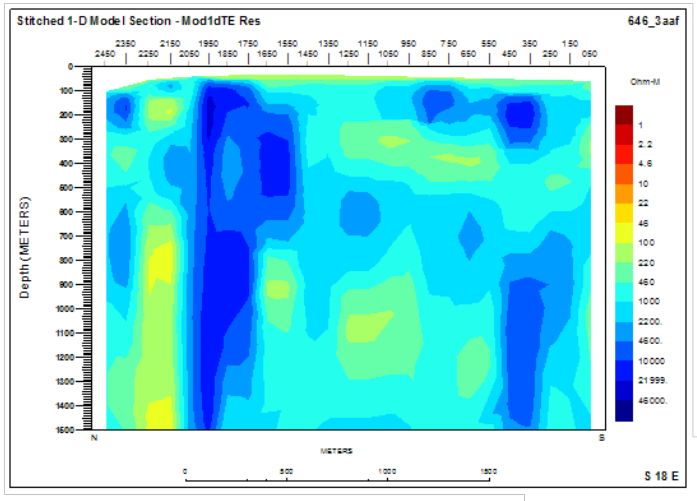

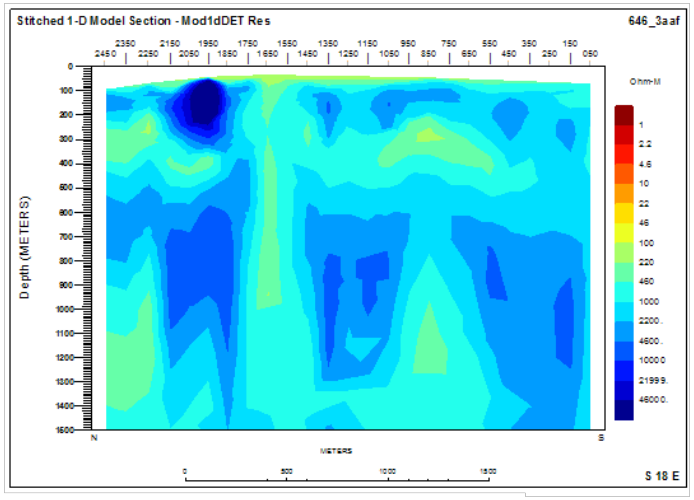

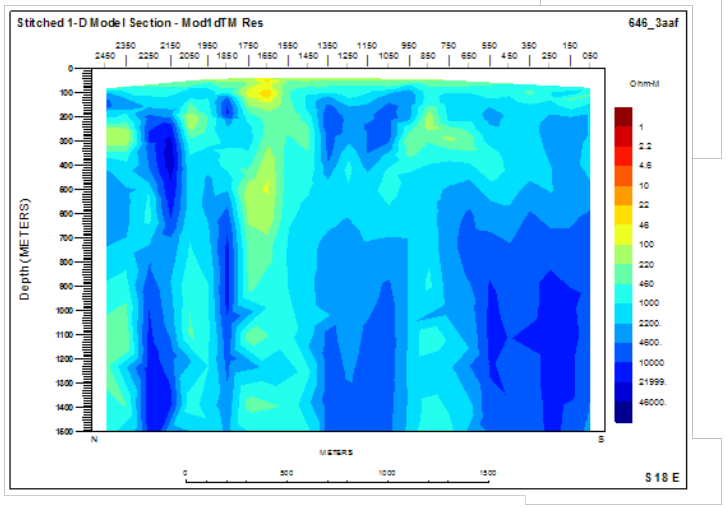

Left top: 1D stitched TE resistivity
Left bottom: 1D stitched TM resistivity
Right top: 1D stitched DET resistivity

titan24

Quantec Geoscience

Preliminary
07.08.09

Capstone Mining Corp.
Minto Mine Project

2D RLM Inversion

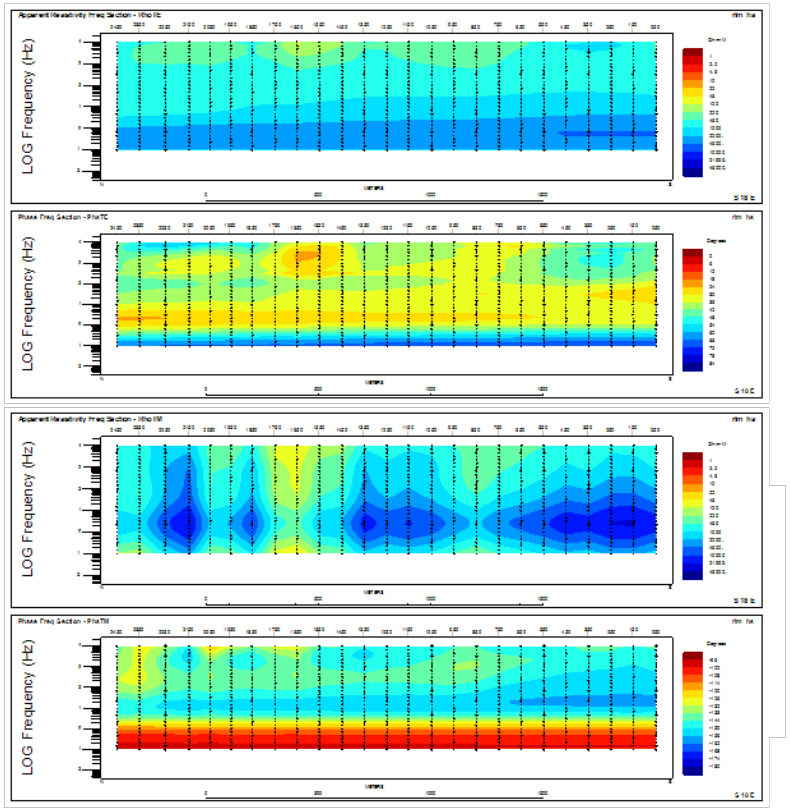

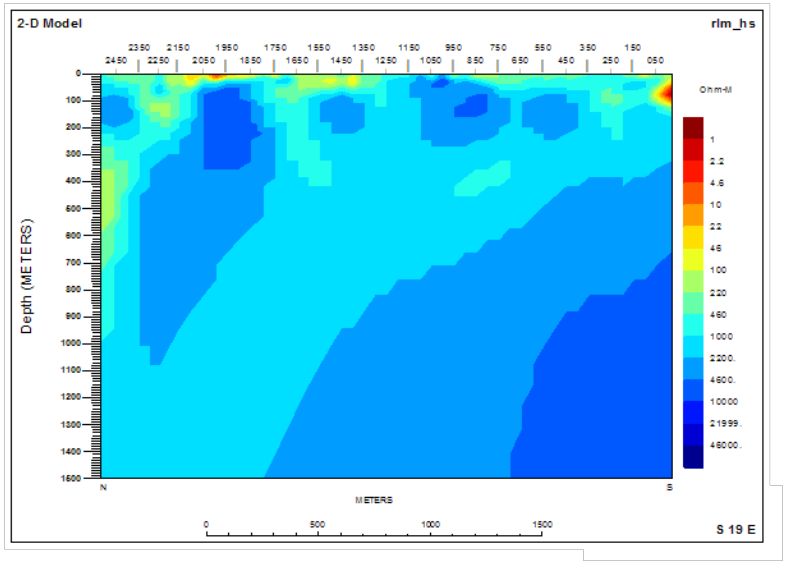

2D RLM TM,TE inversion results:
Starting model: 5000 Ohm-m halfspace
RMS misfit: 0.9573E+01
N iteration: 29

titan24

Quantec Geoscience

Preliminary
07.08.09

Capstone Mining Corp.
Minto Mine Project

2D PW inversion

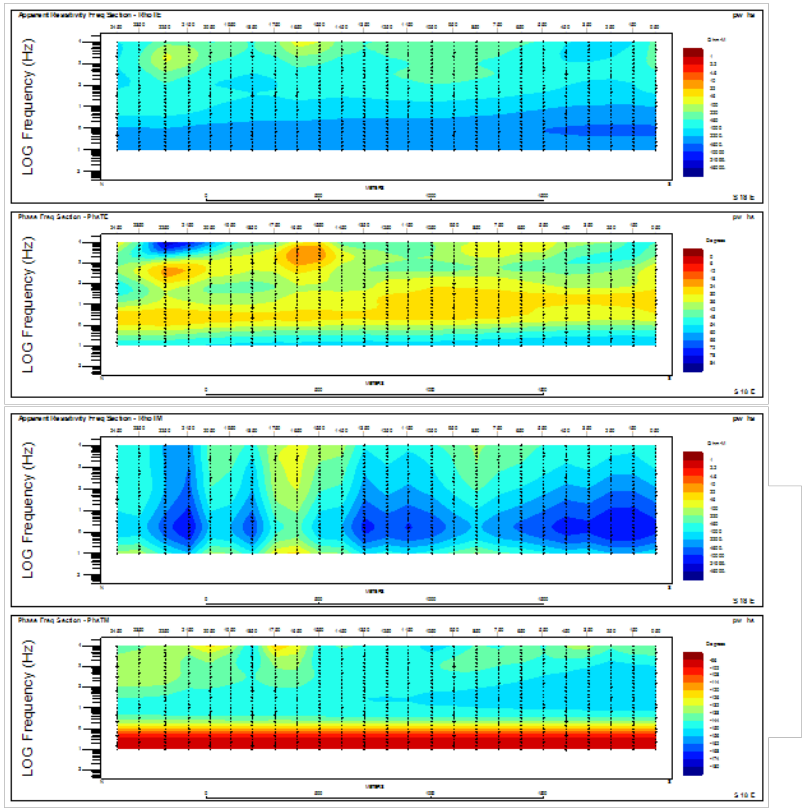

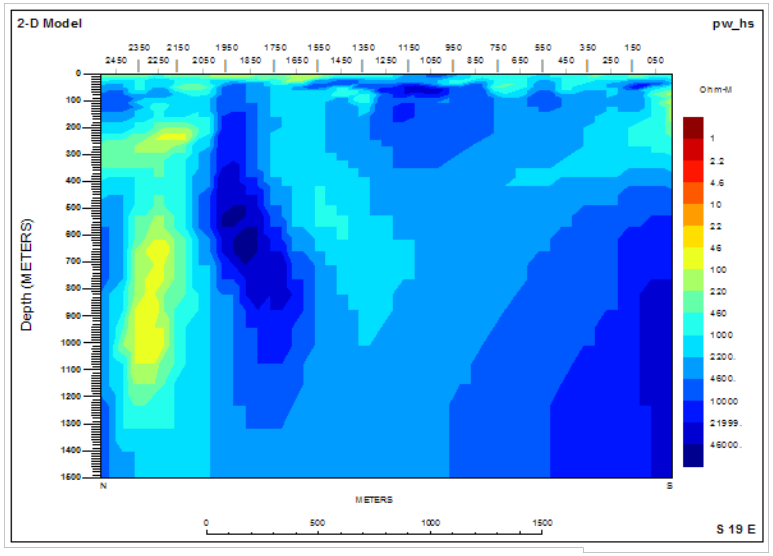

2D PW TM,TE inversion results:
Starting model: 5000 Ohm-m halfspace
RMS misfit: 0.8905E+01
N iteration: 30

titan24

Quantec Geoscience

Preliminary
07.08.09

Capstone Mining Corp.
Minto Mine Project

2D PW inversion

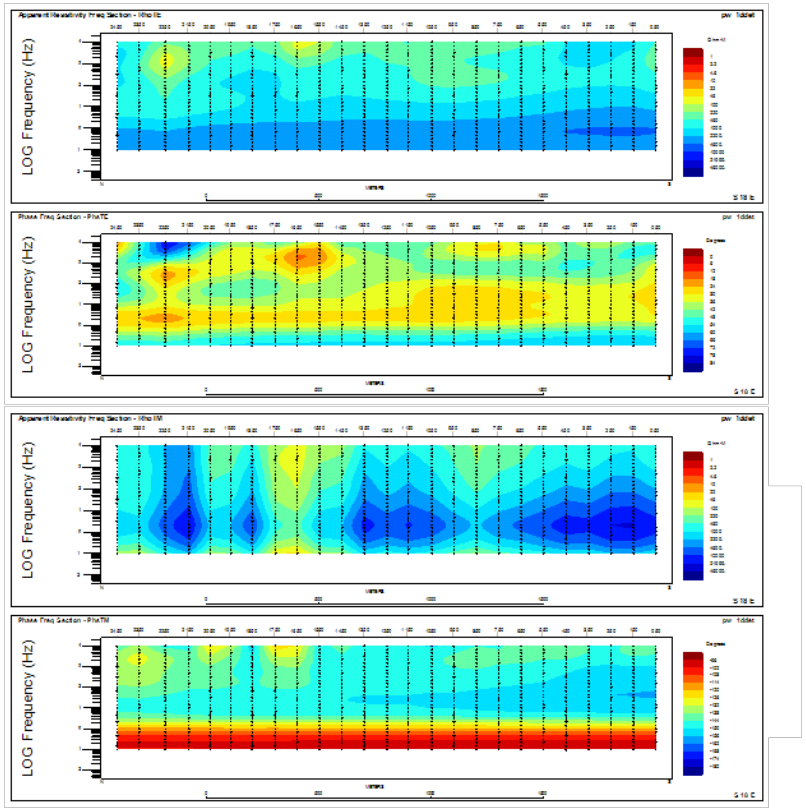

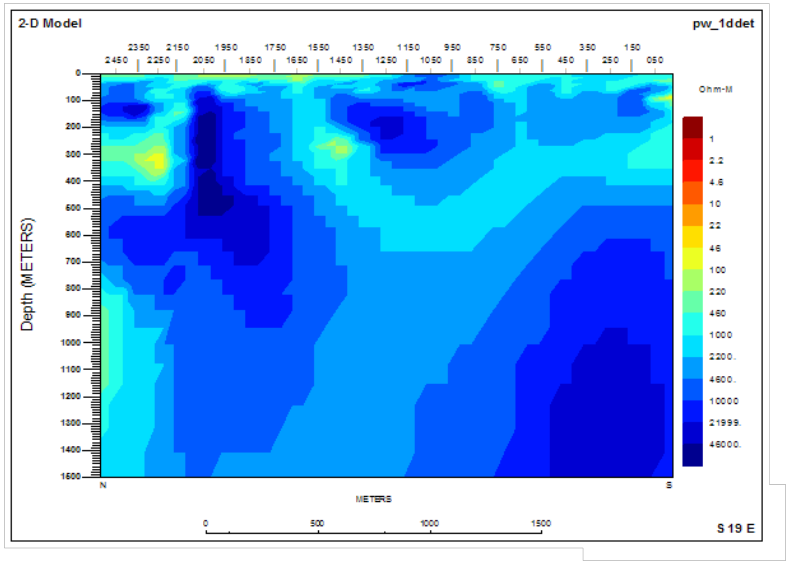

2D PW TM,TE inversion results:
Starting model: Stitched 1D DET
RMS misfit: 0.8881E+01
N iteration: 38

titan24

Quantec Geoscience

Preliminary
07.08.09

Capstone Mining Corp.
Minto Mine Project

Geosoft Images

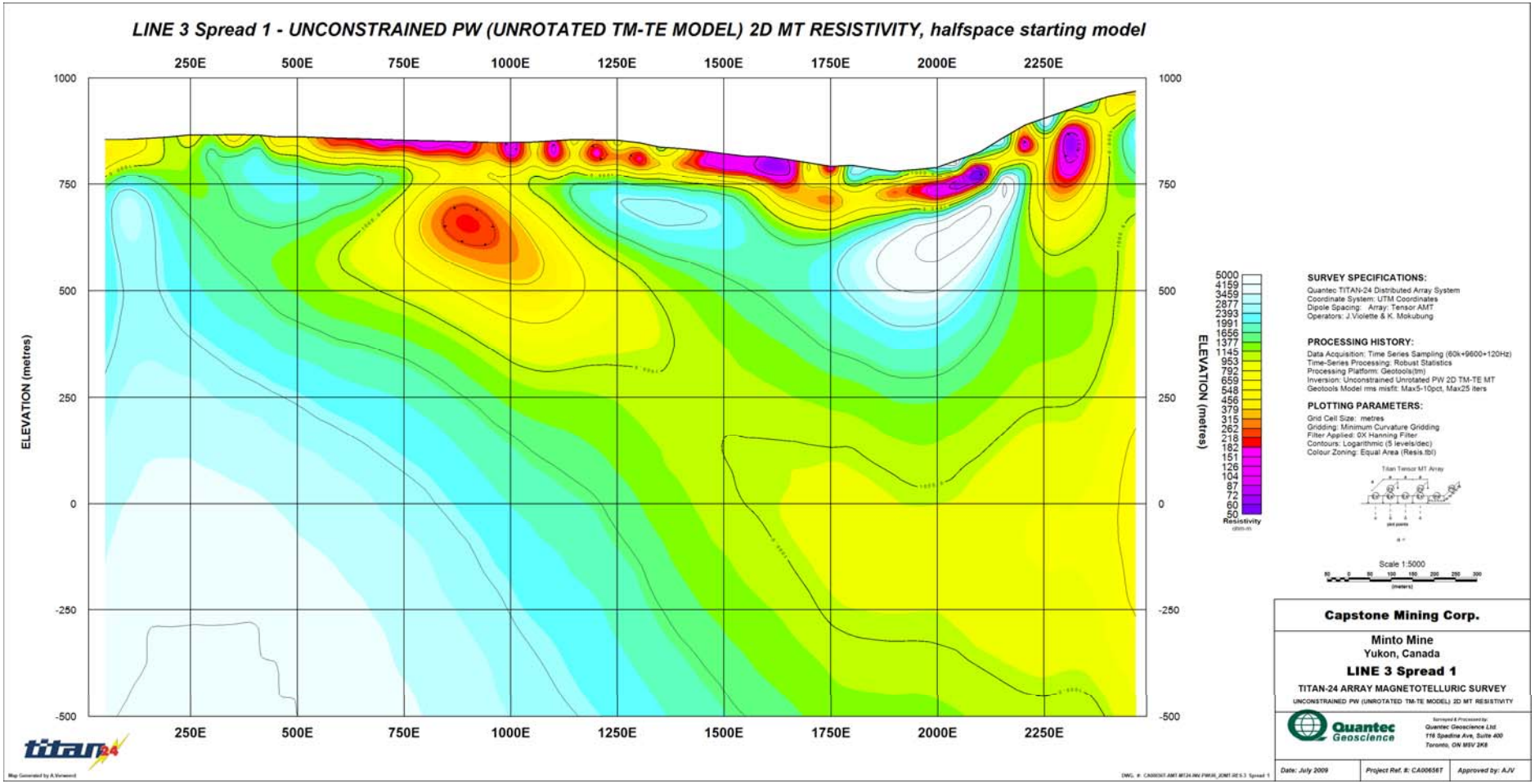

Preliminary
07.08.09

Capstone Mining Corp.
Minto Mine Project

Geosoft Images

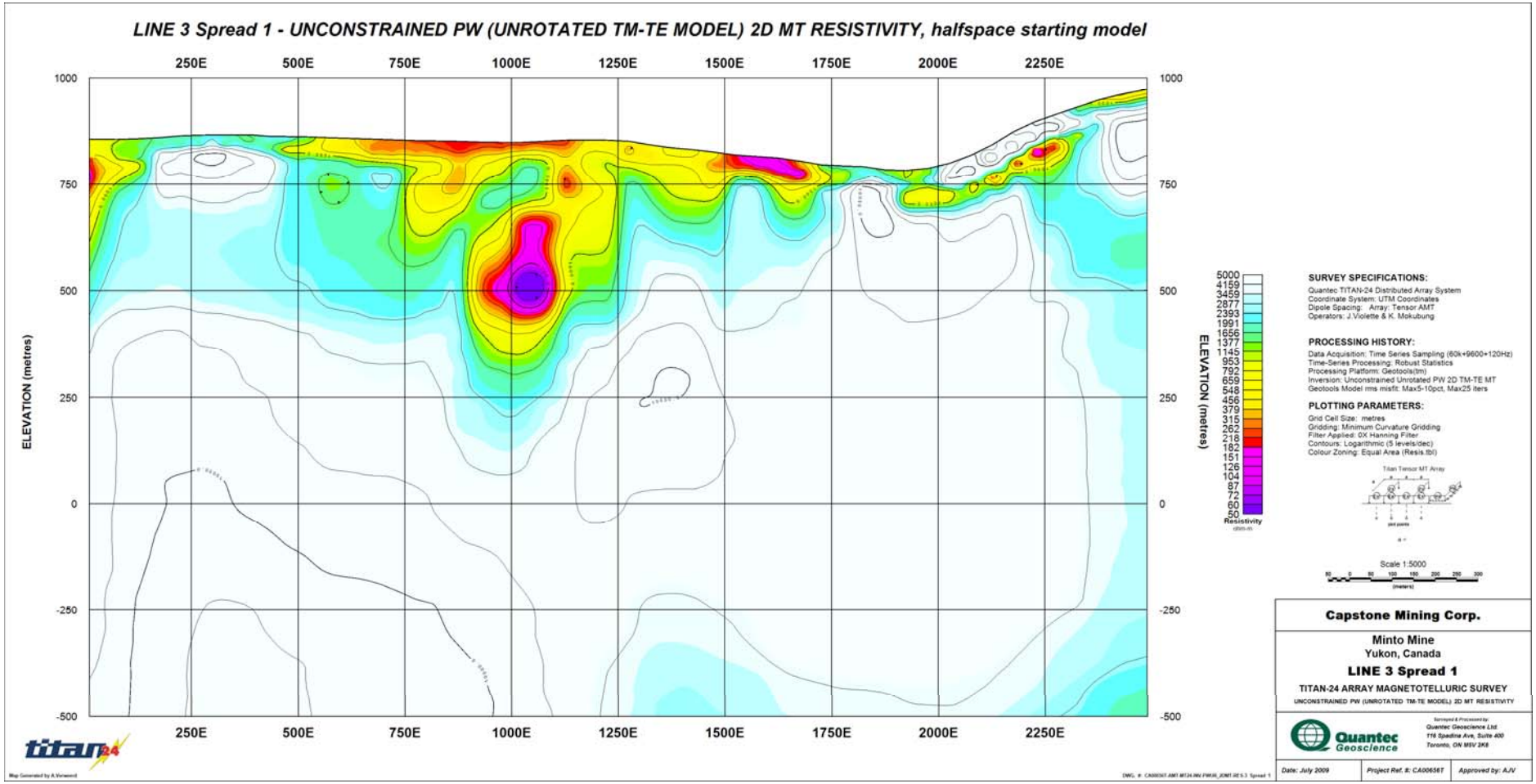

Preliminary
07.08.09

Capstone Mining Corp.
Minto Mine Project

Geosoft Images

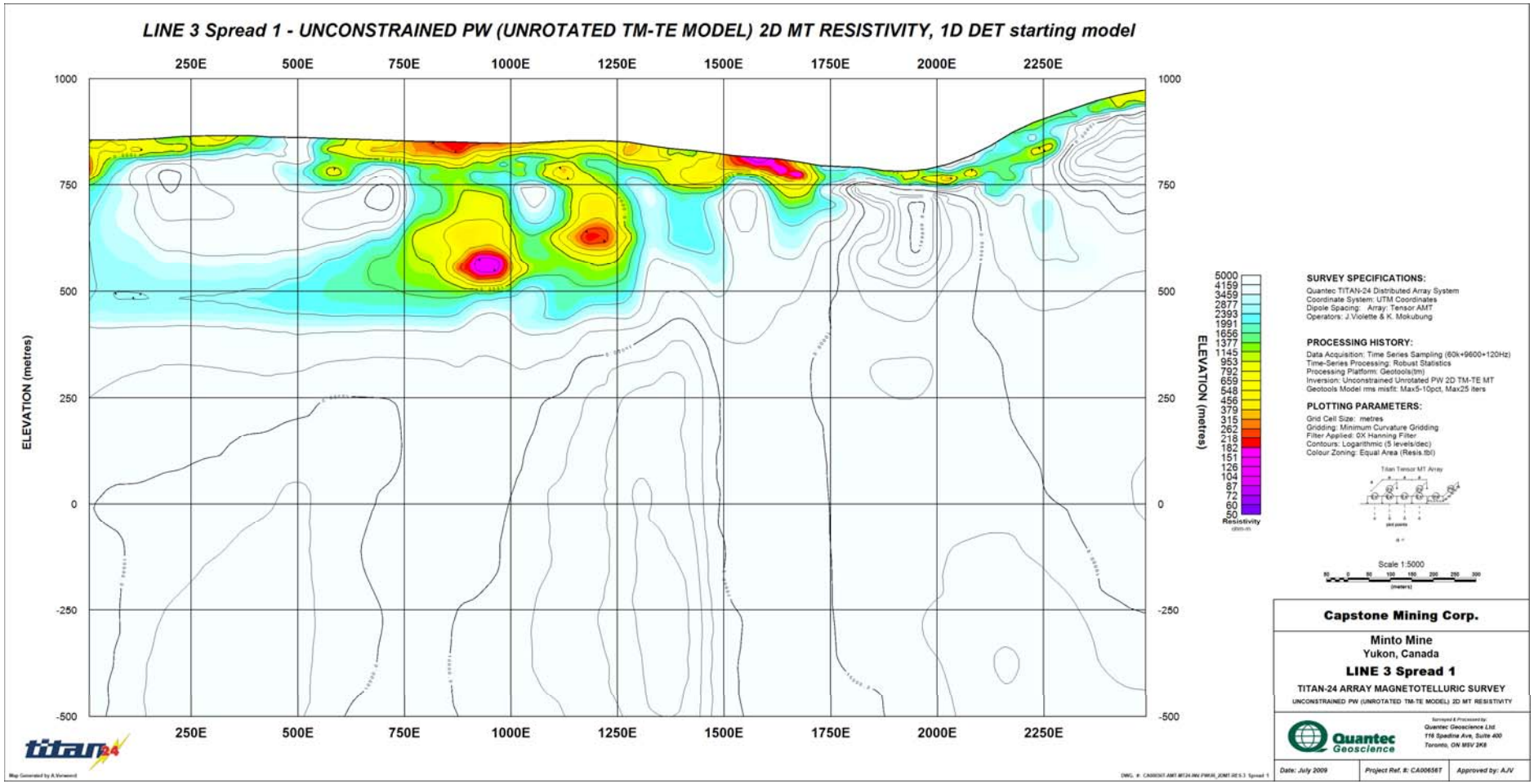

LINE L3 spread 2
TITAN-24 Survey
Minto Mine Project
Capstone Mining Corp - Minto Explorations

Preliminary 2D Inversion

Quantec Geoscience Ltd.
Toronto, Canada

A. Verweerd, Dr. Rer. Nat.

Preliminary
09.08.09

Capstone Mining Corp.
Minto Mine Project

2D DC/IP inversion

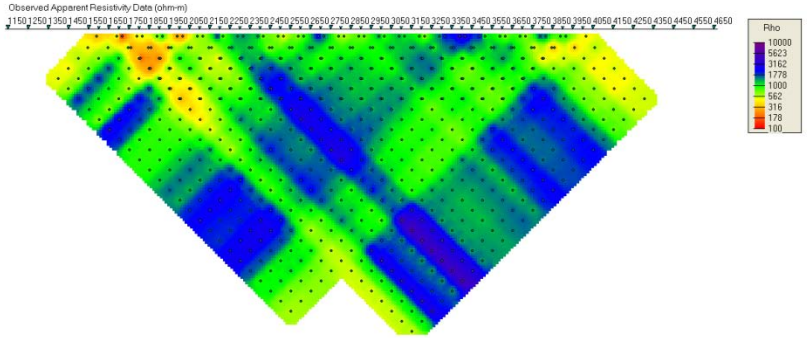

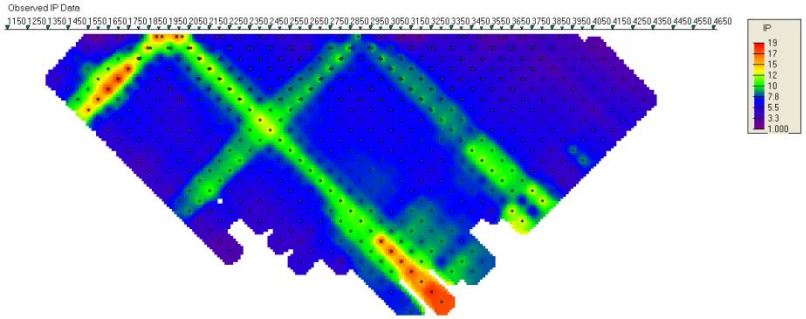

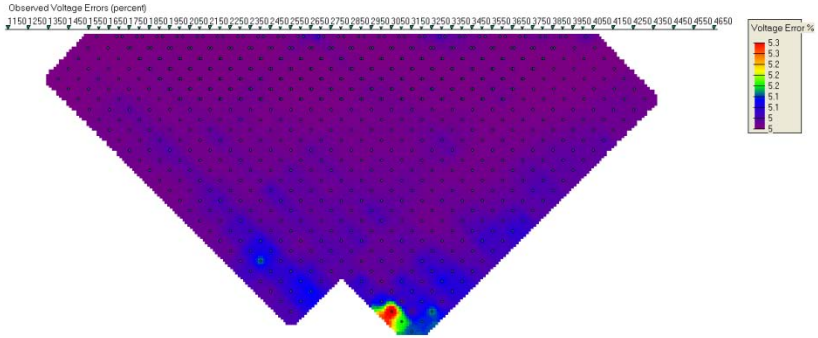

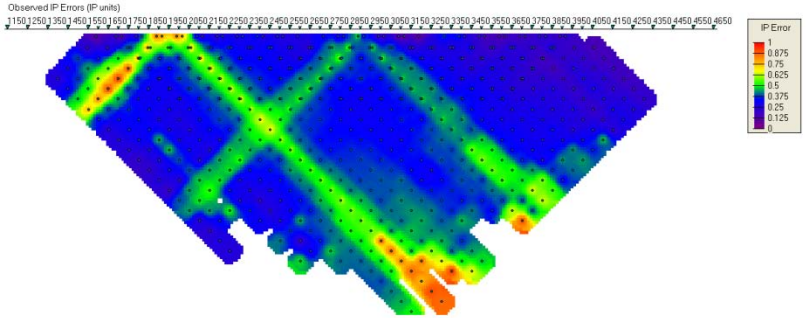

Error assignment:

DC data: Acquisition error + 5%

IP data: Remove acquisition error>25%

if error < 7%, set at 7%, else keep error, outlier rejection

titan24

Quantec Geoscience

Capstone Mining Corp.
Minto Mine Project

Preliminary
09.08.09

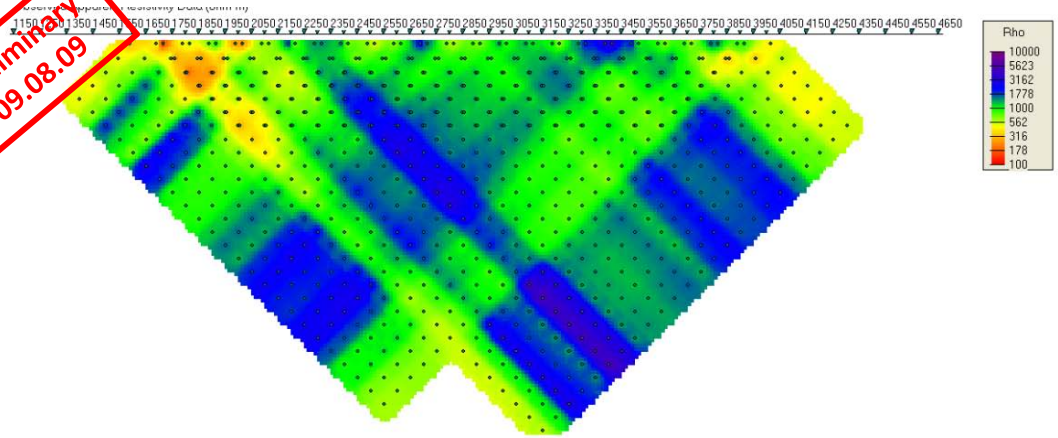

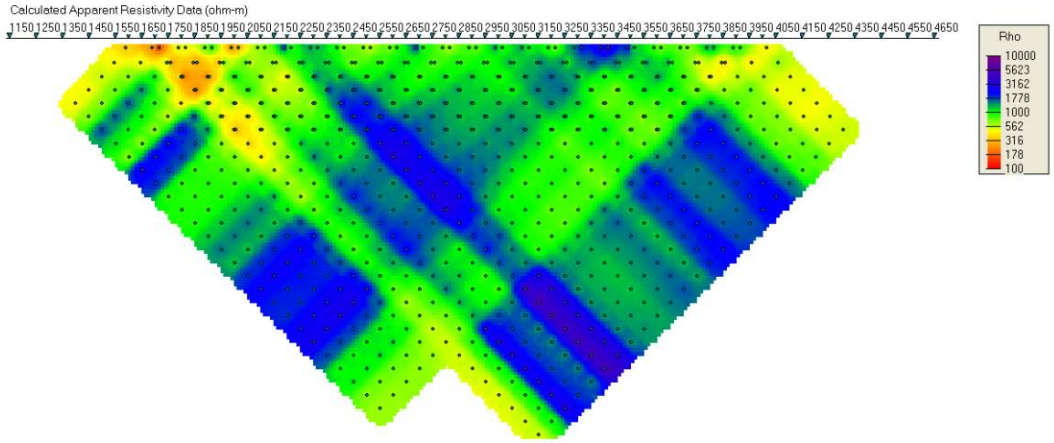

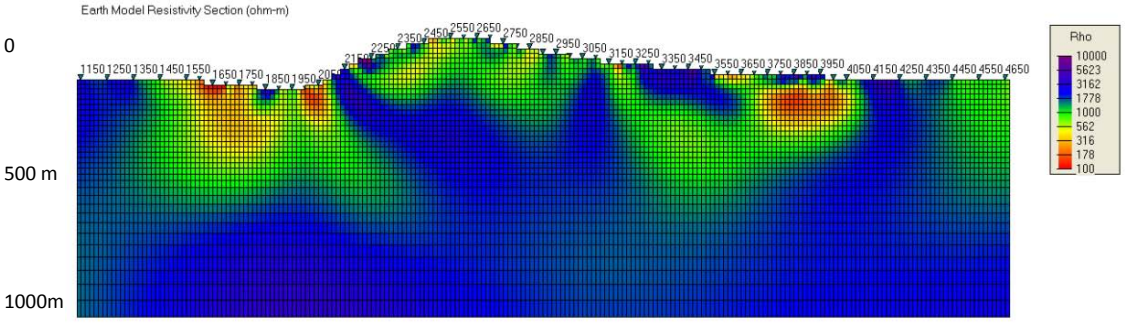

2D DC resistivity inversion results:
N data = 840
Misfit = 8.39989E+02
N iterations = 16

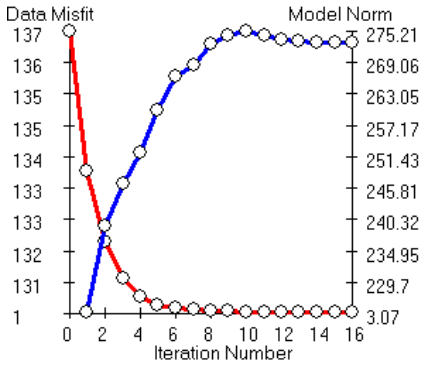

titan24

Note: Depth indications are approximate

Quantec Geoscience

Capstone Mining Corp.
Minto Mine Project

Preliminary
09.08.09

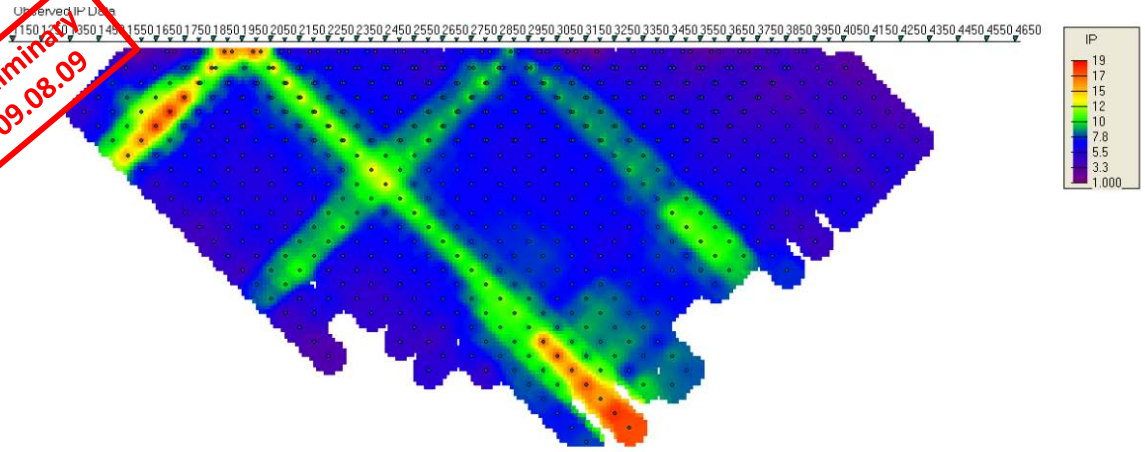

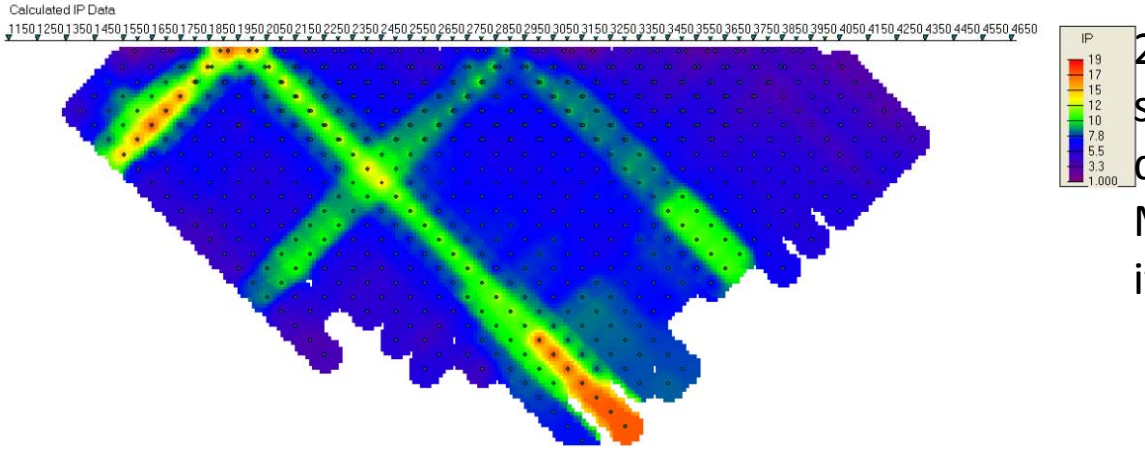

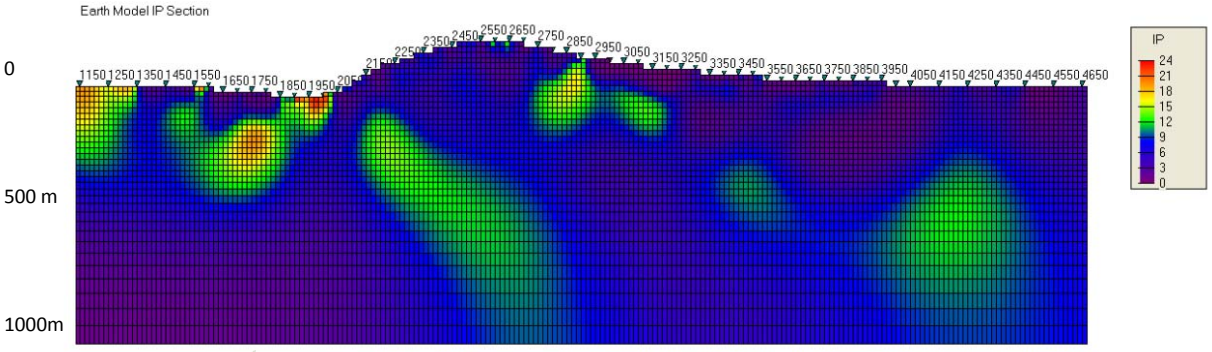

2D IP chargeability inversion results
smooth model:
data = 738
Misfit = 7.38005E+02
iterations = 24

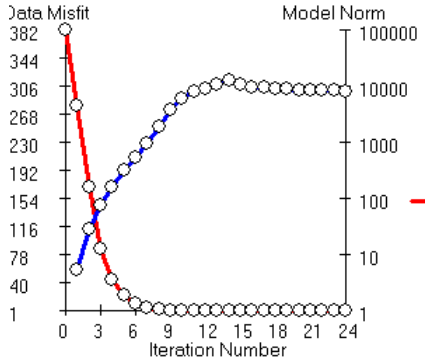

Note: Depth indications are approximate

titan24

Quantec Geoscience

Capstone Mining Corp.
Minto Mine Project

Preliminary
09.08.09

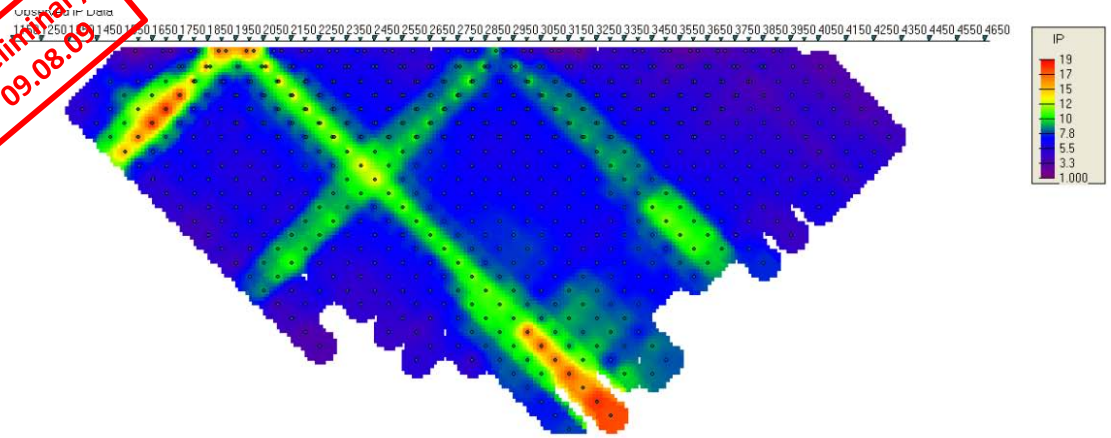

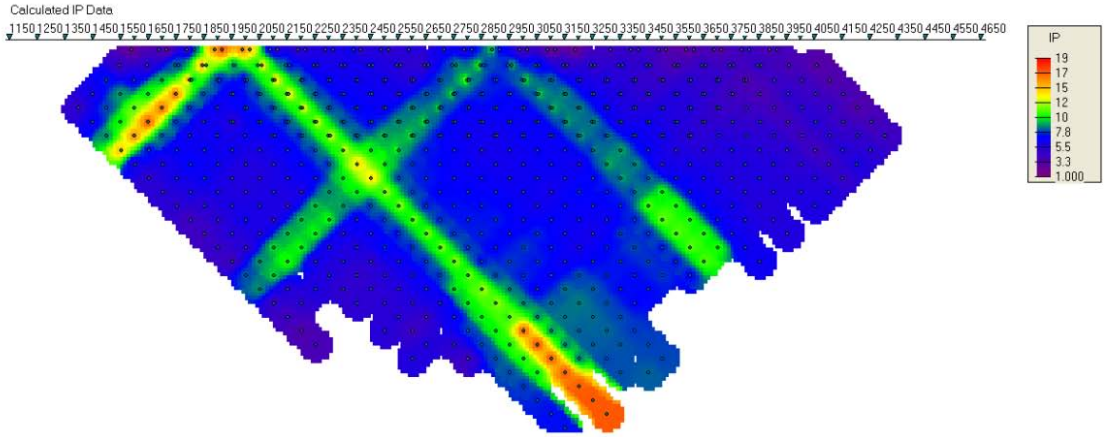

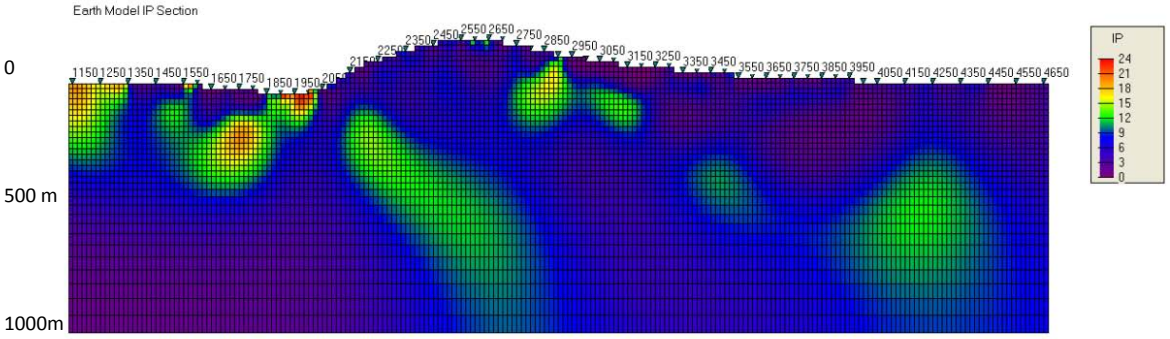

2D IP chargeability inversion results
Null Conductivity model:
N data = 736
Misfit = 7.36302E+02
N iterations = 26

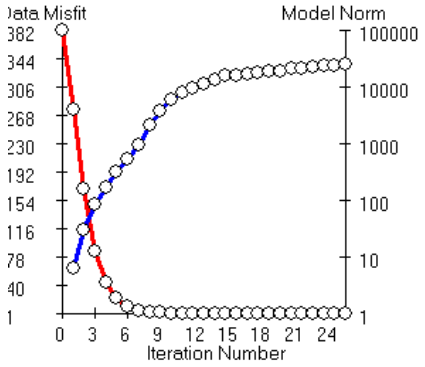

Note: Depth indications are approximate

DOI Investigation

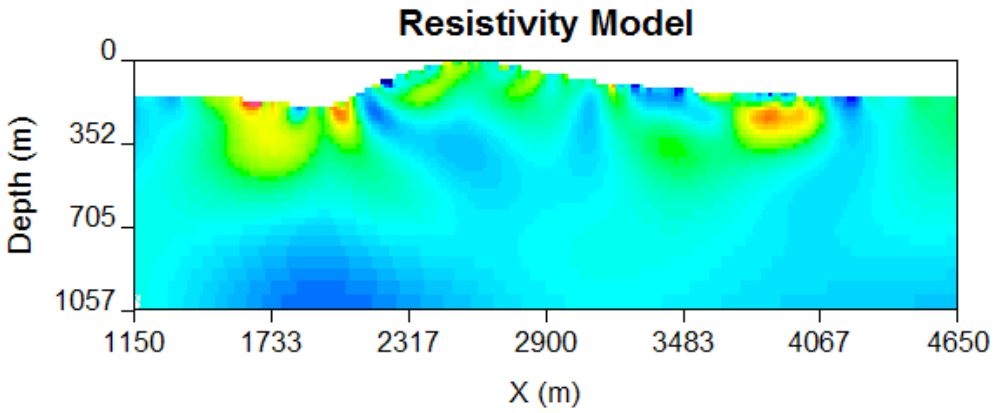

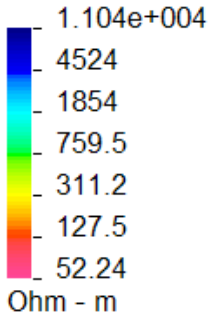

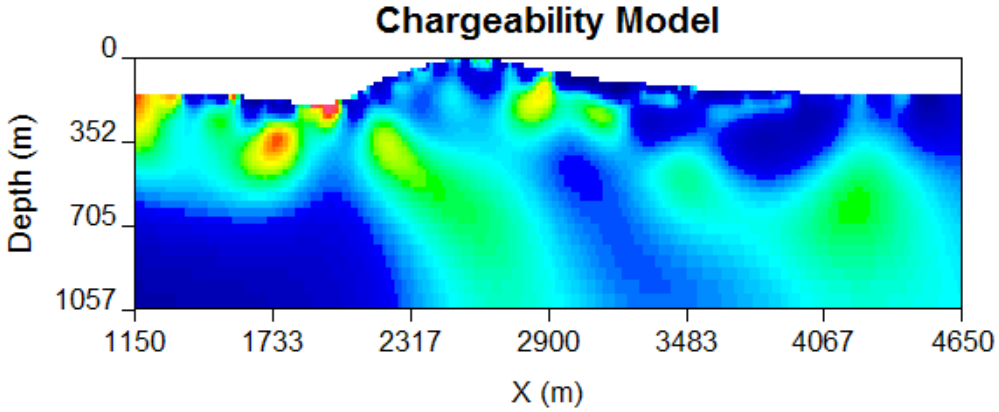

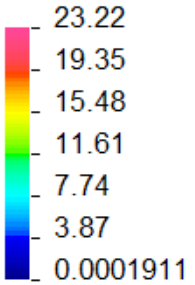

DOI (depth of investigation) is a Tool designed by the UBC-GIF to image the validity of inversion models. It compares two models calculated with different reference models.

Thus creating an image of how regions in the model which are influenced by the choice of reference model and not the actual data.

These zones are indicated with the hatched colours.

For the DC model a 10 kOhm-m and the default reference (average resistivity of the line) was used, in the IP the smooth and null con. Models were compared, a 0.1 cut off value was chosen

See: Oldenburg & Li, "**Estimating depth of investigation in dc resistivity and IP surveys**" GEOPHYSICS, VOL. 64, NO. 2 (MARCH-APRIL 1999); P. 403–416

titan24

Quantec Geoscience

Preliminary
09.08.09

Capstone Mining Corp.
Minto Mine Project

Geosoft Images

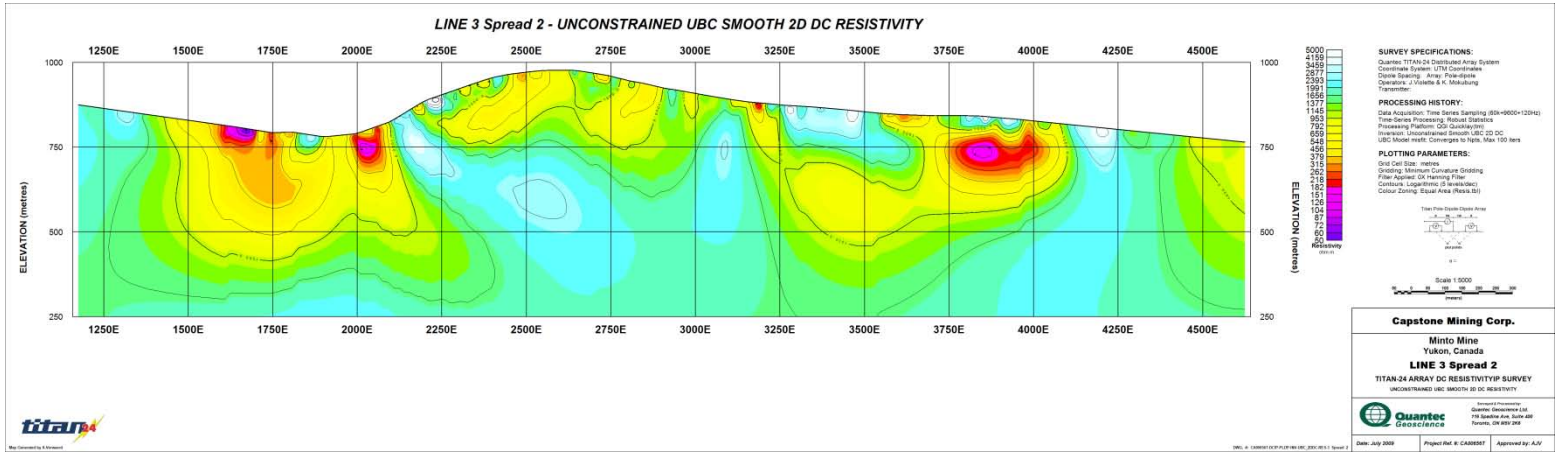

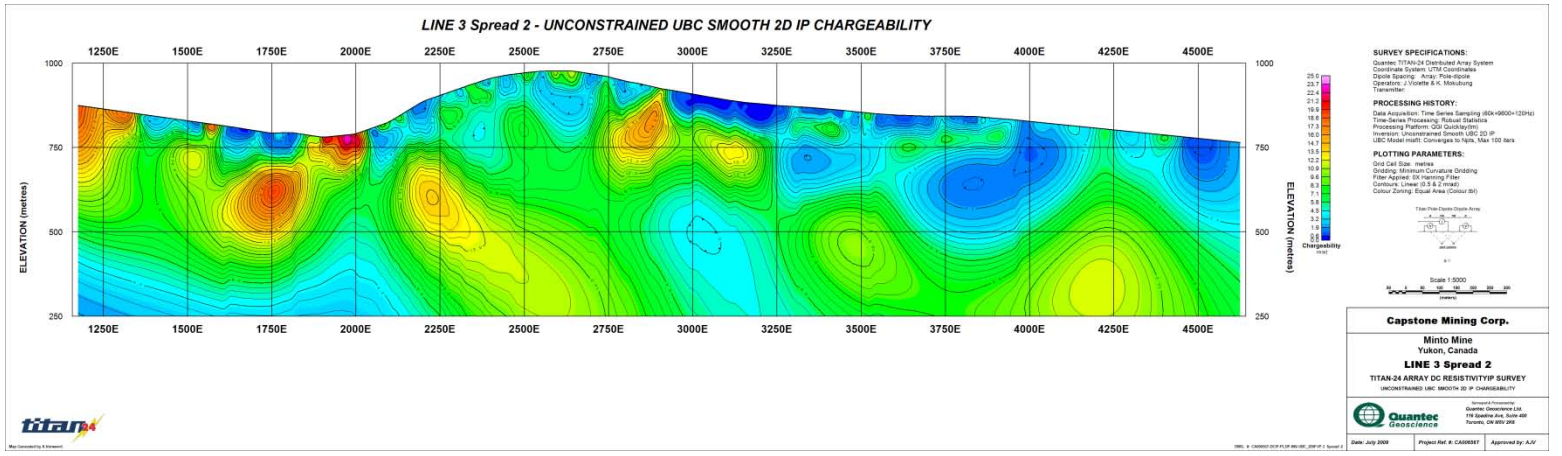

Preliminary
09.08.09

Capstone Mining Corp.
Minto Mine Project

Geosoft Images

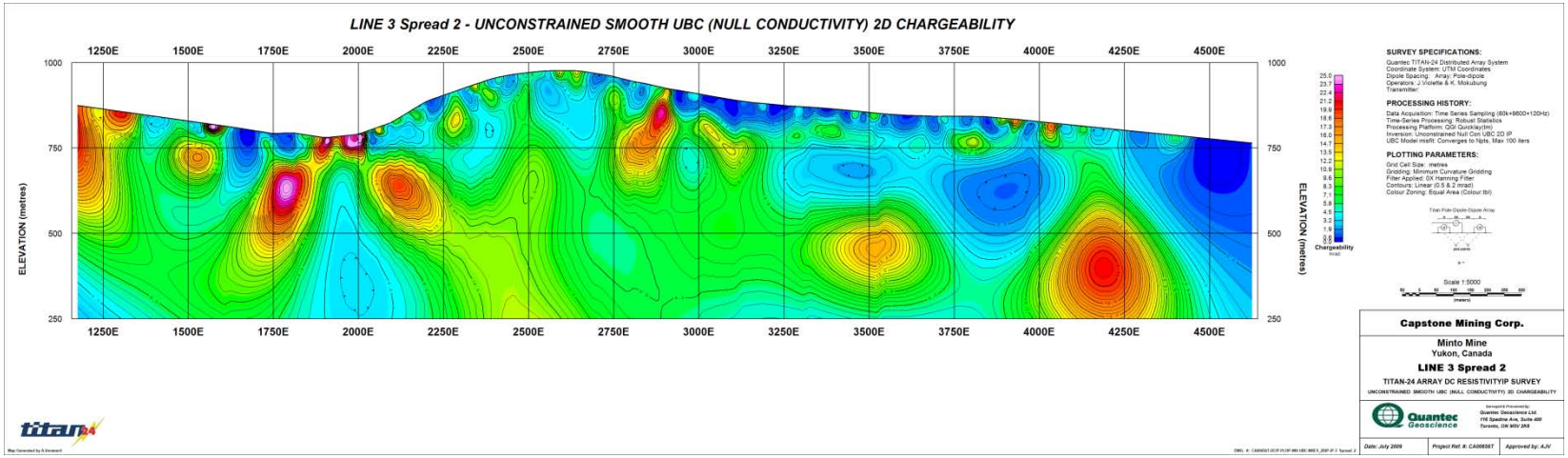

Preliminary
09.08.09

Capstone Mining Corp.
Minto Mine Project

MT inversion

Observed data

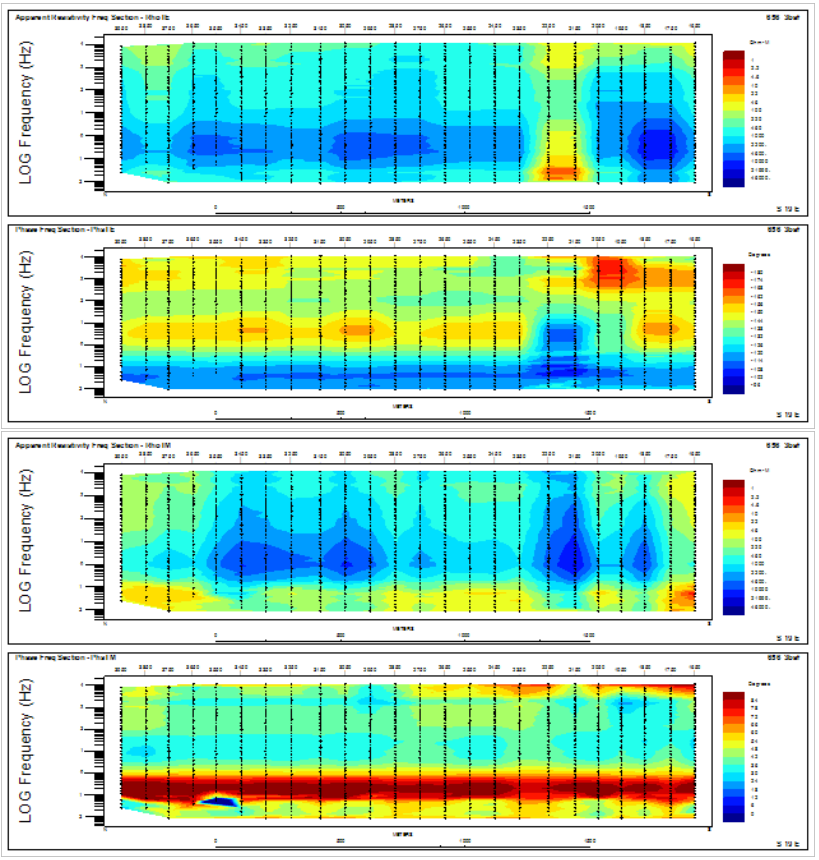

Interpolated data

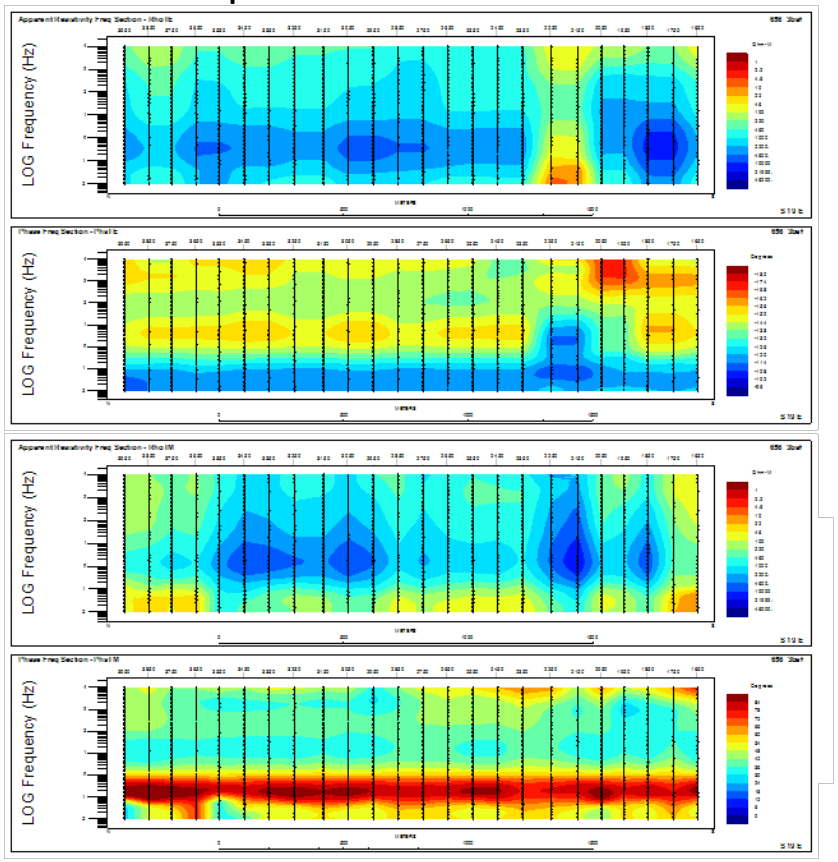

Note: The MT inversion program (GEOTOOLS), has a different plotting convention than the DC/IP inversion program (DCIP2D). Low station numbers are located on the lefts side in the DC/IP images and on the right side in the MT images.

titan24

Quantec Geoscience

Preliminary
09.08.09

Capstone Mining Corp.
Minto Mine Project

1D inversion results

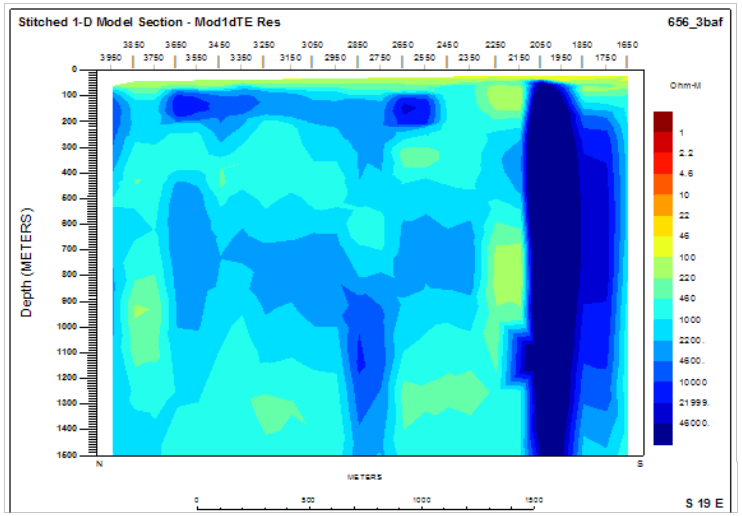

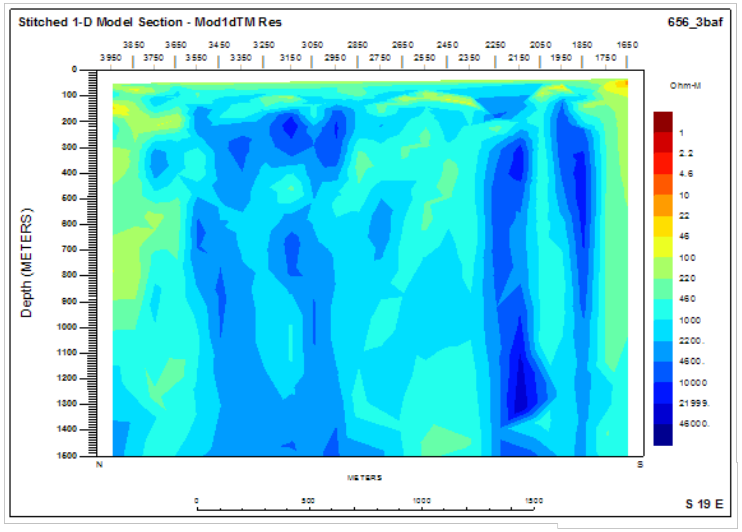

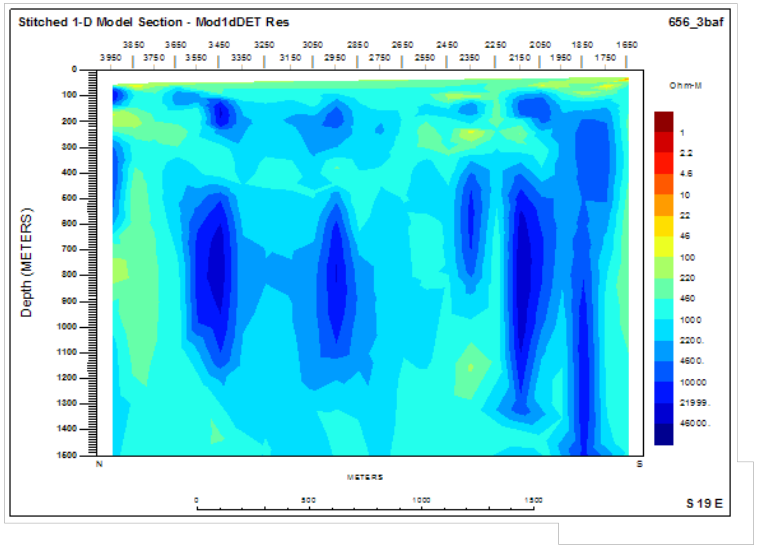

Left top: 1D stitched TE resistivity
Left bottom: 1D stitched TM resistivity
Right top: 1D stitched DET resistivity

titan24

Quantec Geoscience

Preliminary
09.08.09

Capstone Mining Corp.
Minto Mine Project

2D RLM Inversion

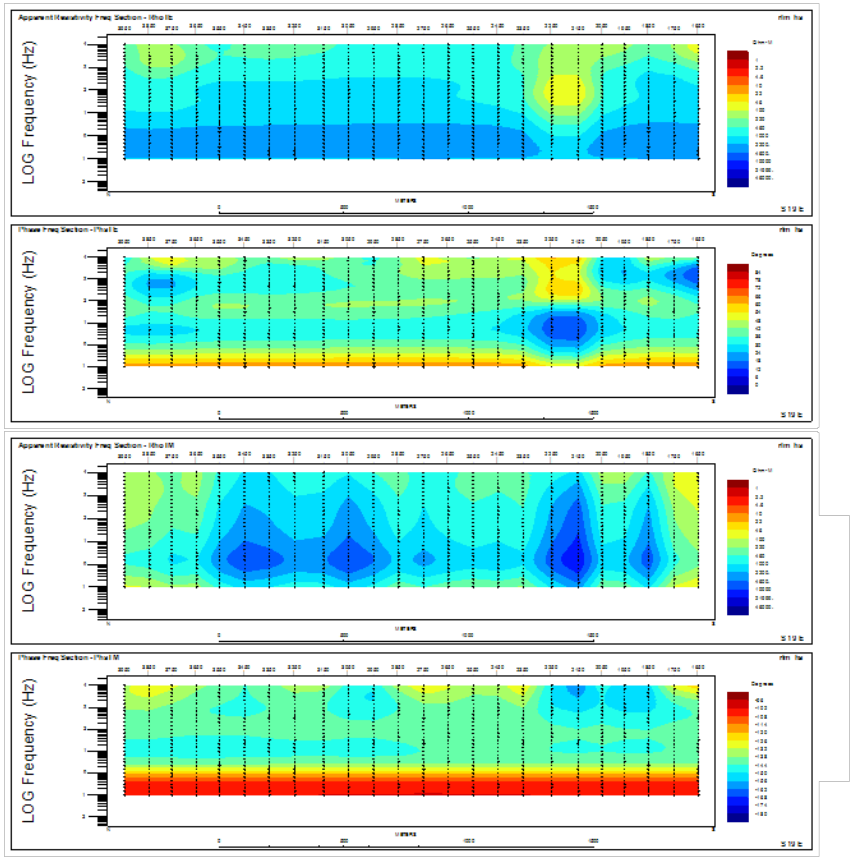

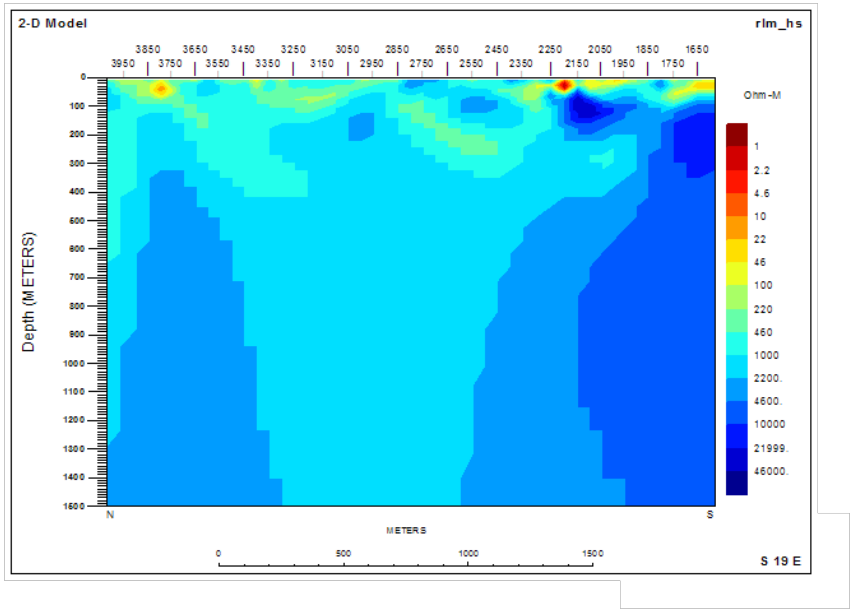

2D RLM TM,TE inversion results:
Starting model: 5000 Ohm-m halfspace
RMS misfit: 0.7234E+01
N iteration: 50 (max)

titan24

Quantec Geoscience

Preliminary
09.08.09

Capstone Mining Corp.
Minto Mine Project

2D PW inversion

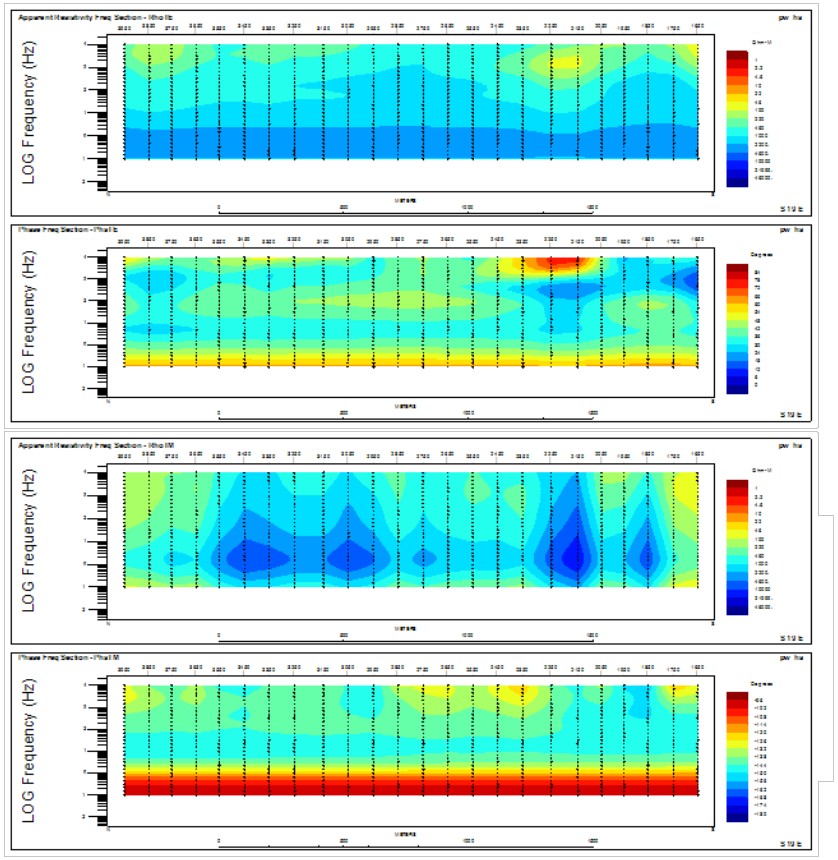

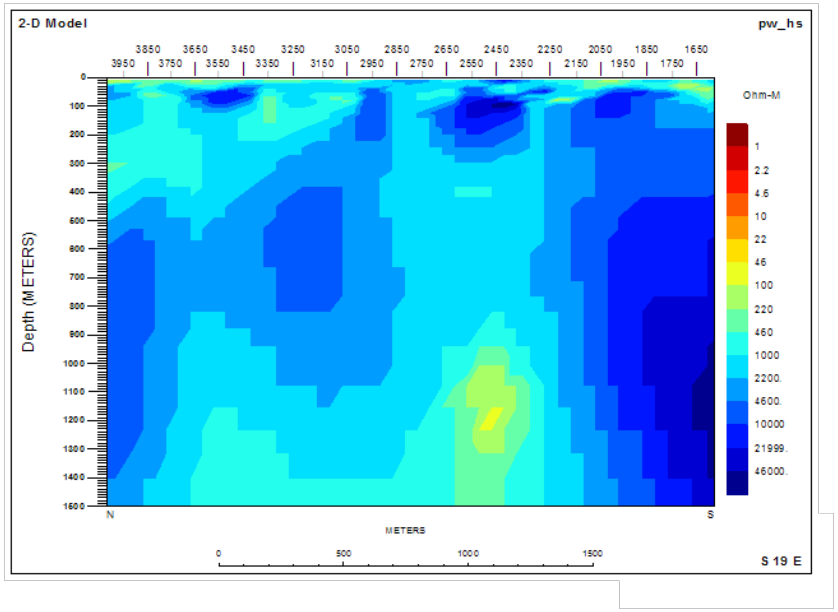

2D PW TM,TE inversion results:
Starting model: 5000 Ohm-m halfspace
RMS misfit: 0.7511E+01
N iteration: 37

titan24

Quantec Geoscience

Preliminary
09.08.09

Capstone Mining Corp.
Minto Mine Project

2D PW inversion

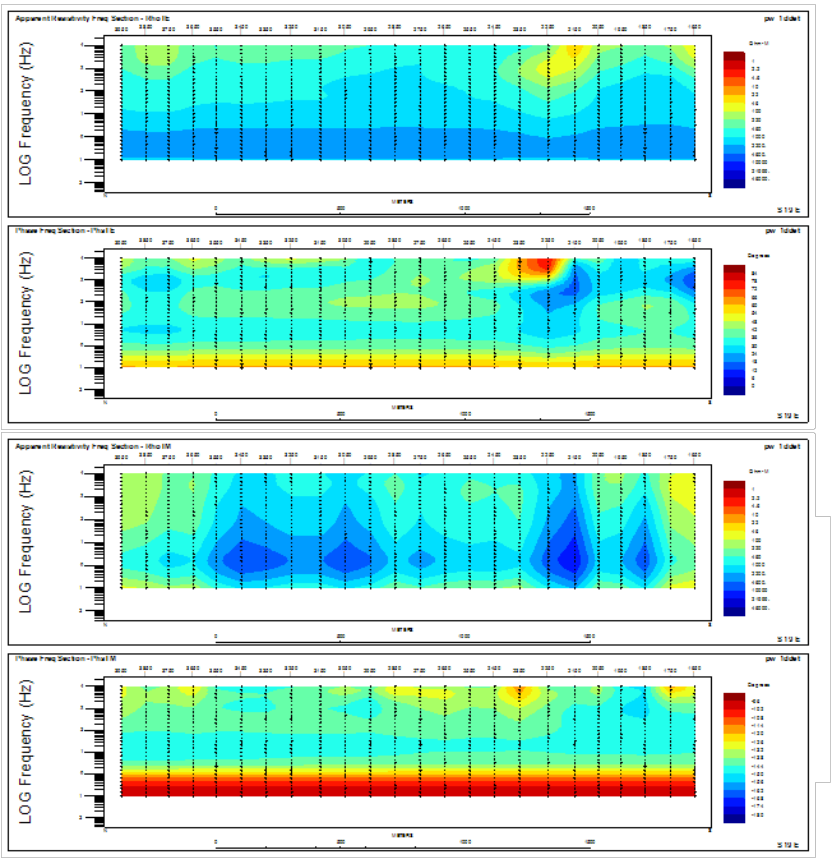

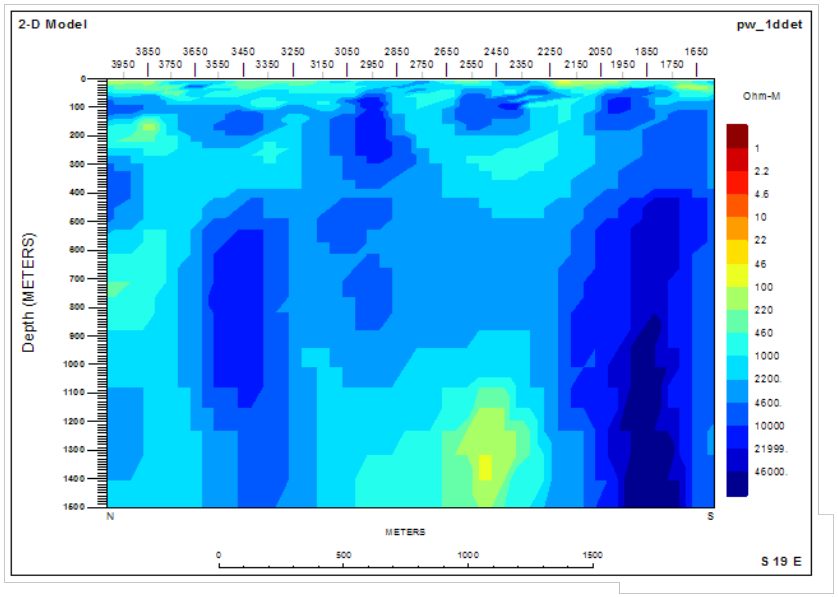

2D PW TM,TE inversion results:
Starting model: Stitched 1D DET
RMS misfit: 0.7406E+01
N iteration: 30

titan24

Quantec Geoscience

Preliminary
09.08.09

Capstone Mining Corp.
Minto Mine Project

Geosoft Images

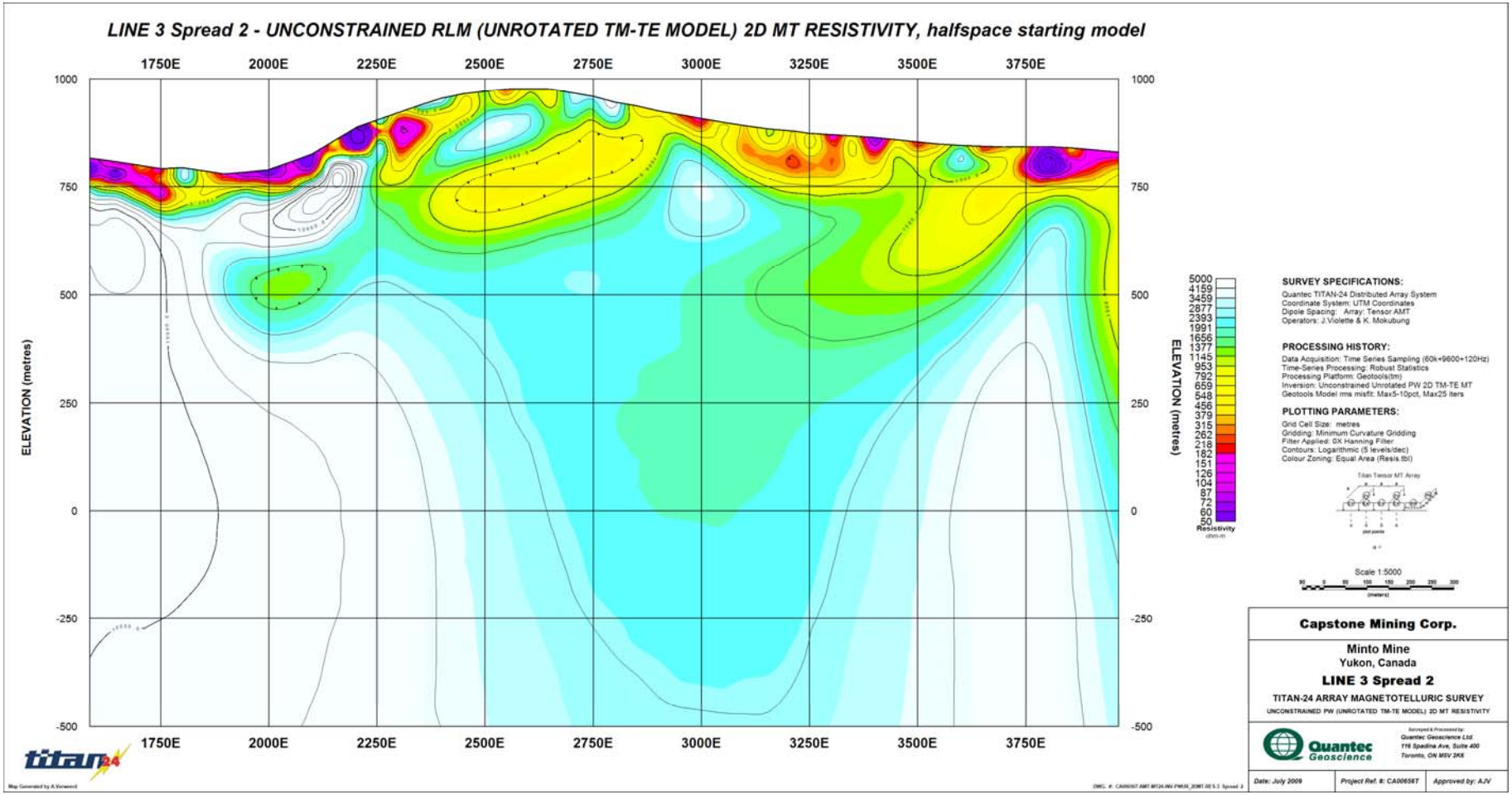

Preliminary
09.08.09

Capstone Mining Corp.
Minto Mine Project

Geosoft Images

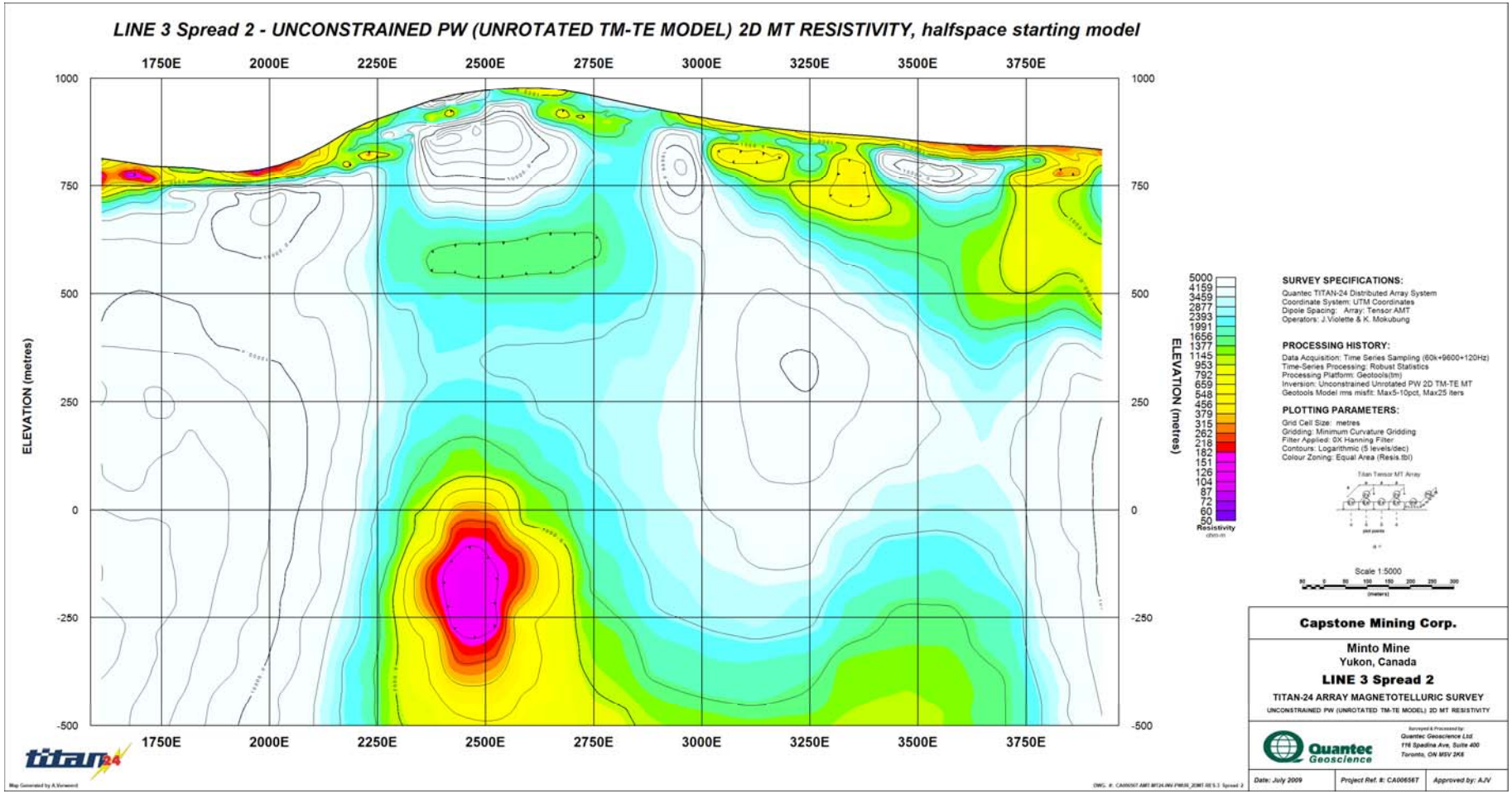

Preliminary
09.08.09

Capstone Mining Corp.
Minto Mine Project

Geosoft Images